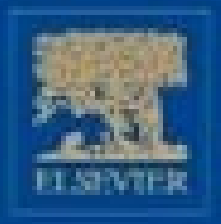

Advances in Molecular Toxicology

Volume 4

VOLUME FOUR

ADVANCES IN MOLECULAR TOXICOLOGY

EDITED BY

JAMES C. FISHBEIN
Department of Chemistry and Biochemistry
University of Maryland, Baltimore County
Baltimore, USA

AMSTERDAM • BOSTON • HEIDELBERG • LONDON
NEW YORK • OXFORD • PARIS • SAN DIEGO
SAN FRANCISCO • SINGAPORE • SYDNEY • TOKYO

Elsevier
Radarweg 29, PO Box 211, 1000 AE Amsterdam, The Netherlands
Linacre House, Jordan Hill, Oxford OX2 8DP, UK
32, Jamestown Road, London NW1 7BY, UK
525 B Street, Suite 1900, San Diego, CA 92101-4495, USA
30 Corporate Drive, Suite 400, Burlington, MA 01803, USA

First edition 2010

British Library Cataloguing in Publication Data
A catalogue record for this book is available from the British Library

Library of Congress Cataloging-in-Publication Data
A catalog record for this book is available from the Library of Congress

ISBN: 978-0-444-53584-9
ISSN: 1872-0854

Printed and bound in Great Britain
10 11 12 13 10 9 8 7 6 5 4 3 2 1

Contributors

Preface

This fourth volume in the series offers a potpourri of chemistries relevant to the broad and diverse discipline of Molecular Toxicology. From single ions to silica nanomaterials, these reviews encompass the best in mechanistic considerations in the discipline. The Editor hopes you enjoy the breadth of this spectrum.

This volume opens with a review of the chemistry and toxicology of a small but highly reactive compound that is pervasive in the human environment—acrolein. Burcham, Thompson, and Henry survey an extensive recent literature on its activity, particularly as a pulmonary toxicant. There has been a rapidly evolving literature on the chemical reactivity of acrolein with biomolecules and its activity in a variety of models. But as the authors demonstrate, our understanding of the detailed molecular basis for the mode of action of acrolein in lung toxicity is relatively fragmentary.

Consumption of cooked poultry, meat, and fish leads to widespread human exposure to heterocyclic aromatic amines. A number of such compounds have been demonstrated to be powerful mutagens and carcinogens. Since Sugimura and coworkers demonstrated the activity in charred fish and meat more than three decades ago, there has been a growing literature on the metabolism and activation of these compounds that have demonstrated arise not only from the initial sources but from diesel and cigarette combustion and endogenous reactions as well. In Chapter 2, Turesky reviews this class of compounds, their metabolism and activation, the products of reactive intermediates interacting with biomolecules, and potential biomarkers for determining their contribution to the human cancer burden.

Nickel and cadmium make up tiny fractions of the earth's crust but they are key elements in many important industrial applications leading to significant human exposure. This is compounded by the presence of significant quantities of these elements in products of combustion—cigarettes smoke, coal, and diesel fly ash. In Chapter 3, Kurowska and Bal take a novel view of commonalities in both the exposure, absorption, and molecular basis of the toxicological activities of nickel and cadmium in this comprehensive review.

Radical intermediates and their consequences are the focus of Chapter 4 which concerns oxidative damage to the sugar moiety of DNA. From the five simple carbon-centered radicals derive a rather large array damage products, some of which are suitably functionalized to form further adducts. The complexity of this chemistry is well elaborated here. The

need to consider the metabolic context in which the radical is formed and the degree to which this can determine its subsequent fate and the ultimate "fingerprint" of the initial oxidation is emphasized.

Nitric oxide, redox inflammation, and cancer are the topics of Chapter 5. Cheng and coauthors elaborate the fundamental chemistry of NO and its Janus-like character in both normal and aberrant biochemical contexts. This modest diatomic radical manifests a profusion of homeostatic and toxic roles. Its role in carcinogenesis and metastatic processes, a form of molecular hijacking, is discussed. A key insight to the contrasting behaviors is that NO levels—"dose"—can be a key determinant to "outcome."

Biological thiols and their redox chemistry are the focus of Nagy and Winterbourn in Chapter 6. The approach is fundamental, as is warranted. The balance of numerous redox couples is integral to the detection of oxidative stress and numerous modifications of small molecule and protein thiols are both key signaling and enzyme activity-modifying events. Activity of thiols as targets is often modulated by microenvironment that controls nucleophilicity and selectivity. The extent of previously little-recognized array of posttranslational modifications of protein cysteine residues is documented. Finally, the newly recognized activity of H_2S as a key signaling agent acting at sulfhydryls is discussed.

Nanomaterials are a current focus of materials development as they offer unique bio- and physicochemical properties that can significantly impact on the properties of the materials themselves and the agents with which they may be coupled or attached. With these new properties accrue new manifestations of toxicity. An aspect of this is the focus of Petushkov and coauthors in Chapter 7. This includes a survey toxicity of zeolites and nanoscale silicalites and mesoporous silicates as well as the impact of surface functionalization. The involvement of reactive oxygen species in toxication is emphasized and the numerous variables that impact on this activity are emphasized. This underscores the need in this area, respecting materials for which application is conceived, for careful characterization of the physicochemical characteristics of the constructs.

The editor wishes to thank all the authors for distinguished contributions and acknowledges the talented Elsevier staff who have put this volume together.

CHAPTER 1

Invited Review

Acrolein and the Lung: Chemical, Molecular, and Pathological Aspects

Philip C. Burcham,* Colin A Thompson, *and* Peter J. Henry

Contents

Pharmacology and Anaesthesiology Unit, School of Medicine and Pharmacology, the University of Western Australia, Crawley, WA, Australia

* Corresponding author. Tel.: 61 8 9346 2986
Email address: Philip.burcham@uwa.edu.au

Advances in Molecular Toxicology, Volume 4
ISSN 1872-0854, DOI 10.1016/S1872-0854(10)04001-4

1. Introduction

1.1. Scope of review

The three-carbon α,β-unsaturated aldehyde acrolein was first identified 170 years ago as a thermal decomposition product of glycerine, the name assigned in recognition of its pungent odor ("acrid") and oil-like constituency ("oleum") [1]. Among the most noxious substances known to toxicology, recent years have witnessed a resurgence of interest in acrolein, partly driven by debate concerning its contribution to smoking-related lung cancer [2]. The renewed interest also reflects the growing awareness that acrolein forms endogenously during oxidative stress, suggesting a role in various degenerative disorders [3]. The rising profile is increasing the application of modern molecular tools to the study of the cellular effects of acrolein, an outcome that should help clarify its role in specific diseases.

In the face of a rapidly expanding literature, this review focuses on the chemical and cellular effects of acrolein within the context of its emerging role as a mediator of human lung disease. As a volatile, airborne toxicant, the lung is the primary port of entry for environmental acrolein, ensuring respiratory epithelium bears the brunt of its cell-damaging properties. An overarching goal is to review existing knowledge with a view to synthesizing understandings of the chemical reactivity of acrolein and its molecular effects at the cellular level with its toxicological and pathological effects on the intact lung. When viewed from this standpoint, the state of knowledge concerning acrolein and the lung appears surprisingly rudimentary.

1.2. Sources of airborne acrolein

Although it forms ubiquitously during a range of natural and human activities, most atmospheric acrolein likely derives from the combustion of organic matter. Based on air measurements within two outdoor urban settings over 1961–1980, the US Environmental Protection Agency reported average ambient concentrations of $14.3\,\mu g\,m^{-3}$ (6.2 ppb) [4]. Corresponding indoor concentrations can be 2–20-fold higher, with the higher levels typically recorded in smoky indoor environments, poorly ventilated kitchens, and dwellings heated with wood stoves [4,5]. Formation during combustion of organic matter ensures particular lifestyle or occupational practices can heighten human exposure to acrolein. For example, as a by-product of the combustion of sugars and to a lesser extent glycerol within tobacco, in excess of 100–200 μg acrolein can be released from a burning cigarette [1,4]. Cigarette smokers likely inhale up to 100 nmol acrolein/puff, with even higher levels present in sidestream smoke [1,5,6]. Acrolein levels in smoke formed upon burning other types

of organic matter can exceed those in tobacco smoke [5]. Wood, vegetation, fossil fuels, and construction materials are all sources for smoke-borne acrolein, with especially high yields released from smouldering synthetic polymers such as polyethylene and polypropylene [7].

While measuring airborne acrolein is straightforward, clarifying the concentrations achieved in lung tissue during either chronic or acute exposure to acrolein-containing smoke is more problematic. This partly reflects the technical challenges accompanying measurement of inhaled toxicants in the fluids that line the respiratory tract, the initial point of contact for inhaled acrolein. Conventional lavage techniques used to collect airway and bronchoalveolar liquid samples cause unpredictable dilution of lung fluids, rendering toxicant concentrations unreliable [8]. Furthermore, the reactivity of acrolein with fluid proteins and epithelial cell constituents ensures any such measurement of "free" acrolein in respiratory fluids is of questionable toxicological significance. Notwithstanding these challenges, some workers have estimated that smoking a single cigarette achieves "micromolar" acrolein concentrations in respiratory fluids, although the quantitative basis for these estimates is uncertain [9]. Concentrations of acrolein within respiratory fluids of heavy, long-term smokers, or victims of high-dose, acute smoke intoxication [e.g., smoke inhalation victims (SII)], are entirely unknown. Future progress awaits translation of knowledge of the chemistry of acrolein adduction of biological macromolecules (e.g., DNA, protein—see Section 2 below) into robust analytical methods that allow the "biologically effective dose" to be estimated for acrolein under different exposure conditions (Figure 1).

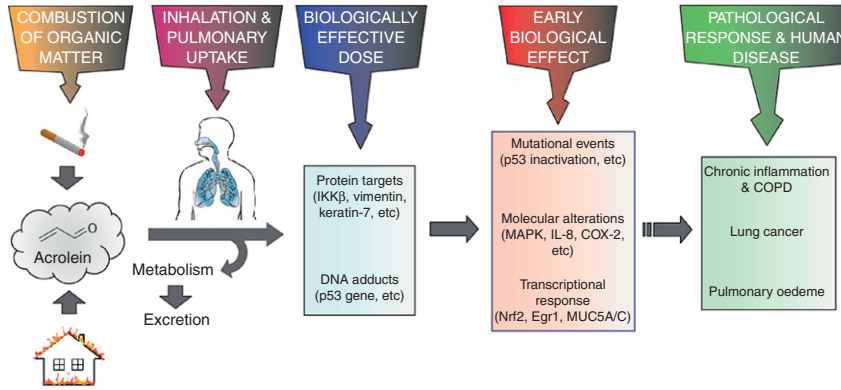

Figure 1 Application of the "toxicological paradigm" to the role of acrolein in various human respiratory disorders. Acrolein may contribute to lung injury following either acute, high-dose exposure to smoke in fire victims (e.g., smoke inhalation injury) or after chronic exposure to tobacco smoke (e.g., COPD or lung cancer). See text for details.

1.3. Involvement in respiratory diseases

While trial as a chemical warfare agent in World War I raised the prospect of acute, single-agent exposure to acrolein, the potential for similar exposures in the modern era seem limited to specific workplace settings (e.g., factories involved in the synthesis of acrylics, etc). Ongoing concern over the pulmonary effects of inhaled acrolein thus mostly centers upon its presence in smoke formed from various combustible materials. A complex mixture of particulates, gases, and organics, the composition of smoke varies according to the flammable material, ignition temperature, oxygen availability, rate of incineration, etc [10]. While the simultaneous exposure to multiple combustion products complicates evaluation of the contribution of acrolein to smoke toxicity, possible toxicological interactions involving acrolein during smoke inhalation are beyond the scope of this review.

Respiratory diseases in which a role for acrolein is suspected include chronic disorders plaguing individuals exposed to first- or second-hand tobacco smoke over an extended period as well as acute, life-threatening disorders seen in fire and SII victims.

1.3.1. Chronic obstructive pulmonary disorder

Chronic obstructive pulmonary disorder (COPD) is a devastating condition that despite the success of smoking cessation initiatives in many countries is of increasing global significance [11]. While COPD occurs most frequently among tobacco smokers, chronic exposure to other forms of air pollution can induce a similar syndrome. The lung pathology underlying COPD is an exaggerated manifestation of the low-grade infiltration of inflammatory cells to the bronchi and peripheral lung of "normal" smokers. In the minority of smokers who develop COPD this process is amplified and accompanied by a tissue-remodeling process that produces lung injury resembling chronic bronchitis. Other features of COPD include mucus hypersecretion, small airways obstruction, emphysematous alveolar damage, and pulmonary hypertension [12]. The airflow limitation and "breathlessness" that is characteristic of COPD is mainly due to permanent enlargement of distal respiratory air spaces following destruction of the alveolar walls [12]. While the pathobiological basis for COPD is complex, it appears the transition from a "normal" inflammatory response to an abnormal innate and adaptive immune response is driven by disparities in the protease–antiprotease and oxidant–antioxidant balance attending the influx of neutrophils, macrophages, and lymphocytes [12]. Together with proinflammatory cytokine production and other tissue responses, these processes trigger apoptosis and failure of repair mechanisms, eliciting alveolar destruction and remodeling of the small airways.

Indications that acrolein participates in COPD include the finding that it is the tobacco smoke constituent which most strongly stimulates mucus hypersecretion. The molecular basis for this response is reviewed in Section 3.2. Acrolein is also implicated in the macrophage adhesion and activation that accompanies the alveolar destruction phase of COPD [13]. Microarray analysis of COPD lung samples also identified Egr1, a transcription factor that is strongly upregulated by acrolein in lung cell lines (Section 3.2 below), as a highly predictive marker of COPD [14]. As Egr1 may promote the expression of proinflammatory cytokines as well as metalloproteinase activation [15,16], acrolein may facilitate COPD pathogenesis by driving the expression of this proinflammatory transcription factor.

1.3.2. Tobacco-related lung cancer

Lung cancer in smokers is insidious since it typically develops over a period of years, partly driven by the accrual of mutations within critical growth regulatory genes [17]. Countless careers within the toxicology and cancer research communities have been devoted to clarifying the pathways of metabolic activation, detoxication, and DNA adduction by classic tobacco-borne carcinogens such as polycyclic aromatic hydrocarbons, nitrosamines, and aromatic amines. While the combustion of a cigarette typically releases just nanogram quantities of these carcinogens, the cumulative doses received over a 40-year period by a pack-a-day smoker (i.e., ~290,000 cigarettes in total) resemble those inducing tumors in rodents [12,18]. However long-standing assumptions concerning the tobacco smoke constituents of greatest toxicological significance are challenged by recent suggestions that acrolein strongly contributes to lung tumorigenesis in smokers [19]. Compared to "classic" tobacco carcinogens that require CYP-catalyzed bioactivation to form DNA adducts, acrolein is a direct-acting genotoxicant that is present in smoke at 1000–10,000-fold greater concentrations. Its potential role in tobacco-related lung cancer is explored further in Section 3.4.

1.3.3. Smoke inhalation injury

Despite significant advances in burns management, the pathological effects of inhaled smoke remain significant contributors to morbidity and mortality among fire victims [20]. As the port of entry, the lung is particularly vulnerable to life-threatening pulmonary edema upon inhalation of large doses of smoke [20,21]. The clinical prognosis after SII is often poor, with mortality rates of 45–78% reported in some studies [20–22]. Respiratory failure in such patients can involve a latency of 24–72 h followed by severe bronchorrhea, bronchospasm, breathing abnormalities, and retrograde alveolar flooding [20–22]. The pathobiology of pulmonary edema in acute lung injury involves loss of vascular and epithelial permeability as well as disruption of ion and fluid transporters that normally maintain "dry"

alveolar airspaces [23,24]. Production of proinflammatory cytokines also accompanies the acute phase of SII [25].

The data implicating acrolein as a mediator of pulmonary edema in SII is long-standing, including early canine work by Zikria *et al.* which compared the edematogenic potential of smoke produced from different combustible materials [26]. Acrolein levels in smoke from burning cotton waste and wood were over 50-fold higher than in smoke formed during kerosene combustion [26]. In clear contrast to animals exposed to the two high-yielding smoke types, no fatalities or edema occurred in dogs exposed to kerosene-derived smoke [26]. Later, using anesthetized sheep, Hales *et al.* performed some compelling studies with synthetic smoke containing different reactive smoke constituents that incriminated acrolein as the primary edematogenic constituent [27–29]. Despite these long-standing observations, existing SII therapies remain poorly directed against the role of toxic smoke constituents such as acrolein.

1.3.4. Cyclophosphamide-induced lung injury

In a minority of patients the anticancer drug cyclophosphamide can induce pulmonary toxicity that involves endothelial swelling, intra-alveolar exudation, interstitial inflammation, pulmonary fibrosis, and fibroblast proliferation [30]. As a major CYP-derived metabolite of cyclophosphamide, a role for acrolein in the pulmonary pathology is suggested by long-standing animal studies [31].

2. Chemical Toxicology of Acrolein

2.1. Chemical properties

The toxicity of acrolein toward lung tissues reflects its strong reactivity with electron-dense centers in target macromolecules. In chemical terms, acrolein is a type-2 alkene, possessing a polarizable alkene (–C=C–) bond in close proximity to an electron-withdrawing carbonyl group. π-Electron mobility within this conjugated system creates a strong electron deficiency at the terminal β-carbon [32]. According to the Hard–Soft theory used to explain the interaction of reactive intermediates with their cellular targets [33], acrolein is a "soft" electrophile that reacts preferentially with "soft" nucleophilic centers. With large atomic radii and polarizable valence electrons, sulfur (S) atoms are the softest nucleophiles within cells and tissues [32]. In recent studies of the reactivity of various α,β–unsaturated carbonyl compounds with model S-containing nucleophiles, a strong correlation was observed between the electrophilic index (ω) and functional deficits elicited by the carbonyl compounds in a synaptosomal bioassay system [34]. Acrolein

was more reactive with soft nucleophiles than other type-2 alkenes such as 4-hydroxynonenal, methyl vinyl ketone, or acrylamide [34]. As the major low-mass S-containing cellular nucleophile, glutathione is a key biological target for acrolein, generating *S*-glutathionyl conjugates that undergo subsequent renal proteolysis and N-acetylation to urinary mercapturates [1]. Since these conjugates undergo spontaneous β-elimination reactions to release acrolein they are proposed to function as "toxic transporters," circulating from the port of entry to induce damage at distal sites [35].

2.2. Chemistry of protein damage

Acrolein displays striking chemical diversity during reactions with proteins (Figure 2). The following discussion will highlight that more work is needed to determine which of the multiple protein adducts formed by acrolein *in vitro* contribute to its pathological effects within the intact lung.

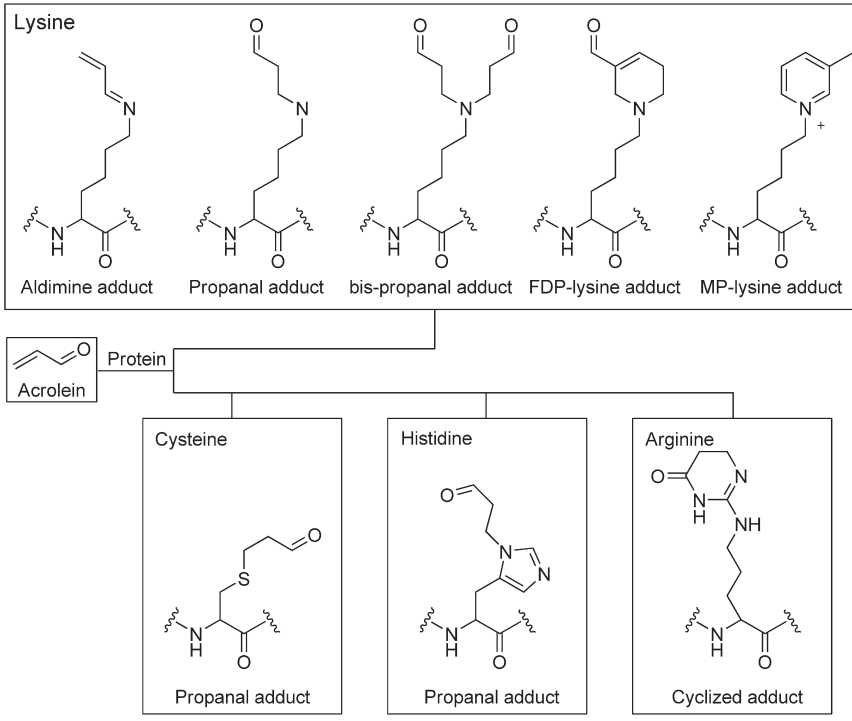

Figure 2 Protein modification by acrolein potentially generates a diversity of adducts at lysine residues as well as species at cysteine, histidine, and arginine residues. The *in vivo* significance of individual adducts awaits confirmation via definitive assay methods. See text for details.

2.2.1. Cysteine

Due to its favored reactivity with S-containing nucleophiles, acrolein readily forms cysteine adducts during Michael addition reactions with proteins [36–38]. Adduction of accessible cysteine residues on such diverse cellular targets as transcription factors (e.g., NF-κB), ion channels (e.g., TRPA1), and caspases likely underlie many of the cellular effects of acrolein [39–41]. To date, quantitative information concerning the levels of cysteine adducts in lung proteins from acrolein-exposed animals or humans is lacking. Nonetheless, since Michael adducts at cysteine are readily derivatized with the carbonyl-modifying reagent 2,4-dinitrophenyl hydrazine, it is likely that cysteine–acrolein adducts are main species detected during Western blotting with anti-DNP serum in acrolein-exposed lung cells [42]. However, the lack of specificity of this approach ensures Michael adducts at histidine and lysine groups are also detected during these assays.

One factor complicating detection of cysteine–acrolein adducts within tissues is their likely instability. In A549 lung cells allowed to "recover" from a brief (30 min) exposure to acrolein, carbonylated adducts decline quickly over 2–3 h, with neither proteasomal nor lysosomal inhibitors slowing the loss [42]. Several mechanisms might underlie such protein decarbonylation, including retrograde Michael addition reactions as well as adduct consumption during cross-linking reactions. Recent studies of the fate of acrolein adducts in a model peptide (insulin) revealed that Michael adducts at cysteine underwent rapid secondary reactions to form Schiff adducts, with mass spectrometry (MS)/MS analysis localizing these species to the N-terminus of modified peptides [37]. Prior blocking of the N-terminus increased the stability of cysteine adducts by impeding Schiff adduction of the terminal nitrogen [37]. Minimal Schiff adduction occurred on peptides that did not contain cysteine residues [37]. The authors concluded that proteins containing cysteine near the N-terminal domain might be especially prone to adduct migration, a possibility that was confirmed using two model proteins [37]. While such reactions have yet to be confirmed within biological settings, the possibility that cysteine adducts formed by acrolein undergo secondary reactions complicates the study of protein modification by this substance, and further explains the paucity of quantitative data concerning the levels of acrolein–cysteine adducts within animal or human lung.

2.2.2. Lysine

The chemistry of lysine modification, while well studied *in vitro* (Figure 2), is also subject to uncertainty concerning which of the known adducts are of *in vivo* relevance. MS of products formed during reactions between acrolein and N^{α}-blocked lysine or model peptides have confirmed expected Michael adduction on the ε-NH_2 group (propanal) as well as a bis-Michael adducted

species involving the same nucleophile [43,44]. Minor Schiff base formation (aldimine) also occurred on lysine side chains and the terminal-NH_2 of model peptides [44]. While mono- and bis-Michael-adducted species predominate in the early stages of peptide modification by acrolein, an additional heterocyclic species also forms, N^{ε}-(3-formyl-3,4-dehydropiperidino)lysine (FDP-lysine, Figure 1), with an analogous adduct also detected on the N-terminus [44]. These cyclic adducts form via condensation of bis-Michael adducted species [43]. FDP-lysine reacts rapidly with glutathione [45], raising the possibility it reacts with protein nucleophiles to form cross-links, although acyclic Michael adducts are also likely mediators of protein cross-linking [42,46]. Another cyclic species, N^{ε}-(3-methylpyridinium)lysine (MP-lysine, Figure 2) forms via sequential Michael and Schiff adduction of a single peptidyl lysine by two acrolein molecules [47,48].

Whether acrolein–lysine adducts form *in vivo* has been explored using antibodies that recognize cyclic lysine adducts, with several studies reporting the formation of modified proteins in the affected tissues of several degenerative diseases [49]. Recently, a rabbit polyclonal antibody against acrolein–lysine adducts was used to detect damaged proteins in the lungs of mice after 5 h exposure to tobacco smoke or acrolein [50]. Acrolein increased the adduction intensity of several proteins (~75, 130, 150, and 250 kDa) in the lungs of exposed animals, with modified proteins also detected in plasma and peripheral tissues [50]. Future identification of the pulmonary targets may provide useful insights into the pathogenetic mechanisms underlying acrolein pneumotoxicity.

Despite these promising observations, quantitative data obtained using structurally definitive analytical methods is lacking in relation to tissue levels of any known acrolein–lysine adduct [43,45,47]. The absence of analytical confirmation of the presence of cyclic acrolein–lysine adducts within biological samples is problematic, given that antibodies raised against acrolein-adducted lysine groups may also detect acyclic species [51]. The advent of specific analytical methods permitting quantification of the multiple acrolein-derived lysine adducts within biological samples would provide important validation of adduction chemistry that to date has been described under test tube conditions or surmised on the basis of immunochemical data.

2.2.3. Other amino acid targets

Recent work using purified actin as a model protein target as well as high molar ratios of acrolein established that modification of several histidine residues (His^{40}, His^{87}, and His^{173}) only occurred after saturation of adduction of the most susceptible residue, Cys^{374} [52]. A role for either Michael- or Schiff-type histidinyl adducts in the formation of cross-linked oligomers was also demonstrated using the β–chain of insulin as a model target [46].

In the main however, the chemistry of histidine modification by acrolein is poorly characterized.

The most basic of all amino acid side chains ($pK_a = 12.48$), the guanidino group of arginine is fully protonated at physiological pH, a factor that is thought to preclude modification by soft electrophiles such as acrolein. During our recent MS studies of peptide modification by acrolein, no adducts were detected on arginine residues under exposure conditions that caused extensive adduction of lysine and N-terminal amines [44]. Surprisingly however, in recent work that explored the distribution of adducts within the p50 subunit of NF-κB, a known target for acrolein, use of MALDI-TOF MS identified novel cyclic adducts on two arginine residues, Arg^{230} and Arg^{307} (Figure 2) [53]. This suggests that local sequence context or other factors may create zones of increased pH within protein microenvironments that enhance the reactivity of specific arginine side chains, an intriguing reminder of the difficulties accompanying extrapolation from simple experimental systems comprising model amino acids or peptides to intact proteins within the tissue setting.

Collectively, acrolein is an efficient electrophile that attacks multiple residues within susceptible proteins, and while cysteine groups are preferred targets on kinetic grounds, the instability of these species may ensure that adduction events at other residues (e.g., lys, his, and arg) may be of comparable toxicological relevance. At present, there is a dearth of qualitative or quantitative information concerning protein adduction within the epithelium or parenchyma of respiratory tissues during either chronic or acute exposure to acrolein. A solid understanding of acrolein toxicity in the lung would thus require knowledge of intraorgan protein adduct distribution under different exposure conditions. To reiterate, development of sensitive assays for the various species of protein adducts formed by acrolein would facilitate achievement of these goals.

2.3. Chemistry of DNA damage by acrolein

Since none of the nucleophiles present in DNA are sufficiently "soft" to allow reactions at rates matching those occurring at cysteine, protein adduction is expected to predominate under conditions of low acrolein exposure, while DNA adducts seem more likely to form at higher levels of exposure. Such assumptions are speculative, however, since no studies have compared dose–response relationships for DNA adduction versus protein modification in acrolein-exposed lung.

Acrolein can react with all four nucleobases within DNA [54–56]. Guanine, the most nucleophilic DNA base, is the major target, undergoing conversion to two hydroxy-1,N^2-propanodeoxyguanosine adducts, hereafter designated α- and γ-OH-Acr-dGua [57,58] (Figure 3).

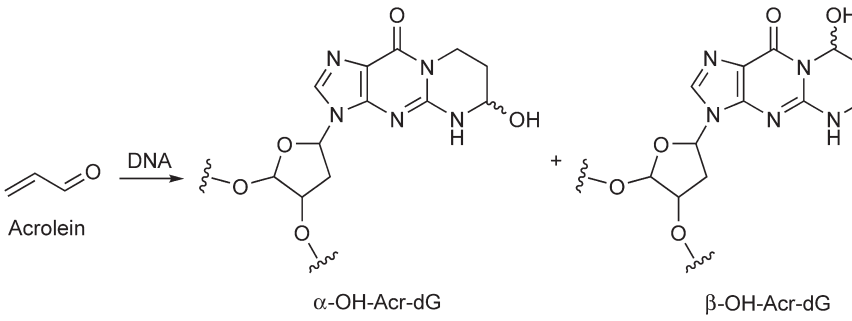

Figure 3 Acrolein attacks guanine bases in DNA to form two isomeric species, both of which have been detected in human tissues. See text for details.

Given the long-standing interest in using DNA adducts as markers of exposure to genotoxic carcinogens, some progress has been made in the quantitation of acrolein-derived DNA adducts in respiratory tissues using either ^{32}P-postlabeling or MS-based techniques. Due to the low levels of DNA adducts in the human genome, such approaches are typically combined with adduct enrichment steps. These sensitive procedures require scrupulous attention to protocol, witnessed by the recent finding that low levels of acrolein in water used to prepare sample buffers may influence baseline levels of acrolein–guanine adducts in DNA [59].

In work conducted by Chung and associates using the ^{32}P-postlabeling-assay, comparatively high levels of γ-OH-Acr-dGua were detected in DNA from the lungs of control rats that had not been deliberately exposed to acrolein [60]. Levels of the α-isomer were below assay detection limits. The same group also used this approach to explore the effects of smoking on adduct levels in humans [61]. Consistent with the presence of acrolein in tobacco smoke, γ-OH-Acr-dGua levels were elevated threefold in DNA collected from the oral cavities of a small sample of tobacco smokers ($N = 11$) relative to nonsmokers ($N = 12$, adduct levels were 1.36 ± 0.9 in the former vs. $0.46 \pm 0.26\,\mu\text{mol}\,\text{mol}^{-1}$ guanine in the latter group, $p = 0.003$) [61].

Newer MS-based methods allow more precise estimation of DNA adducts within biological samples [62]. In the sole definitive study of acrolein-derived macromolecular adducts in human lung, Hecht and associates used liquid chromatography–electrospray ionization tandem MS to measure both α- and γ-OH-Acr-dGua in lung biopsies from smokers and ex-smokers [63]. The two adducts were detected at comparable concentrations in all samples [63]. Moreover, no differences in adduct levels were evident between smokers and ex-smokers, nor did adduct levels correlate with urinary nicotine or cotinine levels, two common markers of tobacco usage [63]. These observations are puzzling given the known

decline in urinary acrolein metabolites on smoking cessation [64]. The inability to observe an effect of smoking cessation on pulmonary DNA adduct levels may partly reflect limited knowledge of DNA adduct distributions within human lung or the repair kinetics for these lesions. The impact of alternative environmental and endogenous acrolein sources on pulmonary DNA adduct levels is also unknown. Clarifying such issues is clearly crucial to the ongoing debate concerning the role of acrolein in smoking-related lung cancer (see below). But work is also needed to clarify the extent and significance of DNA adduction during exposure to acrolein under conditions other than those associated with chronic tobacco smoking, such as SII (Figure 1).

2.4. Macromolecular cross-links

As a bifunctional electrophile, initial reactions of acrolein with protein or DNA generate a Michael adduct that may participate in secondary reactions with neighboring nucleophiles to form cross-linked species (Figure 4). The formation of inter- and intrastrand DNA–DNA, protein–DNA, and protein–protein cross-links can all accompany exposure of respective

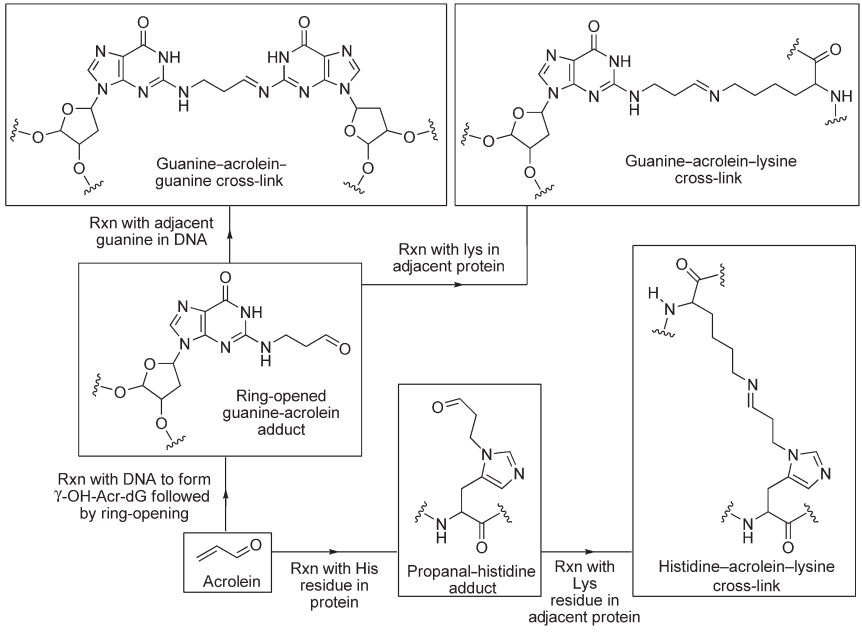

Figure 4 As a bifunctional electrophile, acrolein-adducted cell macromolecules can react further to form DNA–DNA, DNA–protein, or protein–protein cross-links. See text for details.

biomolecules to acrolein, although cross-linked species involving guanine adducts are best characterized in terms of their chemical and biological properties [58].

Given the "crowded" nature of the cytosolic compartment acrolein is likely to elicit extensive protein cross-linking within this subcellular environment, but to date the chemistry of this process is poorly characterized. A species likely formed via reaction of Michael-adducted histidine adducts with the ε-NH_2 group of lysine was recently identified as a contributor to protein–protein cross-linking within a model experimental system [46]. Recent work in our laboratory established that acrolein readily generates intramolecular protein–protein cross-links involving two common targets for electrophiles, heat shock protein-90 (hsp90) and the intermediate filament (IF) vimentin (see below) [42,65]. Although the formation of protein aggregates was potentially inhibited by cytoprotective electrophile scavengers, the relevance of protein–protein cross-linking to the *in vivo* pulmonary toxicity of acrolein is unknown.

3. Cellular Toxicology of Acrolein

3.1. Protein targets

Identifying proteins that incur adduction during the biotransformation of xenobiotics to reactive intermediates is a key objective in modern toxicological research, driven largely by the expectation that such knowledge can clarify the cellular pathways that are disrupted during the onset of any organ-directed pathology [66]. As a reactive electrophile, acrolein attacks numerous cell proteins, but to date the identities of those sustaining damage in the lung during inhalational exposure to acrolein or smoke are poorly defined. As highlighted above, in one of the few efforts to characterize protein damage during pulmonary acrolein exposure, Conklin and associates established that a handful of lung proteins in mice sustained modification during a 5 h inhalational exposure to 5 ppm airborne acrolein [50]. Since these researchers were primarily assessing the cardiovascular impact of inhalational acrolein exposure, neither the protein identities nor the extent of lung injury accompanying acrolein exposure was established.

3.1.1. NF-κB pathway

In contrast to the lack of information concerning *in vivo* pulmonary targets, a number of damaged proteins have been identified in acrolein-exposed lung cells. During a study of its effect on inflammatory processes in immortalized human bronchial epithelial (HBE-1) cells, Valacchi and

associates found that, in keeping with prior observations with other reactive carbonyls, acrolein suppressed the activation of NF-κB signaling by the proinflammatory cytokine TNFα [67]. Activated in response to numerous noxious stimuli, the transcription factor NF-κB drives the production of inflammatory cytokines in pulmonary epithelial cells. The most common form of NF-κB exists as a heterodimer between p50 and p65, with this complex mainly localized in cytoplasm in association with I-κB (the binding of which masks nuclear localization sequences within p65). During exposure to proinflammatory stimuli, I-κB undergoes phosphorylation, ubiquitination, and proteolytic degradation, allowing NF-κB migration to the nucleus where it interacts with κB motifs in target genes [68]. One such gene is the proinflammatory cytokine interleukin-8 (IL-8), a powerful chemoattractant for neutrophils and other immune cells [69]. In HBE-1 cells, a 30 min exposure to acrolein prior to challenge with TNFα reduced cellular IL-8 secretion over the following 24 h while also suppressing IL-8 gene transcripts [67]. Use of an electrophoretic mobility shift assay revealed that acrolein inhibited TNFα-induced relocation of NF-κB to nuclear extracts, an effect that was accompanied by increased cellular levels of its binding partner, I-κBα [67]. The mechanism underlying these effects appeared to involve acrolein adduction on IKKβ, the kinase that regulates the phosphorylation state and cellular persistence of the NF-κB/I-κB complex [67]. This finding is intriguing given the susceptibility of p50 to acrolein adduction discussed in Section 2.2.3 [53]. Since other thiol-reactive electrophiles are known to modulate IKKβ activity via reactions with an active site cysteine in the activation loop [70], these findings highlight a mechanism whereby the reactivity of acrolein disrupts a fundamental biological process (immune signaling) via actions at specific cell targets. While these conclusions are broadly consistent with findings in other laboratories concerning disruption of NF-κB signaling during acrolein exposure in cells of pulmonary origin [71,72], future work is needed to confirm the *in vivo* relevance of these observations.

3.1.2. Intermediate filaments

In recent preliminary work conducted with a view to identifying novel targets for acrolein in human lung cells, we used cellular fractionation, Western blotting, and peptide mass fingerprinting to identify several IFs as targets for acrolein in A549 lung cells [65]. Among the most susceptible family members was vimentin, an IF that participates in many cellular processes and is a known target for diverse electrophiles [65,73–75]. Other targets included various keratins, with the low abundance IF keratin-7 proving especially vulnerable to acrolein, as well as the more abundant and structurally important IF keratins-8 and -18 [65]. Damage to the most abundant keratins was accompanied by a loss of cellular adhesive strength in

A549 cell monolayers, a finding that is consistent with the mechanical functions of IF in providing tensile strength within cellular and tissue networks [76,77]. To determine whether IF sustain damage in other epithelial cells of pulmonary origin, we compared patterns of protein carbonylation in A549 cells (alveolar origin) to Calu-3 cells (bronchiolar origin) following a 60 min exposure to two concentrations of acrolein (Figure 5). The lower concentration of acrolein (25 μM) had no effect upon cell ATP levels during a 4 h incubation in either cell lines, whereas the higher concentration (150 μM) diminished cell ATP in a manner consistent with the onset of overt cell death (Figure 5A and B). While expression of the two most vulnerable IF seemed to differ between the two cell lines (relative to A549 cells vimentin was less abundant in Calu-3 cells while keratin-7 was more abundant), the extent of adduction at these two targets was consistent with its level of expression in the respective cell types (Figure 5C and D). Given that IF appear to be reliable targets for acrolein in epithelial cells originating from different zones of the respiratory tract, future work is needed to determine whether these proteins sustain damage in intact lung during *in vivo* exposure to acrolein.

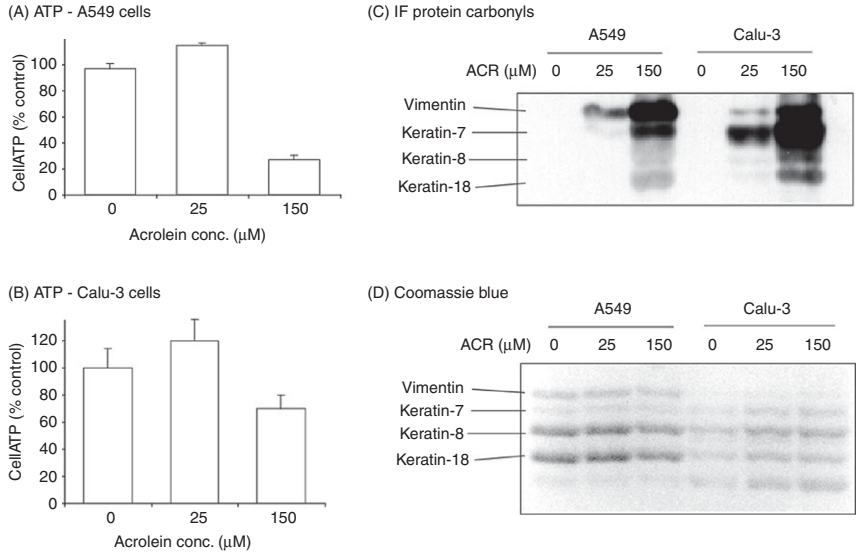

Figure 5 The intermediate filaments vimentin and keratin-7 are targets for acrolein in lung cells of alveolar (A549) and bronchiolar (Calu-3) origin. ATP measurements were made after a 4 h exposure to acrolein (panels A and B) while protein carbonyls were determined following a 30 min exposure (panels C and D). See [65] for a description of the relevant experimental methods.

3.2. Transcriptional responses to acrolein

3.2.1. ARE genes

Cells typically up- and downregulate gene clusters in response to noxious chemicals, with analysis of the affected pathways providing predictive insights into the toxicological effects that might accompany exposure to the substance [78–80]. Interest in the transcriptional responses of cells to acrolein has typically focused on members of the classic antioxidant response element (ARE) locus. This key adaptive pathway is controlled by nuclear factor-erythroid 2-related factor 2 (Nrf2), a cap 'n' collar (CNC) basic-region leucine zipper (bZIP) transcription factor that normally interacts with the intracellular redox sensor KEAP1 [81]. Under regular conditions, Nrf2 transcriptional activity is suppressed due to cytosolic sequestration by actin-associated KEAP1, but exposure to oxidants and electrophiles causes Nrf2 release and its migration to the nucleus, promoting the expression of up to 100 cytoprotective genes that contain ARE sequences in their promoters [81,82]. The mechanisms underlying the loss of KEAP1-mediated restraint on Nrf2 activity on exposure to electrophiles is subject to debate [83]. Acrolein is an especially effective Nrf2 inducer in lung cells, strongly activating hallmark ARE genes such as heme oxygenase-1 (HO-1), NAD(P)H: quinone oxidoreductase-1 (NQO1), glutathione-*S*-transferase (various isoforms), and glutamate-cysteine synthetase (GCS) [83]. Recent findings in HBE1 cells suggest a role for various kinases in acrolein-induced induction of a range of Nrf2-driven genes, including mitogen-activated protein (MAP)- and PI3-kinase family members [84]. In general, increased expression of Nrf2-driven ARE genes is likely to "blunt" the toxic consequences accompanying repeated acrolein exposure.

3.2.2. Mucin-related genes

The role of transcriptional responses in mediating the deleterious effects of inhaled acrolein is also of interest. More needs to be done in this regard, but a useful line of recent research has explored the role of transcriptional events in the mucous hypersecretion that occurs in the airways of animals upon inhalational exposure to acrolein [85]. Mucus is rich in highly glycosylated mucin proteins produced by goblet cells lining secretory ducts in the large airways. Mucins protect the epithelium against damage by infectious particles and noxious airborne substances, but excess production is deleterious in diseases such as COPD. Although several mucin genes are present in the human genome, mucin 5, subtypes A and C (MUC5AC) appear most important in human airway secretions. MUC5AC is upregulated by noxious substances including acrolein, with strong induction seen in the lungs of mice after a 4-week exposure to 2 ppm airborne acrolein (6 h per day, 5 days a week) [86]. Low concentrations of acrolein also upregulated MUC5AC mRNA transcripts in NCI-H292 human lung epithelial cells [87].

MUC5AC upregulation was highly sensitive to acrolein, occurring at concentrations two- to threefold orders of magnitude lower than those that depleted cellular glutathione [87]. MUC5AC upregulation by acrolein proceeds via a multistep process involving activation of the mitogen-activated protein kinase (MAPK) pathway by epidermal growth factor receptor (EGFR) ligands formed via the activity of various matrix metalloproteinases including ADAM17, MMP-9, MMP-12, and MMP-14 [88]. This pathway was confirmed using MAPK inhibitors (e.g., PD98059) and anti-EGF receptor antibodies to suppress acrolein-induced MUC5AC upregulation in cultured cells [87]. Since MAPK activation underlies other cellular responses to acrolein, this pathway will be explored further in Section 3.3 below.

3.2.3. Egr family genes

Transcriptional responses to higher concentrations of acrolein during the onset of cell death might differ from those eliciting mucus hypersecretion at lower concentrations. To explore this issue we used microarrays to study mRNA profiles in A549 human lung cells after 1, 2, or 4 h exposures to a concentration of acrolein that elicited apoptotic changes during a 24 h incubation (cytochrome *c* release and DNA fragmentation) but did not induce the overt necrosis characteristic of short-term exposure to high concentrations of acrolein (e.g., a reduction in cell ATP) [89]. In keeping with its pronounced chemical reactivity, acrolein altered transcript levels for hundreds of genes [89]. Consistent with transcriptional responses to other strong stressors, the initial cellular response was to downregulate large numbers of genes, with the mRNA levels for 478 genes diminished by twofold or more after 1 h (Figure 1B). This "knee-jerk" reaction was offset by a rapid recovery in transcript levels so that after 2 h just 172 genes were downregulated relative to control [89]. This rapid recovery could reflect DNA repair within damaged promoters to restore transcription of attenuated genes, or alternatively, spontaneous reversal of Michael adduction of transcription factors involved in controlling the expression of target genes. After 4 h, gene upregulation had come to dominate the transcriptional response, with 286 transcripts increased over controls (58.1% of total).

Transcripts upregulated by acrolein belonged to numerous biological pathways including genes involved in apoptosis, cell cycle control, antioxidant and heat shock responses, cytoskeletal maintenance, and, for the category containing the largest number of affected genes, transcription [89]. The most strongly induced genes included members of the early growth response family, known to encode a homologous class of DNA-binding proteins belonging to the zinc finger class of transcription factors. The mRNA transcript for the best characterized member of this family, Egr1, was strongly upregulated in a time-dependent manner in A549 cells during acrolein exposure, an effect that was shown by microarray and

RT-PCR analysis (Figure 6). These findings concur with the upregulation of Egr1 in A549 cells during exposure to cigarette smoke [90]. Egr1 is activated by the leucine-zipper transcription factor c-fos, the transcript of which was upregulated by acrolein in a concentration-dependent manner (Figure 6). Acrolein also induced strong but transient upregulation of c-Fos expression prior to the increase in Egr1 protein levels (Figure 6). cFos

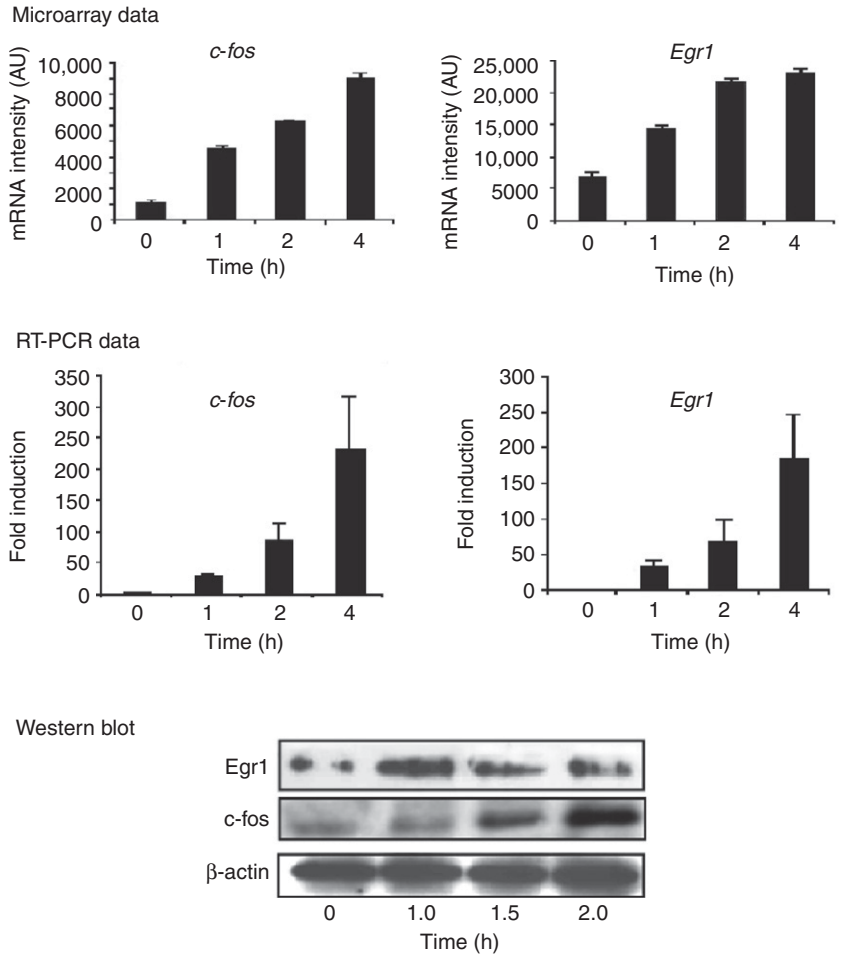

Figure 6 Acrolein elicits strong upregulation of Egr1 and c-fos at both the mRNA and protein levels in A549 lung cells. mRNA levels were measured via microarray analysis (upper panel) or RT-PCR (middle panel) following exposure to 100 μM acrolein for the times indicated in the figure legends. Each data point represents the mean ± SE of four independent determinations. The lower panel depicts immunoblots obtained via Western blotting using antibodies against Egr1, c-fos and the loading control β-actin (25 μg protein/lane). See [89] for details concerning experimental protocols.

activation by acrolein is likely mediated by the classic extracellular MAPK, ERK-1/2, a topic that is explored in Section 3.3.

The fact that Egr1 is upregulated by a range of stimuli including various stresses (e.g., UV irradiation) and physiological stimuli (e.g., hormones, growth factors) while also participating in diverse biological phenomena such as cell growth, differentiation, and mitogenesis, complicates clarification of the significance of any pulmonary Egr1 upregulation elicited by acrolein. Based on *in vitro* studies, a number of Egr1-dependent pathways of toxicological significance seem plausible. One possibility is that Egr1 upregulation drives the activation of matrix metalloproteinases (e.g., MMP-2) that promote activation of the MAPK pathway [91]. Another possibility is that acrolein augments the role of Egr1 in controlling the expression of repressors that regulate the expression of tight-junction proteins (e.g., claudins and cadherins) [92].

Insight into the potential number of Egr1-regulable genes was supplied during recent use of chromatin immunoprecipitation and tiled promoter arrays to identify several thousand Egr1-binding sites in the genome of phorbol ester-stimulated THP-1 monocytes [93]. The most common Egr1-binding sites colocalized with histone acetylation sites within GC-rich consensus sequences located near the transcription start sites of constitutively active promoters [93]. Many of these genes were involved in transcription and translation cascades, indicating that during monocyte differentiation at least, Egr1 is a key initiator of information transmission. Intriguingly, comparison of the findings of Kobosaki *et al.* with results obtained during study of UV irradiation-induced patterns of Egr1 binding to DNA in human prostate M12 cells revealed comparatively few overlapping genes, most of which were involved in regulating transcription and nucleic acid functions [93,94]. These findings indicate that the transcriptional program accompanying Egr1 activation varies among cell types and according to the specific stimuli. Such conclusions highlight the need for careful analysis of acrolein-induced patterns of Egr1 binding to gene targets in human lung cells.

3.3. Molecular effects of acrolein

Knowledge of cellular signaling and cell death pathways that are disrupted by α,β-unsaturated aldehydes and other electrophilic species has greatly expanded in recent decades [68]. As a promiscuous electrophile, acrolein disrupts multiple signaling pathways, but those demonstrated within models relevant to the pulmonary setting will receive most attention here.

3.3.1. MAPK signaling

As with cellular responses to other toxic stresses, acrolein activates one or more of the three main MAPK pathways, namely, the extracellular

signal-regulated kinase (ERK), c-Jun NH2-terminal kinase (JNK), or the p38 kinase cascades. Activation of these stress-activated pathways commonly signals a shift to a proapoptotic environment, but within the lung can accompany a chronic proinflammatory state [95]. Each of these pathways conforms to the common pattern of a MAPK kinase kinase (MAPKKK) activating a MAPK kinase (MAPKK) which activates a MAPK pathway that is variously linked to downstream targets that include various phosphorylation-dependent transcription factors. Phosphorylation of the latter typically boosts transcription of various immediate-early genes. In Chinese hamster ovary cells, acrolein was recently shown to activate both the ERK and p38 MAPK pathways, events that accompanied the induction of apoptosis [96]. However, the relevance of these findings to lung cells is uncertain given that p38 and ERK inhibitors did not block the induction of classic Nrf2-driven genes in HBE-1 cells [84].

While p38 and ERK MAPK pathways may not participate in Nrf2-mediated responses to acrolein in lung cells, these pathways may participate in the chronic pulmonary inflammation that occurs in smokers who are exposed to acrolein over an extended timeframe [97]. As highlighted in Section 1.3.2, COPD is a debilitating respiratory disease that most commonly afflicts smokers. Central to COPD pathogenesis is an inflammatory cascade involving production of cytokines and chemokines that recruit neutrophils and macrophages to the respiratory tract [12]. The barrage of free radical oxidants released upon activation of these immune cells progressively damages the respiratory epithelium and adjacent microvasculature. The powerful chemoattractants IL-8 and TNFα appear to be especially important in initiating and maintaining a chronic inflammatory state during COPD [12].

A role for acrolein in COPD emerged during studies of the stimulatory effects of cigarette smoke extracts on the production of IL-8 and TNFα by model human macrophages [98]. Not only were the IL-8-releasing effects of smoke extracts in macrophages reproducible with equivalent concentrations of acrolein, but prior bubbling with nitrogen gas (which reduced aldehyde contents of the extracts by 70%) produced corresponding reductions in cytokine release from the cells [98]. Likewise, coexposure of the macrophages to carbonyl-trapping reagents but not antioxidants blunted the IL-8 release elicited by cigarette smoke extracts [98]. These findings were recently extended by exploring the role of MAPK in smoke-induced IL-8 production in lung fibroblasts and small airway epithelial cells [97]. In both cell types, cigarette smoke extracts and equivalent concentrations of acrolein elicited IL-8 release that was attenuated by the acrolein scavenger MESNA. In lung fibroblasts the IL-8 upregulation was accompanied by phosphorylation of both ERK1/2 and p38. Moreover, inhibitors of the upstream signaling protein MEK kinase (MAP kinase kinase) and ERK1/2 itself inhibited smoke-induced ERK1/2 phosphorylation and IL-8 release

[97]. While awaiting confirmation within the whole animal setting, these observations implicate acrolein and MAPK pathways as key mediators of the neutrophilia and pulmonary inflammation that plague long-term tobacco smokers.

The precise mechanisms underlying MAPK activation during the progression to a proinflammatory state in smokers are unknown. Ideally, a suitable explanation of the effects of acrolein on MAPK pathways should include demonstrable chemical reactivity with member proteins in this pathway. One possibility could be that acrolein directly modifies MAPK kinases, triggering conformational changes that promote phosphorylation of substrate proteins. Although a precedent for such an mechanism exists for other α,β-unsaturated aldehydes [99], literature support is weak for this mechanism as a general pathway of kinase activation by electrophiles. More feasibly, acrolein might attack critical cysteine residues in phosphatases that regulate MAPKs, a mechanism that is consistent with the vulnerability of MAP kinase phosphatases to thiol oxidants [100]. The finding that acrolein attacks a critical catalytic cysteine on a key protein tyrosine phosphatase, PTP1B, further supports this mechanism [101].

3.3.2. IL-8 synthesis—up- or downregulated by acrolein?

The previously discussed findings concerning upregulation of IL-8 production by acrolein appear contradictory in light of the data discussed in Section 3.1 regarding its inhibitory effects on NF-κB-driven IL-8 expression in bronchiolar epithelial cells [67]. Such reports suggest acrolein may exert opposing actions on IL-8 production; an inhibitory effect involving attenuation of the NF-κB pathway, and a stimulatory action involving activated MAPKs. Perhaps differences in experimental design between the model systems used in these respective studies are relevant to this paradox since the various laboratories used dissimilar culture media conditions that are likely to influence experimental outcomes. In recent work, we found that the presence of nucleophilic acrolein-scavenging constituents such as cysteine or fetal bovine serum (FBS) strongly influenced the transcriptional responses of A549 lung cells to acrolein [102]. Thus ~10-fold higher concentrations of acrolein were needed to upregulate the Nrf2-driven HO-1 gene when cells were intoxicated in the presence of nucleophilic media constituents compared to when cells were maintained in nucleophile-free buffered saline [102]. It thus seems significant that the *in vitro* models used to demonstrate MAPK-mediated upregulation of IL-8 expression by acrolein used cysteine-containing RPMI 1640 media supplemented with 10% FBS, an experimental condition that likely caused extensive scavenging of extracellular acrolein [97,98]. In contrast, the inhibitory effect of acrolein on TNFα-activated, NF-κB-driven synthesis of IL-8 in bronchial epithelial cells was seen in a nucleophile-free exposure

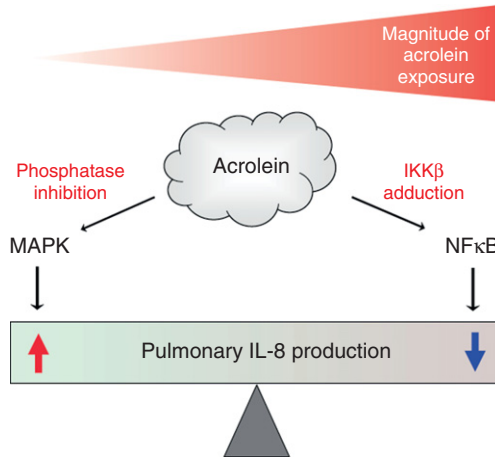

Figure 7 The effect of acrolein on pulmonary production of the proinflammatory chemokine IL-8 is likely a balance of its effect on two opposing pathways. The magnitude of acrolein exposure is a likely determinant of the overall response. See text for details.

medium (Hank's balanced salt solution) which likely allowed much higher intracellular concentrations [67]. The apparently contradictory effects on IL-8 production could thus be reconciled by the likelihood that a MAPK-driven upregulation of IL-8 production predominates under conditions of low acrolein exposure, while at higher levels of exposure, adduction of proteins that regulate NF-κB transcriptional activity effectively inhibit IL-8 release. At any given level of exposure, overall IL-8 production will reflect the net effect of acrolein on these opposing pathways (Figure 7). Once again, these conclusions must be tested in relevant *in vivo* systems that allow clarification of the dose dependence of the effects of acrolein on cytokine production within the lung.

3.4. Mutagenicity of acrolein

The toxicological significance of the DNA damage that is inflicted by acrolein within the lung has generated significant recent controversy within the context of smoking-related human lung cancer [19]. Acrolein is long known to induce base-pair substitution mutations in both bacterial and mammalian cell lines [103–106]. Upon sequence analysis of acrolein-induced mutations in a shuttle vector-based system, mutations mainly occurred at guanine residues, consistent with the tendency of acrolein to target guanine during reactions with DNA to form cyclic α- and γ-OH-Acr-dGua lesions (Figure 3 and Section 2.3 above). While γ-OH-Acr-dG

appears more abundant within the genome of acrolein-exposed cells, molecular studies on the mutagenicity of this lesion during replication in mammalian cells suggests this adduct has less miscoding potential than α-OH-Acr-dG [107]. A number of *in vitro* studies have reported a low incidence of mutational events during translesional bypass of γ-OH-Acr-dG-containing DNA templates [108,109].

Controversy concerning the status of acrolein as a mediator of lung cancer in tobacco smokers arose upon publication of a paper by Feng *et al.* in 2006 [2,19]. These researchers presented data showing a strong similarity between the patterns of DNA damage within a crucial mutational target (the p53 tumor suppressor gene) induced by acrolein and the spectrum of p53 mutations found in lung cancer in smokers [19]. The researchers also noted that acrolein reduced the cellular capacity to repair DNA adducts generated by a major promutagenic species formed from tobacco combustion products, benzo[*a*]pyrene diol epoxide. Weighing these findings against the fact that acrolein concentrations in tobacco smoke are several orders of magnitude higher than those of benzo[*a*]pyrene, the authors suggested acrolein deserves greater attention as a mediator of cigarette smoke-related lung cancer [19].

The above report inspired a subsequent effort by Besaratinia *et al.* to characterize the mutagenicity of acrolein in Big Blue mouse embryonic murine fibroblasts [110]. This experimental system allows screening for chemically induced mutations within the chromosomally incorporated *cII* mutational target gene. As with other comparable attempts in cell-based models, the pronounced cytotoxicity of acrolein toward the embryonic fibroblasts confounded the detection of mutations, necessitating study of mutation frequencies at low acrolein concentrations [110]. Under these conditions, no significant increase in mutation frequencies over controls accompanied acrolein exposure [110]. Following this report, the workers responsible for the initial association of acrolein with p53 mutations in lung cancer conducted a renewed analysis of acrolein mutagenicity in a shuttle vector-based assay system [111]. Such models facilitate study of the genotoxicity of electrophilic chemicals by permitting direct exposure of plasmid DNA to reactive substances prior to cellular transfection. This approach allows removal of unreacted toxicants via plasmid extraction protocols and therefore minimizes direct cellular exposure to toxic compounds [112]. Using this method along with careful attention to determining adduct levels in treated plasmids, these workers found a close correlation between mutation frequencies in viral progeny and the levels of acrolein–guanine adducts [111]. These latter findings provoked a strong exchange of views between the chief investigators involved in these apparently conflicting studies [113,114]. This ongoing debate highlights that the role of acrolein in tobacco-associated pulmonary tumorigenesis is a controversial topic that challenges long-standing assumptions concerning the central roles of such

tobacco carcinogens as nitrosamines, polycyclic aromatic hydrocarbons, and aromatic amines.

3.5. Cell death pathways

As with other cellular responses to acrolein, the cell death pathways it initiates in cells of pulmonary origin have been most commonly defined *in vitro*. In cells of nonpulmonary origin, acrolein has been shown to induce both necrotic and apoptotic forms of cell death, with evidence presented to suggest the latter proceeds via both mitochondrial (intrinsic) and death-receptor-mediated (extrinsic) pathways [41,115–117]. In recent work conducted in A549 lung cells, acrolein initiated cellular changes that are characteristic of both early- and late-stage intrinsic apoptosis, including Bax relocation to the mitochondria, collapse in the mitochondrial membrane potential, cytochrome *c* release, activation of caspases-3 and -7, and redistribution of apoptosis-inducing factor-1 to the nucleus [118].

Our recent microarray study added to the complexity of acrolein-induced cell death pathways in A549 cells by identifying changes in both mitochondrial and death receptor pathways [89]. For example, acrolein strongly induced TNFSF10, an important regulator of the extrinsic apoptotic pathway [89]. We also identified the nuclear receptor Nur77 as a possible pluripotent mediator of A549 cell death by acrolein. Nur77 has analogous actions to p53, helping maintain cell survival under normal conditions while undergoing activation by proapoptotic stimuli to a potent pro-death effector that translocates to mitochondria where it interacts with Bcl-2 to elicit cytochrome *c* release [119]. Nur77 may also translocate to the endoplasmic reticulum to activate a novel nonmitochondrial pathway of intrinsic apoptosis [120]. Moreover, Nur77 can activate receptor-mediated apoptosis in some cells [121,122].

Clearly, more work is needed to define the mechanisms of lung cell death prevailing under conditions of both chronic and acute acrolein exposure within the *in vivo* setting where little is known concerning the molecular events that mediate the epithelial damage elicited by smoke-borne acrolein.

4. Respiratory Effects of Acute Inhaled Acrolein

As a potent irritant to mucosal membranes, inhalational exposure to airborne acrolein produces dose-related symptoms including nose and throat irritation, and important acute reflex responses including reduced

breathing rate, airway constriction, mucus secretion, and cough. These reflex responses are typically mediated through a variable combination of central reflex pathways and local axon-reflex pathways [123], and are evoked to limit further inhalation of the irritant and to promote its rapid removal. At present, these effects of acrolein upon pulmonary physiology are poorly integrated with a chemical description of its effects on key mediators of these processes at the molecular level.

4.1. Bronchoconstriction

Bronchoconstriction appears to be a significant component of the bronchoprotective reflex response that accompanies an acute exposure to acrolein. In animal studies, inhalational exposure to acrolein caused dose-dependent increases in pulmonary resistance in guinea pigs [124,125]. Acrolein-induced bronchoconstrictor responses were diminished by capsaicin treatment and potentiated by thiorphan pretreatment, indicative that acrolein causes an acute release of neuropeptides from bronchopulmonary C-fiber sensory nerves [125]. These earlier findings have been extended by a recent *in vitro* study demonstrating that exposure of guinea pig isolated tracheal preparations to acrolein caused a significant release of the neuropeptides substance P and CGRP, and that acrolein-induced contractions were inhibited a combination of NK_1 and NK_2 receptor antagonists [126]. Acrolein appears to initiate neuropeptide release from capsaicin-sensitive nerve endings in the lung via TRPA1 [127], an excitatory ion channel that has been proposed to function in diverse sensory processes. In summary, acrolein stimulates TRPA1 on C-fiber sensory endings to promote the local axon-reflex release of sensory neuropeptides such as tachykinins, which cause bronchoconstriction via activation of NK_1 and NK_2 receptors on airway smooth muscle cells.

4.2. Airways hyperresponsiveness

In addition to its acute bronchoconstrictor effects, acrolein exposure can induce airways hyperresponsiveness to other spasmogenic stimuli. For example, guinea pigs previously exposed to acrolein were more sensitive to the bronchoconstrictor effects of acetylcholine [124]. In this study, acrolein-induced airways hyperresponsiveness to acetylcholine was maximal between 2 and 6 h after acrolein exposure, and was dependent upon the dose of acrolein [124]. Acrolein-induced airway wall edema and mucus secretion may contribute to *in vivo* airway hyperresponsiveness to spasmogenic stimuli. *In vitro* exposure to acrolein enhanced the responsiveness of airway smooth muscle preparations from humans, ferrets, and rats to a variety of bronchoconstrictor substances, including muscarinic cholinoceptor agonists (carbachol, acetylcholine) and neuropeptides (substance

P, neurokinin A) but not KCl [128–130]. Of particular interest, acrolein potentiated the contractile response of passively sensitized human isolated bronchus to specific antigen stimulation [131]. Several mechanisms for acrolein-induced airways hyperresponsiveness have been proposed including diminution of neutral endopeptidase [129], involvement of lipoxygenase and cyclooxygenase products [130], and altered calcium signaling in airway smooth muscle [132,133]. With respect to the latter mechanism, acrolein may alter calcium signaling in airway smooth muscle by enhancing agonist-induced $InsP_3$ production and the amplitude of the first cytosolic Ca^{2+} concentration peak [132,133], although the molecular target for acrolein (e.g., G proteins, phospholipase C) is not known.

4.3. Protective COX-2-mediated counter responses

In addition to stimulating the rapid release of neuropeptides from sensory nerves, acrolein modulates the production and release of other mediators than alter bronchomotor tone, including prostaglandin E_2 (PGE_2). Acrolein elevated PGE_2 levels in numerous cell types derived from the respiratory tract, including epithelial cells [134,135], fibroblasts [136], and alveolar macrophages [137], as well as in neutrophils [138] and vascular endothelial cells [139]. Current evidence indicates that acrolein-induced increases in PGE_2 levels are the result of the combination effects of increased synthesis and decreased metabolism of PGE_2. For example, in rat lung epithelial cells, acrolein produced time and concentration-dependent increases in the expression of cyclooxygenase-2 (COX-2), a key enzyme in the synthesis of PGH_2, a PGE_2 precursor [140]. Acrolein-induced increases in COX-2 expression were dependent upon a Ca^{2+}-dependent, Ras/Raf/ERK-mediated activation of NF-κB [140]. Interestingly, the expression of microsomal prostaglandin E synthase (mPGES), which is responsible for the conversion of PGH_2 to PGE_2, was markedly increased by acrolein in human lung fibroblasts [136]. Acrolein may also decrease the metabolism of PGE_2 by inactivating NAD^+-linked 15-hydroxyprostaglandin dehydrogenase (PGDH), which enzymatically oxidizes PGE_2 to a 15-keto derivative [141].

It appears that part of the bronchoprotective response to acrolein includes stimulating the delayed expression of enzymes involved in the synthesis of PGE_2. Resultant increases in the levels of PGE_2 are likely to produce a raft of effects within the lung, including bronchodilatation and anti-inflammatory effects [142,143]. PGE_2 produces these effects primarily via activation of E prostanoid receptors, a family of four G-protein-coupled receptors called EP_1, EP_2, EP_3, and EP_4. These four major subtypes of EP receptors are widely expressed within the airways, and the various cell types within the airways have different patterns of EP receptor subtype expression. Thus, PGE_2 can exert a diverse array of biological actions within the

airways depending upon which EP receptor-mediated effects predominate. Typically, PGE_2-induced relaxation of airway smooth muscle occurs via activation of EP_2 receptors which are linked to the $G_{\alpha s}$-adenylate cyclase-cAMP-protein kinase A pathway. However, PGE_2 may also exert a bronchoconstrictor response via the activation of EP_1 receptors expressed on sensory nerves, which causes the reflex activation of parasympathetic, cholinergic nerves and contraction of airway smooth muscle [144]. Interestingly, electrophilic metabolites of PGE_2 may activate TRPA1 on sensory nerves independent of EP receptors [145]. One potential benefit of these latter effects is that the airways will have a heightened sensitivity to the possibility of a subsequent exposure to an irritant.

It is not clear whether the augmented capacity of the airways to generate PGE_2 following acrolein exposure can be exploited in the treatment of acrolein-induced lung damage. A recent study reported that PGE_2 inhibited cigarette smoke extract-induced apoptosis of human lung fibroblasts via an EP_2 receptor-dependent mechanism [146], potentially preventing smoke-induced apoptosis and emphysema. Thus, pathways that stimulate PGE_2 may be bronchoprotective. Activation of epithelial protease-activated receptors (PARs) promotes the generation of PGE_2 via pathways involving phospholipase A_2, COX-2, and mPGES [147,148]. Although hitherto untested, it is possible that the levels of PGE_2 produced in response to PAR_2 activation will be augmented following acrolein exposure, by virtue of the capacity of acrolein to elevate the expression of COX-2 and mPGES, and to inactivate PGDH. The potential beneficial effects produced by elevating PGE_2 levels (bronchodilation, anti-inflammatory effects), will need to be weighed up against the potential for PGE_2 to activate pathways that may contribute to the development of diseases such as lung cancer [146,149,150].

5. Conclusions

As a volatile and reactive electrophile formed upon combustion of organic matter, acrolein is likely to contribute to a range of respiratory conditions. Our survey has attempted to highlight the state of existing knowledge concerning the chemical basis for its diverse biological effects on respiratory tissues. While acrolein toxicity is increasingly well understood at the molecular level, this review has highlighted a need for a heightened effort to show the relevance of *in vitro* findings within whole animal models as well as human tissues from individuals subjected to various degrees of intoxication with acrolein-containing smoke. The goal of such efforts should be to rationalize the profound chemical reactivity of acrolein toward biological macromolecules with its ability to disrupt a wide range of cellular processes and elicit diverse pulmonary pathologies. Our survey has

also demonstrated that the toxicological investigation of the pulmonary effects of acrolein is still very much in its infancy and that many important research questions remain unanswered.

Acknowledgments

The assistance of Albert Raso with aspects of the experimental work is gratefully acknowledged. Work from Prof. Burcham's laboratory reported in this manuscript was supported by NHMRC Project Grants 403967 and 572580 (held with Prof. Henry).

REFERENCES

[1] J.F. Stevens, C.S. Maier, Acrolein: Sources, metabolism, and biomolecular interactions relevant to human health and disease, Mol. Nutr. Food Res. 52 (2008) 7–25.
[2] S.S. Hecht, Smoking and lung cancer—a new role for an old toxicant? Proc. Natl. Acad. Sci. U. S. A. 103 (2006) 15725–15726.
[3] R.M. Adibhatla, J.F. Hatcher, Lipid oxidation and peroxidation in CNS health and disease: From molecular mechanisms to therapeutic opportunities, Antioxid. Redox Signal. 12 (2010) 125–169.
[4] Anonymous, Toxicological review of acrolein CAS No. 107-02-8, US EPA, EPA/635/R-03/003 (2003) 1–106.
[5] T. Vermeire, Acrolein, Environmental Health Criteria 127 (1992), IPCS, WHO, Geneva.
[6] L. Li, A. Holian, Acrolein: A respiratory toxin that suppresses pulmonary host defense, Rev. Environ. Health 13 (1998) 99–108.
[7] T. Morikawa, Acrolein, formaldehyde, and volatile fatty acids from smouldering combustion, J. Combust. Toxicol. 3 (1976) 135–151.
[8] J.P. Eiserich, A. van der Vliet, G.J. Handelman, B. Halliwell, C.E. Cross, Dietary antioxidants and cigarette smoke-induced biomolecular damage: A complex interaction, Am. J. Clin. Nutr. 62 (1995) 1490S–1500S.
[9] E.I. Finkelstein, M. Nardini, A. van der Vliet, Inhibition of neutrophil apoptosis by acrolein: A mechanism of tobacco-related lung disease? Am. J. Physiol. Lung Cell Mol. Physiol. 281 (2001) L732–L739.
[10] G.E. Hartzell, Overview of combustion toxicology, Toxicology 115 (1996) 7–23.
[11] A.S. Buist, M.A. McBurnie, W.M. Vollmer, S. Gillespie, P. Burney, D.M. Mannino, A.M. Menezes, S.D. Sullivan, T.A. Lee, K.B. Weiss, R.L. Jensen, G.B. Marks, A. Gulsvik, E. Nizankowska-Mogilnicka, BOLD Collaborative Research Group. International variation in the prevalence of COPD (the BOLD Study): A population-based prevalence study, Lancet 370 (2007) 741–750.
[12] J.C. Hogg, W. Timens, The pathology of chronic obstructive pulmonary disease, Annu. Rev. Pathol. 4 (2009) 435–459.
[13] P.A. Kirkham, G. Spooner, C. Ffoulkes-Jones, R. Calvez, Cigarette smoke triggers macrophage adhesion and activation: Role of lipid peroxidation products and scavenger receptor, Free Radic. Biol. Med. 35 (2003) 697–710.

[14] W. Ning, C.J. Li, N. Kaminski, C.A. Feghali-Bostwick, S.M. Alber, Y.P. Di, S.L. Otterbein, R. Song, S. Hayashi, Z. Zhou, D.J. Pinsky, S.C. Watkins, J.M. Pilewski, F.C. Sciurba, D.G. Peters, J.C. Hogg, A.M. Choi, Comprehensive gene expression profiles reveal pathways related to the pathogenesis of chronic obstructive pulmonary disease, Proc. Natl. Acad. Sci. U. S. A. 101 (2004) 14895–14900.
[15] P.R. Reynolds, M.G. Cosio, J.R. Hoidal, Cigarette smoke-induced Egr-1 upregulates proinflammatory cytokines in pulmonary epithelial cells, Am. J. Respir. Cell Mol. Biol. 35 (2006) 314–319.
[16] W. Ning, Y. Dong, J. Sun, C. Li, M.A. Matthay, C.A. Feghali-Bostwick, A.M. Choi, Cigarette smoke stimulates matrix metalloproteinase-2 activity via EGR-1 in human lung fibroblasts, Am. J. Respir. Cell Mol. Biol. 36 (2007) 480–490.
[17] F.J. Kaye, Molecular biology of lung cancer, Lung Cancer 34 (Suppl. 2) (2001) S35–S41.
[18] S.S. Hecht, Tobacco carcinogens, their biomarkers and tobacco-induced cancer, Nat. Rev. Cancer. 3 (2003) 733–744.
[19] Z. Feng, W. Hu, Y. Hu, M.S. Tang, Acrolein is a major cigarette-related lung cancer agent: Preferential binding at p53 mutational hotspots and inhibition of DNA repair, Proc. Natl. Acad. Sci. U. S. A. 103 (2006) 15404–15409.
[20] P. Enkhbaatar, D.L. Traber, Pathophysiology of acute lung injury in combined burn and smoke inhalation injury, Clin. Sci. (Lond.). 107 (2004) 137–143.
[21] R.H. Demling, Smoke inhalation lung injury: An update, Eplasty 8 (2008) e27.
[22] D.M. Heimbach, J.F. Waeckerle, Inhalation injuries, Ann. Emerg. Med. 17 (1988) 1316–1320.
[23] M.A. Matthay, H.G. Folkesson, C. Clerici, Lung epithelial fluid transport and the resolution of pulmonary oedema, Physiol. Rev. 82 (2002) 569–600.
[24] Y. Berthiaume, M.A. Matthay, Alveolar edema fluid clearance and acute lung injury, Respir. Physiol. Neurobiol. 159 (2007) 350–359.
[25] P.C. Fuchs, E. Demir, K. Reuber, P. Stromps, T. Wolter, N. Pallua, Intra-alveolar IL-6 levels following burn and inhalation injury, Burns 35 (2009) 840–844.
[26] B.A. Zikria, J.M. Ferrer, H.F. Floch, The chemical factors contributing to pulmonary damage in "smoke poisoning", Surgery 71 (1972) 704–709.
[27] C.A. Hales, P.W. Barkin, W. Jung, E. Trautman, D. Lamborghini, N. Herrig, J. Burke, Synthetic smoke with acrolein but not HCl produces pulmonary edema, J. Appl. Physiol. 64 (1988) 1121–1133.
[28] O. Efimova, A.B. Volokhov, S. Iliaifar, C.A. Hales, Ligation of the bronchial artery in sheep attenuates early pulmonary changes following exposure to smoke, J. Appl. Physiol. 88 (2000) 888–893.
[29] C.A. Hales, S.W. Musto, S. Janssens, W. Jung, D.A. Quinn, M. Witten, Smoke aldehyde component influences pulmonary edema, J. Appl. Physiol. 72 (1992) 555–561.
[30] J.M. Patel, Metabolism and pulmonary toxicity of cyclophosphamide, Pharmacol. Ther. 47 (1990) 137–146.
[31] J.M. Patel, E.R. Block, C.L. Hood, Biochemical indices of cyclophosphamide-induced lung toxicity, Toxicol. Appl. Pharmacol. 76 (1984) 128–138.
[32] R.M. LoPachin, T. Gavin, D.R. Petersen, D.S. Barber, Molecular mechanisms of 4-hydroxy-2-nonenal and acrolein toxicity: Nucleophilic targets and adduct formation, Chem. Res. Toxicol. 22 (2009) 1499–1508.
[33] F.P. Guengerich, D.C. Liebler, Enzymatic activation of chemicals to toxic metabolites, Crit. Rev. Toxicol. 14 (1985) 259–307.
[34] R.M. LoPachin, T. Gavin, B.C. Geohagen, S. Das, Neurotoxic mechanisms of electrophilic type-2 alkenes: Soft-soft interactions described by quantum mechanical parameters, Toxicol. Sci. 98 (2007) 561–570.
[35] K. Ramu, C.S. Perry, T. Ahmed, G. Pakenham, J.P. Kehrer, Studies on the basis for the toxicity of acrolein mercapturates, Toxicol. Appl. Pharmacol. 140 (1996) 487–498.

[36] H. Esterbauer, A. Ertl, N. Scholz, The reaction of cysteine with α,β-unsaturated aldehydes, Tetrahedron 32 (1976) 285–289.
[37] J. Cai, A. Bhatnagar, W.M. Pierce, Jr, Protein modification by acrolein: Formation and stability of cysteine adducts, Chem. Res. Toxicol. 22 (2009) 708–716.
[38] I. Dalle-Donne, M. Carini, G. Vistoli, L. Gamberoni, D. Giustarini, R. Colombo, R. Maffei Facino, R. Rossi, A. Milzani, G. Aldini, Actin-Cys374 as a nucleophilic target of α,β-unsaturated aldehydes, Free Radic. Biol. Med. 42 (2007) 583–598.
[39] N.D. Horton, S.S. Biswal, L.L. Corrigan, J. Bratta, J.P. Kehrer, Acrolein causes inhibitor kB-independent decreases in nuclear factor kB activation in human lung adenocarcinoma (A549) cells, J. Biol. Chem. 274 (1999) 9200–9206.
[40] L.J. Macpherson, A.E. Dubin, M.J. Evans, F. Marr, P.G. Schultz, B.F. Cravatt, A. Patapoutian, Noxious compounds activate TRPA1 ion channels through covalent modification of cysteines, Nature 445 (2007) 541–545.
[41] J.C. Kern, J.P. Kehrer, Acrolein-induced cell death: A caspase-influenced decision between apoptosis and oncosis/necrosis. Chem. Biol. Interact. 139 (2002) 79–95.
[42] P.C. Burcham, A. Raso, C. Thompson, D. Tan, Intermolecular protein cross-linking during acrolein toxicity: Efficacy of carbonyl scavengers as inhibitors of heat shock protein-90 cross-linking in A549 cells, Chem. Res. Toxicol. 20 (2007) 1629–1637.
[43] K. Uchida, M. Kanematsu, Y. Morimitsu, T. Osawa, N. Noguchi, E. Niki, Acrolein is a product of lipid peroxidation reaction. Formation of free acrolein and its conjugate with lysine residues in oxidized low density lipoproteins, J. Biol. Chem. 273 (1998) 16058–16066.
[44] L.M. Kaminskas, S.M. Pyke, P.C. Burcham, Michael addition of acrolein to lysinyl and N-terminal residues of a model peptide: Targets for cytoprotective hydrazino drugs. Rapid Commun. Mass Spectrom. 21 (2007) 1155–1164.
[45] A. Furuhata, M. Nakamura, T. Osawa, K. Uchida, Thiolation of protein-bound carcinogenic aldehyde. An electrophilic acrolein-lysine adduct that covalently binds to thiols, J. Biol. Chem. 277 (2002) 27919–27926.
[46] T. Ishii, T. Yamada, T. Mori, S. Kumazawa, K. Uchida, T. Nakayama, Characterization of acrolein-induced protein cross-links, Free Radic. Res. 41 (2007) 1253–1260.
[47] A. Furuhata, T. Ishii, S. Kumazawa, T. Yamada, T. Nakayama, K. Uchida, N(ε)-(3-methylpyridinium)lysine, a major antigenic adduct generated in acrolein-modified protein, J. Biol. Chem. 278 (2003) 48658–48665.
[48] T. Obama, R. Kato, Y. Masuda, K. Takahashi, T. Aiuchi, H. Itabe, Analysis of modified apolipoprotein B-100 structures formed in oxidized low-density lipoprotein using LC-MS/MS, Proteomics 7 (2007) 2132–2141.
[49] P.C. Burcham, L.M. Kaminskas, D. Tan, S.M. Pyke, Carbonyl-scavenging drugs & protection against carbonyl stress-associated cell injury, Mini Rev. Med. Chem. 8 (2008) 319–330.
[50] D.J. Conklin, P. Haberzettl, R.A. Prough, A. Bhatnagar, Glutathione-S-transferase P protects against endothelial dysfunction induced by exposure to tobacco smoke, Am. J. Physiol. Heart Circ. Physiol. 296 (2009) H1586–H1597.
[51] P.C. Burcham, F.R. Fontaine, D.R. Petersen, S.M. Pyke, Reactivity with Tris (hydroxymethyl)aminomethane confounds immunodetection of acrolein-adducted proteins, Chem. Res. Toxicol. 16 (2003) 1196–1201.
[52] I. Dalle-Donne, M. Carini, G. Vistoli, L. Gamberoni, D. Giustarini, R. Colombo, R. Maffei Facino, R. Rossi, A. Milzani, G. Aldini, Actin-Cys374 as a nucleophilic target of α,β-unsaturated aldehydes, Free Radic. Biol. Med. 42 (2007) 583–598.
[53] C. Lambert, J. Li, K. Jonscher, T.C. Yang, P. Reigan, M. Quintana, J. Harvey, B.M. Freed, Acrolein inhibits cytokine gene expression by alkylating cysteine and arginine residues in the NF-κB1 DNA binding domain, J. Biol. Chem. 282 (2007) 19666–19675.

[54] R.A. Smith, D.S. Williamson, S.M. Cohen, Identification of 3,N^4-propanodeoxycytidine 5′-monophosphate formed by the reaction of acrolein with deoxycytidine 5′-monophosphate, Chem. Res. Toxicol. 2 (1989) 267–271.
[55] R.A. Smith, D.S. Williamson, R.L. Cerny, S.M. Cohen, Detection of 1,N^6-propanodeoxyadenosine in acrolein-modified polydeoxyadenylic acid and DNA by ^{32}P-postlabeling, Cancer Res. 50 (1990) 3005–3012.
[56] A. Chenna, R.A. Rieger, C.R. Iden, Characterization of thymidine adducts formed by acrolein and 2-bromoacrolein, Carcinogenesis 13 (1992) 2361–2365.
[57] P.C. Burcham, Genotoxic lipid peroxidation products: Their DNA damaging properties and role in formation of endogenous DNA adducts, Mutagenesis 13 (1998) 287–305.
[58] I.G. Minko, I.D. Kozekov, T.M. Harris, C.J. Rizzo, R.S. Lloyd, M.P. Stone, Chemistry and biology of DNA containing 1,N(2)-deoxyguanosine adducts of the α,β-unsaturated aldehydes acrolein, crotonaldehyde, and 4-hydroxynonenal. Chem. Res. Toxicol. 22 (2009) 759–778.
[59] A. Emami, M. Dyba, A.K. Cheema, J. Pan, R.G. Nath, F.L. Chung, Detection of the acrolein-derived cyclic DNA adduct by a quantitative ^{32}P-postlabeling/solid-phase extraction/HPLC method: Blocking its artifact formation with glutathione, Anal. Biochem. 374 (2008) 163–172.
[60] R.G. Nath, J.E. Ocando, F.L. Chung, Detection of 1, N^2-propanodeoxyguanosine adducts as potential endogenous DNA lesions in rodent and human tissues, Cancer Res. 56 (1996) 452–456.
[61] R.G. Nath, J.E. Ocando, J.B. Guttenplan, F.L. Chung, 1,N^2-propanodeoxyguanosine adducts: Potential new biomarkers of smoking-induced DNA damage in human oral tissue, Cancer Res. 58 (1998) 581–584.
[62] X. Liu, M.A. Lovell, B.C. Lynn, Development of a method for quantification of acrolein-deoxyguanosine adducts in DNA using isotope dilution-capillary LC/MS/MS and its application to human brain tissue, Anal. Chem. 77 (2005) 5982–5989.
[63] S. Zhang, P.W. Villalta, M. Wang, S.S. Hecht, Detection and quantitation of acrolein-derived 1,N^2-propanodeoxyguanosine adducts in human lung by liquid chromatography-electrospray ionization-tandem mass spectrometry, Chem. Res. Toxicol. 20 (2007) 565–571.
[64] S.G. Carmella, M. Chen, S. Han, A. Briggs, J. Jensen, D.K. Hatsukami, S.S. Hecht, Effects of smoking cessation on eight urinary tobacco carcinogen and toxicant biomarkers, Chem. Res. Toxicol. 22 (2009) 734–741.
[65] P.C. Burcham, A. Raso, C.A. Thompson, Intermediate filament carbonylation during acute acrolein toxicity in A549 lung cells: Functional consequences, chaperone redistribution and protection by bisulfite, Antioxid. Redox Signal. 12 (2010) 337–347.
[66] D.C. Liebler, Protein damage by reactive electrophiles: Targets and consequences, Chem. Res. Toxicol. 21 (2008) 117–128.
[67] G. Valacchi, E. Pagnin, A. Phung, M. Nardini, B.C. Schock, C.E. Cross, A. van der Vliet, Inhibition of NFκB activation and IL-8 expression in human bronchial epithelial cells by acrolein, Antioxid. Redox Signal. 7 (2005) 25–31.
[68] J.D. West, L.J. Marnett, Endogenous reactive intermediates as modulators of cell signaling and cell death, Chem. Res. Toxicol. 19 (2006) 173–194.
[69] N. Mukaida, Pathophysiological roles of interleukin-8/CXCL8 in pulmonary diseases, Am. J. Physiol. Lung Cell Mol. Physiol. 284 (2003) L566–L577.
[70] C. Ji, K.R. Kozak, L.J. Marnett, IκB kinase, a molecular target for inhibition by 4-hydroxy-2-nonenal, J. Biol. Chem. 276 (2001) 18223–18228.
[71] L. Li, R.F. Hamilton, Jr, A. Holian, Effect of acrolein on human alveolar macrophage NF-κB activity, Am. J. Physiol. 277 (1999) L550–L557.

[72] N.D. Horton, S.S. Biswal, L.L. Corrigan, J. Bratta, J.P. Kehrer, Acrolein causes inhibitor κB-independent decreases in nuclear factor κB activation in human lung adenocarcinoma (A549) cells, J. Biol. Chem. 274 (1999) 9200–9206.
[73] T. Kueper, T. Grune, S. Prahl, H. Lenz, W. Welge, T. Biernoth, Y. Vogt, G.M. Muhr, A. Gaemlich, T. Jung, G. Boemke, H.P. Elsässer, K.P. Wittern, H. Wenck, F. Stäb, T. Blatt, Vimentin is the specific target in skin glycation: Structural prerequisites, functional consequences, and role in skin aging, J. Biol. Chem. 282 (2007) 23427–23436.
[74] B.W. Meier, J.D. Gomez, A. Zhou, J.A. Thompson, Immunochemical and proteomic analysis of covalent adducts formed by quinone methide tumor promoters in mouse lung epithelial cell lines, Chem. Res. Toxicol. 18 (2005) 1575–1585.
[75] S. Gharbi, B. Garzón, J. Gayarre, J. Timms, D. Pérez-Sala, Study of protein targets for covalent modification by the antitumoral and anti-inflammatory prostaglandin PGA_1: Focus on vimentin, J. Mass Spectrom. 42 (2007) 1474–1484.
[76] B.B. Omary, Intermediate filaments and their associated diseases, N.Engl. J. Med. 351 (2004) 2087–2100.
[77] M. Pekny, E.B. Lane, Intermediate filaments and stress, Exp. Cell Res. 313 (2007) 2244–2254.
[78] H.K. Hamadeh, P.R. Bushel, S. Jayadev, O. DiSorbo, L. Bennett, L. Li, R. Tennant, R. Stoll, J.C. Barrett, R.S. Paules, K. Blanchard, C.A. Afshari, Prediction of compound signature using high density gene expression profiling, Toxicol. Sci. 67 (2002) 232–240.
[79] J.F. Waring, R.A. Jolly, R. Ciurlionis, P.Y. Lum, J.T. Praestgaard, D.C. Morfitt, B. Buratto, C. Roberts, E. Schadt, R.G. Ulrich, Clustering of hepatotoxins based on mechanism of toxicity using gene expression profiles, Toxicol. Appl. Pharmacol. 175 (2001) 28–42.
[80] L. Huang, A.N. Heinloth, Z.B. Zeng, R.S. Paules, P.R. Bushel, Genes related to apoptosis predict necrosis of the liver as a phenotype observed in rats exposed to a compendium of hepatotoxicants, BMC Genomics 9 (2008) 288.
[81] W.O. Osburn, T.W. Kensler, Nrf2 signaling: An adaptive response pathway for protection against environmental toxic insults, Mutat. Res. 659 (2008) 31–39.
[82] K. Itoh, K.I. Tong, M. Yamamoto, Molecular mechanism activating Nrf2-Keap1 pathway in regulation of adaptive response to electrophiles, Free Radic. Biol. Med. 36 (2004) 1208–1213.
[83] J.D. Hayes, M. McMahon, NRF2 and KEAP1 mutations: Permanent activation of an adaptive response in cancer, Trends Biochem. Sci. 34 (2009) 176–188.
[83] R. Tirumalai, T. Rajesh Kumar, K.H. Mai, S. Biswal, Acrolein causes transcriptional induction of phase II genes by activation of Nrf2 in human lung type II epithelial (A549) cells, Toxicol. Lett. 132 (2002) 27–36.
[84] H. Zhang, H.J. Forman, Signaling pathways involved in phase II gene induction by α,β-unsaturated aldehydes, Toxicol. Ind. Health 25 (2009) 269–278.
[85] J.P. Lyon, L.J. Jenkins, R.A. Jones, R.A. Coon, J. Siegel, Repeated and continuous exposure of laboratory animals to acrolein, Toxicol. Appl. Pharmacol. 17 (1970) 726–732.
[86] H.S. Deshmukh, C. Shaver, L.M. Case, M. Dietsch, S.C. Wesselkamper, W.D. Hardie, T.R. Korfhagen, M. Corradi, J.A. Nadel, M.T. Borchers, G.D. Leikauf, Acrolein-activated matrix metalloproteinase 9 contributes to persistent mucin production, Am. J. Respir. Cell Mol. Biol. 38 (2008) 446–454.
[87] H.S. Deshmukh, L.M. Case, S.C. Wesselkamper, M.T. Borchers, L.D. Martin, H.G. Shertzer, J.A. Nadel, G.D. Leikauf, Metalloproteinases mediate mucin 5AC expression by epidermal growth factor receptor activation, Am. J. Respir. Crit. Care Med. 171 (2005) 305–314.
[88] H.S. Deshmukh, C. Shaver, L.M. Case, M. Dietsch, S.C. Wesselkamper, W.D. Hardie, T.R. Korfhagen, M. Corradi, J.A. Nadel, M.T. Borchers, G.D. Leikauf,

Acrolein-activated matrix metalloproteinase 9 contributes to persistent mucin production, Am. J. Respir. Cell Mol. Biol. 38 (2008) 446–454.
[89] C.A. Thompson, P.C. Burcham, Genome-wide transcriptional responses to acrolein, Chem. Res. Toxicol. 21 (2008) 2245–2256.
[90] P.R. Reynolds, M.G. Cosio, J.R. Hoidal, Cigarette smoke-induced Egr-1 upregulates proinflammatory cytokines in pulmonary epithelial cells, Am. J. Respir. Cell Mol. Biol. 35 (2006) 314–319.
[91] W. Ning, Y. Dong, J. Sun, C. Li, M.A. Matthay, C.A. Feghali-Bostwick, A.M. Choi, Cigarette smoke stimulates matrix metalloproteinase-2 activity via EGR-1 in human lung fibroblasts, Am. J. Respir. Cell Mol. Biol. 36 (2007) 480–490.
[92] S. Grotegut, D. von Schweinitz, G. Christofori, F. Lehembre, Hepatocyte growth factor induces cell scattering through MAPK/Egr-1-mediated upregulation of Snail, EMBO J. 25 (2006) 534–545.
[93] A. Kubosaki, Y. Tomaru, M. Tagami, E. Arner, H. Miura, T. Suzuki, M. Suzuki, H. Suzuki, Y. Hayashizaki, Genome-wide investigation of *in vivo* EGR-1 binding sites in monocytic differentiation, Genome Biol. 10 (2009) R41.
[94] S. Arora, Y. Wang, Z. Jia, S. Vardar-Sengul, A. Munawar, K.S. Doctor, M. Birrer, M. McClelland, E. Adamson, D. Mercola, Egr1 regulates the coordinated expression of numerous EGF receptor target genes as identified by ChIP-on-chip, Genome Biol. 9 (2008) R166.
[95] B.T. Mossman, K.M. Lounsbury, S.P. Reddy, Oxidants and signaling by mitogen-activated protein kinases in lung epithelium, Am. J. Respir. Cell Mol. Biol. 34 (2006) 666–669.
[96] A. Tanel, D.A. Averill-Bates, P38 and ERK mitogen-activated protein kinases mediate acrolein-induced apoptosis in Chinese hamster ovary cells, Cell Signal. 19 (2007) 968–977.
[97] N. Moretto, F. Facchinetti, T. Southworth, M. Civelli, D. Singh, R. Patacchini, α,β-Unsaturated aldehydes contained in cigarette smoke elicit IL-8 release in pulmonary cells through mitogen-activated protein kinases, Am. J. Physiol. Lung Cell Mol. Physiol. 296 (2009) L839–L848.
[98] F. Facchinetti, F. Amadei, P. Geppetti, F. Tarantini, C. Di Serio, A. Dragotto, P.M. Gigli, S. Catinella, M. Civelli, R. Patacchini, α,β-unsaturated aldehydes in cigarette smoke release inflammatory mediators from human macrophages, Am. J. Respir. Cell Mol. Biol. 37 (2007) 617–623.
[99] M. Parola, G. Robino, F. Marra, M. Pinzani, G. Bellomo, G. Leonarduzzi, P. Chiarugi, S. Camandola, G. Poli, G. Waeg, P. Gentilini, M.U. Dianzani, HNE interacts directly with JNK isoforms in human hepatic stellate cells, J. Clin. Invest. 102 (1998) 1942–1950.
[100] H. Kamata, S. Honda, S. Maeda, L. Chang, H. Hirata, M. Karin, Reactive oxygen species promote TNFα-induced death and sustained JNK activation by inhibiting MAP kinase phosphatases, Cell 120 (2005) 649–661.
[101] D.R. Seiner, J.N. LaButti, K.S. Gates, Kinetics and mechanism of protein tyrosine phosphatase 1B inactivation by acrolein, Chem. Res. Toxicol. 20 (2007) 1315–1320.
[102] C.A. Thompson, P.C. Burcham, Protein alkylation, transcriptional responses and cytochrome c release during acrolein toxicity in A549 cells: Influence of nucleophilic culture media constituents, Toxicol. In Vitro 22 (2008) 844–853.
[103] R.A. Smith, S.M. Cohen, T.A. Lawson, Acrolein mutagenicity in the V79 assay Carcinogenesis 11 (1990) 497–498.
[104] L.J. Marnett, H.K. Hurd, M.C. Hollstein, D.E. Levin, H. Esterbauer, B.N. Ames, Naturally occurring carbonyl compounds are mutagens in Salmonella tester strain TA104 Mutat. Res. 148 (1985) 25–34.

[105] R.D. Curren, L.L. Yang, P.M. Conklin, R.C. Grafstrom, C.C. Harris, Mutagenesis of xeroderma pigmentosum fibroblasts by acrolein, Mutat. Res. 209 (1988) 17–22.
[106] M. Kawanishi, T. Matsuda, A. Nakayama, H. Takebe, S. Matsui, T. Yagi, Molecular analysis of mutations induced by acrolein in human fibroblast cells using supF shuttle vector plasmids, Mutat. Res. 417 (1998) 65–73.
[107] L.A. VanderVeen, M.F. Hashim, L.V. Nechev, T.M. Harris, C.M. Harris, L.J. Marnett, Evaluation of the mutagenic potential of the principal DNA adduct of acrolein, J. Biol. Chem. 276 (2001) 9066–9070.
[108] I.Y. Yang, M. Hossain, H. Miller, S. Khullar, F. Johnson, A. Grollman, M. Moriya, Responses to the major acrolein-derived deoxyguanosine adduct in Escherichia coli, J. Biol. Chem. 276 (2001) 9071–9076.
[109] M. Kanuri, I.G. Minko, L.V. Nechev, T.M. Harris, C.M. Harris, R.S. Lloyd, Error prone translesion synthesis past γ-hydroxy-propanodeoxyguanosine, the primary acrolein-derived adduct in mammalian cells, J. Biol. Chem. 277 (2002) 18257–18265.
[110] S.I. Kim, G.P. Pfeifer, A. Besaratinia, Lack of mutagenicity of acrolein-induced DNA adducts in mouse and human cells, Cancer Res. 67 (2007) 11640–11647.
[111] H.T. Wang, S. Zhang, Y. Hu, M.S. Tang, Mutagenicity and sequence specificity of acrolein-DNA adducts, Chem. Res. Toxicol. 22 (2009) 511–517.
[112] P.C. Burcham, L.A. Harkin, Mutations at G:C base pairs predominate after replication of peroxyl radical-damaged pSP189 plasmids in human cells, Mutagenesis 14 (1999) 135–140.
[113] A. Besaratinia, Acrolein: Excessive cytotoxicity or potent mutagenicity? Chem. Res. Toxicol. 22 (2009) 751–753.
[114] H.T. Wang, M.S. Tang, Acrolein adducts are mutagenic, Chem. Res. Toxicol. 22 (2009) 753–754.
[115] J.P. Kehrer, S.S. Biswal, The molecular effects of acrolein, Toxicol. Sci. 57 (2000) 6–15.
[116] A. Tanel, D.A. Averill-Bates, The aldehyde acrolein induces apoptosis via activation of the mitochondrial pathway, Biochim. Biophys. Acta 1743 (2005) 255–267.
[117] A. Tanel, D.A. Averill-Bates, Activation of the death receptor pathway of apoptosis by the aldehyde acrolein, Free Radic. Biol. Med. 42 (2007) 798–810.
[118] J. Roy, P. Pallepati, A. Bettaieb, A. Tanel, D.A. Averill-Bates, Acrolein induces a cellular stress response and triggers mitochondrial apoptosis in A549 cells, Chem. Biol. Interact. 181 (2009) 154–167.
[119] U.M. Moll, N. Marchenko, X. Zhang, p53 and Nur77/TR3—transcription factors that directly target mitochondria for cell death induction, Oncogene 25 (2006) 4725–4743.
[120] B. Liang, X. Song, G. Liu, R. Li, J. Xie, L. Xiao, M. Du, Q. Zhang, X. Xu, X. Gan, D. Huang, Involvement of TR3/Nur77 translocation to the endoplasmic reticulum in ER stress-induced apoptosis, Exp. Cell Res. 313 (2007) 2833–2844.
[121] S.O. Kim, K. Ono, P.S. Tobias, J. Han, Orphan nuclear receptor Nur77 is involved in caspase-independent macrophage cell death, J. Exp. Med. 197 (2003) 1441–1452.
[122] S. Chintharlapalli, R. Burghardt, S. Papineni, S. Ramaiah, K. Yoon, Safe, Activation of Nur77 by selected 1,1-Bis(3′-indolyl)-1-(p-substituted phenyl)methanes induces apoptosis through nuclear pathways, J. Biol. Chem. 280 (2005) 24903–24914.
[123] L.Y. Lee, Respiratory sensations evoked by activation of bronchopulmonary C-fibers, Respir. Physiol. Neurobiol. 167 (2009) 26–35.
[124] G.D. Leikauf, L.M. Leming, J.R. O'Donnell, C.A. Doupnik, Bronchial responsiveness and inflammation in guinea pigs exposed to acrolein, J. Appl. Physiol. 66 (1989) 171–178.
[125] C.R. Turner, R.B. Stow, S.D. Talerico, E.P. Christian, J.C. Williams, Protective role for neuropeptides in acute pulmonary response to acrolein in guinea pigs, J. Appl. Physiol. 75 (1993) 2456–2465.

[126] E. Andrè, B. Campi, S. Materazzi, M. Trevisani, S. Amadesi, D. Massi, C. Creminon, N. Vaksman, R. Nassini, M. Civelli, P.G. Baraldi, D.P. Poole, N.W. Bunnett, P. Geppetti, R. Patacchini, Cigarette smoke-induced neurogenic inflammation is mediated by α,β-unsaturated aldehydes and the TRPA1 receptor in rodents, J. Clin. Invest. 118 (2008) 2574–2582.
[127] D.M. Bautista, S.E. Jordt, T. Nikai, P.R. Tsuruda, A.J. Read, J. Poblete, E.N. Yamoah, A.I. Basbaum, D. Julius, TRPA1 mediates the inflammatory actions of environmental irritants and proalgesic agents, Cell 124 (2006) 1269–1282.
[128] A. Ben-Jebria, Y. Crozet, M.L. Eskew, B.L. Rudeen, J.S. Ultman, Acrolein-induced smooth muscle hyperresponsiveness and eicosanoid release in excised ferret tracheae, Toxicol. Appl. Pharmacol. 135 (1995) 35–44.
[129] A. Ben-Jebria, R. Marthan, M. Rossetti, J.P. Savineau, J.S. Ultman, Human bronchial smooth muscle responsiveness after in vitro exposure to acrolein, Am. J. Respir. Crit. Care Med. 149 (1994) 382–386.
[130] A. Ben-Jebria, R. Marthan, M. Rossetti, J.P. Savineau, J.S. Ultman, Effect of in vitro exposure to acrolein on carbachol responses in rat trachealis muscle, Respir. Physiol. 93 (1993) 111–123.
[131] E. Roux, N. Ouedraogo, J.M. Hyvelin, J.P. Savineau, R. Marthan, In vitro effect of air pollutants on human bronchi, Cell Biol. Toxicol. 18 (2002) 289–299.
[132] J.M. Hyvelin, J.P. Savineau, R. Marthan, Selected contribution: Effect of the aldehyde acrolein on acetylcholine-induced membrane current in airway smooth muscle cells, J. Appl. Physiol. 90 (2001) 750–754.
[133] J.M. Hyvelin, E. Roux, M.C. Prévost, J.P. Savineau, R. Marthan, Cellular mechanisms of acrolein-induced alteration in calcium signaling in airway smooth muscle, Toxicol. Appl. Pharmacol. 164 (2000) 176–183.
[134] C.A. Doupnik, G.D. Leikauf, Acrolein stimulates eicosanoid release from bovine airway epithelial cells, Am. J. Physiol. 259 (1990) L222–L229.
[135] P.M. Joseph, M.L. Witten, C.H. Burke, C.A. Hales, The effects of chronic sidestream cigarette smoke exposure on eicosanoid production by tracheal epithelium, Exp. Lung Res. 22 (1996) 317–335.
[136] C.A. Martey, S.J. Pollock, C.K. Turner, K.M. O'Reilly, C.J. Baglole, R.P. Phipps, P.J. Sime, Cigarette smoke induces cyclooxygenase-2 and microsomal prostaglandin E_2 synthase in human lung fibroblasts: Implications for lung inflammation and cancer, Am. J. Physiol. Lung Cell Mol. Physiol. 287 (2004) L981–L991.
[137] C.C. Grundfest, J. Chang, D. Newcombe, Acrolein: A potent modulator of lung macrophage arachidonic acid metabolism, Biochim. Biophys. Acta 713 (1982) 149–159.
[138] K.A. Berry, P.M. Henson, R.C. Murphy, Effects of acrolein on leukotriene biosynthesis in human neutrophils, Chem. Res. Toxicol. 21 (2008) 2424–2432.
[139] Y.S. Park, J. Kim, Y. Misonou, R. Takamiya, M. Takahashi, M.R. Freeman, N. Taniguchi, Acrolein induces cyclooxygenase-2 and prostaglandin production in human umbilical vein endothelial cells: Roles of p38 MAP kinase, Arterioscler. Thromb. Vasc. Biol. 27 (2007) 1319–1325.
[140] P. Sarkar, B.E. Hayes BE, Induction of COX-2 by acrolein in rat lung epithelial cells, Mol. Cell Biochem. 301 (2007) 191–199.
[141] Y. Liu, H.H. Tai, Inactivation of pulmonary NAD^+-dependent 15-hydroxyprostaglandin dehydrogenase by acrolein, Biochem. Pharmacol. 34 (1985) 4275–4278.
[142] C. Vancheri, C. Mastruzzo, M.A. Sortino, N. Crimi, The lung as a privileged site for the beneficial actions of PGE_2, Trends Immunol. 25 (2004) 40–46.
[143] P.J. Henry, The protease-activated $receptor_2$ (PAR_2)-prostaglandin E_2-prostanoid EP receptor axis: A potential bronchoprotective unit in the respiratory tract? Eur. J. Pharmacol. 533 (2006) 156–170.

[144] S.L. Tilley, J.M. Hartney, C.J. Erikson, C. Jania, M. Nguyen, J. Stock, J. McNeisch, C. Valancius, R.A. Panettieri, R.B. Penn, B.H. Koller, Receptors and pathways mediating the effects of prostaglandin E_2 on airway tone, Am. J. Physiol. Lung Cell Mol. Physiol. 284 (2003) L599–L606.

[145] T.E. Taylor-Clark, B.J. Undem, D.W. Macglashan, S. Ghatta, M.J. Carr, M.A. McAlexander, Prostaglandin-induced activation of nociceptive neurons via direct interaction with transient receptor potential A1 (TRPA1), Mol. Pharmacol. 73 (2008) 274–281.

[146] H. Sugiura, X. Liu, S. Togo, T. Kobayashi, L. Shen, S. Kawasaki, K. Kamio, X.Q. Wang, L.J. Mao, S.I. Rennard, Prostaglandin E_2 protects human lung fibroblasts from cigarette smoke extract-induced apoptosis via EP_2 receptor activation, J. Cell Physiol. 210 (2007) 99–110.

[147] A. Kawabata, S. Kubo, T. Ishiki, N. Kawao, F. Sekiguchi, R. Kuroda, M.D. Hollenberg, T. Kanke, N. Saito, Proteinase-activated receptor-2-mediated relaxation in mouse tracheal and bronchial smooth muscle: Signal transduction mechanisms and distinct agonist sensitivity, J. Pharmacol. Exp. Ther. 311 (2004) 402–410.

[148] N. Kawao, M. Nagataki, K. Nagasawa, S. Kubo, K. Cushing, T. Wada, F. Sekiguchi, S. Ichida, M.D. Hollenberg, W.K. MacNaughton, H. Nishikawa, A. Kawabata, Signal transduction for proteinase-activated receptor-2-triggered prostaglandin E_2 formation in human lung epithelial cells, J. Pharmacol. Exp. Ther. 315 (2005) 576–589.

[149] S. Hazra, K.A. Peebles, S. Sharma, J.T. Mao, S.M. Dubinett, The role of PPARγ in the cyclooxygenase pathway in lung cancer, PPAR Res. 2008 (2008) 790568.

[150] J.M. Lee, J. Yanagawa, K.A. Peebles, S. Sharma, J.T. Mao, S.M. Dubinett, Inflammation in lung carcinogenesis: New targets for lung cancer chemoprevention and treatment, Crit. Rev. Oncol. Hematol. 66 (2008) 208–217.

CHAPTER 2

Heterocyclic Aromatic Amines

Potential Human Carcinogens

Robert J. Turesky*

Contents

1. Introduction

The diet provides key nutritents and minerals for sustenance and well-being of the body; however, hazardous chemicals present in the diet can also contribute to the development of diseases such as cancer [1]. Heterocyclic aromatic amines (HAAs) are a class of compounds in the diet that are

Division of Environmental Health Sciences, Wadsworth Center, New York State Department of Health, Empire State Plaza, Albany, NY, USA

* Corresponding author. Tel.: 518-474-4151; Fax: 518-473-2095
Email address: Rturesky@wadsworth.org

Advances in Molecular Toxicology, Volume 4
ISSN 1872-0854, DOI 10.1016/S1872-0854(10)04002-6

receiving widening attention as a risk factor for human cancer. HAAs were discovered more than 30 years ago by Professor Sugimura and his colleagues in Japan [2], who showed that the charred parts and smoke generated from broiled fish and beef contained potent activity in *Salmonella typhimurium*-based mutagenicity assays. Since that discovery, more than 20 HAAs have been identified in cooked meats, fish, and poultry [3–6]. Several HAAs have also been identified in cigarette smoke condensate and diesel exhaust [7,8]. HAAs induce cancer of the oral cavity, liver, stomach, lung, colorectum, prostate, and mammary glands of rodents, during long-term feeding studies [5]. It is noteworthy that the colon, prostate, and female mammary glands are common sites of cancer in the Western countries in which well-done cooked meats containing HAAs are frequently consumed [9]; and the rates of cancer in these organs are increasing in Japan and other countries that are adapting western dietary habits [5]. Therefore, questions have been raised about the safety of foods containing HAAs, and much research has already been devoted to the biochemical toxicology of HAAs and their potential role in the etiology of human cancer. The recent *Report on Carcinogens*, Eleventh Edition, of the National Toxicology Program concluded that several prevalent HAAs are "reasonably anticipated" to be human carcinogens [10].

1.1. Mechanisms of formation of HAAs

There are two major classes of HAAs. One class of compounds is known as "pyrolytic HAAs." These compounds arise during the high-termperature pyrolysis (>250 °C) of individual amino acids. HAAs are formed during the pyrolysis of tryptophan, glutamic acid, phenylalanine, or ornithine. Several HAAs also arise during the pyrolysis of proteins such as soybean globulin and casein [2,11]. The reactions of these amino acids or proteins at high temperature produce deaminated and decarboxylated products and reactive radical fragments, which can combine to form heterocyclic ring structures. The known pyrolytic HAAs comprise five structurally distinct groups that contain pyridoindoles, pyridoimidazoles, phenylpyridine, tetraazofluoranthene, or benzmidazole moieties (Figure 1). The tryptophan pyrolysates 2-amino-1,4-dimethyl-5*H*-pyrido[4,3-*b*]indole (Trp-P-1) and 2-amino-1-dimethyl-5*H*-pyrido[4,3-*b*]indole (Trp-P-2), and the soybean globulin pyrolysates 2-amino-9*H*-pyrido[2,3-*b*]indole (AαC) and 2-amino-3-methyl-9*H*-pyrido[2,3-*b*]indole (MeAαC) each contain an indole moiety as a part of their structure, which may be derived from tryptophan. The high temperature of burning cigarettes catalyzes the formation of several pyrolytic HAAs [12]. AαC and MeAαC are the two most abundant HAAs that arise in mainstream cigarette smoke [13], with levels reported up to 258 and 37 ng per cigarette, respectively. These levels are considerably higher than the levels reported for many polycyclic aromatic

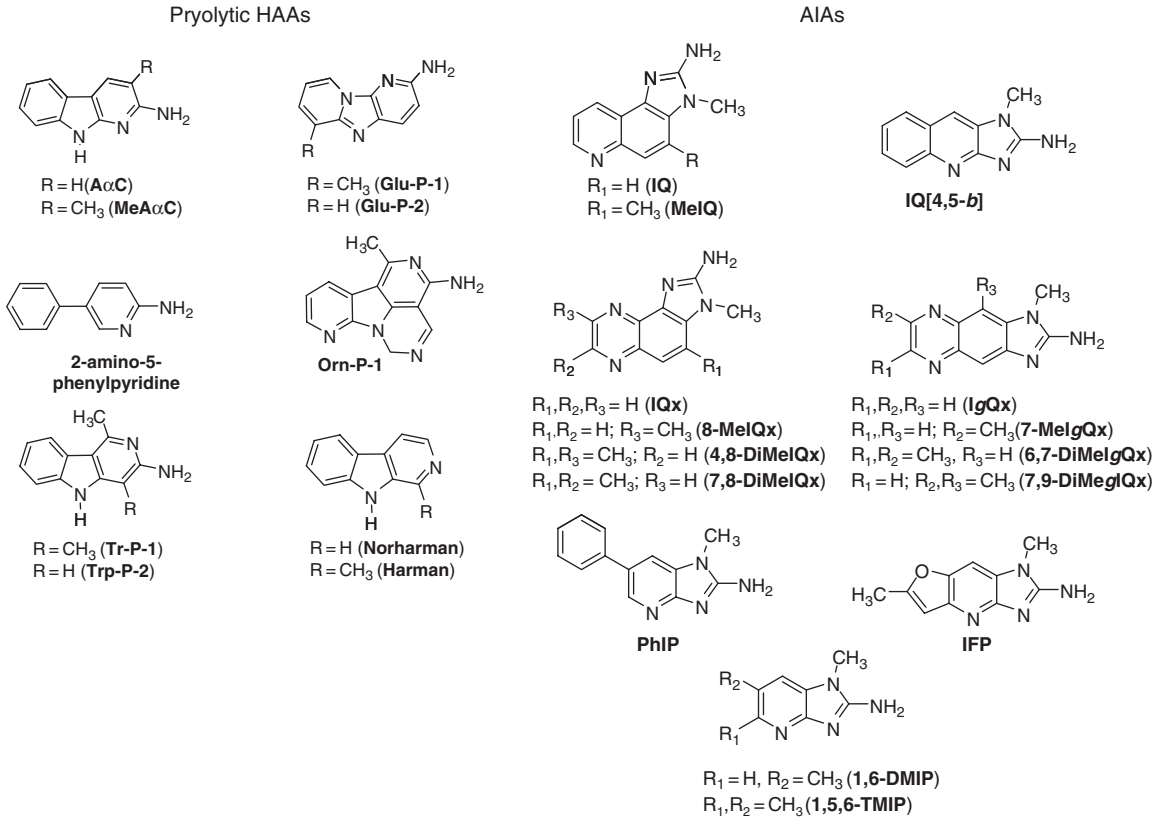

Figure 1 Chemical structures of prominent pyrolysate HAAs and AIAs formed during cooking of meat.

hydrocarbons and aromatic amines, which are established human carcinogens [14]. Several pyrolytic HAAs are formed at low nanogram per gram concentrations in some broiled or grilled fish and meats that are cooked very well-done or burnt [15–21]. However, concentrations of pyrolytic HAAs are typically formed below the nanogram per gram range in cooked meat prepared under common household cooking practices, because the temperatures of the cooking surfaces are below 250 °C: this heat level is insufficient to catalyze the production of pyrolytic HAAs.

The second class of HAAs, named aminoimidazoarenes (AIAs) (Figure 1), are formed in meats cooked at temperatures (150–250 °C) commonly used in the household kitchen. The Maillard reaction is thought to play an important role in the formation of AIAs. Jägerstad and coworkers employed a model system that contained creatine, free amino acids, and hexoses, constituents present in uncooked meats, and they refluxed these components at temperatures ≥130 °C to produce 2-amino-3-methylimidazo[4,5-*f*]quinoline (IQ), 2-amino-3-methylmidazo[4,5-*f*]quinoxaline (IQx), 2-amino-3,8-dimethylimidazo[4,5-*f*]quinoxaline (MeIQx), and 2-amino-3,4,8-trimethylimidazo[4,5-*f*]quinoxaline (4,8-DiMeIQx) [22,23]. The proposed pathways of AIA formation are shown in Figure 2A and B. The *N*-methyl-2-aminoimidazole portion of the molecule is derived from creatine, and the remaining parts of the IQ and IQx skeleton are assumed to arise from Strecker degradation products (e.g., pyridines or pyrazines), formed in the Maillard reaction between hexoses and amino acids [22,24]. An aldol condensation is thought to link the two molecules through an aldehyde or related Schiff base, to form IQ- and IQx-ring-structured HAAs. 2-Amino-1-methyl-6-phenylimidazo[4,5-*b*]pyridine (PhIP) can form in a model system containing phenylalanine, creatinine, and glucose [25]; however, PhIP can also form in the absence of sugar. Phenylalanine and creatine were shown, by dry heating of ^{13}C-labeled phenylalanine and creatine, to be precursors of PhIP [3]; the Strecker aldehyde phenylacetaldehyde was identified as a critical intermediate [26] (Figure 2B). Free radical intermediates have also been suggested to be involved in AIA formation [24,27,28]. IQx-type compounds arise in model systems containing glucose, glycine, and creatine through formation of pyrazine cation radical and carbon-centered radicals [28]; evidence for this pathway was obtained by heating of creatinine with 2,5-dimethylpyrazine or 2-methylpyridine and acetaldehyde, to produce 4,8-DiMeIQx or IQ, respectively [24].

1.2. Endogenous formation of HAAs

The β-carboline compounds 9*H*-pyrido[3,4-*b*]indole (norharman) and 1-methyl-9*H*-pyrido[3,4-*b*]indole (harman) are formed at considerably higher levels in tobacco condensates and cooked foods than are other HAAs (Figure 1) [29]. Norharman and harman are not mutagenic in *S. typhimurium* in the

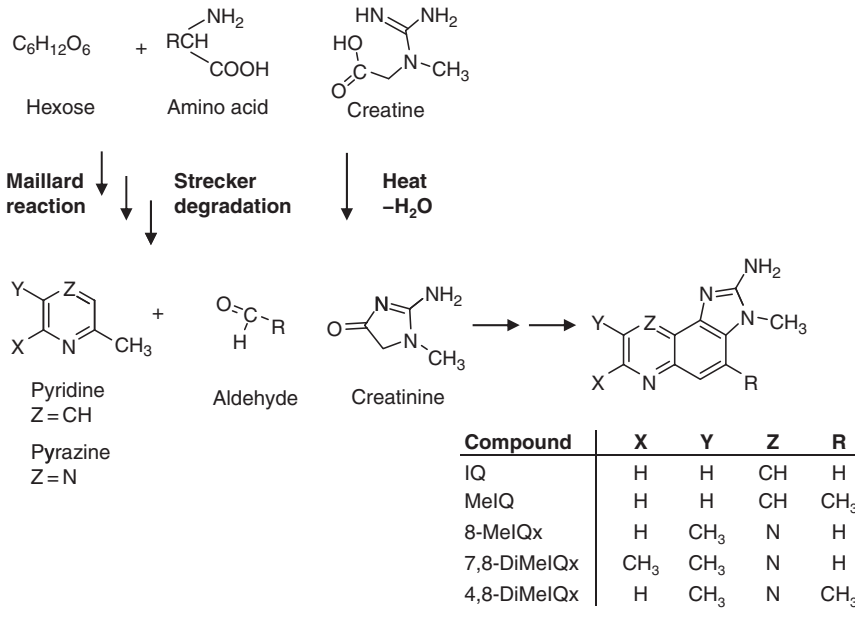

Compound	X	Y	Z	R
IQ	H	H	CH	H
MeIQ	H	H	CH	CH_3
8-MeIQx	H	CH_3	N	H
7,8-DiMeIQx	CH_3	CH_3	N	H
4,8-DiMeIQx	H	CH_3	N	CH_3

Figure 2A Mechanism of AIA formation. Adapted from Jagerstad *et al.* [22] with permission.

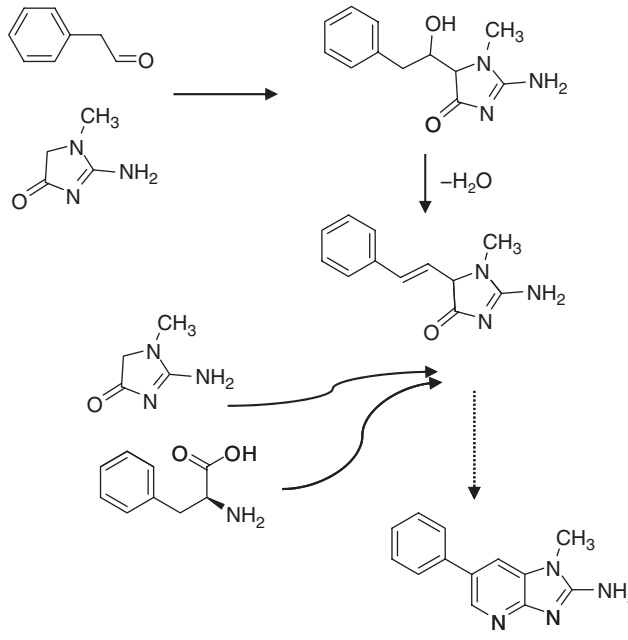

Figure 2B Mechanism of PhIP formation. Adapted from Murkovic [26] with permission.

presence or absence of liver S9 fraction mixture; however, a mutagenic effect is observed when these compounds are coincubated with aniline or *o*-toluidine [30]. This comutagenic effect is attributed to the formation of novel, mutagenic HAAs [31]. The structures of the compounds formed are 9-(4′-aminophenyl)-9*H*-pyrido[3,4-*b*]indole (amino-phenylnorharman, APNH), 9-(4′-amino-3-methyl-phenyl)-9*H*-pyrido[3,4-*b*]indole (aminomethyl-phenylnorharman, AMPNH), and 9-(4′-aminophenyl)-1-methyl-9*H*-pyrido[3,4-*b*]indole (amino-phenylharman, APH). The compounds are produced by the respective reactions of norharman with aniline; norharman with *o*-toluidine; and harman with aniline [32], during metabolism of the arylamines by a P450 complex. In the metabolism, an *ipso* attack on the aniline (or toluidine) can occur by norhaman or harman to produce these novel compounds (Figure 3A). Human P450s 1A2 and 3A4 catalyze the process [33]. APNH is a liver and colon carcinogen in F344 rats [34]. APNH has been detected at comparable concentrations in urine of smokers, nonsmokers, and patients receiving parenteral alimentation [35]. These results suggest that APNH is a novel mutagen/carcinogen that is produced endogenously.

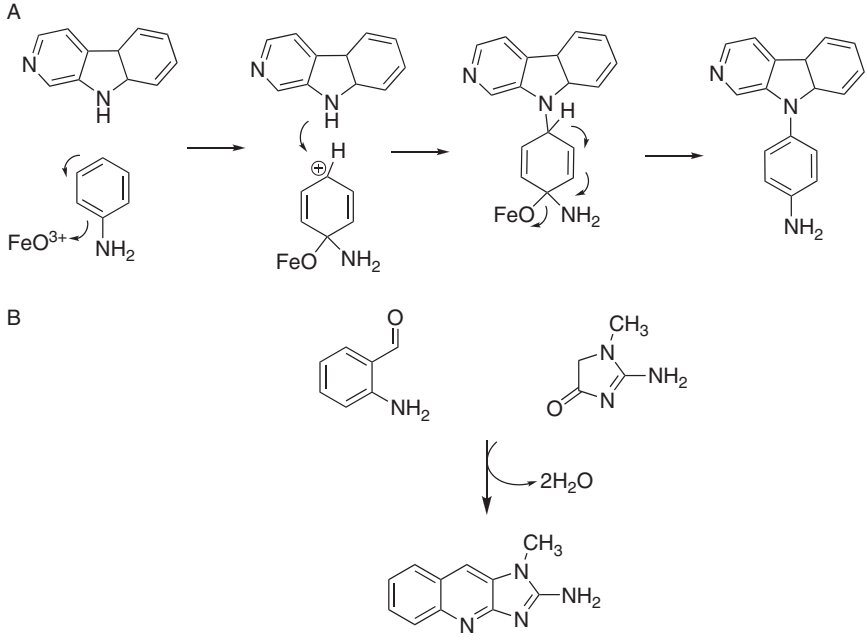

Figure 3 Endogenous AIA formation. (A) Formation of 9-(4′-aminophenyl)-1-methyl-9*H*-pyrido[3,4-*b*]indole (APH) via a P450 complex with aniline. Adapted from Oda *et al.* [32] with permission. (B) Formation of IQ[4,5-b] by reaction of 2-aminobenzaldehyde with creatinine. Adapted from Holland *et al.* [38] with permission.

2-Amino-1-methylimidazo[4,5-*b*]quinoline (IQ[4,5-*b*]) is a weak bacterial mutagen [36,37] and an isomer of IQ, a powerful animal carcinogen [5]. The amounts of IQ[4,5-*b*] measured in the urine of some human volunteers who consumed grilled beef exceeded the ingested dose [38], and base treatment of urine at 70 °C increased the amount of IQ[4,5-*b*] by more than 100-fold in urine of meat-eaters and vegetarians. IQ[4,5-*b*], but not IQ, 8-MeIQx, or PhIP was produced in urine incubated for 3 h at 37 °C: creatinine and 2-aminobenzaldehyde are the likely precursors of IQ[4,5-*b*] (Figure 3B). IQ[4,5-*b*] may form endogenously within the urine or other biological fluids. The contribution of these endogenously formed HAAs to the daily genotoxic burden of dietary HAAs remains to be investigated.

1.3. Estimates of HAAs in cooked meat, poultry, and fish

The amounts of HAAs formed in many types of meats, poultry, and fish, prepared under various cooking conditions, have been summarized in several review articles [3,39,40]. AIAs are the principal class of HAAs formed in meats prepared under common household cooking conditions [21,41–46]. The levels of HAAs formed are dependent upon the type of meat and the method of cooking: HAAs form in cooked meats at levels that can range from 0.01 up to several hundred nanograms per gram cooked meat. Panfrying or barbecuing of meats at high temperatures produces the greatest concentrations of HAAs. The roasting or broiling of meats generates lower amounts of HAAs, perhaps because less efficient heat transfer occurs, thereby retarding the migration of HAA precursors to the meat surface, where HAA formation occurs [44,45,47].

The influence of both the temperature of the cooking surface and the length of time of cooking on the amounts of HAAs formed in fried hamburgers is shown in Figure 4 (panels A and B). A cooking temperature of 160 °C gives rise to low concentrations of HAAs over time, but both the concentrations and the numbers of individual HAAs increase significantly at higher temperatures [21,43,47]. AIAs containing the 2-amino-1-methylimidazo[4,5-*g*]quinoxaline (I*g*Qx) skeleton, linear tricyclic ring isomers of the angular tricyclic ring-structured IQx compounds [6,48], are among the most abundant HAAs formed in cooked meats. The biochemical toxicology of these compounds warrants further investigation.

2. Mutagenesis and Carcinogenesis

2.1. Bioactivation of HAAs and DNA adduct formation

The mutagenic potency of an HAA is dependent upon the chemical structure and the ability of the molecule to undergo N-oxidation to form the reactive nitrenium ion [49]. Cytochrome P450s catalyze the oxidation

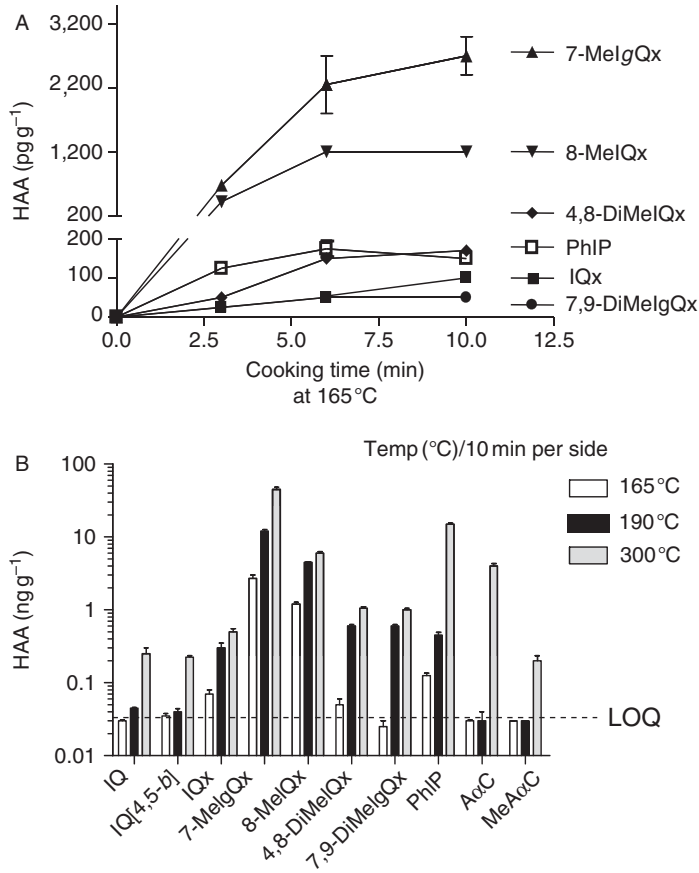

Figure 4 HAA formation as a function of (A) cooking time and (B) temperature. Adapted from Turesky *et al.* [6] with permission.

of the exocyclic amine groups of the HAAs to produce the genotoxic *N*-hydroxy-HAA metabolites [50–52]. Hepatic P450 1A2 and extrahepatic P450s 1A1 and 1B1 are the principal P450s that catalyze this reaction. The *N*-hydroxy-HAA metabolites can directly react with DNA, but the penultimate carcinogenic species are thought to be acetate or sulfate esters of the *N*-hydroxy-HAAs, esters that are produced by *N*-acetyltransferases (NATs) or sulfotransferases (SULTs) expressed in liver or extrahepatic tissues [53,54]. These esters undergo heterolytic cleavage to produce the reactive nitrenium ion that binds to DNA.

The reaction of the *N*-hydroxy HAA derivatives with DNA occurs at deoxyguanosine (dG) to produce dG-C8-HAA adducts: bond formation occurs between the C-8 atom of dG and the oxidized, exocyclic amine

group of the HAA [53,54]. DNA adducts also form at the N^2 atom of dG and the C-5 atom of the heterocyclic ring structures of IQ and MeIQx, indicating charge delocalization of the nitrenium ion over the heteronuclei of these HAAs (Figure 5) [53]. Recently, dA adducts of both IQ and MeIQx were identified; bond formation was proposed to occur between the N^6 atom of adenine and the C-5 atom of the IQ or MeIQx heteronucleus, to form 5-(deoxyadenosin-N^6-yl)-IQ (dA-N^6-IQ) [55] and 5-(deoxyadenosin-N^6-yl)-MeIQx (dA-N^6-MeIQx) [56], via a carbenium ion intermediate of the *N*-acetoxy-HAAs [57].

2.2.1. Biological effects of AA–DNA and HAA–DNA adducts

The conformational changes in DNA induced by HAA–purine base modifications are believed to be important determinants of the adduct's biological activity, and its propensity to induce frameshift mutations or base-pair substitutions during translesional synthesis [58–60]. The potential for an adduct to induce mutations or to block DNA polymerase activity is a function of the adduct structure, but the biological effects are strongly influenced by the sequence context of the oligonucleotide neighboring the adduct [58–60], as well as the particular polymerase or the host cell [61].

The isomeric *N*-(deoxyguanosin-8-yl)-IQ (dG-C8-IQ) and dG-N^2-IQ adducts were placed at the G_1 or G_3 site of the *NarI* recognition sequence (5′$\underline{G}_1\underline{G}_2C\underline{G}_3$CC-3′) [62]. The G_3 site is a known "hotspot" for frameshift mutation with the model arylamine N^2-acetyl-aminoflourene (AAF), but the G_1 site is not [58]. Human DNA polymerase (pol) η extended primers beyond template G-IQ adducts more efficiently than did pol κ, pol ι, or pol δ. Mass spectrometry (MS) of the pol η extension products revealed a single major product in each of four adduct templates. A cytosine was incorporated across the G_1 or G_3 modified with the dG-C8-IQ adduct; the extension product was largely error free. With the dG-N^2-IQ adduct placed at the G_3 position, a –2 deletion occurred in the newly formed sequence across the site of the adduct; however, when the dG-N^2-IQ adduct was placed at the G_1 position, the product formed at the site opposite the adducted base was error free and then the polymerase stalled. Thus, the pol η products yielded frameshifts with the dG-N^2-IQ adduct but not with the dG-C8-IQ adduct [62]. The translesional synthesis products of these isomeric dG-IQ adducts in the same sites of the *Narl* sequence were examined with *Escherichia coli* pol I Klenow fragment exo$^-$, *E. coli* pol II exo$^-$, and *Sulfolobus solfataricus* P2 DNA polymerase IV (Dpo4) [63]. The end products were profoundly different from those obtained with the human polymerases. The dG-C8-IQ adduct located at the G_3 position induced a two-base deletion in the sequences produced by all three bacterial polymerases, whereas error-free bypass and extension were observed for the adduct situated at the G_1 position. In contrast, the

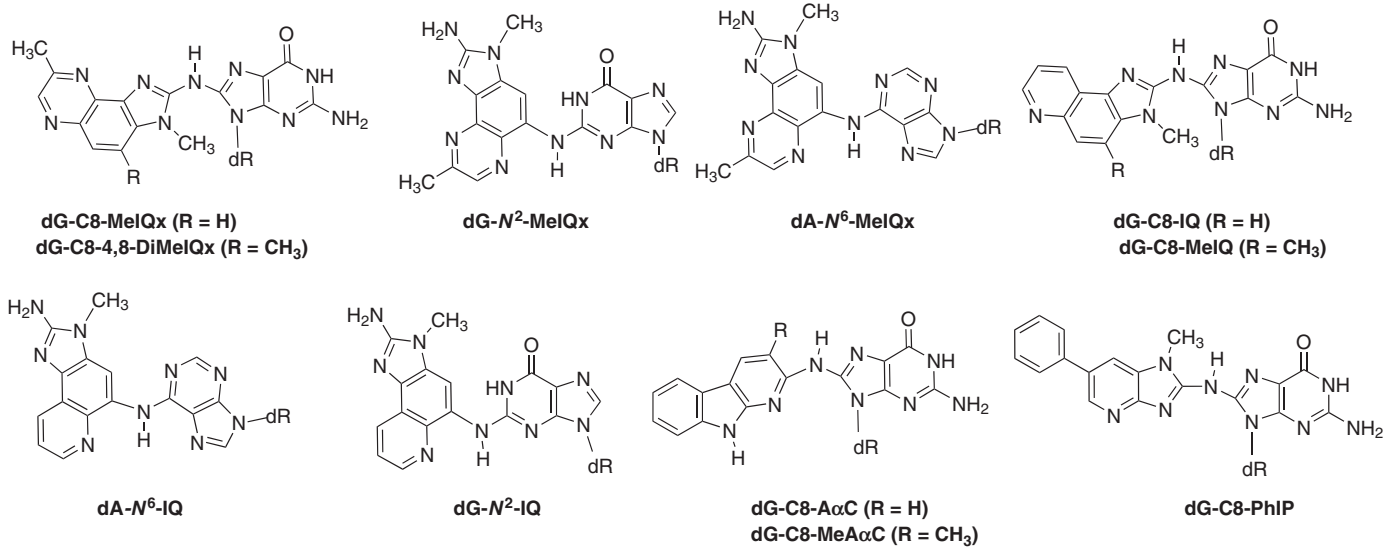

Figure 5 Structures of some representative HAA-DNA adducts.

dG-N^2-IQ adduct was bypassed and extended by all three polymerases, when placed at the G_1 position, and the error-free product was observed. However, when the dG-N^2-IQ adduct was situated at the G_3 position, the adduct exerted blocking effects, and it was bypassed and extended only by Dpo4 to produce an error-free product.

The mutagenic effects of *N*-(deoxyguanosin-8-yl)-PhIP (dG-C8-PhIP) were assessed in oligonucleotides containing a single dG-C8-PhIP adduct in the sequence context 5′-CCTCCTXGCCTCTC-3′, where $X = C$, A, G, or T was placed immediately at the 5′-flanking position to the dG-C8-PhIP. Translesional synthesis across the adduct was assessed by placement of the adducted oligonucleotide into a single-strand plasmid vector, in replicating simian kidney (COS-7) cells [64]. The GC → TA transversions were the most frequent mutations observed, particularly when dC was at the 5′-flanking position to the adduct. Single-base deletions were detected only when either dG or dT was 5′ to dG-C8-PhIP. The mutational frequency of dG-C8-PhIP (27.5%) was ninefold higher than that observed in a similar sequence with dG-C8-2-aminofluorene (AF) [65].

General frameshift or base-slippage models have been proposed to explain the mechanism of GC base-pair deletion for dG-C8-IQ and dG-C8-PhIP adducts [62–64]; these models have been based upon the NMR solution structural conformations of the adducts within oligodeoxynucleotide duplexes [66–68]. The glycosidic torsion angle of the dG-C8 adducts of PhIP and IQ exists in the *syn* form in some oligonucleotide sequence contexts, thus favoring a base-displaced intercalated model. Such a conformation can help explain the mechanism of frameshift mutations of these two adducts [66,68] (Figures 5 and 6). Neither the NMR structural conformations of the dG-N^2-IQ adduct within oligonucelotides, nor the mechanisms by which these structural perturbations influence translesional synthesis have not been investigated. In summary, the studies above show that each individual HAA-DNA adduct structure and the location of the adduct within the sequence context of the oligonucleotide can affect the fidelity and the catalytic efficiency of each of the polymerases in a unique manner.

The structural conformation of the HAA-DNA adduct can also influence the persistence and rate of removal of the adduct *in vivo*. Some dG-C8 arylamine and HAA-DNA adducts that adopt the glycosidic torsion angle in the *syn* conformation can cause greater perturbation of the DNA duplex at the site of carcinogen adduction than is seen for the glycosidic linkage of the dG-N^2 adducts; the latter often adopt the normally-occuring *anti* conformation [66–71] (Figure 6). The differing extents of structural perturbation induced by these adducts in duplex DNA are believed to result in variable degrees of recognition and extents of enzymatic removal of the adduct, by the nucleotide excision repair complex. The dG-C8-IQ and dG-C8-AAF adducts both of which can

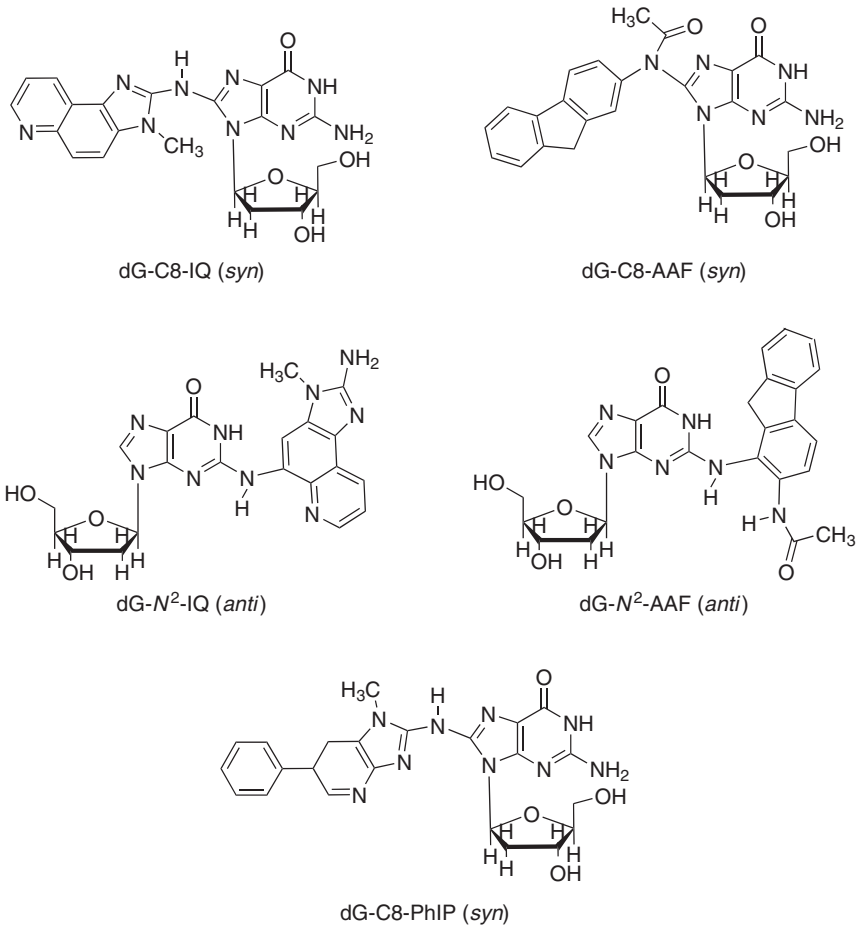

Figure 6 DNA adducts of IQ, AAF, and PhIP. The dG-C8 adducts are drawn with glycosidic linkage occurring in the *syn* conformation and the dG-N^2 adducts are drawn with the glycosidic linkage existing in the normally occuring *anti* conformation.

exist in the *syn* conformation, are rapidly removed from tissues in rodents, whereas the isomeric dG-N^2-IQ and dG-N^2-AAF, which exist in the normally occuring *anti* conformation, persist [72,73]. In the case of IQ, the proportion of dG-N^2-IQ among the total adducts increased in slowly dividing tissues of nonhuman primates over time, apparently due to the much slower repair rate than is seen for dG-C8-IQ, and the dG-N^2-IQ adduct became the predominant lesion during long-term feeding studies [73]. Because of their persistence, the dG-N^2 adducts are expected to play a significant role in the tumorigenic properties of aromatic amines and HAAs [73,74].

2.2. Bacterial and mammalian mutagenesis

The early investigations on bacterial mutagenesis of HAAs were conducted with liver homogenates from rodents pretreated with polychlorinated biphenyls (PCBs), so as to augment the levels of P450s (P450 1A1 and 1A2) that N-hydroxylate HAAs. 2-amino-3,4-dimethylimidazo[4,5-*f*]quinoline (MeIQ), IQ, and MeIQx rank among the most potent mutagens ever tested in the Ames bacterial reversion assay [5,75,76], while PhIP and AαC are, respectively, about 100-fold and 1,000-fold weaker in potency, under similar assay conditions. The strong propensity of some HAAs to induce frameshift revertant mutations in *S. typhimurium* TA98 and TA1538 tester strains is attributed to a preference by these compounds to react at a site about nine base pairs upstream of the original CG deletion in the *his*D^+ gene sequence, within a run of GC repeats [77]. The existence of this "hotspot" is consistent with the presence of dG–HAA adducts, which can induce CG deletions during translesional DNA synthesis [62,64]. Several HAAs also induce strong genotoxic effects in strain TA100, which reverts to the wild type through point mutations. Many HAA–DNA lesions can be repaired, since the mutagenic potencies of several HAAs are 100-fold less active in the uvrB^+ proficient *S. typhimurium* strain [78]. The mutagenic potencies of even some of the weaker HAAs can be increased by up to 250-fold in *S. typhimurium* TA1538/1,8-DNP-derived strains that have been engineered to express NAT or SULT proteins [79,80], and also in mammalian cells [79,81,82], thereby demonstrating the importance of xenobiotic metabolism enzymes (XMEs) in the biological properties of HAAs [83].

The mutagenic effects of HAAs in other bacterial genes such as *lacZ, lacZ*α, and *lacI* of *E. coli* also occur primarily at GC base pairs. The types of mutations are dependent upon DNA sequence context and upon the assay system. The genotoxicity of aromatic amines and HAAs has been studied in *E. coli* cells carrying a mutated copy of the *lacZ* gene that reverts back to the wild-type gene by a –2 GC frameshift mutation [84]. These bacteria have been genetically engineered to simultaneously express human P450 1A2, NADPH cytochrome P450 reductase, and NAT, so that the bioactivation of HAAs occurs within the cell. Thus, the formation of the chemically reactive metabolites occurs in close proximity to the target gene, which enhances the sensitivity of the mutagenicity assay.

Other bacterial systems have used the induction of the SOS response in *S. typhimurium* NM2009 as a measure of DNA damage induced by HAAs; these systems possess high bacterial *O*-acetyltransferase (OAT) activity and contain a *umuC* regulatory sequence attached to the *lacZ* reporter gene [85]. More recently, such strains have been modified to express human P450 enzymes, NADPH-cytochrome P450 reductase, and bacterial OAT [86]. These tester strains have been used to compare genotoxic potencies of HAAs and to identify specific human P450s that are involved in the

biotransformation of HAAs. The findings confirm that P450 1A2 is a principal cytochrome P450 involved in bioactivation of HAAs.

Short-term bacterial mutagenesis assays have served as an effective screening tool for the identification of mutagenic HAAs in complex food matrices and for the characterization of enzymes involved in bioactivation of HAA; however, these assays cannot reliably predict carcinogenic potency. The huge differences in range seen for the mutagenic potencies of HAAs in bacteria are not observed in mammalian cell assays or in long-term carcinogen bioassays, where the total doses required to induce cancer at 50% incidence (TD_{50}) fall generally within a tenfold range [5].

In mammalian cells, HAAs often induce base-pair substitutions at guanines as the prominent mutations; however, frameshift mutations at guanines also occur, depending upon the base sequence context and the assay employed. The occurrence of these mutational events is consistent with the chemical DNA binding data, which show that guanine is the principal target for HAA-DNA adduct formation [53,54]. The PhIP-induced mutations at the *hgprt* locus in human lymphoblastoid cells occur predominantly through GC → TA transversions [87], while CG → AT and GC → TA transversions have been reported at PhIP-induced mutants in the *aprt* and *dhfr* genes of Chinese hamster ovary (CHO) cells [88,89]. PhIP also predominantly induced GC → TA transversions at the *hprt* locus in Chinese hamster V79 cells; however, 13% of the mutants displayed a –1 frameshift mutation in the 5′-GGGA-3′ sequence [90], which is identical to a sequence that is mutated in the *Apc* tumor suppressor gene of rat colon tumors induced by PhIP [91]. In CHO cells, 80% of the mutations induced by PhIP were single-base substitutions at GC base pairs, with 57% of those reported as GC → TA transversions. The study on the mutagenicity of IQ at the *hgprt* locus in human lymphoblastoid cells also revealed that about 30% of the mutations were guanine deletions, principally occurring in a run of six guanines in exon III [92]. GC → TA and GC → CG transversions were also noted. The majority of the identified mutations occurred at GC pairs, suggesting that either the dG-C8-IQ or the dG-N^2-IQ adduct is the premutagenic lesion.

The mutagenic potencies of MeIQx, PhIP, and AαC were investigated in nucleotide excision repair-deficient CHO cells that had been constructed with a stable transfection of human P450 1A1 or 1A2, plus either human *NAT2*4* (rapid acetylator) or *NAT2*5B* (slow acetylator) allele. The capacity of the cells to bioactivate the HAAs, to form DNA adducts and induce mutations in the *hprt* locus, was dependent upon the expression of P450s and NAT. In the case of MeIQx [81], DNA adduct formation and genotoxicity occurred only in cells expressing both P450 1A2 and NAT2 4 protein, AαC was bioactivated most efficiently by cells expressing P450 1A2 and NAT2 4 protein, followed by lesser activation in cell lines expressing P450 1A2 and the NAT2 5 protein, whereas no adduct

formation or genotoxicity was observed in cells just expressing P450 1A2 [93]. For PhIP, the differences in bioactivation were only modest among the various cell lines expressing only P450 1A2, or P450 1A2 and NAT2 4, or P450 1A2 and NAT2 5 proteins [82]. The N-hydroxylated metabolite of PhIP appears to be a poor substrate for NAT2; an endogenous SULT in the CHO cells may have catalyzed the binding of PhIP to DNA [82]. CHO cells stably transfected with mouse *P450 1A2* and human *NAT2*4* alleles were also shown to efficiently activate IQ, but not PhIP, to a genotoxicant [79,94]. Thus, the genotoxic potencies of AαC, MeIQx, and PhIP are affected differently by *NAT2* polymorphisms. These findings signify that the identification of the specific HAA exposure is very important in any molecular epidemiological investigation that seeks to assess the roles of HAAs and *NAT2* genetic polymorphism in cancer risk [93].

Transgenic (TG) mouse and rat models have been established to enable the measurent of genotoxicity *in vivo*, with the *lacZ* or *lacI* transgene used as the target gene. The TG mutation assays use λ phage-based TG rodents: Muta™ Mouse [95,96] or Big Blue® Mouse or Big Blue®Rat models [97]. These assays employ reporter genes of the bacterial *lac* operon. The *lacZ* encodes β-galactosidase and is the reporter gene in Muta Mouse, and the *lacI* gene, which encodes the repressor protein of the *lacZ* gene, is the reporter gene in the Big Blue® Mouse and Rat models. Either gene is stably incorporated into mouse or rat chromosomes as part of a λ shuttle vector; the vector is easily recovered as phage particles from genomic DNA, by *in vitro* packaging reactions [98]. In an assay, TG rodents are exposed to the putative mutagen, followed by a suitable expression period to "fix" the mutation. The shuttle vector is recovered from various tissues and incubated with λ *in vitro* packaging extracts, which initiate packaging of the shuttle vector into infectious lambda bacteriophage. The recovered shuttle-vector phage is then used to infect restriction-deficient *E. coli* K12 cells, and mutants are screened.

PhIP induced a number of one-base deletions in the *lacI* gene of the colon mucosa of the TG Big Blue® Mice and Big Blue® Rats [99]. A characteristic deletion of a guanine base at 5′-GGGA-3′ sequence reported in the *Apc* gene of rat colon cancers induced by PhIP [91] accounted for 7 and 10% of the total mutations of this *lacI* gene in Big Blue® Mice and Big Blue® Rats, respectively. This mutation was also observed in mammary glands of female Big Blue® Rats treated with PhIP: 6% of the mutations that were found displayed a GC base-pair deletion at the 5′-GGGA-3′ site [100]. If this GC base-pair deletion at the 5′-GGGA-3′ sequence can be shown to be a specific and unique mutation induced by PhIP, it may be used as a molecular marker for evaluating the role of PhIP in human cancers. The prostate is a target tissue of cancer induced by PhIP in male rats [101], and PhIP was also reported to induce both GC → TA transversions and –1G frameshifts of GC base pairs in the *lacI* gene of prostate of Big Blue® male rats, at high frequency [102,103].

The *lacI* and *lacZ* reporter genes appear to be useful predictors of PhIP-induced carcinogenesis, and the mutational characteristics of MeIQ in the *lac* genes correlated well with those characterized in the *Ha-ras* gene of MeIQ-induced mouse forestomach tumors and rat Zymbal gland tumors [104]. These results suggest that the mutational characteristics of each chemical are conserved across different genes in multiple species, in the processes of carcinogenesis induced by genotoxic carcinogens. However, the relationship linking DNA adduct formation, mutation frequencies in the *lacI/lacZ* gene, and cancer incidences of HAAs, including MeIQ [105] and IQ [106], has not been shown to be a quantitative correlation. Moreover, HAAs induce mutations in *lacI or lacZ* in organs that do not develop tumors. Some of the discrepancies between mutagenesis and carcinogenesis can be attributed to different cell proliferation rates in different organs that affect mutation frequencies. In addition, the number of mutations and the specific types of genetic alterations required for cancer development can also vary across different organs [105].

Other *in vivo* mutation systems have been used to assess HAA carcinogenesis. PhIP, but not MeIQx, was shown to induce intestinal stem-cell mutations at the Dlb-1 locus in Dlb-1a/b heterozygous mice [107]. PhIP was also reported to induce tumors in the C57B/6J-Min/+ (multiple intestinal neoplasia) mouse model and to truncate the Apc protein at an elevated frequency [108].

2.3. Experimental animal carcinogenesis

Long-term 2-year feeding studies have been conducted on the tryptophan (Trp-P-1, Trp-P-2) and glutamic acid (2-amino-6-methyldiprido[1,2-a:3′,2′-*d*]imidazole (Glu-P-1), 2-aminodiprido[1,2-a:3′,2′-*d*]imidazole (Glu-P-2)) pyrolysates, AαC, MeAαC, IQ, MeIQ, MeIQx, and PhIP, in both mice (CDF_1) and F-344 rats, of both genders. All 10 HAAs tested in rodents have been found to be carcinogenic. These compounds induce tumors at multiple organs, including liver, lung, hematopoietic system, forestomach, and blood vessels in mice; and colon, small intestine, prostate, hematopoietic system, liver, Zymbal gland, skin, clitoral gland, mammary gland, oral cavity, and urinary bladder in rats [5,109]. The C57BL/6 (B6) mouse model has recently been used in carcinogenesis studies [99,110]. This mouse strain is more susceptible than is the CDF_1 mouse to intestinal carcinogenesis of several classes of genotoxicants, including alkylating agents [111] and HAAs [112]. In long-term feeding studies, MeIQ induced cancer of the cecum and colon [112] and PhIP induced small intestinal tumors [113] in C57BL/6 mice. IQ was also reported to be a powerful liver carcinogen in nonhuman primates [114].

Genetic alterations arise in tumor-related genes of experimental animals during long-term feeding studies with HAAs ([104,115–117] and

references therein). The GC → TA transversion at codon 13 at the second position in the *Ha-ras* gene was predominantly observed in mouse forestomach and rat Zymbal gland tumors induced by MeIQ. In contrast, several types of mutation were detected in the *ras* family genes in rat Zymbal gland tumors induced by IQ; the presence of an additional methyl group at position 4 of MeIQ gave rise to a remarkable difference in the mutational fingerprint. The *K-ras* mutations were rare, and no mutations were detected in either the *N-ras* or the *Ha-ras* gene in any of the tumors of the colon. Similarly, *p53* gene mutations were not detected in any rat colon tumors induced by these HAAs even though 60–70% of human colon cancers have mutations in the *p53* gene [104]. Therefore, HAAs could represent suitable model compounds for use in investigations of sporadic colon carcinogenesis, a process which does not involve mutations in the *p53* gene [104]. However, mutations in either *Ha-ras* or *Ki-ras* and the *p53* genes were found in rat Zymbal gland tumors induced by IQ [104]. IQ also induced mutations in the *p53* gene in 4 of 20 nonhuman primate subjects that developed hepatocellular carcinoma during long-term feeding studies; three of the mutations contained GC → TA transversions, and one possessed a GC → AT transition [118].

The *APC* gene plays a major role in human colon carcinogenesis and its genetic alteration is considered to be an initial or early mutational event in that process [119]. Alterations of the *APC* gene were more prominent in PhIP-induced than in IQ-induced rat colon carcinogenesis [91]. In that study, four of the eight colon tumors caused by PhIP had mutations in the rat *Apc* gene and featured a guanine deletion from 5′-GGGA-3′ sequences. This specific GC base-pair deletion in 5′-GTGGGAT-3′ at codon 635 of the *Apc* gene occurs as an early mutation in the colon of male rats exposed to PhIP for as little as 1 week [120]. One of the hotspots of PhIP-induced mutation at the 5′-GTGGGAT-3′ sequence around codon 635 in the rat is conserved in the human *APC* gene and may be a signature mutation of this HAA [116]. The mutations in the *Apc* gene of IQ-induced colon tumors in rats were detected in only 2 of 13 tumors, and no specific or characteristic mutations were identified [91,116].

3. Metabolism and Biomarkers

3.1. Phase I and phase II enzymes

HAAs undergo extensive metabolism, by phase I and II enzymes, in experimental animals and humans [83,121–123]. The major pathways of HAA metabolism are depicted in Figure 7. Cytochrome P450 1A2 primarily expressed in liver [126] and P450s 1A1 and 1B1 expressed in extrahepatic tissues [51,127] are the principal P450 enzymes (http://www.cypalleles.ki.se)

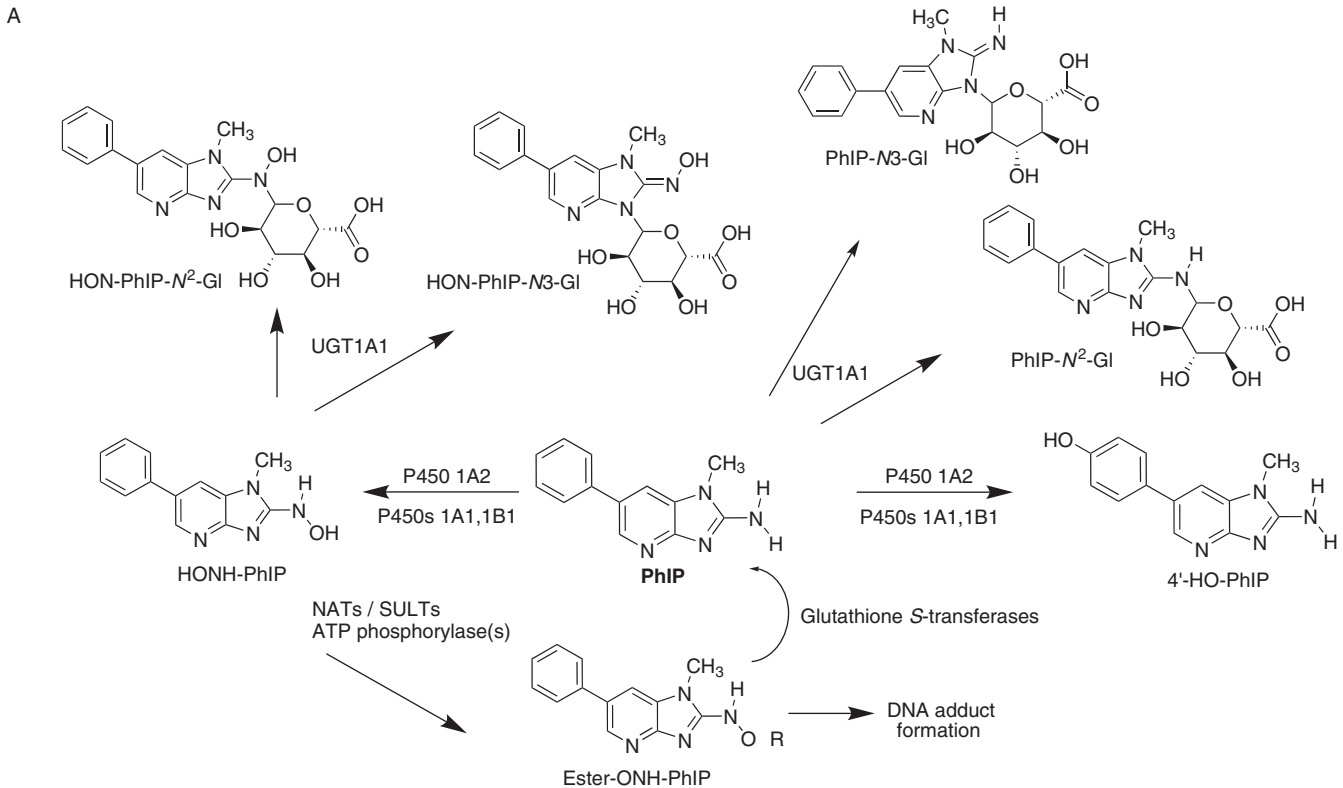

Figure 7 (Continued)

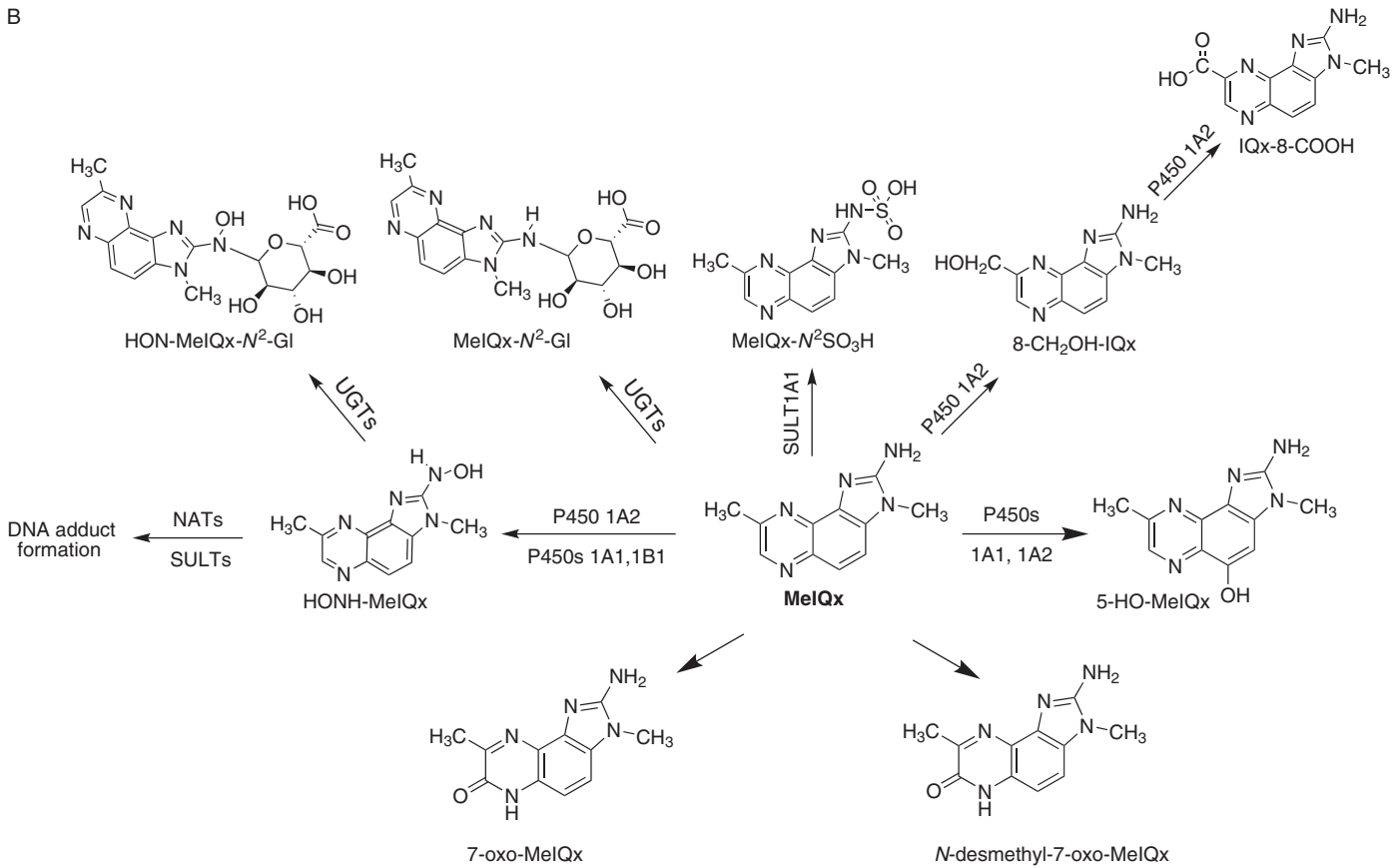

Figure 7 Major pathways of PhIP and MeIQx metabolism in experimental animal models and humans. 2-Amino-3,8-dimethyl-6-hydro-7*H*-imidazo[4,5-*f*]quinoxalin-7-one (7-oxo-MeIQx) formation is catalyzed by bacteria in the fecal flora [124], but the P450s or oxidases present in human hepatocytes [125] that catalyze this reaction have not been determined.

involved in oxidation of HAAs. Metabolic studies revealed that *P450 1A2*-null mice still possess significant activities of N^2-hydroxylation and DNA adduction of PhIP: mouse P450 2C enzymes may be the major P450 isoform involved in N-oxidation of PhIP, in livers of *P450 1A2*-null mice [128].

There are important species differences in the regioselectivity of P450-mediated oxidation of HAAs. P450-mediated N-demethylation of IQ and MeIQx occurs in rodents and nonhuman primates [129,130], but this metabolic pathway is not prominent in the metabolism of these HAAs in experiments conducted *in vitro* with human liver microsomes or *in vivo* [50,131–135]. Both the human and rodent orthologues of P450 1A2 catalyze the bioactivation of HAAs through N-oxidation of the exocyclic amine groups. However, human P450 1A2 catalyzes the detoxication of PhIP by 4′hydroxylation only poorly, while the rat orthologue efficiently carries out this reaction [50,121]. In the case of MeIQx, human P450 1A2 catalyzes the oxidation of the C^8-methyl group of 8-MeIQx, to form 2-amino-3-methylimidazo[4,5-*f*]quinoxaline-8-carboxylic acid (IQx-8-COOH); this reaction is the major pathway of metabolism and detoxication of 8-MeIQx in humans [131,132]. The rat P450 1A2 orthologue does not catalyze IQx-8-COOH formation, but it does catalyze the detoxication of MeIQx through C-5 hydroxylation [131]. However, human P450 1A2 does not catalyze C-5 hydroxylation of MeIQx.

Phase II conjugation reactions occur at the exocyclic amino group of HAAs, to form detoxication products in both experimental animals and humans. The uridine diphosphate glucuronosyltransferases (UGTs) are a superfamily of enzymes that catalyze the glucuronidation of many endogenous and xenobiotic compounds. UGT proteins are divided into two families, UGT1A and UGT2B, based on sequence homologies (http://www.pharmacogenomics.pha.ulaval.ca/sgc/ugt_alleles/index.html) [136]. Both PhIP and *N*-hydroxy-2-amino-1-methyl-6-phenylmidazo[4,5-*b*]pyridine (HONH-PhIP) undergo conjugation by multiple human UGT1A isoforms to produce N^2- and N^3-glucuronide conjugates [121,134,135,137–139]. UGT activity toward PhIP and HONH–PhIP has been detected in human liver and in colon microsome samples [137,140–143]. The glucuronide conjugates of HONH-PhIP have been viewed as detoxication products [144], although bacterial glucuronidases can hydrolyze N^3-(β-1-glucosiduronyl-2-(hydroxyimino)-1-methyl-6-phenylimidazo[4,5-*b*]pyridine (HON-PhIP-N^3-Gl) to liberate HONH-PhIP for further metabolism and potential DNA adduct formation [145]. There are interspecies differences in the regioselectivity of glucuronidation of PhIP and HONH-PhIP. In rodents, the endocyclic N^3 atom is the preferential site of glucuronidation [121,146], whereas the exocyclic N^2 atom is the principal site of glucuronidation in humans [134,135,137]. Both MeIQx and *N*-hydroxy-2-amino-3,8-dimethylimidazo[4,5-*f*]quinoxaline (HONH-MeIQx) also undergo glucuronidation in rodents, nonhuman primates, and humans [132,141].

There are two distinct NAT isoenzymes, designated NAT1 and NAT2 (http://louisville.edu/medschool/pharmacology/nat/). NAT2 is expressed primarily in the liver, whereas NAT1 appears to be more prominently expressed in extrahepatic tissues [147,148]. N-Acetylation is an important mechanism of detoxication of primary arylamines [148]. NATs do not catalyze the detoxication of HAAs containing the *N*-methyl-2-aminoimidazole moiety [149], but both NAT1 and NAT2 isoforms do N-acetylate AαC and several other pyrolysate HAAs [122]. The HONH-AIA and pyrolytic HONH-HAAs serve as substrates for NATs and undergo O-acetylation, primarily by NAT2, to form the *N*-acetoxy species, which then binds to DNA [149,150]; HONH-AαC undergoes bioactivation by both NAT1 and NAT2 isoforms [151].

The SULTs belong to a superfamily of genes that is divided into two subfamilies [152]: the phenol SULTs (SULT1) and the hydroxysteroid SULTs (SULT2). A third, less well-characterized subfamily of brain-specific SULTs has also been reported [153]. SULT1A1 and SULT1A2 preferentially catalyze the sulfation of small planar phenols such as 4-nitrophenol and the estrogens, while SULT1A3 preferentially catalyzes the sulfate conjugation of monoamine derivatives. Human SULT1A1 catalyzes the detoxication of IQ and MeIQx to form sulfamates [122,154]. These SULTs can also bioactivate the N-hydroxyated HAA metabolites, presumably by formation of the reactive *N*-sulfate esters. Human SULT1A1 and SULT1A2 catalyze the binding of the *N*-hydroxy metabolites of the aromatic amine 4-aminobiphenyl, as well as PhIP and AαC, to DNA. SULTs also increase the genotoxic effects of IQ, *N*-hydroxy-2-amino-3-methylimidazo[4,5-*f*]quinoline (HONH-IQ), AαC, and MeAαC in bacterial or mammalian cells [83]. SULT1E1, which is under hormonal regulation, catalyzes the binding of HONH-PhIP to DNA in cultured human mammary cells; this SULT may play a role in carcinogen bioactivation in breast tissue [155].

3.2. Nitrosation reactions

HAAs, such as IQ and MeIQx, that contain the 2-amino-*N*-methylimidazo moiety are resistant to nitrosation under acidic conditions, whereas many pyrolytic HAAs readily undergo nitrosation, followed by oxidation [156]. However, IQ and MeIQx can undergo nitrosation with nitric oxide, under neutral pH conditions, to form 2-nitrosoamino-3-methylimidazo[4,5-*f*] quinoline (N-NO-IQ) and 2-nitrosoamino-3,8-dimethylimidazo[4,5-*f*] quinoxaline (N-NO-MeIQx). Both N-NO-IQ and N-NO-MeIQx are converted to reactive species that can form covalent DNA adducts [157,158]. A mechanism for the NAT2-catalyzed bioactivation of N-NO-MeIQx has been proposed (Figure 8) [159]. Reactive intermediates derived from N-NO-IQ and N-NO-MeIQx have also been suggested to form under acidic pH, on the basis of detection of azo intermediates that are

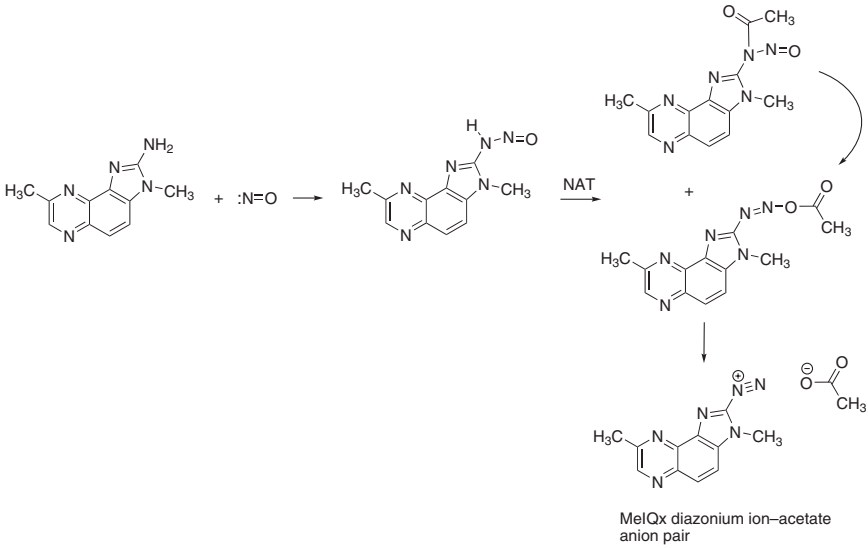

Figure 8 NO-N-MeIQx formation and metabolic activation by NAT. Adapted from Zenser *et al.* [159] with permission.

dimerization products derived from the nitrenium ion [157,158]. The bioactivation of AIAs via nitrosation could be an alternative mechanism to P450-mediated N-oxidation of HAAs and contribute to their genotoxicity, under inflammatory conditions, during which elevated levels of NO can arise [159].

3.3. Genetic polymorphisms in genes that encode xenobiotic enzymes involved in HAA bioactivation

Genetic polymorphisms in genes that encode for enzymes that catalyze the activation and/or detoxification of HAAs could account for interindividual differences in susceptibility to this group of carcinogens [160]. The constitutive P450 1A2 mRNA expression levels in human liver can vary by as much as 15-fold [161], and interindividual expression of P450 1A2 protein can vary by 60-fold [50,162]. Environmental and dietary factors [163], varying extents of CpG methylation [164], and genetic polymorphisms in the upstream 5′-regulatory region of the *P450 1A2* gene [165,166], which affect the level of P450 1A2 mRNA expression, can all lead to variations in P450 1A2 protein levels. However, the genotype responsible for the >60-fold range of interindividual differences in human hepatic P450 1A2 constitutive expression is still not well understood [167]. In contrast to what is seen in humans, the amount of P450 1A2 protein in the liver of inbred rodent varies by only severalfold across different strains [50]. The

level of P450 1A2 protein expression in human liver, on average, is several- to 10-fold or greater than the level of P450 1A2 expression in liver of inbred rodents [50,162]. The interspecies differences in the level of P450 1A2 expression, catalytic activity, and regioselectivity of P450 1A2-catalyzed oxidation influence the toxicological properties of HAAs and must be considered in any assessment of human risk.

More than 20 genetic polymorphisms have been identified in these NAT genes; these polymorphisms can affect the catalytic activity of NATs toward AAs and HAAs [147,168]. In humans, a common genetic polymorphism is seen in arylamine NAT2, giving rise to rapid and slow acetylator phenotypes. The *NAT2*4* wild-type allele is associated with the rapid acetylator phenotype, whereas the *NAT2*5B* allele is the most common haplotype associated with the slow acetylator phenotype [147,148]. Some *N*-hydroxy-AIA and *N*-hydroxy-pyrolytic HAAs are preferentially or exclusively activated by the NAT2 4 protein, but not by the NAT2 5 protein [81,82,93]. The role of NAT2 genetic polymorphism in urinary bladder cancer risk, in factory workers or tobacco smokers exposed to aromatic amines, is well documented [168,169]. This increased cancer risk has been attributed to the impaired capacity of slow N-acetylator individuals to detoxify aromatic amines, which are human bladder carcinogens [168]. The epidemiological data on the role of NAT2 genetic polymorphism, in susceptibility to various cancers, suggest that the role of this polymorphism varies both with the specific carcinogen and with the organ site [147,148].

In contrast to aromatic amines, many HAAs are not detoxified by NAT2, but their N-hydroxylated metabolites undergo O-acetylation by NAT2 to form reactive *N*-acetoxy intermediates that bind to DNA [54]. The epidemiological studies on the role of NAT2 genetic polymorphisms and cancer risk of HAAs have provided inconsistent findings [147,148]. Since both phase I and II enzymes are required to bioactivate HAAs, risk may be markedly elevated in individuals who are both rapid N-oxidizers and rapid *O*-acetylators. Cigarette smoking is a known risk factor for colorectal cancer [170]. Two epidemiological studies reported a marked increased risk of colorectal cancer among individuals who were tobacco smokers and who frequently ate meats cooked well done. Both tobacco smoke and well-done meats are sources of exposures to HAAs. The elevated cancer risk was observed only in individuals possessing high activities of both the P450 1A2 and NAT2 enzymes; these subjects had up to an 8.8-fold increased risk of colorectal cancer [171,172]. It is noteworthy that AαC, a carcinogen formed in substantial amounts in tobacco smoke and well-done cooked meats, is a potent genotoxicant in the colon of rodents [173,174].

Single-nucleotide polymorphisms (SNPs) in the *SULT* genes can result in functional changes in the stability or catalytic activity of the translated

protein. In general, these SNPs are fairly uncommon in the population but some, most notably for SULT isoform 1A1, are common. They have been associated not only with cancer risk for a variety of tumor sites, but also with response to therapeutic agents [153]. The epidemiological studies on genetic polymorphisms of the SULTs and the cancer risk posed by HAAs are limited and have provided inconsistent results. A GC → AT transition at codon 213 (CGC/Arg to CAC/His) of the *SULT1A1* gene is a common genetic polymorphism [175]. The gene product of this allele has substantially lower enzyme activity than does the gene product of the wild-type allele. Women who possess the *Arg/Arg* genotype *(SULT1A1*1)* and who frequently ate well-done cooked meats were found to be at an elevated risk for breast cancer (odds ratio 3.6); no such association was evident in women with the *His/His* genotype, in that subpopulation of women who ate meat [176]. Thus, the *His/His* genotype, characterized by poor bioactivation of HONH-HAAs and HONH-AAs [177], was protective against breast cancer in this above-described exposed population. Other studies are warranted to confirm this observation. However, genetic polymorphisms in *SULT1A1* and *SULT1A2* have not been demonstrated to influence colorectal cancer risk [178], and the variant *SULT1A1*2* allele did not show an association with prostate cancer risk [179].

3.4. Measurement of HAAs and their metabolites in human urine

Urine is a useful biological matrix for the measurement of HAAs and their metabolites, given that large quantities can be obtained noninvasively. The measurements of urinary HAAs and their metabolites do not shed light on DNA damage, but they can reflect the relative capacity of an individual to bioactivate and detoxicate the procarcinogen. HAA urinary biomarkers can be used to probe the interrelationship between HAA exposure and P450 1A2 and phase II enzyme metabolism, which can affect the cancer risk [180]. A recent study reported that elevated urinary mutagenicity of meat-eaters ascribed to HAAs is positively associated with an increase in colorectal adenoma risk [181]: this finding reinforces the hypothesis that HAAs may contribute to the etiology of colorectal cancer.

Several different analytical approaches have been devised to isolate HAAs and/or their metabolites from human urine. The analysis is technically challenging, because the concentrations of HAAs and their metabolites are often below the parts per billion (ppb) level in urine. Moreover, the polar and ionic nature of the metabolites presents difficulties for their selective isolation from thousands of other components in the urine matrix [182]. The isolation techniques include organic solvent extraction [183,184], solid-phase extraction (SPE) with reverse-phase resin [185] or a mixed-mode reverse-phase cation exchange resin [135], use of molecularly imprinted polymers [186], or immunoaffinity methods [187,188]. The

quantification of HAAs has been done by gas chromatography and negative-ion chemical ionization mass spectrometry (GC-NICI-MS) [183,184,188], by liquid chromatography-electrospray ionization/tandem mass spectrometry (LC-ESI/MS/MS) [185,186], and by fluorescence detection [189]. Urinary metabolites of HAAs have been detected by LC-ESI/MS/MS, following SPE [133–135], or indirectly after chemical reduction or acid hydrolysis of HONH-PhIP or HONH-MeIQx glucuronide conjugates, employing either LC-ESI/MS/MS or GC-NICI-MS [190,191]. A facile extraction method, employing a mixed-mode reverse-phase cation exchange SPE resin, was recently reported [135] for the simultaneous isolation of PhIP, its glucuronide conjugates, and the glucuronide conjugates of HONH-PhIP, from urine of meat-eaters. The quantification of the analytes was done by LC/MS: the limit of quantification (LOQ) of PhIP was five parts per trillion (ppt) and the LOQ values for the glucuronide conjugates were at 50 ppt. The use of this method of analysis should aid in identifying genetic polymorphisms in xenobiotic metabolism enzymes that influence the biotransformation of PhIP and should allow us to assess chemoprotective agents that inhibit the metabolism and the potential deleterious effects of PhIP.

Most of the human urinary metabolism studies have been conducted on MeIQx or PhIP. Both compounds are rapidly absorbed from the gastrointestinal tract and eliminated in urine as multiple metabolites and only several percent or less of the dose is excreted in urine as the unaltered parent compound within 24 h of consumption of grilled meats [132–135,183,187,192]. In the case of MeIQx, lower levels of the unaltered compound were found in urine from individuals with high P450 1A2 activity than in urine from subjects with low P450 1A2 activity, thus demonstrating the importance of this enzyme in the metabolism of MeIQx [193]. In pharmacokinetic studies with furafylline, a selective mechanism-based inhibitor of P450 1A2 [194], up to 91% of the elimination of MeIQx and 70% of the elimination of PhIP, could be accounted for by P450 1A2-catalyzed metabolism [183]. The major metabolite of MeIQx in human urine, accounting for ~50–70% of the dose in urine, is the 8-carboxylic acid derivative IQx-8-COOH; its formation is catalyzed by P450 1A2 [132,195]. Thus, human P450 1A2 serves a dual role in the metabolism of MeIQx: it can both bioactivate and detoxicate this procarcinogen.

In a pilot study that analyzed urine from 10 volunteers, the N^2-(β-1-glucosiduronyl-2-(hydroxyamino)-1-methyl-6-phenylimidazo[4,5-*b*]pyridine (HON-PhIP-N^2-glucuronide) was the most abundant of the 12 metabolites of PhIP identified, by accelerator MS, in urine from all of the subjects [144]. The levels of this metabolite varied significantly among the individuals. In the same study, interindividual differences in colon PhIP-DNA adduct levels were noted. The individuals with a rapid P450 1A2

phenotype and a high level of urinary HON-PhIP-N^2-glucuronide showed the lowest level of colon PhIP-DNA adducts. This negative correlation suggested that glucuronidation plays an important role in the detoxication of HONH-PhIP and protects against colorectal DNA adduct formation. A larger study group will be required for investigatiors to firmly establish the role of UGT in protection against PhIP-mediated DNA damage and consequent colorectal cancer risk.

The effect of a diet high in cruciferous vegetables, on the metabolism of PhIP, was investigated in a group of volunteers [134]. Components of cruciferous vegetables significantly increased the hepatic P450 1A2 activity, measured by changes in the kinetics of caffeine metabolism and by the increases in levels of urinary HON-PhIP-N^2-glucuronide. This latter urinary biomarker was 32% higher in urine from subjects on a cruciferous diet, as compared to the level in urine from the same subjects when they consumed a diet not containing cruciferous vegetables [134]. That study confirmed the observation that HON-PhIP-N^2-glucuronide is the major metabolite of PhIP eliminated in human urine [133]. The consumption of cruciferous vegetables was postulated to increase the production and elimination of HON-PhIP-N^2-glucuronide through an induction of UGT activities, resulting in an overall reduction of the HONH-PhIP available for reaction with DNA. At the same time, however, the consumption of cruciferous vegetables also increased the expression of hepatic P450 1A2 protein. Unfortunately, the balance between the enhanced formation of HNOH-PhIP and the UGT-mediated detoxication of HON-PhIP, as might have been assessed through measurement of the change in the levels of PhIP-DNA adduct formation in the colon, was not examined. Therefore, the potential beneficial chemoprotective effects of cruciferous vegetables toward HAAs remain uncertain.

3.5. DNA and Protein Adducts of HAAs

Although short-term urinary biomarkers of PhIP and MeIQx and their metabolites have been established [133–135,183,196,197], such biomarkers are transient, and they capture only the preceding 24–48 h of exposure. For individuals who chronically but intermittently consume cooked meats, urinary HAA biomarkers can be undetected, and these individuals can be misclassified. Thus, long-lived biomarkers of HAAs are required for a reliable assessment of HAA exposure in epidemiological investigations.

Putative HAA-DNA adducts have been detected in human colon, breast, and lymphocytes, in assays employing ^{32}P-postlabeling, immunohistochemical, or accelerator mass spectrometric (AMS) methods [198–202]. The putative *N*-(deoxyguanosin-8-yl)-MeIQx (dG-C8-MeIQx) adduct was detected in colon and kidney of some individuals at levels of several adducts per 10^9 DNA bases, when assayed by ^{32}P-postlabeling [203].

A GC/MS assay, based upon alkaline hydrolysis of putative dG-C8-HAA adducts back to the parent HAAs, was employed to measure putative PhIP-DNA adducts in the colorectal mucosa of individuals, at levels of several adducts per 10^8 DNA bases [204]. A base-labile adduct of PhIP, presumably dG-C8-PhIP, was also detected in long-lived lymphocytes of colorectal cancer subjects, at levels of several adducts per 10^8 DNA bases [200]. The adduct was detected in about 30% of subjects, and its level varied across a >10-fold range. The adduct levels were not significantly higher either in smokers or in subjects who frequently consumed well-done cooked meat as compared to individuals who ate meat less frequently. Moreover, relationships were not observed between PhIP-DNA adduct formation and alleles of *NAT1, NAT2*, or *SULT1A1*, the genes encoding the XMEs that are involved in bioactivation of PhIP [160]. However, a subset of younger individuals who carried two mutated *GSTA1* alleles had higher adduct levels than did homozygous wild-type or heterozygous subjects [200]. The GSTA1 protein is known to detoxicate *N*-acetoxy-PhIP [205,206].

A DNA adduct of PhIP, presumably, dG-C8-PhIP, was detected by immunohistochemistry, in human breast tissue biopsy samples [207], by ^{32}P-postlabeling of DNA obtained from exfoliated breast epithelial cells in milk of lactating mothers [208]. PhIP-DNA adducts were detected at high frequency (>50% positivity) in both studies: Adduct levels were approximately one adduct per 10^7 bases [207,208]. Putative PhIP-DNA adducts were also detected at high levels and high frequency in prostate tissue from cancer patients, by immunohistochemical methods [209]. Collectively, the data suggest that HAA-DNA adducts can form in human tissues even when the concentrations of HAAs in the diet are at the low ppb range.

Caveats are associated with the measurements of HAA-DNA adducts in all of the adduct studies cited above: identities of the adducts are equivocal. The ^{32}P-postlabeling and immunohistochemical methods lack specificity and are not quantitative [53]; AMS is a specific method of detection, but it does not provide confirmatory spectral data. Robust and sensitive LC-ESI/MS/MS-based methods have emerged as essential tools for biomonitoring of intact DNA adducts of diverse carcinogens at levels of less than or equal to one adduct per 10^8 DNA bases in experimental animal models and in humans [53,210–214]. The incorporation of LC-ESI/MS/MS methods can permit corroboration or refutation of the validity of the HAA-DNA adduct biomaker data generated from the less specific bioanalytical methods.

Carcinogen adducts of abundant blood proteins, such as hemoglobin (Hb) and serum albumin (SA), have also been investigated as potential biomarkers for various genotoxicants [215]. HAA–protein adducts can form by the reaction between nucleophilic amino acid residues within proteins and the metabolically activated HAAs. On the basis of experimental animal model studies and pilot human studies, the levels of IQ, 8-MeIQx, and PhIP bound to Hb are low (~0.01% of the dose)

[199,215,216]. Such a low level of protein binding will probably preclude the development of Hb–HAA adducts as biomarkers in humans, because the LOQ values for the adducts are below the limits of current MS instruments. However, the reaction product(s) of PhIP with serum albumin (SA) show promise as biomarker(s) [199]. Human SA is the most abundant protein in plasma (~45 mg ml^{-1}). The cys^{34} is one of 35 cysteine residues that are conserved in SA across species [217]. Thirty-four of these cysteines are involved in 17 disulfide bonds. The single unpaired cys^{34} is present either as a free thiol or in an oxidized form: this singular residue is present partially as disulfide linkages with low-molecular-weight thiols. Albumin functions as an antioxidant and scavenges reactive oxygen and nitrogen species that are generated by basal aerobic metabolism. The cys^{34} of SA is believed to be responsible for many of the antioxidant properties of SA and accounts for ~80% of the net free thiols in plasma [218,219], and it is a major transporter of NO in blood [220]. The scavenging properties of this cys^{34} residue with respect to reactive carcinogens and some toxic electrophiles are well documented. Adducts at the cys^{34} residue have been identified with reactive metabolites of various toxicants *in vitro* in rodent SA and human SA, which include IQ [221], MeIQx [222], PhIP [223,224], acrylamide [225], sulfur mustard [226], benzene [227], and acetaminophen [228].

An adduct formed between IQ and SA in the rat was characterized, by MS, ^{1}H NMR, and amino acid analysis, as a sulfinamide adduct (Figure 9). The adduct was formed by a nucleophilic reaction of the sulfhydryl group of the cys^{34} residue of SA with nitroso-IQ, an oxidation product of HONH-IQ. This sulfinamide adduct was estimated to account for about 10% of the total adducts of SA in the rat [221]. The adduct was characterized following enzymatic hydrolysis of SA with pronase, to produce a tripeptide-containing sulfinamide–IQ adduct, or by mild acid hydrolysis of SA, to regenerate IQ and produce a sulfonic acid at the cys^{34} residue of SA (Figure 9). In a human study, one or more acid-labile PhIP–SA adducts were detected in human subjects on a noncontrolled diet; levels were 10-fold higher in meat-eaters than in vegetarians (6.7 ± 1.6 vs. 0.7 ± 0.3 fmol PhIP-SA/mg protein; mean $\pm$ SE) [230]. The structure(s) of the adduct(s) attributed to the acid-labile lesion remain to be determined. It is plausible that some proportion of the acid-labile PhIP adduction products were formed at the cys^{34} residue in human SA. Additional studies are required to elucidate the structure of the adduct(s) and to validate the biomarker prior to its use in population-based studies.

3.6. Biomonitoring of HAAs in hair

Various drugs and contaminants are known to accumulate in human hair, and it has served as a matrix for the biomonitoring of chemicals such as

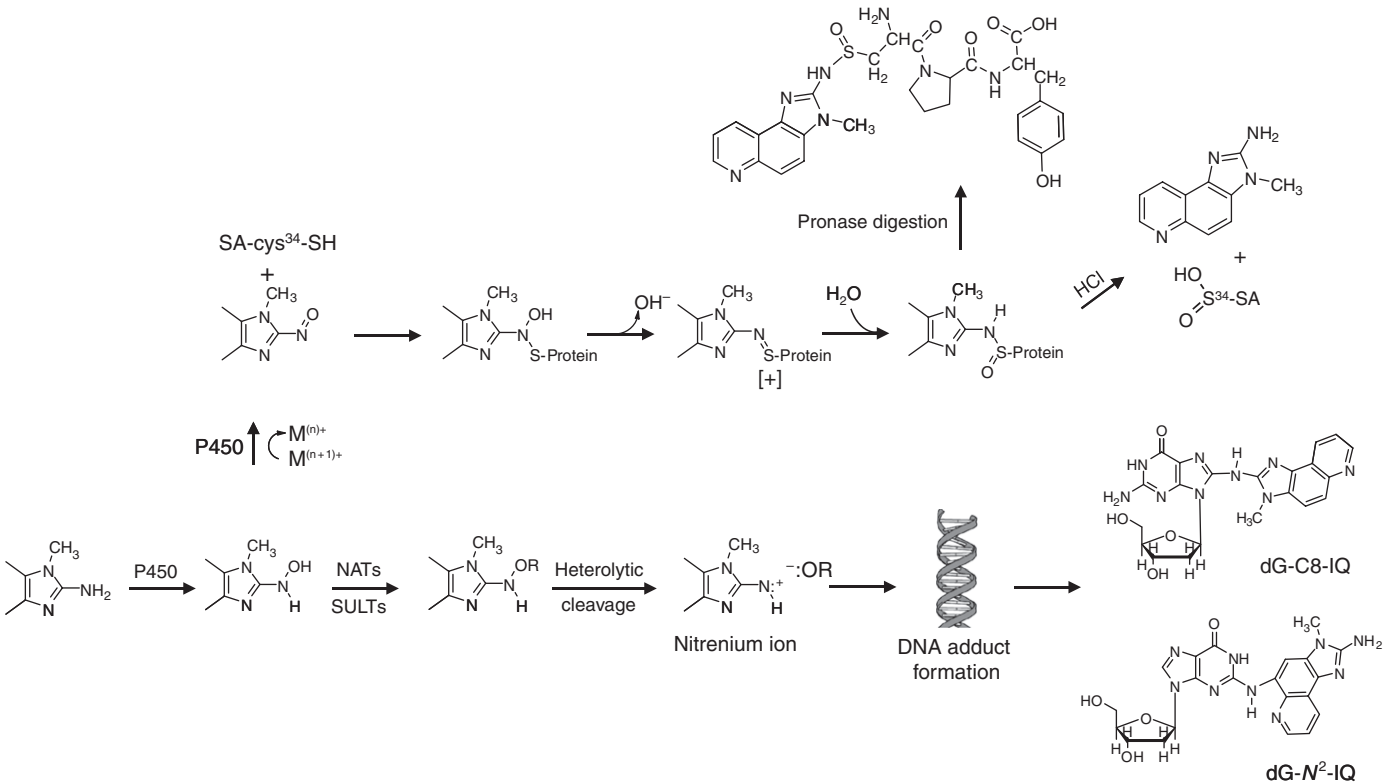

Figure 9 Metabolic activation of IQ to form DNA adducts and a protein adduct with serum albumin (SA) in the rat. Isomeric dG-C8- and dG-N^2-IQ adducts are formed by reaction of *N*-hydroxy-IQ or by its sulfate or acetate esters with DNA [53,54]. Oxidation of the *N*-hydroxy-IQ metabolite to the nitroso intermediate can occur by P4501A2 or metal-catalyzed oxidation [229]. The nitroso-IQ can then react with the cys^{34} sulfhydryl group of SA to form a sulfinamide adduct [221]. The adduct can be digested with pronase to produce a tripeptide containing the adduct, or the adduct can be hydrolyzed by acid treatment to regenerate IQ [221].

nicotine, narcotics, and other drugs [231,232]. However, such exposures occur at levels that exceed the levels of HAAs by at least 3 orders of magnitude. Studies with experimental laboratory animals have shown that ^{14}C-labeled PhIP accumulates in melanin-rich tissues, including fur [184]. A method was established to quantitate PhIP in mouse fur and human hair by GC-NICI-MS [184,233], and more recently a method to quantitate PhIP in human hair was conducted by LC-ESI/MS [234,235]. Both methods require elaborate purification procedures prior to the MS assay. PhIP was identified at high frequency, but at variable levels in hair of Norwegian subjects (60–7500 pg g^{-1} hair) [236] and Japanese subjects (180–3600 pg g^{-1} hair) [235]. A more recent analytical method was reported to require considerably less hair (50 mg) and includes a simplified HAA extraction procedure [237]. Hair samples are digested by base hydrolysis, and the liberated HAAs are then isolated by tandem solvent/solid-phase extraction, followed by quantification by LC/MS/MS [237]. In the latter study, PhIP was detected in hair of all six meat-eaters at levels ranging from 290 to 890 pg g^{-1} hair, while MeIQx and AαC were below the LOQ (50 pg g^{-1} hair) in hair from meat-eaters and also from six vegetarians. PhIP was detected in the hair from one vegetarian, and that occurrence was at a level (65 pg g^{-1} hair) just above the LOQ (50 pg g^{-1} hair). These data suggest that the exposure to PhIP occurs primarily through consumption of cooked meats or poultry [238,239] and that nonmeat-derived sources of exposure to PhIP [240,241] are probably negligible. The levels of PhIP in hair samples from two meat-eaters varied by less than 24% over a 6-month interval, signifying that the exposure to PhIP and its accumulation in hair are relatively constant over time [237].

The wide range of PhIP accumulation levels in hair of subjects of the above studies is due to several variables. The concentration of PhIP in the individual's diet constitutes one critical variable. The pharmacokinetics and metabolism of PhIP represent another important variable. There are large interindividual differences in the hepatic P450 1A2 protein content, which can vary by more than 50-fold [50]; this enzyme accounts for ~70% of the metabolism of PhIP in humans [183]. Thus, the amount of unmetabolized PhIP in the bloodstream that reaches the hair follicle, following first-pass metabolism, can widely range and may affect the levels of PhIP accrued in hair. The pigmentation of hair also affects the amount of PhIP incorporated into hair. PhIP has a high binding affinity for eumelanin [242], a pigment that is more predominant in black hair than in lighter colored hair [243]. The accumulation of PhIP in hair can be used as an integrative dose of exposure and can serve as a marker of exposure to this dietary carcinogen. However, studies that examine the interrelationship among dietary exposure to PhIP, P450 1A2 activity, and the melanin content of hair will be required, before we can determine how these factors affect the level of PhIP

accumulated in hair and the accuracy of this hair biomarker as a measure of dietary intake of PhIP.

4. Conclusions

Humans are continuously exposed to HAAs in their diet. With the recent improvements in the sensitivity of mass spectometric instrumentation, it is now possible to probe for HAA biomarkers in sampled biological fluids and tissues. The challenge remains to develop rapid and robust methods to analyze these biomarkers; such methods can then be employed in epidemiological studies that investigate HAA exposures, together with metabolic phentotypes/genotypes in determination of cancer risk. With such data available, we can define more accurately the human health risk posed by these HAAs.

Acknowledgment

A portion of the reported research that was conducted in the author's laboratory was funded by R01CA122320 from the National Cancer Institute.

REFERENCES

[1] B.N. Ames, L.S. Gold, W.C. Willet, The causes and prevention of cancer, Proc. Natl. Acad. Sci. U. S. A. 92 (1995) 5258–5265.
[2] T. Sugimura, N. Nagao, T. Kawachi, M. Honda, T. Yahagi, Y. Seino, S. Stao, N. Matsukura, T. Matsushima, A. Shirai, M. Sawamura, H. Matsumoto, Mutagen-carcinogens in food, with special reference to highly mutagenic pyrolytic products in broiled foods, in: H.H. Hiatt, J.D. Watson, J.A. Winstein (Eds.), Origins of Human Cancer, Book C, Cold Spring Harbor Laboratory, Cold Spring Harbor, NY, 1977, pp. 1561–1577.
[3] J.S. Felton, M. Jagerstad, M.G. Knize, K. Skog, K. Wakabayashi, Contents in foods, beverages and tobacco, in: M. Nagao, T. Sugimura (Eds.), Food Borne Carcinogens Heterocyclic Amines, John Wiley & Sons Ltd., Chichester, England, 2000, pp 31–71.
[4] K.I. Skog, M.A. Johansson, M.I. Jagerstad, Carcinogenic heterocyclic amines in model systems and cooked foods: A review on formation, occurrence and intake, Food Chem. Toxicol. 36 (1998) 879–896.
[5] T. Sugimura, K. Wakabayashi, H. Nakagama, M. Nagao, Heterocyclic amines: Mutagens/carcinogens produced during cooking of meat and fish, Cancer Sci. 95 (2004) 290–299.
[6] R.J. Turesky, A.K. Goodenough, W. Ni, L. McNaughton, D.M. LeMaster, R.D. Holland, R.W. Wu, J.S. Felton, Identification of 2-amino-1,7-dimethylimidazo[4,5-

g]quinoxaline: An abundant mutagenic heterocyclic aromatic amine formed in cooked beef, Chem. Res. Toxicol. 20 (2007) 520–530.
[7] S. Manabe, S. Izumikawa, K. Asakuno, O. Wada, Y. Kanai, Detection of carcinogenic amino-alpha-carbolines and amino-gamma-carbolines in diesel-exhaust particles, Environ. Pollut. 70 (1991) 255–265.
[8] S. Manabe, K. Tohyama, O. Wada, T. Aramaki, Detection of a carcinogen, 2-amino-1-methyl-6-phenylimidazo[4,5-*b*]pyridine, in cigarette smoke condensate, Carcinogenesis 12 (1991) 1945–1947.
[9] G.A. Keating, K.T. Bogen, Estimates of heterocyclic amine intake in the US population, J. Chromatogr. B Analyt. Technol. Biomed. Life Sci. 802 (2004) 127–133.
[10] *National Toxicology Program, Report on Carcinogenesis, Eleventh Edition, U.S. Department of Health and Human Services, Public Health Service, Research Triangle Park, N.C.,* 2005.
[11] T. Sugimura, Multistep carcinogenesis: A 1992 perspective, Science 258 (1992) 603–607.
[12] S. Manabe, O. Wada, Y. Kanai, Simultaneous determination of amino-alpha-carbolines and amino-gamma-carbolines in cigarette smoke condensate by high-performance liquid chromatography, J. Chromatogr. 529 (1990) 125–133.
[13] D. Yoshida, T. Matsumoto, Amino-alpha-carbolines as mutagenic agents in cigarette smoke condensate, Cancer Lett. 10 (1980) 141–149.
[14] S.S. Hecht, Tobacco carcinogens, their biomarkers and tobacco-induced cancer, Nat. Rev. Cancer 3 (2003) 733–744.
[15] Z. Yamaizumi, T. Shiomi, H. Kasai, S. Nishimura, Y. Takahashi, M. Nagao, T. Sugimura, Detection of potent mutagens, Trp-P-1 and Trp-P-2, in broiled fish, Cancer Lett. 9 (1980) 75–83.
[16] T. Matsumoto, D. Yoshida, H. Tomita, Determination of mutagens, amino-alpha-carbolines in grilled foods and cigarette smoke condensate, Cancer Lett. 12 (1981) 105–110.
[17] U. Brockstedt, W. Pfau, Formation of 2-amino-α-carbolines in pan-fried poultry and ^{32}P-postlabelling analysis of DNA adducts, Z. Lebensm Unters Forsch A, 207 (1998) 472–476.
[18] G.A. Gross, A. Gruter, Quantitation of mutagenic/carcinogenic heterocyclic aromatic amines in food products, J. Chromatogr. 592 (1992) 271–278.
[19] K. Skog, K. Augustsson, G. Steineck, M. Stenberg, M. Jagerstad, Polar and non-polar heterocyclic amines in cooked fish and meat products and their corresponding pan residues, Food Chem. Toxicol. 35 (1997) 555–565.
[20] K. Skog, A. Solyakov, P. Arvidsson, M. Jagerstad, Analysis of nonpolar heterocyclic amines in cooked foods and meat extracts using gas chromatography-mass spectrometry, J. Chromatogr. A. 803 (1998) 227–233.
[21] R.J. Turesky, J. Taylor, L. Schnackenberg, J.P. Freeman, R.D. Holland, Quantitation of carcinogenic heterocyclic aromatic amines and detection of novel heterocyclic aromatic amines in cooked meats and grill scrapings by HPLC/ESI-MS, J. Agric. Food Chem. 53 (2005) 3248–3258.
[22] M. Jagerstad, K. Skog, S. Grivas, K. Olsson, Formation of heterocyclic amines using model systems, Mutat. Res. 259 (1991) 219–233.
[23] K. Skog, M. Jagerstad, Incorporation of carbon atoms from glucose into the food mutagens MeIQx and 4,8-DiMeIQx using 14C-labelled glucose in a model system, Carcinogenesis 14 (1993) 2027–2031.
[24] B.L. Milic, S.M. Djilas, J.M. Candadanoic-Brunet, Synthesis of some heterocyclic aminoimidazoarenes, Food Chem. 46 (1993) 273–276.
[25] M. Shioya, K. Wakabayashi, S. Sato, M. Nagao, T. Sugimura, Formation of a mutagen, 2-amino-1-methyl-6-phenylimidazo[4,5-b]-pyridine (PhIP) in cooked beef, by heating a mixture containing creatinine, phenylalanine and glucose, Mutat. Res. 191 (1987) 133–138.

[26] M. Murkovic, Formation of heterocyclic aromatic amines in model systems, *J. Chromatogr. B.* 802 (2004) 3–10.
[27] A.M. Pearson, C. Chen, J.I. Gray, S.D. Aust, Mechanism(s) involved in meat mutagen formation and inhibition, Free Radic. Biol. Med. 13 (1992) 161–167.
[28] T. Kato, T. Harashima, N. Moriya, K. Kikugawa, K. Hiramoto, Formation of the mutagenic/carcinogenic imidazoquinoxaline-type heterocyclic amines through the unstable free radical Maillard intermediates and its inhibition by phenolic antioxidants, Carcinogenesis 17 (1996) 2469–2476.
[29] Y. Totsuka, H. Ushiyama, J. Ishihara, R. Sinha, S. Goto, T. Sugimura, K. Wakabayashi, Quantification of the co-mutagenic beta-carbolines, norharman and harman, in cigarette smoke condensates and cooked foods, Cancer Lett. 143 (1999) 139–143.
[30] T. Totsuka, R. Nishigaki, T. Sugimura, K. Wakabayashi, The possible involvement of mutagenic and carcinogenic heteroyclic amines in human cancer, in: K. Skog, J. Alexander (Eds.), Acrylamide and Other Hazardous Compounds in Heat-Treated Foods, Woodhead Publisher, Boca Raton, Fl, 2006, pp. 296–515.
[31] N. Hada, Y. Totsuka, T. Enya, K. Tsurumaki, M. Nakazawa, N. Kawahara, Y. Murakami, Y. Yokoyama, T. Sugimura, K. Wakabayashi, Structures of mutagens produced by the co-mutagen norharman with o- and m-toluidine isomers, Mutat. Res. 493 (2001) 115–126.
[32] Y. Oda, Y. Totsuka, K. Wakabayashi, F.P. Guengerich, T. Shimada, Activation of aminophenylnorharman, aminomethylphenylnorharman and aminophenylharman to genotoxic metabolites by human N-acetyltransferases and cytochrome P450 enzymes expressed in Salmonella typhimurium umu tester strains, Mutagenesis 21 (2006) 411–416.
[33] R. Nishigaki, Y. Totsuka, T. Takamura-Enya, T. Sugimura, K. Wakabayashi, Identification of cytochrome P-450s involved in the formation of APNH from norharman with aniline, Mutat. Res. 562 (2004) 19–25.
[34] T. Kawamori, Y. Totsuka, N. Uchiya, T. Kitamura, H. Shibata, T. Sugimura, K. Wakabayashi, Carcinogenicity of aminophenylnorharman, a possible novel endogenous mutagen, formed from norharman and aniline, in F344 rats, Carcinogenesis 25 (2004) 1967–1972.
[35] R. Nishigaki, Y. Totsuka, H. Kataoka, H. Ushiyama, S. Goto, T. Akasu, T. Watanabe, T. Sugimura, K. Wakabayashi, Detection of aminophenylnorharman, a possible endogenous mutagenic and carcinogenic compound, in human urine samples, Cancer Epidemiol. Biomarkers Prev. 16 (2007) 151–156.
[36] E. Ronne, K. Olsson, S. Grivas, One-step synthesis of 2-amino-1-methylimidazo [4,5-*b*]quinoline, Synthetic Commun. 24 (1994) 1363–1366.
[37] R. Vikse, F.T. Hatch, N.W. Winter, M.G. Knize, S. Grivas, J.S. Felton, Structure-mutagenicity relationships of four amino-imidazonaphthyridines and imidazoquinolines, Environ. Mol. Mutagen. 26 (1995) 79–85.
[38] R.D. Holland, T. Gehring, J. Taylor, B.G. Lake, N.J. Gooderham, R.J. Turesky, Formation of a mutagenic heterocyclic aromatic amine from creatinine in urine of meat eaters and vegetarians, Chem. Res. Toxicol. 18 (2005) 579–590.
[39] K. Skog, Cooking procedures and food mutagens: A literature review, Food Chem. Toxicol. 31 (1993) 655–675.
[40] K. Skog, A. Solyakov, Heterocyclic amines in poultry products: A literature review, Food Chem. Toxicol. 40 (2002) 1213–1221.
[41] K. Skog, G. Steineck, K. Augustsson, M. Jagerstad, Effect of cooking temperature on the formation of heterocyclic amines in fried meat products and pan residues, Carcinogenesis 16 (1995) 861–867.
[42] J.S. Felton, M.G. Knize, Heterocyclic amine mutagens/carcinogens in foods, in: C.S. Cooper, P.L. Grover (Eds.), Handbook of Experimental Pharmacology, Springer-Verlag, Berlin Heidelberg, 1990, pp. 471–502.

[43] M.G. Knize, F.A. Dolbeare, K.L. Carroll, D.H. Moore, J.S. Felton, Effect of cooking time and temperature on the heterocyclic amine content of fried beef patties, Food Chem. Toxicol. 32 (1994) 595–603.
[44] R. Sinha, N. Rothman, C.P. Salmon, M.G. Knize, E.D. Brown, C.A. Swanson, D. Rhodes, S. Rossi, J.S. Felton, O.A. Levander, Heterocyclic amine content in beef cooked by different methods to varying degrees of doneness and gravy made from meat drippings, Food Chem. Toxicol. 36 (1998) 279–287.
[45] R. Sinha, M.G. Knize, C.P. Salmon, E.D. Brown, D. Rhodes, J.S. Felton, O.A. Levander, N. Rothman, Heterocyclic amine content of pork products cooked by different methods and to varying degrees of doneness, Food Chem. Toxicol. 36 (1998) 289–297.
[46] A. Solyakov, K. Skog, M. Jagerstad, Heterocyclic amines in process flavours, process flavour ingredients, bouillon concentrates and a pan residue, Food Chem Toxicol. 37 (1999) 1–11.
[47] R. Sinha, N. Rothman, E.D. Brown, C.P. Salmon, M.G. Knize, C.S. Swanson, S.C. Rossi, S.D. Mark, O.A. Levander, J.S. Felton, High concentrations of the carcinogen 2-amino-1-methyl-6-phenylimidazo[4,5-*b*]pyridine (PhIP) occur in chicken but are dependent on the cooking method, Cancer Res. 55 (1995) 4516–4519.
[48] H. Nukaya, S. Koyota, F. Jinno, H. Ishida, K. Wakabayashi, R. Kurosaka, I.S. Kim, Z. Yamaizumi, H. Ushiyama, T. Sugimura, Structural determination of a new mutagenic heterocyclic amine, 2-amino-1,7,9-trimethylimidazo[4,5-g]quinoxaline (7,9-DiMeI*g*Qx), present in beef extract, Carcinogenesis 15 (1994) 1151–1154.
[49] F.T. Hatch, M.G. Knize, M.E. Colvin, Extended quantitative structure-activity relationships for 80 aromatic and heterocyclic amines: Structural, electronic, and hydropathic factors affecting mutagenic potency, *Environ. Mol. Mutagen* 38 (2001) 268–291.
[50] R.J. Turesky, A. Constable, J. Richoz, N. Varga, J. Markovic, M.V. Martin, F.P. Guengerich, Activation of heterocyclic aromatic amines by rat and human liver microsomes and by purified rat and human cytochrome P450 1A2, Chem. Res. Toxicol. 11 (1998) 925–936.
[51] F.G. Crofts, T.R. Sutter, P.T. Strickland, Metabolism of 2-amino-1-methyl-6-phenylimidazo[4,5-b]pyridine by human cytochrome P4501A1, P4501A2 and P4501B1, Carcinogenesis 19 (1998) 1969–1973.
[52] G.J. Hammons, D. Milton, K. Stepps, F.P. Guengerich, F.F. Kadlubar, Metabolism of carcinogenic heterocyclic and aromatic amines by recombinant human cytochrome P450 enzymes, Carcinogenesis 18 (1997) 851–854.
[53] R.J. Turesky, P. Vouros, Formation and analysis of heterocyclic aromatic amine-DNA adducts in vitro and in vivo, J. Chromatogr. B Analyt. Technol. Biomed. Life Sci. 802 (2004) 155–166.
[54] H.A. Schut, E.G. Snyderwine, DNA adducts of heterocyclic amine food mutagens: Implications for mutagenesis and carcinogenesis, Carcinogenesis 20 (1999) 353–368.
[55] E.L. Jamin, D. Arquier, C. Canlet, E. Rathahao, J. Tulliez, L. Debrauwer, New insights in the formation of deoxynucleoside adducts with the heterocyclic aromatic amines PhIP and IQ by means of ion trap MSn and accurate mass measurement of fragment ions, J. Am. Soc. Mass Spectrom. 18 (2007) 2107–2118.
[56] E.E. Bessette, A.K. Goodenough, S. Langouet, I. Yasa, I.D. Kozekov, S.D. Spivack, R.J. Turesky, Screening for DNA adducts by data-dependent constant neutral loss-triple stage mass spectrometry with a linear quadrupole ion trap mass spectrometer, Anal. Chem. 81 (2009) 809–819.
[57] R.J. Turesky, S.C. Rossi, D.H. Welti, Jr, J.O. Lay, F.F. Kadlubar, Characterization of DNA adducts formed in vitro by reaction of *N*-hydroxy-2-amino-3-methylimidazo[4,5-*f*]quinoline and *N*-hydroxy-2-amino-3,8-dimethylimidazo[4,5-*f*]quinoxaline at the C-8 and N^2 atoms of guanine, Chem. Res. Toxicol. 5 (1992) 479–490.

[58] G.R. Hoffmann, R.P. Fuchs, Mechanisms of frameshift mutations: Insight from aromatic amines, Chem Res. Toxicol. 10 (1997) 347–359.
[59] S. Broyde, L. Wang, L. Zhang, O. Rechkoblit, N.E. Geacintov, D.J. Patel, DNA adduct structure-function relationships: Comparing solution with polymerase structures, Chem. Res. Toxicol. 21 (2008) 45–52.
[60] J.C. Delaney, J.M. Essigmann, Biological properties of single chemical-DNA adducts: A twenty year perspective, Chem. Res. Toxicol. 21 (2008) 232–252.
[61] X. Tan, N. Suzuki, A.P. Grollman, S. Shibutani, Mutagenic events in Escherichia coli and mammalian cells generated in response to acetylaminofluorene-derived DNA adducts positioned in the Nar I restriction enzyme site, Biochemistry 41 (2002) 14255–14262.
[62] J.Y. Choi, J.S. Stover, K.C. Angel, G. Chowdhury, C.J. Rizzo, F.P. Guengerich, Biochemical basis of genotoxicity of heterocyclic arylamine food mutagens: Human DNA polymerase eta selectively produces a two-base deletion in copying the N2-guanyl adduct of 2-amino-3-methylimidazo[4,5-f]quinoline but not the C8 adduct at the NarI G3 site, J. Biol. Chem. 281 (2006) 25297–25306.
[63] J.S. Stover, G. Chowdhury, H. Zang, F.P. Guengerich, C.J. Rizzo, Translesion synthesis past the C8- and N2-deoxyguanosine adducts of the dietary mutagen 2-Amino-3-methylimidazo[4,5-f]quinoline in the NarI recognition sequence by prokaryotic DNA polymerases, Chem. Res. Toxicol. 19 (2006) 1506–1517.
[64] S. Shibutani, A. Fernandes, N. Suzuki, L. Zhou, F. Johnson, A.P. Grollman, Mutagenesis of the *N*-(deoxyguanosin-8-yl)-2-amino-1-methyl-6-phenylimidazo[4,5-*b*] pyridine DNA adduct in mammalian cells. Sequence context effects, J. Biol. Chem. 274 (1999) 27433–27438.
[65] S. Shibutani, N. Suzuki, A.P. Grollman, Mutagenic specificity of (acetylamino) fluorene-derived DNA adducts in mammalian cells, Biochemistry 37 (1998) 12034–12041.
[66] K. Brown, B.E. Hingerty, E.A. Guenther, V.V. Krishnan, S. Broyde, K.W. Turteltaub, M. Cosman, Solution structure of the 2-amino-1-methyl-6-phenylimidazo [4,5-*b*]pyridine C8-deoxyguanosine adduct in duplex DNA, Proc. Natl. Acad. Sci. U. S. A. 98 (2001) 8507–8512.
[67] C.E. Elmquist, J.S. Stover, Z. Wang, C.J. Rizzo, Site-specific synthesis and properties of oligonucleotides containing C8-deoxyguanosine adducts of the dietary mutagen IQ, J. Am. Chem. Soc. 126 (2004) 11189–11201.
[68] F. Wang, N.E. DeMuro, C.E. Elmquist, J.S. Stover, C.J. Rizzo, M.P. Stone, Base-displaced intercalated structure of the food mutagen 2-amino-3-methylimidazo[4,5-f] quinoline in the recognition sequence of the NarI restriction enzyme, a hotspot for -2 bp deletions, J. Am. Chem. Soc. 128 (2006) 10085–10095.
[69] D.J. Patel, B. Mao, Z. Gu, B.E. Hingerty, A. Gorin, A.K. Basu, S. Broyde, Nuclear magnetic resonance solution structures of covalent aromatic amine-DNA adducts and their mutagenic relevance, Chem Res. Toxicol. 11 (1998) 391–407.
[70] M. Lukin, S.C. de Los, NMR structures of damaged DNA, Chem. Rev. 106 (2006) 607–686.
[71] T. Zaliznyak, R. Bonala, F. Johnson, S.C. de Los, Structure and stability of duplex DNA containing the 3-(deoxyguanosin-N2-yl)-2-acetylaminofluorene (dG(N2)-AAF) lesion: A bulky adduct that persists in cellular DNA, Chem. Res. Toxicol. 19 (2006)745–752.
[72] S.J. Culp, M.C. Poirier, F.A. Beland, Biphasic removal of DNA adducts in a repetitive DNA sequence after dietary administration of 2-acetylaminofluorene, Environ. Health Perspect. 99 (1993) 273–275.
[73] R.J. Turesky, R.M. Box, J. Markovic, E. Gremaud, E.G. Snyderwine, Formation and persistence of DNA adducts of 2-amino-3-methylimidazo[4,5-*f*]quinoline in the rat and nonhuman primates, Mutat. Res. 376 (1997) 235–241.

[74] F.A. Beland, F.F. Kadlubar, Formation and persistence of arylamine DNA adducts *in vivo*, Environ. Health Perspect. 62 (1985) 19–30.
[75] D.M. Maron, B.N. Ames, Revised methods for the Salmonella mutagenicity test, Mutat. Res. 113 (1983) 173–215.
[76] T. Sugimura, Successful use of short-term tests for academic purposes: Their use in identification of new environmental carcinogens with possible risk for humans, Mutat. Res. 205 (1988) 33–39.
[77] J.C. Fuscoe, R. Wu, N.H. Shen, S.K. Healy, J.S. Felton, Base-change analysis of revertants of the hisD3052 allele in *Salmonella typhimurium*, Mutat. Res. 201 (1988) 241–251.
[78] J.S. Felton, M.G. Knize, F.A. Dolbeare, R. Wu, Mutagenic activity of heterocyclic amines in cooked foods, Environ. Health Perspect. 102 (Suppl. 6) (1994) 201–204.
[79] R.W. Wu, J.D. Tucker, K.J. Sorensen, L.H. Thompson, J.S. Felton, Differential effect of acetyltransferase expression on the genotoxicity of heterocyclic amines in CHO cells, Mutat. Res. 390 (1997) 93–103.
[80] H. Glatt, U. Pabel, W. Meinl, H. Frederiksen, H. Frandsen, E. Muckel, Bioactivation of the heterocyclic aromatic amine 2-amino-3-methyl-9H-pyrido [2,3-b]indole (MeAalphaC) in recombinant test systems expressing human xenobiotic-metabolizing enzymes, Carcinogenesis 25 (2004) 801–807.
[81] J. Bendaly, S. Zhao, J.R. Neale, K.J. Metry, M.A. Doll, J.C. States, W.M. Pierce, Jr, D.W. Hein, 2-Amino-3,8-dimethylimidazo-[4,5-f]quinoxaline-induced DNA adduct formation and mutagenesis in DNA repair-deficient Chinese hamster ovary cells expressing human cytochrome P4501A1 and rapid or slow acetylator N-acetyltransferase 2, Cancer Epidemiol, Biomarkers Prev. 16 (2007) 1503–1509.
[82] K.J. Metry, S. Zhao, J.R. Neale, M.A. Doll, J.C. States, W.G. McGregor, W.M. Pierce, Jr, D.W. Hein, 2-amino-1-methyl-6-phenylimidazo [4,5-b] pyridine-induced DNA adducts and genotoxicity in chinese hamster ovary (CHO) cells expressing human CYP1A2 and rapid or slow acetylator N-acetyltransferase 2, Mol. Carcinog. 46 (2007) 553–563.
[83] H. Glatt, Metabolic factors affecting the mutagenicity of heteroyclic amines, in: K. Skog, J. Alexander (Eds.), Acrylamide and Other Hazardous Compounds in Heat-Treated Foods, Woodhead Publishing Ltd., Cambridge, England, 2006, pp. 358–404.
[84] P.D. Josephy, Genetically-engineered bacteria expressing human enzymes and their use in the study of mutagens and mutagenesis, Toxicology 181–182 (2002) 255–260.
[85] Y. Oda, H. Yamazaki, M. Watanabe, T. Nohmi, T. Shimada, Development of high sensitive *umu* test system: Rapid detecton of genotoxicity of promutagenic aromatic amines by *Salmonella typhimurium* strain NM2009 possessing high *O*-acetyltransferase activity, Mutat. Res. 334 (1995) 145–156.
[86] Y. Oda, P. Aryal, T. Terashita, E.M. Gillam, F.P. Guengerich, T. Shimada, Metabolic activation of heterocyclic amines and other procarcinogens in Salmonella typhimurium umu tester strains expressing human cytochrome P4501A1, 1A2, 1B1, 2C9, 2D6, 2E1, and 3A4 and human NADPH-P450 reductase and bacterial O-acetyltransferase, Mutat. Res. 492 (2001) 81–90.
[87] P.M. Morgenthaler, D. Holzhauser, Analysis of mutations induced by 2-amino-1-methyl-6-phenylimidazo[4,5-*b*]pyridine (PhIP) in human lymphoblastoid cells, Carcinogenesis, 16 (1995) 713–718.
[88] A.M. Carothers, W. Yuan, B.E. Hingerty, S. Broyde, D. Grunberger, E.G. Snyderwine, Mutation and repair induced by the carcinogen 2-(hydroxyamino)-1-methyl-6-phenylimidazo[4,5-*b*]pyridine (N-OH-PhIP) in the dihydrofolate reductase gene of Chinese hamster ovary cells and conformational modeling of the dG-C8-PhIP adduct in DNA, Chem. Res. Toxicol. 7 (1994) 209–218.

[89] R.W. Wu, E.M. Wu, L.H. Thompson, J.S. Felton, Identification of aprt gene mutations induced in repair-deficient and P450-expressing CHO cells by the food-related mutagen/carcinogen, PhIP, Carcinogenesis 16 (1995) 1207–1213.
[90] M. Yadollahi-Farsani, N.J. Gooderham, D.S. Davies, A.R. Boobis, Mutational spectra of the dietary carcinogen 2-amino-1-methyl-6-phenylimidazo[4,5-*b*]pyridine(PhIP) at the Chinese hamsters hprt locus, Carcinogenesis 17 (1996) 617–624.
[91] H. Kakiuchi, M. Watanabe, T. Ushijima, M. Toyota, K. Imai, J.H. Weisburger, T. Sugimura, N. Nagao, Specific 5′-GGGA-3′ --> 5′-GGA-3′ mutation of the APC gene in rat colon tumors induced by 2-amino-1-methyl-6-phenylimidazo[4,5-*b*] pyridine, Proc. Natl. Acad. Sci. U. S. A. 92 (1995) 910–914.
[92] P.M. Leong-Morgenthaler, H. Op, V.E. Jaccaud, R.J. Turesky, Mutagenicity of 2-amino-3-methylimidazo[4,5-*f*]quinoline in human lymphoblastoid cells, Carcinogenesis 19 (1998) 1749–1754.
[93] R.J. Turesky, J. Bendaly, I. Yasa, M. A. Doll, D.W. Hein, The impact of NAT2 acetylator genotype on mutagenesis and DNA adducts from 2-amino-9*H*-pyrido[2,3-*b*]indole, Chem Res. Toxicol. (2009), in press.
[94] R.W. Wu, F.N. Panteleakos, J.S. Felton, Development and characterization of CHO repair-proficient cell lines for comparative mutagenicity and metabolism of heterocyclic amines from cooked food, Environ. Mol. Mutagen. 41 (2003) 7–13.
[95] J.A. Gossen, W.J. de Leeuw, C.H. Tan, E.C. Zwarthoff, F. Berends, P.H. Lohman, D.L. Knook, J. Vijg, Efficient rescue of integrated shuttle vectors from transgenic mice: A model for studying mutations in vivo, Proc. Natl. Acad. Sci. U. S. A. 86 (1989) 7971–7975.
[96] J.A. Gossen, W.J. de Leeuw, J. Vijg, LacZ transgenic mouse models: Their application in genetic toxicology, Mutat. Res. 307 (1994) 451–459.
[97] S.W. Kohler, G.S. Provost, P.L. Kretz, A. Fieck, J.A. Sorge, J.M. Short, The use of transgenic mice for short-term, in vivo mutagenicity testing, Genet. Anal. Tech. Appl. 7 (1990) 212–218.
[98] J.A. Heddle, S. Dean, T. Nohmi, M. Boerrigter, D. Casciano, G.R. Douglas, B.W. Glickman, N.J. Gorelick, J.C. Mirsalis, H.J. Martus, T.R. Skopek, V. Thybaud, K.R. Tindall, N. Yajima, In vivo transgenic mutation assays, Environ. Mol. Mutagen. 35 (2000) 253–259.
[99] H. Okonogi, T. Ushijima, X.B. Zhang, J.A. Heddle, T. Suzuki, T. Sofuni, J.S. Felton, J.D. Tucker, T. Sugimura, M. Nagao, Agreement of mutational characteristics of heterocyclic amines in lacI of the Big Blue mouse with those in tumor related genes in rodents, Carcinogenesis 18 (1997) 745–748.
[100] E. Okochi, N. Watanabe, Y. Shimada, S. Takahashi, K. Wakazono, T. Shirai, T. Sugimura, M. Nagao, T. Ushijima, Preferential induction of guanine deletion at 5′-GGGA-3′ in rat mammary glands by 2-amino-1-methyl-6-phenylimidazo[4,5-*b*] pyridine, Carcinogenesis 20 (1999) 1933–1938.
[101] T. Shirai, M. Sano, S. Tamano, S. Takahashi, M. Hirose, M. Futakuchi, R. Hasegawa, K. Imaida, K. Matsumoto, K. Wakabayashi, T. Sugimura, N. Ito, The prostate: A target for carcinogenicity of 2-amino-1-methyl-6-phenylimidazo[4,5-*b*]pyridine (PhIP) derived from cooked foods, Cancer Res. 57 (1997) 195–198.
[102] G.R. Stuart, J. Holcroft, J.G. de Boer, B.W. Glickman, Prostate mutations in rats induced by the suspected human carcinogen 2-amino-1-methyl-6-phenylimidazo [4,5-*b*]pyridine, Cancer Res. 60 (2000) 266–268.
[103] Y. Nakai, W.G. Nelson, A.M. De Marzo, The dietary charred meat carcinogen 2-amino-1-methyl-6-phenylimidazo[4,5-b]pyridine acts as both a tumor initiator and promoter in the rat ventral prostate, Cancer Res. 67 (2007) 1378–1384.
[104] M. Nagao, T. Ushijima, M. Toyota, R. Inoue, T. Sugimura, Genetic changes induced by heterocyclic amines, Mutat. Res. 376 (1997) 161–167.

[105] M. Nagao, M. Ochiai, E. Okochi, T. Ushijima, T. Sugimura, LacI transgenic animal study: Relationships among DNA-adduct levels, mutant frequencies and cancer incidences, Mutat. Res. 477 (2001) 119–124.
[106] S.A. Bol, J. Horlbeck, J. Markovic, J.G. de Boer, R.J. Turesky, A. Constable, Mutational analysis of the liver, colon and kidney of Big Blue rats treated with 2-amino-3-methylimidazo[4,5-*f*]quinoline, Carcinogenesis 21 (2000) 1–6.
[107] R.A. Brooks, N.J. Gooderham, K. Zhao, R.J. Edwards, L.A. Howard, A.R. Boobis, D.J. Winton, 2-Amino-1-methyl-6-phenylimidazo[4,5-*b*]pyridine is a potent mutagen in the mouse small intestine, Cancer Res. 54 (1994) 1665–1671.
[108] A. Andreassen, R. Vikse, I.L. Steffensen, J.E. Paulsen, J. Alexander, Intestinal tumours induced by the food carcinogen 2-amino-1-methyl-6- phenylimidazo[4,5-*b*]pyridine in multiple intestinal neoplasia mice have truncation mutations as well as loss of the wild-type Apc^{+} allele, Mutagenesis 16 (2001) 309–315.
[109] H. Ohgaki, H. Hasegawa, T. Kato, M. Suenaga, M. Ubukata, S. Sato, S. Takayama, T. Sugimura, Carcinogenicity in mice and rats of heterocyclic amines in cooked foods, Environ. Health Perspect. 67 (1986) 129–134.
[110] G.R. Stuart, E. Thorleifson, E. Okochi, J.G. de Boer, T. Ushijima, M. Nagao, B.W. Glickman, Interpretation of mutational spectra from different genes: Analyses of PhIP-induced mutational specificity in the lacI and cII transgenes from colon of Big Blue rats, Mutat. Res. 452 (2000) 101–121.
[111] B.A. Diwan, K.E. Blackman, Differential susceptibility of 3 sublines of C57BL/6 mice to the induction of colorectal tumors by 1,2-dimethylhydrazine, Cancer Lett. 9 (1980) 111–115.
[112] H. Fujita, K. Nagano, M. Ochiai, T. Ushijima, T. Sugimura, M. Nagao, T. Matsushima, Difference in target organs in carcinogenesis with a heterocyclic amine, 2-amino-3,4-dimethylimidazo[4,5-f]quinoline, in different strains of mice, Jpn. J. Cancer Res. 90 (1999) 1203–1206.
[113] M. Ochiai, H. Imai, T. Sugimura, M. Nagao, H. Nakagama, Induction of intestinal tumors and lymphomas in C57BL/6N mice by a food-borne carcinogen, 2-amino-1-methyl-6-phenylimidazo[4,5-b]pyridine, Jpn. J Cancer Res. 93 (2002) 478–483.
[114] R.H. Adamson, U.P. Thorgeirsson, E.G. Snyderwine, J. Reeves, D.W. Dalgard, S. Takayama, T. Sugimura, Carcinogenicity of 2-amino-3-methylimidazo[4,5-*f*]quinoline in nonhuman primates: Induction of tumors in three macaques, Jpn. J. Cancer Res. 81 (1990) 10–14.
[115] M. Toyota, T. Ushijima, H. Kakiuchi, F. Canzian, M. Watanabe, K. Imai, T. Sugimura, M. Nagao, Genetic alterations in rat colon tumors induced by heterocyclic amines, Cancer 77 (1996) 1593–1597.
[116] N. Nagao, K. Wakabayashi, U. Ushijima, M. Toyota, Y. Totsuka, T. Sugimura, Human exposure to carcinogenic heterocyclic amines and their mutational fingerprints in animals, Environ. Health Perspect. 104 (Suppl. 3) (1996) 497–501.
[117] M. Nagao, Mutagenicity, in: M. Nagao, T. Sugimura (Eds.), Food Borne Carcinogens Heterocyclic Amines, John Wiley & Sons Ltd., Chichester, England, 2000, pp. 163–195.
[118] Y. Fujimoto, L.L. Hampton, E.G. Snyderwine, M. Nagao, T. Sugimura, R.H. Adamson, S.S. Thorgeirsson, p53 gene mutation in hepatocellular carcinoma induced by 2-amino-3-methylimidazo[4,5-*f*]quinoline in nonhuman primates, Jpn. J. Cancer Res. 85 (1994) 506–509.
[119] S.M. Powell, N. Zilz, Y. Beazer-Barclay, T.M. Bryan, S.R. Hamilton, S.N. Thibodeau, B. Vogelstein, K.W. Kinzler, APC mutations occur early during colorectal tumorigenesis, Nature 359 (1992) 235–237.
[120] D. Burnouf, R. Miturski, M. Nagao, H. Nakagama, M. Nothisen, J. Wagner, R.P. Fuchs, Early detection of 2-amino-1-methyl-6-phenylimidazo[4,5-*b*]pyridine(PhIP)-induced mutations within the *Apc* gene of rat colon, Carcinogenesis 22 (2001) 329–335.

[121] J. Alexander, B. Heidenreich, R. Reistad, J.A. Holme, Metabolism of the food carcinogen 2-amino-1-methyl-6-phenylimidazo[4,5-*b*]pyridine (PhIP) in the rat and other rodents, in: R.H. Adamson, J.-A. Gustafsson, N. Ito, M. Nagao, T. Sugimura, K. Wakabayashi, Y. Yamazoe (Eds.), Heterocyclic amines in cooked foods: Possible human carcinogens. 23rd Proceedings of the Princess Takamatusu Cancer Society, Princeton Scientific Publishing Co. Inc., NJ, 1995, pp. 59–68.
[122] R.S. King, F.F. Kadlubar, R.J. Turesky, In vivo metabolism of heterocyclic amines, in: M. Nagao, T. Sugimura (Eds.), Food Borne Carcinogens: Heterocyclic Amines, John Wiley & Sons Ltd., Chichester, England, 2000, pp. 90–111.
[123] Y. Yamazoe, K. Nagata, In vitro metabolism, in: T. Sugimura, M. Nagao (Eds.), Food Borne Carcinogens Heterocyclic Amines, John Wiley & Sons Ltd., Chichester, England, 2000, pp. 74–89.
[124] M. Bashir, D.G. Kingston, R.J. Carman, R.L. Van Tassell, T.D. Wilkins, Anaerobic metabolism of 2-amino-3-methyl-3H-imidazo[4,5-f]quinoline (IQ) by human fecal flora, Mutat. Res. 190 (1987) 187–190.
[125] R.J. Turesky, F.P. Guengerich, A. Guillouzo, S. Langouet, Metabolism of heterocyclic aromatic amines by human hepatocytes and cytochrome P4501A2, Mutat. Res. 506–507 (2002), 187–195.
[126] M.A. Butler, M. Iwasaki, F.P. Guengerich, F.F. Kadlubar, Human cytochrome P-450_{PA} (P450IA2), the phenacetin *O*-deethylase, is primarily responsible for the hepatic 3-demethylation of caffeine and N-oxidation of carcinogenic arylamines, Proc. Natl. Acad. Sci. U. S. A. 86 (1989) 7696–7700.
[127] T. Shimada, F.P. Guengerich, Activation of amino-α-carboline, 2-amino-1-methyl-6-phenylimidazo[4,5-*b*]pyridine, and a copper phthalocyanine cellulose extract of cigarette smoke condensate by cytochrome P-450 enzymes in rat and human liver microsomes, Cancer Res. 51 (1991) 5284–5291.
[128] C. Chen, X. Ma, M.A. Malfatti, K.W. Krausz, S. Kimura, J.S. Felton, J.R. Idle, F.J. Gonzalez, A comprehensive investigation of 2-amino-1-methyl-6-phenylimidazo [4,5-b]pyridine (PhIP) metabolism in the mouse using a multivariate data analysis approach, Chem Res. Toxicol. 20 (2007) 531–542.
[129] V.M. Lakshmi, F.F. Hsu, T.V. Zenser, N-Demethylation is a major route of 2-amino-3-methylimidazo[4,5-f]quinoline metabolism in mouse, Drug Metab Dispos. 36 (2008) 1143–1152.
[130] E.G. Snyderwine, R.J. Turesky, K.W. Turteltaub, C.D. Davis, N. Sadrieh, H.A. Schut, M. Nagao, T. Sugimura, U.P. Thorgeirsson, R.H. Adamson, S.S. Thorgeirsson, Metabolism of food-derived heterocyclic amines in nonhuman primates, Mutat. Res. 376 (1997) 203–210.
[131] S. Langouët, D.H. Welti, N. Kerriguy, L.B. Fay, T. Huynh-Ba, J. Markovic, F.P. Guengerich, A. Guillouzo, R.J. Turesky, Metabolism of 2-amino-3,8-dimethylimidazo [4,5-*f*]quinoxaline in human hepatocytes: 2-amino-3-methylimidazo[4,5-*f*]quinoxaline-8-carboxylic acid is a major detoxification pathway catalyzed by cytochrome P450 1A2, Chem. Res. Toxicol. 14 (2001) 211–221.
[132] R.J. Turesky, R.C. Garner, D.H. Welti, J. Richoz, S.H. Leveson, K.H. Dingley, K.W. Turteltaub, L.B. Fay, Metabolism of the food-borne mutagen 2-amino-3,8-dimethylimidazo[4,5-*f*]quinoxaline in humans, Chem. Res. Toxicol. 11 (1998) 217–225.
[133] K.S. Kulp, M.G. Knize, N.D. Fowler, C.P. Salmon, J.S. Felton, PhIP metabolites in human urine after consumption of well-cooked chicken, J. Chromatogr. B Analyt. Technol. Biomed. Life Sci. 802 (2004) 143–153.
[134] D.G. Walters, P.J. Young, C. Agus, M.G. Knize, A.R. Boobis, N.J. Gooderham, B.G. Lake, Cruciferous vegetable consumption alters the metabolism of the dietary carcinogen 2-amino-1-methyl-6-phenylimidazo[4,5-b]pyridine (PhIP) in humans, Carcinogenesis 25 (2004) 1659–1669.

[135] J.M. Fede, A.P. Thakur, N.J. Gooderham, R.J. Turesky, Biomonitoring of 2-amino-1-methyl-6-phenylimidazo[4,5-b]pyridine (PhIP) and its carcinogenic metabolites in urine, Chem Res. Toxicol. 22 (2009) 1096–1105.
[136] P.I. Mackenzie, K.W. Bock, B. Burchell, C. Guillemette, S. Ikushiro, T. Iyanagi, J.O. Miners, I.S. Owens, D.W. Nebert, Nomenclature update for the mammalian UDP glycosyltransferase (UGT) gene superfamily, Pharmacogenet. Genomics 15 (2005) 677–685.
[137] S.A. Nowell, J.S. Massengill, S. Williams, A. Radominska-Pandya, T.R. Tephly, Z. Cheng, C.P. Strassburg, R.H. Tukey, S.L. MacLeod, N.P. Lang, F.F. Kadlubar, Glucuronidation of 2-hydroxyamino-1-methyl-6-phenylimidazo[4,5-*b*]pyridine by human microsomal UDP-glucuronosyltransferases: Identification of specific UGT1A family isoforms involved, Carcinogenesis 20 (1999) 1107–1114.
[138] M.A. Malfatti, J.S. Felton, Human UDP-glucuronosyltransferase 1A1 is the primary enzyme responsible for the N-glucuronidation of N-hydroxy-PhIP in vitro, Chem. Res. Toxicol. 17 (2004) 1137–1144.
[139] R.W. Dellinger, G. Chen, A.S. Blevins-Primeau, J. Krzeminski, S. Amin, P. Lazarus, Glucuronidation of PhIP and N-OH-PhIP by UDP-glucuronosyltransferase 1A10, Carcinogenesis 28 (2007) 2412–2418.
[140] P.B. Styczynski, R.C. Blackmon, J.D. Groopman, T.W. Kensler, The direct glucuronidation of 2-amino-1-methyl-6-phenylimidazo[4,5-*b*]pyridine (PhIP) by human and rabbit liver microsomes, Chem. Res. Toxicol. 6 (1993) 846–851.
[141] S. Langouët, A. Paehler, D.H. Welti, N. Kerriguy, A. Guillouzo, R.J. Turesky, Differential metabolism of 2-amino-1-methyl-6-phenylimidazo[4,5- b]pyridine in rat and human hepatocytes, Carcinogenesis 23 (2002) 115–122.
[142] H. Girard, J. Thibaudeau, M.H. Court, L.C. Fortier, L. Villeneuve, P. Caron, Q. Hao, L.L. von Moltke, D.J. Greenblatt, C. Guillemette, UGT1A1 polymorphisms are important determinants of dietary carcinogen detoxification in the liver, Hepatology 42 (2005) 448–457.
[143] C.P. Strassburg, A. Vogel, S. Kneip, R.H. Tukey, M.P. Manns, Polymorphisms of the human UDP-glucuronosyltransferase (UGT) 1A7 gene in colorectal cancer, Gut 50 (2002) 851–856.
[144] M.A. Malfatti, K.H. Dingley, S. Nowell-Kadlubar, E.A. Ubick, N. Mulakken, D. Nelson, N.P. Lang, J.S. Felton, K.W. Turteltaub, The urinary metabolite profile of the dietary carcinogen 2-amino-1-methyl-6-phenylimidazo[4,5-b]pyridine is predictive of colon DNA adducts after a low-dose exposure in humans, Cancer Res. 66 (2006) 10541–10547.
[145] J. Alexander, H. Wallin, O.J. Rossland, K.E. Solberg, J.A. Holme, G. Becher, R. Andersson, S. Grivas, Formation of a glutathione conjugate and a semistable transportable glucuronide conjugate of N^2-oxidized species of 2-amino-1-methyl-6-phenylimidazo[4,5-*b*]pyridine (PhIP) in rat liver, Carcinogenesis 12 (1991) 2239–2245.
[146] K.R. Kaderlik, G.J. Mulder, R.J. Turesky, N.P. Lang, C.H. Teitel, M.P. Chiarelli, F.F. Kadlubar, Glucuronidation of *N*-hydroxy heterocyclic amines by human and rat liver microsomes, Carcinogenesis 15 (1994) 1701.
[147] D.W. Hein, M.A. Doll, A.J. Fretland, M.A. Leff, S.J. Webb, G.H. Xiao, U.S. Devanaboyina, N.A. Nangju, Y. Feng, Molecular genetics and epidemiology of the NAT1 and NAT2 acetylation polymorphisms, Cancer Epidemiol. Biomarkers Prev. 9 (2000) 29–42.
[148] D.W. Hein, Molecular genetics and function of NAT1 and NAT2: Role in aromatic amine metabolism and carcinogenesis, Mutat. Res. 506–507 (2002) 65–77.
[149] R.F. Minchin, P.T. Reeves, C.H. Teitel, M.E. McManus, B. Mojarrabi, K.F. Ilett, F.F. Kadlubar, *N*- and *O*-acetylation of aromatic and hetercyclic amine carcinogens by human monomorphic and polymorphic acetyltransferases expressed in *COS-1* cells, Biochem. Biophys. Res. Commun. 185 (1992) 839–844.

[150] R.J. Turesky, N.P. Lang, M.A. Butler, C.H. Teitel, F.F. Kadlubar, Metabolic activation of carcinogenic heterocyclic aromatic amines by human liver and colon, Carcinogenesis 12 (1991) 1839–1845.
[151] R.S. King, C.H. Teitel, F.F. Kadlubar, In vitro bioactivation of N-hydroxy-2-amino-alpha-carboline, Carcinogenesis 21 (2000) 1347–1354.
[152] R.L. Blanchard, R.R. Freimuth, J. Buck, R.M. Weinshilboum, M.W. Coughtrie, A proposed nomenclature system for the cytosolic sulfotransferase (SULT) superfamily, Pharmacogenetics 14 (2004) 199–211.
[153] S. Nowell, C.N. Falany, Pharmacogenetics of human cytosolic sulfotransferases, Oncogene 25 (2006) 1673–1678.
[154] S. Ozawa, K. Nagata, Y. Yamazoe, R. Kato, Formation of 2-amino-3-methylimidazo[4,5-f]quinoline- and 2-amino-3,8-dimethylimidazo[4,5-f]quinoxaline-sulfamates by cDNA-expressed mammalian phenol sulfotransferases, Jpn. J. Cancer Res. 86 (1995) 264–269.
[155] A.J. Lewis, U.K. Walle, R.S. King, F.F. Kadlubar, C.N. Falany, T. Walle, Bioactivation of the cooked food mutagen N-hydroxy-2-amino-1-methyl-6-phenylimidazo [4,5-b]pyridine by estrogen sulfotransferase in cultured human mammary epithelial cells, Carcinogenesis 19 (1998) 2049–2053.
[156] M. Tsuda, C. Negishi, R. Makino, S. Sato, Z. Yamaizumi, T. Hirayama, T. Sugimura, Use of nitrite and hypochlorite treatments in determination of the contributions of IQ-type and non-IQ-type heterocyclic amines to the mutagenicities in crude pyrolyzed materials, Mutat. Res. 147 (1985) 335–341.
[157] V.M. Lakshmi, H.A. Schut, T.V. Zenser, 2-Nitrosoamino-3-methylimidazo[4,5-f] quinoline activated by the inflammatory response forms nucleotide adducts, Food Chem. Toxicol. 43 (2005) 1607–1617.
[158] V.M. Lakshmi, M.L. Clapper, W.C. Chang, T.V. Zenser, Hemin potentiates nitric oxide-mediated nitrosation of 2-amino-3-methylimidazo[4,5-f]quinoline (IQ) to 2-nitrosoamino-3-methylimidazo[4,5-f]quinoline, Chem. Res. Toxicol. 18 (2005) 528–535.
[159] T.V. Zenser, V.M. Lakshmi, H.A. Schut, H.J. Zhou, P.D. Josephy, Activation of aminoimidazole carcinogens by nitrosation: mutagenicity and nucleotide adducts, Mutat. Res. 673 (2009) 109–115.
[160] R.J. Turesky, The role of genetic polymorphisms in metabolism of carcinogenic heterocyclic aromatic amines, Curr. Drug Metab. 5 (2004) 169–180.
[161] D.L. Eaton, E.P. Gallagher, T.K. Bammler, K.L. Kunze, Role of cytochrome P450 1A2 in chemical carcinogenesis: Implications for human variability in expression and enzyme activity, Pharmacogenetics 5 (1995) 259–274.
[162] C. Belloc, S. Baird, J. Cosme, S. Lecoeur, J.-C. Gautier, D. Challine, I. de Waziers, J.-P. Flinois, P.H. Beaune, Human cytochrome P450 expressed in *Escherichia coli*: Production of specific antibodies, Toxicology 106 (1996) 207–219.
[163] A.H. Conney, Induction of microsomal enzymes by foreign chemicals and carcinogenesis by polycyclic aromatic hydrocarbons: G. H. A. Clowes Memorial Lecture, Cancer Res. 42 (1982) 4875–4917.
[164] G.J. Hammons, Y. Yan-Sanders, B. Jin, E. Blann, F.F. Kadlubar, B.D. Lyn-Cook, Specific site methylation in the 5′-flanking region of CYP1A2 interindividual differences in human livers, Life Sci. 69 (2001) 839–845.
[165] M. Nakajima, T. Yokoi, M. Mizutani, M. Kinoshita, M. Funayama, T. Kamataki, Genetic polymorphism in the 5′-flanking region of human CYP1A2 gene: Effect on the CYP1A2 inducibility in humans, J. Biochem. (Tokyo) 125 (1999) 803–808.
[166] C. Sachse, U. Bhambra, G. Smith, T.J. Lightfoot, J.H. Barrett, J. Scollay, R.C. Garner, A.R. Boobis, C.R. Wolf, N.J. Gooderham, Polymorphisms in the cytochrome P450 CYP1A2 gene (CYP1A2) in colorectal cancer patients and controls:

Allele frequencies, linkage disequilibrium and influence on caffeine metabolism, Br. J. Clin. Pharmacol. 55 (2003) 68–76.
[167] Z. Jiang, N. Dragin, L.F. Jorge-Nebert, M.V. Martin, F.P. Guengerich, E. Aklillu, M. Ingelman-Sundberg, G.J. Hammons, B.D. Lyn-Cook, F.F. Kadlubar, S.N. Saldana, M. Sorter, A.A. Vinks, N. Nassr, R.O. von, L. Jin, D.W. Nebert, Search for an association between the human CYP1A2 genotype and CYP1A2 metabolic phenotype, Pharmacogenet. Genomics 16 (2006) 359–367.
[168] D.W. Hein, N-acetyltransferase 2 genetic polymorphism: effects of carcinogen and haplotype on urinary bladder cancer risk, Oncogene 25 (2006) 1649–1658.
[169] M. Garcia-Closas, N. Malats, D. Silverman, M. Dosemeci, M. Kogevinas, D.W. Hein, A. Tardon, C. Serra, A. Carrato, R. Garcia-Closas, J. Lloreta, G. Castano-Vinyals, M. Yeager, R. Welch, S. Chanock, N. Chatterjee, S. Wacholder, C. Samanic, M. Tora, F. Fernandez, F.X. Real, N. Rothman, NAT2 slow acetylation, GSTM1 null genotype, and risk of bladder cancer: Results from the Spanish Bladder Cancer Study and meta-analyses, Lancet 366 (2005) 649–659.
[170] E. Giovannucci, An updated review of the epidemiological evidence that cigarette smoking increases risk of colorectal cancer, Cancer Epidemiol. Biomarkers Prev. 10 (2001) 725–731.
[171] N.P. Lang, M.A. Butler, J.P. Massengill, M. Lawson, R.C. Stotts, M. Hauer-Jensen, F.F. Kadlubar, Rapid metabolic phenotypes for acetyltransferase and cytochrome P4501A2 and putative exposure to food-borne heterocyclic amines increase the risk for colorectal cancer or polyps, Cancer Epidemiol. Biomarkers Prev. 3 (1994) 675–682.
[172] L. Le Marchand, J.H. Hankin, L.M. Pierce, R. Sinha, P.V. Nerurkar, A.A. Franke, L.R. Wilkens, L.N. Kolonel, T. Donlon, A. Seifried, L.J. Custer, A. Lum-Jones, W. Chang, Well-done red meat, metabolic phenotypes and colorectal cancer in Hawaii, Mutat. Res. 506–507 (2002) 205–214.
[173] X.B. Zhang, J.S. Felton, J.D. Tucker, C. Urlando, J.A. Heddle, Intestinal mutagenicity of two carcinogenic food mutagens in transgenic mice: 2-amino-1-methyl-6-phenylimidazo[4,5-b]pyridine and amino(alpha)carboline, Carcinogenesis 17 (1996) 2259–2265.
[174] H. Okonogi, T. Ushijima, H. Shimizu, T. Sugimura, M. Nagao, Induction of aberrant crypt foci in C57BL/6N mice by 2-amino-9H-pyrido[2,3-b]indole (A alphaC) and 2-amino-3,8-dimethylimidazo[4,5-f]quinoxaline (MeIQx), Cancer Lett. 111 (1997) 105–109.
[175] R.B. Raftogianis, T.C. Wood, R.M. Weinshilboum, Human phenol sulfotransferases SULT1A2 and SULT1A1: Genetic polymorphisms, allozyme properties, and human liver genotype-phenotype correlations, Biochem. Pharmacol. 58 (1999) 605–616.
[176] W. Zheng, D. Xie, J.R. Cerhan, T.A. Sellers, W. Wen, A.R. Folsom, Sulfotransferase 1A1 polymorphism, endogenous estrogen exposure, well-done meat intake, and breast cancer risk, Cancer Epidemiol. Biomarkers Prev. 10 (2001) 89–94.
[177] S. Nowell, C.B. Ambrosone, S. Ozawa, S.L. MacLeod, G. Mrackova, S. Williams, J. Plaxco, F.F. Kadlubar, N.P. Lang, Relationship of phenol sulfotransferase activity (SULT1A1) genotype to sulfotransferase phenotype in platelet cytosol, Pharmacogenetics 10 (2000) 789–797.
[178] V. Moreno, H. Glatt, E. Guino, E. Fisher, W. Meinl, M. Navarro, J.M. Badosa, H. Boeing, Polymorphisms in sulfotransferases SULT1A1 and SULT1A2 are not related to colorectal cancer, Int. J. Cancer 113 (2005) 683–686.
[179] M. Steiner, M. Bastian, W.A. Schulz, T. Pulte, K.H. Franke, A. Rohring, J.M. Wolff, H. Seiter, P. Schuff-Werner, Phenol sulphotransferase SULT1A1 polymorphism in prostate cancer: lack of association, Arch. Toxicol. 74 (2000) 222–225.
[180] S.S. Hecht, Human urinary carcinogen metabolites: biomarkers for investigating tobacco and cancer, Carcinogenesis 23 (2002) 907–922.

[181] U. Peters, D.M. DeMarini, R. Sinha, L.R. Brooks, S.H. Warren, N. Chatterjee, N. Rothman, Urinary mutagenicity and colorectal adenoma risk, Cancer Epidemiol. Biomarkers Prev. 12 (2003) 1253–1256.
[182] D.S. Wishart, D. Tzur, C. Knox, R. Eisner, A.C. Guo, N. Young, D. Cheng, K. Jewell, D. Arndt, S. Sawhney, C. Fung, L. Nikolai, M. Lewis, M.A. Coutouly, I. Forsythe, P. Tang, S. Shrivastava, K. Jeroncic, P. Stothard, G. Amegbey, D. Block, D.D. Hau, J. Wagner, J. Miniaci, M. Clements, M. Gebremedhin, N. Guo, Y. Zhang, G.E. Duggan, G.D. Macinnis, A.M. Weljie, R. Dowlatabadi, F. Bamforth, D. Clive, R. Greiner, L. Li, T. Marrie, B.D. Sykes, H.J. Vogel, L. Querengesser, HMDB: The Human Metabolome Database, Nucleic Acids Res. 35 (2007) D521–D526.
[183] A.R. Boobis, A.M. Lynch, S. Murray, R. de la Torre, A. Solans, M. Farré, J. Segura, N.J. Gooderham, D.S. Davies, CYP1A2-catalyzed conversion of dietary heterocyclic amines to their proximate carcinogens is their major route of metabolism in humans, Cancer Res. 54 (1994) 89–94.
[184] J. Alexander, R. Reistad, S. Hegstad, H. Frandsen, K. Ingebrigtsen, J.E. Paulsen, G. Becher, Biomarkers of exposure to heterocyclic amines: Approaches to improve the exposure assessment, Food Chem. Toxicol. 40 (2002) 1131–1137.
[185] R.D. Holland, J. Taylor, L. Schoenbachler, R.C. Jones, J.P. Freeman, D.W. Miller, B.G. Lake, N.J. Gooderham, R.J. Turesky, Rapid biomonitoring of heterocyclic aromatic amines in human urine by tandem solvent solid phase extraction liquid chromatography electrospray ionization mass spectrometry, Chem. Res. Toxicol. 17 (2004) 1121–1136.
[186] H. Frandsen, Biomonitoring of urinary metabolites of 2-amino-1-methyl-6-phenylimidazo[4,5-b]pyridine (PhIP) following human consumption of cooked chicken, Food Chem Toxicol. 46 (2008) 3200–3205.
[187] W.G. Stillwell, L.-C.K.S.-B. Kidd, J.W. Wishnok, S.R. Tannenbaum, R. Sinha, Urinary excretion of unmetabolized and phase II conjugates of 2-amino-1-methyl-6-phenylimidazo[4,5-*b*]pyridine and 2-amino-3,8-dimethylimidazo[4,5-*f*]quinoxaline in humans: Relationship to cytochrome P450 1A2 and *N*-acetyltransferase activity, Cancer Res. 57 (1997) 3457–3464.
[188] W.G. Stillwell, R.J. Turesky, R. Sinha, P.L. Skipper, S.R. Tannenbaum, Biomonitoring of heterocyclic aromatic amine metabolites in human urine, Cancer Lett. 143 (1999) 145–148.
[189] P.T. Strickland, Z. Qian, M.D. Friesen, N. Rothman, R. Sinha, Metabolites of 2-amino-1-methyl-6-phenylimidazo[4,5-*b*]pyridine (PhIP) in human urine after consumption of charbroiled or fried beef, Mutat. Res. 506–507 (2002) 163–173.
[190] H. Frandsen, Deconjugation of N-glucuronide conjugated metabolites with hydrazine hydrate–biomarkers for exposure to the food-borne carcinogen 2-amino-1-methyl-6-phenylimidazo[4,5-b]pyridine (PhIP), Food Chem Toxicol. 45 (2007) 863–870.
[191] W.G. Stillwell, R. Sinha, S.R. Tannenbaum, Excretion of the N(2)-glucuronide conjugate of 2-hydroxyamino-1-methyl-6-phenylimidazo[4,5-b]pyridine in urine and its relationship to CYP1A2 and NAT2 activity levels in humans, Carcinogenesis 23 (2002) 831–838.
[192] W.G. Stillwell, R.J. Turesky, G.A. Gross, P.L. Skipper, S.R. Tannenbaum, Human urinary excretion of sulfamate and glucuronde conjugates of 2-amino-3,8-dimethylimdazo[4,5-*f*]quinoxaline (MeIQx), Cancer Epidemiol. Biomarkers Prev. 3 (1994) 399–405.
[193] R. Sinha, N. Rothman, S.D. Mark, S. Murray, E.D. Brown, O.A. Levander, D.S. Davies, N.P. Lang, F.F. Kadlubar, R.N. Hoover, Lower levels of urinary 2-amino-3,8-dimethylimidazo[4,5-f]-quinoxaline (MeIQx) in humans with higher CYP1A2 activity, Carcinogenesis 16 (1995) 2859–2861.
[194] K.L. Kunze, W.F. Trager, Isoform-selective mechanism-based inhibition of human cytochrome P450 1A2 by furafylline, Chem. Res. Toxicol. 6 (1993) 649–656.

[195] R.J. Turesky, V. Parisod, T. Huynh-Ba, S. Langouet, F.P. Guengerich, Regioselective differences in C(8)- and N-oxidation of 2-amino-3,8- dimethylimidazo[4,5-*f*] quinoxaline by human and rat liver microsomes and cytochromes P450 1A2, Chem. Res. Toxicol. 14 (2001) 901–911.

[196] L.C. Kidd, W.G. Stillwell, M.C. Yu, J.S. Wishnok, P.L. Skipper, R.K. Ross, B.E. Henderson, S.R. Tannenbaum, Urinary excretion of 2-amino-1-methyl-6-phenylimidazo[4,5-b]pyridine (PhIP) in White, African-American, and Asian-American men in Los Angeles County, Cancer Epidemiol. Biomarkers Prev. 8 (1999) 439–445.

[197] W.G. Stillwell, R.J. Turesky, R. Sinha, S.R. Tannenbaum, N-oxidative metabolism of 2-amino-3,8-dimethylimidazo[4,5-*f*]quinoxaline (MeIQx) in humans: Excretion of the N^2-glucuronide conjugate of 2-hydroxyamino-MeIQx in urine, Cancer Res. 59 (1999) 5154–5159.

[198] K.W. Turteltaub, R.J. Mauthe, K.H. Dingley, J.S. Vogel, C.E. Frantz, R.C. Garner, N. Shen, MeIQx-DNA adduct formation in rodent and human tissues at low doses, Mutat. Res. 376 (1997) 243–252.

[199] K.H. Dingley, K.D. Curtis, S. Nowell, J.S. Felton, N.P. Lang, K.W. Turteltaub, DNA and protein adduct formation in the colon and blood of humans after exposure to a dietary-relevant dose of 2-amino-1-methyl-6-phenylimidazo[4,5-*b*]pyridine, Cancer Epidemiol. Biomarkers Prev. 8 (1999) 507–512.

[200] C. Magagnotti, R. Pastorelli, S. Pozzi, B. Andreoni, R. Fanelli, L. Airoldi, Genetic polymorphisms and modulation of 2-amino-1-methyl-6-phenylimidazo[4,5-b]pyridine (PhIP)-DNA adducts in human lymphocytes, Int. J Cancer 107 (2003) 878–884.

[201] K.W. Turteltaub, K.H. Dingley, K.D. Curtis, M.A. Malfatti, R.J. Turesky, R.C. Garner, J.S. Felton, N.P. Lang, Macromolecular adduct formation and metabolism of heterocyclic amines in humans and rodents at low doses, Cancer Lett. 143 (1999) 149–155.

[202] T.J. Lightfoot, J.M. Coxhead, B.C. Cupid, S. Nicholson, R.C. Garner, Analysis of DNA adducts by accelerator mass spectrometry in human breast tissue after administration of 2-amino-1-methyl-6-phenylimidazo[4,5-b]pyridine and benzo[a]pyrene, Mutat. Res. 472 (2000) 119–127.

[203] Y. Totsuka, K. Fukutome, M. Takahashi, S. Takashi, A. Tada, T. Sugimura, K. Wakabayashi, Presence of N^2-(deoxyguanosin-8-yl)-2-amino-3,8-dimethylimidazo[4,5-*f*]quinoxaline (dG-C8-MeIQx) in human tissues, Carcinogenesis 17 (1996) 1029–1034.

[204] M.D. Friesen, K. Kaderlik, D. Lin, L. Garren, H. Bartsch, N.P. Lang, F.F. Kadlubar, Analysis of DNA adducts of 2-amino-1-methyl-6-phenylimidazo[4,5-*b*]pyridine in rat and human tissues by alkaline hydrolysis and gas chromatography/electron capture mass spectrometry: Validation by comparison with ^{32}P-postlabeling, Chem. Res. Toxicol. 7 (1994) 733–739.

[205] D.-X. Lin, D.J. Meyer, B. Ketterer, N.P. Lang, F.F. Kadlubar, Effects of human and rat glutathione-S-transferase on the covalent binding of the *N*-acetoxy derivatives of heterocyclic amine carcinogens *in vitro*: A possible mechanism of organ specificity in their carcinogensis, Cancer Res. 54 (1994) 4920–4926.

[206] B.F. Coles, F.F. Kadlubar, Detoxification of electrophilic compounds by glutathione S-transferase catalysis: Determinants of individual response to chemical carcinogens and chemotherapeutic drugs? *Biofactors* 17 (2003) 115–130.

[207] J. Zhu, P. Chang, M.L. Bondy, A.A. Sahin, S.E. Singletary, S. Takahashi, T. Shirai, D. Li, Detection of 2-amino-1-methyl-6-phenylimidazo[4,5-b]-pyridine-DNA adducts in normal breast tissues and risk of breast cancer, Cancer Epidemiol. Biomarkers Prev. 12 (2003) 830–837.

[208] K. Gorlewska-Roberts, B. Green, M. Fares, C.B. Ambrosone, F.F. Kadlubar, Carcinogen-DNA adducts in human breast epithelial cells, Environ. Mol. Mutagen. 39 (2002) 184–192.

[209] D. Tang, J.J. Liu, A. Rundle, C. Neslund-Dudas, A.T. Savera, C.H. Bock, N.L. Nock, J.J. Yang, B.A. Rybicki, Grilled meat consumption and PhIP-DNA adducts in prostate carcinogenesis, Cancer Epidemiol. Biomarkers Prev. 16 (2007) 803–808.
[210] R. Singh, P.B. Farmer, Liquid chromatography-electrospray ionization-mass spectrometry: the future of DNA adduct detection, Carcinogenesis 27 (2006) 178–196.
[211] E.M. Ricicki, J.R. Soglia, C. Teitel, R. Kane, F. Kadlubar, P. Vouros, Detection and quantification of N-(deoxyguanosin-8-yl)-4-aminobiphenyl adducts in human pancreas tissue using capillary liquid chromatography-microelectrospray mass spectrometry, Chem Res. Toxicol. 18 (2005) 692–699.
[212] F.A. Beland, M.I. Churchwell, L.S. Von Tungeln, S. Chen, P.P. Fu, S.J. Culp, B. Schoket, E. Gyorffy, J. Minarovits, M.C. Poirier, E.D. Bowman, A. Weston, D.R. Doerge, High-performance liquid chromatography electrospray ionization tandem mass spectrometry for the detection and quantitation of benzo[a]pyrene-DNA adducts, Chem. Res. Toxicol. 18 (2005) 1306–1315.
[213] A.P. Grollman, S. Shibutani, M. Moriya, F. Miller, L. Wu, U. Moll, N. Suzuki, A. Fernandes, T. Rosenquist, Z. Medverec, K. Jakovina, B. Brdar, N. Slade, R.J. Turesky, A.K. Goodenough, R. Rieger, M. Vukelic, B. Jelakovic, Aristolochic acid and the etiology of endemic (Balkan) nephropathy, Proc. Natl. Acad. Sci. U. S. A. 104 (2007) 12129–12134.
[214] L. Chen, M. Wang, P.W. Villalta, X. Luo, R. Feuer, J. Jensen, D.K. Hatsukami, S.S. Hecht, Quantitation of an acetaldehyde adduct in human leukocyte DNA and the effect of smoking cessation, Chem. Res. Toxicol. 20 (2007) 108–113.
[215] P.L. Skipper, X. Peng, C.K. SooHoo, S.R. Tannenbaum, Protein adducts as biomarkers of human carcinogen exposure, Drug Metab. Rev. 26 (1994) 111–124.
[216] K.H. Dingley, S.P. Freeman, D.O. Nelson, R.C. Garner, K.W. Turteltaub, Covalent binding of 2-amino-3,8-dimethylimidazo[4,5-*f*]quinoxaline to albumin and hemoglobin at environmentally relevant doses. Comparison of human subjects and F344 rats, Drug Metab. Dispos. 26 (1998) 825–828.
[217] T. Peters, Jr, All about Albumin. Biochemistry, Genetics, and Medical applications, Academic Press, San Diego, 1996.
[218] S. Carballal, R. Radi, M.C. Kirk, S. Barnes, B.A. Freeman, B. Alvarez, Sulfenic acid formation in human serum albumin by hydrogen peroxide and peroxynitrite, Biochemistry 42 (2003) 9906–9914.
[219] J.L. Beck, S. Ambahera, S.R. Yong, M.M. Sheil, J.J. de, S.F. Ralph, Direct observation of covalent adducts with Cys34 of human serum albumin using mass spectrometry, Anal. Biochem. 325 (2004) 326–336.
[220] J.F. Keaney, Jr, D.I. Simon, J.S. Stamler, O. Jaraki, J. Scharfstein, J.A. Vita, J. Loscalzo, NO forms an adduct with serum albumin that has endothelium-derived relaxing factor-like properties, J. Clin. Invest. 91 (1993) 1582–1589.
[221] R.J. Turesky, P.L. Skipper, S.R. Tannenbaum, Binding of 2-amino-3-methylimidazo[4,5-*f*]quinoline to hemoglobin and alubmin in the rat. Identificaiton of an adduct suitable for dosimetry, Carcinogenesis 8 (1987) 1537–1542.
[222] A.M. Lynch, S. Murray, K. Zhao, N.J. Gooderham, A.R. Boobis, D.S. Davies, Molecular dosimetry of the food-borne carcinogen MeIQx using adducts of serum albumin, Carcinogenesis 14 (1993) 191–194.
[223] R. Reistad, H. Frandsen, S. Grivas, J. Alexander, In vitro formation and degradation of 2-amino-1-methyl-6- phenylimidazo[4,5-*b*]pyridine (PhIP) protein adducts, Carcinogenesis 15 (1994) 2547–2552.
[224] C.L. Chepanoske, K. Brown, K.W. Turteltaub, K.H. Dingley, Characterization of a peptide adduct formed by N-acetoxy-2-amino-1-methyl-6-phenylimidazo[4,5-b] pyridine (PhIP), a reactive intermediate of the food carcinogen PhIP, Food Chem Toxicol. 42 (2004) 1367–1372.

[225] D. Noort, A. Fidder, A.G. Hulst, Modification of human serum albumin by acrylamide at cysteine-34: A basis for a rapid biomonitoring procedure, Arch. Toxicol. 77 (2003) 543–545.
[226] D. Noort, A.G. Hulst, L.P. de Jong, H.P. Benschop, Alkylation of human serum albumin by sulfur mustard in vitro and in vivo: Mass spectrometric analysis of a cysteine adduct as a sensitive biomarker of exposure, Chem. Res. Toxicol. 12 (1999) 715–721.
[227] W.E. Bechtold, J.K. Willis, J.D. Sun, W.C. Griffith, T.V. Reddy, Biological markers of exposure to benzene: S-phenylcysteine in albumin, Carcinogenesis 13 (1992) 1217–1220.
[228] K.J. Hoffmann, A.J. Streeter, D.B. Axworthy, T.A. Baillie, Structural characterization of the major covalent adduct formed in vitro between acetaminophen and bovine serum albumin, Chem Biol. Interact. 53 (1985) 155–172.
[229] D. Kim, F.F. Kadlubar, C.H. Teitel, F.P. Guengerich, Formation and reduction of aryl and heterocyclic nitroso compounds and significance in the flux of hydroxylamines, Chem. Res. Toxicol. 17 (2004) 529–536.
[230] C. Magagnotti, F. Orsi, R. Bagnati, N. Celli, D. Rotilio, R. Fanelli, L. Airoldi, Effect of diet on serum albumin and hemoglobin adducts of 2-amino-1-methyl-6-phenylimidazo[4,5-b]pyridine (PhIP) in humans, Int. J. Cancer 88 (2000) 1–6.
[231] R.L. DuPont, W.A. Baumgartner, Drug testing by urine and hair analysis: Complementary features and scientific issues, Forensic Sci. Int. 70 (1995) 63–76.
[232] Y. Nakahara, K. Takahashi, R. Kikura, Hair analysis for drugs of abuse. X. Effect of physicochemical properties of drugs on the incorporation rates into hair, Biol. Pharm. Bull. 18 (1995) 1223–1227.
[233] S. Hegstad, R. Reistad, L.S. Haug, J. Alexander, Eumelanin is a major determinant for 2-amino-1-methyl-6-phenylimidazo[4,5-*b*]pyridine (PhIP) incorporation into hair of mice, Pharmacol. Toxicol. 90 (2002) 333–337.
[234] H. Hashimoto, T. Hanaoka, M. Kobayashi, S. Tsugane, Analytical method of 2-amino-1-methyl-6-phenylimidazo[4,5-b]pyridine in human hair by column-switching liquid chromatography-mass spectrometry, J. Chromatogr. B Analyt. Technol. Biomed. Life Sci. 803 (2004) 209–213.
[235] M. Kobayashi, T. Hanaoka, H. Hashimoto, S. Tsugane, 2-Amino-1-methyl-6-phenylimidazo[4,5-b]pyridine (PhIP) level in human hair as biomarkers for dietary grilled/stir-fried meat and fish intake, Mutat. Res.588 (2005) 136–142.
[236] R. Reistad, S.H. Nyholm, L.S. Huag, G. Becher, J. Alexander, 2-Amino-1-methyl-6-phenylimidazo[4,5-*b*]pyridine (PhIP) in human hair as biomarker for dietary exposure, *Biomarkers*, 4 (1999) 263–271.
[237] E.E. Bessette, I. Yasa, D. Dunbar, L. Wilkens, L. Le Marchand, R.J. Turesky, Biomonitoring of carcinogenic heterocyclic aromatic amines in hair: a validation assay. Chem. Res. Toxic. 22 (2009) 1454–1463.
[238] J.S. Felton, M.G. Knize, L.M. Bennett, M.A. Malfatti, M.E. Colvin, K.S. Kulp, Impact of environmental exposures on the mutagenicity/carcinogenicity of heterocyclic amines, Toxicology 198 (2004) 135–145.
[239] W. Ni, L. McNaughton, D.M. LeMaster, R. Sinha, R.J. Turesky, Quantitation of 13 heterocyclic aromatic amines in cooked beef, pork, and chicken by liquid chromatography-electrospray ionization/tandem mass spectrometry, J. Agric. Food Chem. 56 (2008) 68–78.
[240] S. Manabe, N. Kurihara, O. Wada, K. Tohyama, T. Aramaki, Formation of PhIP in a mixture of creatinine, phenylalanine and sugar or aldehyde by aqueous heating, Carcinogenesis 13 (1992) 827–830.
[241] S. Manabe, H. Suzuki, O. Wada, A. Ueki, Detection of the carcinogen 2-amino-1-methyl-6-phenylimidazo[4,5-*b*]pyridine (PhIP) in beer and wine, Carcinogenesis 14 (1993) 899–901.

[242] S. Hegstad, R. Reistad, L.S. Haug, J. Alexander, Eumelanin is a major determinant for 2-amino-1-methyl-6-phenylimidazo[4,5-*b*]pyridine (PhIP) incorporation into hair of mice, Pharmacol. Toxicol. 90 (2002) 333–337.
[243] H. Ozeki, S. Ito, K. Wakamatsu, A.J. Thody, Spectrophotometric characterization of eumelanin and pheomelanin in hair, Pigment Cell Res. 9 (1996) 265–270.

CHAPTER 3

Recent Advances in Molecular Toxicology of Cadmium and Nickel

Ewa Kurowska[1] *and* Wojciech Bal[1,2,*]

Contents

1. Introduction

Factors eliciting toxicity can be subdivided into physical, chemical, and biological ones. Physical toxic agents include a wide section of the electromagnetic radiation spectrum, from gamma rays through X-rays and

[1] Institute of Biochemistry and Biophysics, Polish Academy of Sciences, Pawińskiego, Warsaw, Poland

[2] Central Institute for Labour Protection—National Research Institute, Czerniakowska, Warsaw, Poland

[*] Corresponding author. Tel.: +48 22 592 2346; Fax: +48 22 658 4636
Email address: wbal@ibb.waw.pl

Advances in Molecular Toxicology, Volume 4
ISSN 1872-0854, DOI 10.1016/S1872-0854(10)04003-8

ultraviolet, to infrared and microwaves, corpuscular radiation, and other physical processes capable of delivering enough uncontrolled energy to interfere with biological processes. Biological toxic agents include parasites, infectious fungi, bacteria, and viruses, as well as toxins produced by infectious organisms *in vivo*. Chemical toxic factors cover the field in-between, with significant overlaps. An example from the physics/chemistry borderline is provided by radioactive elements introduced into the organism. They generally act as sources of highly energetic photons and particles, which elicit cascades of ionizing radiation intermediates. Their actual toxicities will, however, depend on their biodistribution, which in turn depends on their nonradiative, chemical properties. Moreover, many radioactive elements, uranium for example, are definite chemical poisons as well [1]. Toxins present in venoms of such organisms as marine snails or snakes serve as an example from the biology/chemistry borderline. These toxins have an obvious biological origin and are introduced into their victims by a definitely biological act of stinging or biting. From this moment, however, they act solely by the virtue of their chemical properties.

In molecular terms toxic agents can be divided into organic poisons (such as ethylene glycol, sarin, and strychnine) and inorganic poisons (such as chlorine, cyanide, and phosgene). The latter ones are distinguished somewhat formally by the absence of carbon–carbon bonds. In this simplistic classification, toxins produced by living organisms generally, but not exclusively, belong to the organic chemistry realm. Proteins (e.g., botulinum toxin or ricin) or alkaloids (e.g., atropine or tubocurarine) are typical organic toxins, but, for example, the toxicity of cyanogenetic glycosides, such as amygdalin, is due to the release of a classical inorganic poison, hydrogen cyanide, from their molecules upon the action of β-galactosidase.

Toxic metal ions have a specific property that differentiates them from all other poisons. Inorganic or organic toxins are multiatomic molecules, which, at least in principle, can be detoxicated by chemical modification, in particular, by decomposition into nontoxic derivatives. A toxic metallic element cannot be transmuted into another, nontoxic one by biological means. (Transmutation is an alchemy term for changing lead into gold. In modern terms transmutation is equivalent to nuclear reaction which can be accomplished in a controlled fashion in an accelerator, and nuclear explosion is an example of uncontrolled transmutation.) Therefore, the means of defense against toxic metal ions are seriously limited, only to immobilization or excretion. Furthermore, a toxic metal ion can act by many molecular pathways. Being indestructible, it can migrate from one interaction with a protein, nucleic acid, or small molecule to another. Many toxic metal ions act indirectly, as catalysts facilitating the formation of inorganic or organic toxins.

In this context, we need to make a note regarding two styles of naming partners in such interactions. A biochemical convention uses the term ligand for small molecules, including metal ions that bind to macromolecules such as proteins. In coordination chemistry, however, the term ligand is used to label all molecules, big or small, which form bonds with metal ions, assumed to be the center of the complex. The latter convention seems to be more appropriate for describing interactions of toxic metals with biomolecules. Toxic metals usually do not have their specific physiological binding partners (they are not dedicated to macromolecules of any specific kind). Instead, they are "free to choose"—it is their binding preferences that define toxic interactions.

The toxicity of metal ions is aggravated by the fact that many of them are either absent from the natural environment, or present there in such chemical forms that make them inaccessible for a living system. Such metals are particularly dangerous, when introduced into the environment or mobilized from hitherto safe stores as a result of industrial activity, because no defense mechanisms have had a chance to evolve against them. Aluminum poisoning of fish in Northeast United States and Scandinavian lakes several decades ago, caused by the dissolution of soil aluminosilicates by acid rain of industrial origin is a classical example of such an event [2,3].

Mercury and lead are two very toxic elements, which have been present in human environment in very large quantities, due to their widespread technological usage since antiquity [4]. The increasing awareness of their toxicity, particularly neurotoxicity in children [5,6], led to a gradual withdrawal of these metals and their compounds from materials and objects accessible to general public. Lead was first to go. Lead metal water pipes (the memory of this technology frozen in the word plumber, from Latin *plumbum* for lead) and toy soldiers, pigments in paints, such as yellow lead (II) chromate ($PbCrO_4$) and white lead(II) carbonate ($PbCO_3$), and tetraethyllead additive to gasoline [7] have been gradually vanishing from the human environment in most countries. Somewhat surprisingly, extremely toxic mercury has been slower to depart. Recent European Union (EU) decisions to promote energy-saving light sources may even result in the increase of environmental mercury burden. However, such potentially hazardous mercury applications, as amalgam dental fillings [8], spill-prone mercury thermometers, and mercury-containing drug preservatives (sodium ethylmercurithiosalicylate—thimerosal) [9] are being gradually removed from the global market (the latter has been banned in EU since 2001, but is still approved in the United States and many other countries).

The aim of this review is to summarize the current state of knowledge about molecular mechanisms of toxicity of two other, very toxic, metals: cadmium (Cd) and nickel (Ni). These two elements are abundant in the human environment, largely due to their applications in the articles of everyday use. The amount of evidence of their toxicity and carcinogenesis

at low doses is rising continuously. Health hazards to large communities due to current exposures to these two elements are likely. Yet, the awareness of their toxic properties seems to be limited, compared to that related to lead and mercury.

2. Chemical Properties and Routes of Exposure to Cadmium and Nickel Compounds

2.1. Chemical properties of cadmium

Cd, element no. 48, belongs to the 12th group of the periodic table (together with zinc and mercury), due to its electron configuration [Kr] $4d^{10}5s^2$. Natural Cd is a mixture of eight isotopes with isotopic masses between 106 and 116. Its standard atomic weight is 112.41 Da. In its elemental metallic form Cd is soft and malleable at room temperature. It undergoes passivation in contact with oxygen, being covered with a layer of Cd oxide. Chemistry of Cd includes 0, +1, and +2 oxidation states; however, only Cd(II) compounds are stable under ambient conditions. In complexes Cd(II) coordination numbers vary from 2 to 8, with 4 (tetrahedral) and 6 (octahedral) being the most frequent ones [10]. The d-electron shell of Cd(II) is filled, therefore, its chemical behavior is similar to that of main group rather than transition metals. Cd(II) is a moderately soft metal ion, forming particularly strong bonds with thiolates, but can also interact effectively with oxygen and nitrogen donors [11,12]. Consequently, CdS and CdO are the most important binary Cd(II) compounds. Thiolate Cd(II) complexes are tetrahedral, and isostructural with Zn(II) complexes [11,13]. Higher coordination numbers are encountered in oxygen donor environments, by analogy to Ca(II) [11].

2.2. Chemical properties of nickel

Ni, element no. 28 belongs to the 10th group of the periodic table (together with palladium and platinum), due to its electron configuration [Ar]$3d^8 4s^2$. Natural Ni is a mixture of five stable isotopes with isotopic masses between 58 and 64, with 58 and 60 being most abundant. Its standard atomic weight is 58.69 Da. Elemental Ni is a white metal with a yellowish shade. It is malleable, melts in high temperatures, and is ferromagnetic up to 627 K (Curie temperature for Ni). Metallic Ni is resistant to corrosion in humid air. In chemical compounds Ni can be encountered at oxidation levels from −1 to +4, but Ni(II) is by far the most important oxidation level at ambient conditions. Its most common coordination numbers are 4, 5, and 6 [10]. The existence of readily interconvertible high- and low-spin Ni(II)

compounds is the most characteristic feature of Ni(II) chemistry, because of the accompanying changes of color (Ni(II) termochromism). High-spin Ni(II) complexes are usually octahedral (six-coordinate) and the low-spin complexes are typically square-planar (four-coordinate). Much less frequent square-pyramidal (five-coordinate) species occur for both high- and low-spin configurations. Ni(II) readily accepts oxygen, nitrogen, and sulfur ligands. Harder ligands, like water or carboxylate oxygens, stabilize high-spin complexes, whereas softer donors, like thiolate sulfurs promote the formation of low-spin complexes [13].

Low oxidation levels, –1 and 0, are encountered in organometallic complexes (defined as those containing metal–carbon bonds). The very stable Ni(0) tetracarbonyl is the most important of them. Ni(I) complexes are very unstable in air. This oxidation level is stabilized by thiolate coordination and is known mostly from bioinorganic studies of redox enzymes of anaerobic microorganisms [14]. Ni(III) is a strong oxidant, stabilized by strong nitrogen ligands [15,16]. Compounds of the even stronger oxidant, Ni(IV) are very rare and unstable. Characteristically, the spin state of a Ni(II) complex controls its redox properties: the Ni(I) and Ni (III) state are accessible only from the low-spin complexes, while Ni(IV) complexes can only be obtained from high-spin species [17]. This phenomenon is due to Jahn–Teller effect, which precludes the octahedral geometry for d-electron configurations of d7 and d9, corresponding to Ni(III) and Ni (I), respectively.

2.3. Exposures to cadmium

Cd is widespread in the natural environment at low levels, comprising ~1.5×10^{-5}% of the earth's crust. It accompanies mainly zinc and also calcium (e.g., otavite, $CdCO_3$) [18,19]. Grenockite, CdS, the most important specific Cd mineral, is very rare in nature, and industrial Cd is obtained as a by-product of refinement of copper and zinc. Cd is not considered to be essential for life in general. However, an interesting exception is provided by marine diatoms grown under zinc deficiency. The addition of Cd (II) can restore growth in these organisms, apparently by taking up key enzymatic functions of Zn(II), including that in carbonic anhydrase [20,21]. As mentioned above, due to chemical similarities with Ca(II), Cd(II) is sometimes present in limestone soils and often accompanies phosphates. Several anthropogenic sources of Cd(II) are relevant for the general population. Large-scale burning of materials containing Cd is one of them. Energetic coal burning spreads very fine dusts and ashes containing Cd oxide and inorganic salts over large areas [22]. There is, however, a very large variation of Cd contents depending on geological origin of the solid fossil fuel [23]. Municipal solid waste incinerators (MSWI) appear to be

important sources of Cd enriched fly ash. Their overall emissions are much smaller, than the energetic ones, but MSWI are often located close to human settlements [24]. The speciation of Cd in MSWI fly ashes is more complex, with "hot spots" made of water soluble, and thus readily bioavailable Cd halides and sulfate ($CdCl_2$, $CdBr_2$, and $CdSO_4$), accompanied by less bioavailable Cd silicate, oxide, and metallic Cd [25–27]. Further sources include phosphate fertilizers, which may contain up to 0.01% of Cd, depending on the geological source of the phosphate [28], and calcium carbonate used for re-cultivation of acidified soils and waters (however, the liming process may actually reduce bioavailability of Cd from natural acid soils [29]). Industrial emissions of Cd are related to its usage in the manufacturing of Ni–Cd accumulators, pigments, alloys (addition of Cd lowers the melting point), and organic polymers (e.g., Cd(II) compounds are used as stabilizers in plastics such as PVC). Some plants, including tobacco, are efficient Cd(II) bioaccumulators. As a result, tobacco smoking is perhaps the most relevant source of Cd exposure to persons not exposed occupationally [30]. Both first- and second-hand smoke is dangerous, as air exhaled by a smoker is enriched in Cd [31].

Accumulation in farm animals is strongly organ-specific, with kidney as a prime target [32]. Doses of Cd at the level of 1–3 μg Cd per day approximately, ingested with food and drink in industrialized areas, such as EU, are not considered hazardous [33,34]. However, the bioavailability of food Cd depends on a person's nutritional status. The intestinal absorption of Cd, generally proportional to the concentration in the diet, is reduced, if the nutritional status of zinc, iron, or calcium of a person is high, and correspondingly, the low general nutritional status of these metals enhances Cd absorption [34]. A significant consumption of specific foods may affect both factors. For example, rice accumulates Cd into grain, when available, but excludes zinc, even when grown on soils rich in zinc. Consumption of such rice leads to zinc/iron malnutrition and increase of Cd intestinal absorption and accumulation. On the other hand, the consumption of foods rich in Cd, iron, and zinc, such as seafood, does not increase Cd absorption [35]. This fact is especially important with respect to premenopausal women, who commonly have low body iron stores [35]. Recent studies indicate that divalent metal transporter-1 (DMT-1) is partially, but not exclusively responsible for increased Cd absorption in the presence of a nutritional deficit of other metal ions transported by DMT-1 [36].

Occupational exposures to Cd relevant to human health are mainly of respiratory nature, and are related to mining or manufacturing of batteries and pigments. The average consumption of Cd with tobacco smoke, ~1–3 μg of Cd per pack of cigarettes is considered to be of a higher toxicological importance. The Cd turnover in the human body is slow, with a biological half-life of ~10–20 or more years, significantly higher in

women [37,38]. Consequently, Cd tends to accumulate in human body with age, and heavy smokers accumulate significantly more Cd than non-smokers [37–39]. Also, the environmental exposure in childhood aggravates the Cd status in adults [40].

2.4. Exposures to nickel

Ni is widespread in the environment at levels generally higher than those of Cd. It comprises 0.0084% of the Earth's crust, existing mostly as soluble salts (sulfate, chloride, etc.) and insoluble compounds (sulfides, oxide). Major ores of Ni include pentlandite $(Fe,Ni)_9S_8$ accompanied by other sulfide minerals, and are excavated, for example, in the world's largest deposits in Sudbury in Canada, Norilsk in Russia, and most other mining sites, except for New Caledonia, where garnierite [hydrous Ni silicate $(Ni, Mg)_3Si_2O_5(OH)$] ores are exploited. Higher soil Ni(II) levels are encountered locally, due to particular geological conditions and in the areas of Ni ore mining and smelting, such as Sudbury [41].

Ni-containing cofactors are crucial components of several enzymes key to metabolism of archaeons and anaerobic bacteria, providing redox chemistry for functions such as energy generation and utilization, akin to those assumed by copper enzymes in aerobic organisms [14]. Ni is also essential for legumes, and some other higher plants, and for many species of aerobic bacteria and fungi. Two Ni(II) ions constitute the active site of ureases, a unique class of nonredox enzymes breaking down urea to ammonia, which is an appropriate nitrogen source for plants [42,43]. Apart from this specific usage, Ni(II) is bioaccumulated in some plant foods such as spinach, cocoa, and nuts [44]. Tobacco also accumulates Ni (II).

The literature provides conflicting data on the extent of intestinal absorption of Ni(II) salts, from as low, at 1–5% of the dose to as high as 20–25% [45–47]. The nutritional status and mode of administration seem to be crucial in this respect. The urinary elimination of Ni(II) is rather rapid—with a half-life of approximately a couple of days [48]. A high proportion of ingested Ni(II) is removed from the human body with urine within several days. Opposite Cd, the retention of Ni is lower in women than in men, by a factor of 2 [49]. Oral exposure to low doses of Ni(II) compounds is not considered to be hazardous. This notion is supported by animal experiments [50]. However, a prolonged elevation of respiratory cancer risk in retired Ni refinery workers, has been related to continuous presence of accumulated Ni(II) in their airways [51,52]. The clearance of insoluble Ni(II) compounds is about 10 times slower than that of soluble compounds [53].

Ni is listed in many textbooks as an essential microelement in humans, on the basis of experiments on animals fed on Ni-deficient

diets (reviewed in [54]). The lack of specificity of effects observed, seems to be associated with an absence of any Ni-specific physiological process in animals, including humans. In contrast, many bacteria, including the notorious *Helicobacter pylori*, which causes peptic ulcers, require Ni(II) for urease, which is similar to that described above [55]. The opinion that Ni is required by (not necessarily beneficial) bacteria inhabiting our digestive tracts, rather than ourselves, was expressed some time ago [54]. We are not aware of any new facts that could challenge it. On the contrary, all recent research, reviewed below, provided evidence for toxic effects of Ni(II) in human body.

Major industrial uses of Ni include stainless steel and other alloys. White Ni alloy with copper (75% Cu, 25% Ni), other Cu–Ni and Cu–Ni–Zn alloys, and sometimes even pure metallic Ni are used worldwide for coin production. Other uses of Ni include Ni plating of corrosion-prone metals, such as iron, manufacturing of Ni–Cd batteries, and Ni-based catalysts, including those for industrial hydrogenation processes (such as that of edible oil) and carbon nanoparticle manufacturing.

Occupational exposure to Ni compounds is mostly respiratory, similarly to Cd. It is associated with Ni mining and refinement, electroplating, metallurgy of Ni-containing alloys and stainless-steel welding. Another type of respiratory exposure, affecting the general public, is due to residual fly ash containing bioavailable Ni(II) compounds [56]. There are two types of such ash. Residual oil fly ash (ROFA) is generated in the course of combustion of heavier fractions of oil products in diesel car engines and power plants. Its Ni contents can be as high as 1.5% [57], and the resulting air level of Ni in large cities and industrial areas is increased by a factor of 10–20, compared to suburban areas [58]. Some coal burning electric power plants and MSWI also emit fly ash containing significant amounts of Ni [59,60]. The presence of Ni in oil and coal reflects its physiological functions in anaerobic bacteria and plants, respectively. Ni is present in ROFA predominantly as water-soluble $NiSO_4$, with varied amounts of insoluble salts, including little or no sulfides [57,61]. In contrast, other types of fly ash contain mainly Ni oxide and sulfides, followed by insoluble Ni(II) compounds and metallic Ni, and generally little amounts of $NiSO_4$ [60,62]. Ni is bioavailable from ROFA to airways and may be partially responsible for acute toxic effects of ROFA inhalations, as determined using experiments on cell lines and laboratory animals [63–68]. These studies point, however, toward vanadium(IV) and vanadium(V) compounds, which always accompany Ni in ROFA, as the major source of direct oxidative damage to cells, observed as a result of acute exposure.

3. Health Hazards Due to Exposures to Cadmium and Nickel Compounds

3.1. Health hazards related to cadmium exposure

Nephropathy associated with the characteristic Cd proteinuria is the most prevalent result of Cd intoxication, observed for all routes and modes of exposure [69,70]. Acute Cd intoxications are rare and confined to occupational accidents. Acute respiratory exposure to airborne Cd or Cd oxide gives symptoms of Cd fever, similar to that of much more common zinc fever but much more persistent, due to a slow clearance of CdO from the lung tissue. However, for Cd, such exposure may also result in lung fibrosis, atherosclerosis of pulmonary arteries, and nephropathy [71]. Acute oral poisoning may evoke circulatory insufficiency [72]. Major health hazards of chronic respiratory exposure to Cd include carcinogenesis in respiratory tract and internal organs, as well as reproductive disorders, such as derangement of spermatogenesis and impairment of hormonal balance [73–75]. Osteoporosis is a very characteristic effect of chronic oral intake of large doses of soluble Cd compounds, accompanying nephropathy [76,77]. The itai-itai disease was described in Japan in areas heavily polluted with Cd-rich industrial waste. This condition affected mostly postmenopausal women, prone to osteoporosis. Despite a rather weak ability of Cd to substitute calcium in bones directly, at levels 30-fold lower from those detected in the liver, significant bone mass loss occurred. This led to the loss of the bone resistance to weak mechanical stress and multiple recurring fractures. The mechanism of this process is likely based on the interference with calcium metabolism in bone remodeling cells—osteoblasts and osteoclasts [76]. The improved environmental protection makes itai-itai largely a historical condition. Notably, long-term Japanese studies indicated that there was no elevation of cancer incidence in populations suffering long-term exposure to environmental Cd [78].

3.1.1. Cadmium nephropathy

Kidneys are the main and ultimate Cd target in the human body. This feature of Cd toxicity is seen most clearly in chronic exposures to low levels of Cd, which are most relevant to the general public. Cd(II) nephrotoxicity is observed with no regard to the intake route, be it oral or respiratory. It is characterized by a specific form of proteinuria, which manifests itself clinically upon a prolonged duration of exposure, typically of 20 years or more [79]. Tubular resorption impairment in kidneys results in the appearance of low-molecular-weight proteins and metabolites in urine, while glomerular dysfunction leads to the leakage of high-molecular-weight

proteins [79,80]. The proteinuria is generally irreversible, despite of the cessation of exposure, except for very mild cases. This fact is related to the very long biological half-life of Cd, mentioned above [37,38]. The renal abnormalities are accompanied by elevated Cd(II) levels in the kidney tissue. The element is then also present in urine [80–82].

There is a threshold level for Cd in the renal cortex, above which tubular damage occurs. The older data indicated the threshold value of ~200–250 ppm [81]. Now the limit has been lowered to ~150–200 ppm [83]. The levels of Cd in whole blood, kidney, liver, and urine of exposed subjects are correlated, signifying high mobility of Cd among the compartments of human body. Cd(II) is transported to kidney as a complex with metallothionein (MT), a metal ion storage protein. The exchange of this complex between kidney and liver is thought to be responsible for the paradoxical lowering of kidney Cd burden along with the progression of renal dysfunction [84]. There are, however, no epidemiologic data that would link Cd intoxication with liver disease.

Recent studies indicate that Cd exposure may be linked to diabetic nephropathy and to diabetes itself. Epidemiology suggests that the body Cd(II) burden may exacerbate kidney damage due to diabetes, and diabetes may aggravate Cd nephropathy. Animal studies confirm these observations and demonstrate a direct action of Cd(II) on Langerhans islets, resulting in the pancreatic Cd accumulation and decrease of blood insulin [85]. These results suggest that Cd toxicity is more widespread and more severe in broad populations than hitherto estimated.

3.1.2. Reproductive disorders due to cadmium exposure

Exposure to Cd causes reduced male fertility (reduced sperm count and poor semen quality), disruption of blood–testes barrier (BTB), germ cell loss, testicular edema, hemorrhage, necrosis, and, eventually, sterility [86]. In women Cd influences oocyte maturation, oocyte pickup and development of the preimplantation embryo, which have obvious clinical implications. As mentioned above, tobacco smoke is one of the main sources of Cd in the human organism. Consequently, the concentration of Cd(II) in the follicular fluid of female smokers undergoing *in vitro* fertilization was reported to be elevated by 15% compared with nonsmokers [87]. Elevated Cd(II) levels have also been associated with a higher risk of ectopic pregnancy and with recurrent miscarriages. Cd exposure is also teratogenic [87].

The reproductive toxicity of Cd(II) is largely related to its hormone mimicking activity. Cd binds to estrogen (ER) and androgen receptors. Ovariectomized female rats exposed to Cd showed increase of the uterus weight and increased growth of mammary glands. The effects were suppressed by administration of an antiestrogen [88]. In castrated rat males,

Cd(II) had an androgenic effect also suppressed by administration of the antiandrogen. Therefore, the data suggest that Cd is a potent endocrine disruptor acting via binding to hormone receptors [88]. Recent cell line experiments also provide evidence for the interference of Cd(II) with ER-related signal transduction pathways [89].

3.1.3. Cadmium and COPD

Chronic obstructive pulmonary disease (COPD) is a life-threatening disorder of pandemic proportions, considered as one of the major global causes of morbidity and mortality [90]. COPD involves small airways disease, mucus hypersecretion, and chronic bronchitis, which lead to the progressive impairment of lung function, decrease of air-flow, and shortness of breath. The disease, clearly associated with smoking, is likely to have multiple triggering factors, related to the exposure to environmental pollutants, including metal ions [91]. There is also evidence for the relationship of COPD with the occupational exposure to metals [92]. Exposure to Cd, measured by urinary Cd excretion, has recently been correlated with the severity of pulmonary function decrease, and there is mounting evidence for the causative relationship between the Cd exposure and COPD [93,94].

3.1.4. Cadmium carcinogenesis

The World Health Organization's International Agency for Research on Cancer (IARC) rates chemical elements and compounds according to their carcinogenicity. Group 1 includes confirmed human carcinogens, and Groups 2A and 2B include substances assigned as probable and possible carcinogens, respectively. Group 3 contains chemicals declared noncarcinogenic according to the current state of knowledge [95]. Cd and its compounds were declared as definitely carcinogenic (Group 1) in 1993, on the basis of substantial epidemiological evidence of lung cancer incidence in workers exposed occupationally to Cd-containing fumes [74]. These data were complemented by the abundant evidence of pulmonary adenocarcinomas in rats which inhaled either soluble Cd chloride aerosols or insoluble Cd oxide fumes [96,97]. Occupational and nonoccupational Cd exposure has also been implicated in the etiology of transitional cell carcinoma of the urinary bladder [98,99]. Smoking-related Cd seems to be responsible for most, or even all excess risk of this cancer [100,101]. These epidemiological studies are supported by cell culture studies, which demonstrate the ability of Cd(II) ions to directly cause the malignant transformation of bladder epithelial cells [102].

Weaker, but still accumulating evidence is available for the causative involvement of Cd in carcinogenesis in several other human organs. While

epidemiological studies of prostate cancer etiology yielded conflicting results with respect to Cd [103], animal and cell culture studies support the involvement of Cd in the development of prostate adenocarcinoma [96,104–106]. Results of a recent analytical study indicate that the Cd accumulation does not differentiate the prostatic cancer from the benign prostatic hyperplasia (BPH), both significantly elevated above the control level, but suggest that the elevated MT level, observed specifically in BPH could provide protection against malignancy [107].

The incidence of pancreatic cancers is related to cigarette smoking, chronic pancreatitis, diabetes, and occupational exposures to toxins and heavy metals. Cd is represented in the first and the last of these factors, and has been implicated in the etiology of diabetes and diabetic nephropathy [85,108]. A significant increase of blood Cd was also recorded in pancreatic cancer patients [109]. These coincidences warrant further studies within this research area, which is very important due to the extreme malignancy and very low survival ratio in pancreatic cancer patients [110].

Renal cancer also seems to be associated with occupational exposure to Cd [111,112]. The nephropathy develops into kidney cancer rarely, indicating a requirement for additional causative factors for the latter to occur. Per analogy with prostate, is seems likely that Cd carcinogenesis in kidney also depends on the intracellular level of MT.

Interestingly, Cd has not been demonstrated directly to cause breast cancer, in spite of its estrogen-mimicking activity, which seems to predestinate it to such an ability. This striking contradiction has been ascribed to antiangiogenic properties of Cd(II) [113]. On the other hand, epidemiological studies indicate an association between the increased incidence of breast cancer and occupational Cd exposure [114]. Also this area of research can be expected to grow rapidly, due to the populational significance of breast cancer.

Recently, an epidemiological correlation of long-term non-occupational Cd exposure with a slightly increased risk of endometrial cancer was demonstrated in postmenopausal women [115]. An association of this fact with hormone-mimicking Cd activity is very likely.

3.2. Health hazards related to nickel exposure

Health effects exerted by exposure to Ni and its compounds can be subdivided into three major groups: acute toxicity related to respiratory or oral exposure, carcinogenesis in respiratory organs, resulting from chronic inhalation of Ni compounds, and Ni allergy, related to dermal and oral exposure. Other health hazards include hard metal asthma, which has a Ni-specific component [116] and teratogenicity, observed in extreme industrial exposures, but not pronounced at lower exposures near Ni refineries [117,118].

3.2.1. Acute nickel toxicity

Nickel tetracarbonyl [$Ni(CO)_4$] is a Ni compound responsible for the majority of known cases of acute Ni toxicity. It is a gas formed upon the direct reaction of CO (carbon monoxide) gas with metallic Ni, used for obtaining very pure Ni for industrial applications in the Mond process [119]. Human exposure to $Ni(CO)_4$ occurs only occupationally, as a result of rare industrial accidents [120,121]. The immediate symptoms include respiratory tract irritation and headache, followed by an asymptomatic period and delayed pulmonary symptoms similar to a pneumonia, accompanied by cardiological and cerebral problems. Depending on the dose and individual susceptibility, the exposures may be deadly, and in the survivors the long-term neurasthenic syndrome and weakness may last for as long as 6 months [121]. On the other hand, the accidental ingestion of water containing a high concentration of soluble Ni(II) salts by a group of workers resulted in transient symptoms, largely of gastrointestinal character. No long-term health problems were detected in this group [122].

3.2.2. Nickel allergy

Ni is the most frequent of all allergens causing allergic contact dermatitis (ACD) [123]. Consequently, Ni allergy is a worldwide health problem. It affects one of every six persons on average. Women exhibit hypersensitivity to Ni four times more frequently than men [124]. This prevalence is currently thought to result from the frequent childhood exposure of women to Ni-containing fashion jewelry [125]. The EU acknowledged Ni allergy to be a major social health problem for European societies and issued a directive posing limits on Ni release from materials coming into prolonged contact with skin [126]. In the light of recent epidemiological data indicating the increase of incidence of Ni hypersensitivity in general population, and particularly in children in North America, a similar regulation has been proposed for the United States [127–129]. ACD to nickel (Ni-ACD) is the most frequent clinical manifestation of Ni allergy, but general allergic symptoms, like conjunctivitis, rhinitis, bronchial asthma, or disseminated eczema are also prevalent. There is no medication available, and the only way to alleviate the symptoms is to avoid contact with objects made of stainless steel and other Ni-containing alloys, including tools, door handles, some arts of silver jewelry, coins, and many others. Coins in particular are difficult to avoid, and they are usually made of alloys with high Ni(II) content. The common name "Nickel" for the American 5 cent coin made of the typical 75% Cu, 25% Ni alloy is indicative of a long history of this issue, but it was Euro coins, which contain the same alloy in their white parts and a 5% Ni alloy in their yellow parts, that attracted public attention more recently [130,131]. A severe manifestation of Ni allergy has therefore obvious deleterious consequences in life and work, and there is urgent need for active remedies against this disease.

3.2.3. Nickel carcinogenesis

Carcinogenicity of Ni was first reported in the occupational context, and solid medical evidence on incidence of cancer resulting from Ni exposure remains to be largely associated with workplace exposure [54,132,133]. The first reports regarded rather spectacular cancers of the nasal cavities in workers employed in a Ni refinery (Mond Nickel Works in Clydach, Wales), soon to be complemented with lung cancers [134]. The incidence of malignancies was horrific: 35.5% of employees died of these cancers, as compared to 1.5% incidence in coal miners [135]. In the light of these findings, Ni-related cancer of upper and lower airways has been the first officially recognized occupational disease, in Great Britain and worldwide [132,133]. The locations of malignancies clearly suggested the inhalatory route of exposure. Subsequent epidemiological studies confirmed exposure to airborne Ni(II) compounds as the cause of cancer in chronically exposed individuals [136,137]. Dusts containing insoluble compounds, mostly Ni_3S_2, NiS, and NiO, as well as aerosols of soluble Ni(II) salts bear a risk of cancer, confirmed by the IARC assignment of these compounds as confirmed (Group 1) human carcinogens. Metallic Ni dusts are currently rated as possibly carcinogenic to humans (IARC Group 2B)[132].

There is no single type of tumor resulting from inhalatory Ni(II) exposures. A careful histopathological study of a large number of respiratory tract tumors developed in Ni refinery workers in Wales, Canada, and Norway indicated a prevalence of squamous cell carcinomas, followed by a number of other carcinomas, with a small incidence of adenocarcinomas and several other tumor types [138].

The location of tumors within airways was found to be related to the size of Ni-containing particles, due to their ability to penetrate the airways. The largest, millimeter size grains are deposited in the nose and mouth, while the finest of micrometer and smaller sizes can penetrate all the way down to the lungs [139].

While causative relations between Ni exposure and other malignancies, for example, larynx, kidney, prostate, and stomach carcinomas and soft-tissue sarcomas were suggested, they have not been demonstrated in humans in a statistically relevant fashion [133]. On the other hand, there is some evidence for such malignancies in laboratory animals, as reviewed [54,133]. Ni compounds induce local tumors at virtually all sites of application. Water-insoluble sulfides and oxides are more active than soluble salts, which is due to a rapid clearance of soluble Ni(II) compounds from the site of application [140,141]. Interestingly, intraperitoneal injections of soluble Ni(II) acetate resulted in both local and distant tumorigenesis, including lung tumors in strain A mice and renal cortical adenomas in F344 rats, the latter, when accompanied by a prolonged administration of sodium barbital, a cancer promoter [142,143]. Intraperitoneal administration of Ni(II) acetate in pregnant F344 rats produced pituitary (without barbital) and renal

(with barbital) tumors [144]. As mentioned above, the administration of soluble Ni(II) salts in drinking water did not yield tumors in experimental animals [50].

A phenomenon of transgenerational, paternally inherited carcinogenesis was noted in epidemiological studies of children whose fathers were occupationally exposed to toxic metal mixtures (e.g., welders) [145]. Nevertheless, the direct association of this rare phenomenon with exposure to Ni specifically, however likely, seems premature at this moment.

Endoprostheses and other implantable surgical devices made of Ni-containing alloys have been suspected to cause tumors locally due to Ni leaking by corrosion in body fluids [133,146]. The evidence has not been ruled conclusive, but convincing enough to assign these implants to Group 2B by IARC [147]. These alloys have been subsequently phased out in favor of alloys based on metals considered noncarcinogenic, ceramics, or materials coated with biocompatible organic polymers.

As mentioned above, general populations are exposed to Ni compounds in food, tobacco, and urban air. These exposures have not been considered to pose Ni-specific health hazards, as no direct epidemiological evidence for such is available. Nevertheless, the combination of facts reviewed briefly above suggests that such analysis might be worthwhile. In particular, the chemical forms of Ni in inhaled particulate matter, such as ROFA, are sufficiently similar to those considered carcinogenic in the occupational setting. Of course, doses of Ni inhaled occupationally are much higher than the environmental ones. The levels of total Ni in lung wet tissue were found to be higher than controls by a factor of 112–5800 in Ni refinery workers and by a factor of 500 in stainless-steel welders [148,149]. However, the populations exposed are about as much bigger, and huge differences in individual susceptibilities to Ni carcinogenicity are evident. Further studies are definitely required to clarify the issue of environmental hazard of airborne Ni, but this issue should not be neglected, as stated already 15 years ago by Canadian Environmental Health Directorate [150].

4. Molecular Mechanisms of Cadmium and Nickel Toxicity

4.1. Molecular mechanisms of cadmium toxicity

The molecular toxicology of Cd is an interplay between extracellular transport phenomena, which govern the distribution of this metal in the organism and intracellular interactions, predominantly involving proteins. The following paragraphs cover three major areas of cellular and molecular research in this area: MTs and Cd redistribution, mechanisms of Cd carcinogenesis, and effects of Cd on cellular junctions.

4.1.1. Metallothionein and extracellular transport of Cd(II) ions

Both inhalatory and gastrointestinal ways of exposure to Cd yield, eventually, Cd(II) ions into the bloodstream. Albumin is a major Cd-binding protein of human serum, capable of simultaneous binding of two Cd(II) ions [151,152]. Other proteins, including transferrin and α-2-macroglobulin were also implicated in blood transport of Cd on the basis of *in vitro* experiments and animal studies [153,154]. These proteins bind Cd(II) ions with their oxygen and nitrogen donors, despite the preference of Cd(II) ions for thiol ligands. This is due to a low availability of thiol ligands in the bloodstream. The resulting binding is in the micromolar affinity range, enabling facile and rapid (in a minutes to hours timescale) transport of Cd (II) ions to the liver [155]. Two pathways of further Cd(II) transport are known. Intracellularly, Cd(II) spontaneously forms relatively strong complexes with reduced glutathione (GSH, γ-Glu–Cys–Gly) [156,157]. The Cd $(GSH)_2$ complex is a molecular mimic of glutathione disulfide (GSSG) and is exported out of the cell along with GSSG, through the ABC transporter system [158]. In liver, this pathway results in the secretion of Cd into the bile, and its transfer down the digestive tract. This Cd fraction is largely excreted with the feces, as Cd resorption in the gut is low [159].

An alternative pathway includes the Cd(II) binding to MTs. MTs are a family of small proteins of ~60 amino acids, very rich in cysteines (20 residues), involved in intracellular storage and buffering of Zn(II) and Cu(I) ions [160,161]. There are three major human MTs: MT1, MT2, and MT3. The former two are expressed in many organs, including the liver and kidney, MT3 is brain-specific. The Zn(II)-saturated MT contains seven metal ions, forming two metal–sulfur clusters: Zn_3S_9 and Zn_4S_{11}. The recent detailed study on Zn(II) binding to MT2 revealed that the binding is fully cooperative and stronger for the four-zinc domain, while the three-zinc domain demonstrates less cooperative and weaker interactions [162].

The Cd(II) binding to MT is nearly isostructural with the Zn(II) binding, and mixed Zn/Cd forms are known to exist *in vivo* [163,164]. Cd(II) ions induce expression of MT1 and MT2 in hepatocytes, so that a 24 h pretreatment with subtoxic Cd doses protects liver from injury due to a subsequent treatment with a higher dose of Cd(II) [165,166]. The resulting cadmium metallothionein (Cd–MT) is stored in the hepatocyte cytosol, preventing injury to cellular organelles. Such Cd is not prone to induce apoptosis or necrosis, but can impair DNA repair (see below) [167]. The net result of Cd–MT storage is positive anyway, as poor MT expression was demonstrated to enhance Cd carcinogenesis [168]. It is very interesting to note that MT expression is very highly variable in humans. Differences between individuals in a given population in hepatic MT expression are very large, up to a factor of 50 or 100 [169,170]. Genetic variability in the promoter region of MT2A gene was recently discussed as a possible source of this effect [170].

Small portions of liver-bound Cd-MT can be released back to circulation from damaged hepatocytes, upon prolonged exposure, resulting in the slow decrease of liver Cd burden [77,171]. The tight binding of Cd(II) ions to MT prevents their unspecific leakage and there is little uptake of Cd-MT in most tissues. The epithelial cells of the S1 segment of kidney proximal tubules, however, absorb these complexes, which pass kidney glomeruli due to their low molecular weight of ~7 kDa. This scenario was considered to be responsible for Cd nephropathy, and supported by nephrotoxicity observed in rats receiving transplants of Cd-loaded livers [172]. Studies on MT-null mice and renal cell culture experiments demonstrated, however, that $CdCl_2$ is much more toxic that Cd-MT in kidney cells [173–175]. The exact molecular mechanism of Cd nephropathy remains, therefore, to be elucidated [165].

4.1.2. Cadmium carcinogenesis: oxidative stress and DNA repair inhibition

As mentioned above, Cd, in the form of Cd(II) compounds, is one of the most potent metallic carcinogens [74]. Several molecular mechanisms apparently coexist in Cd carcinogenesis, including oxidative stress, inhibition of DNA repair and apoptosis, and alterations of gene expression. Also, some of these mechanisms are more important than others in specific cell types.

Oxidative stress has been proposed to be a unifying theme, manifesting itself in other mechanistic trails listed [176]. It is a common feature of metal carcinogenesis [177]. However, unlike arsenic, Ni, and chromium, the redox silent Cd is unable to oxidize biomolecules or to catalyze the formation of reactive intermediates. Therefore, indirect mechanisms must be involved. Furthermore, Cd is only weakly genotoxic, and typical results of direct oxidative damage to DNA, such as strand breaks or 8-oxo-dG formation were detected only at high micromolar levels of intracellular Cd(II) ions [178,179]. Other mechanisms of Cd carcinogenesis manifest themselves at much lower Cd exposures, which makes them more relevant at realistic long-term Cd exposures in humans [180].

Depletion of GSH and (partially interdependent) impairment of mitochondrial control of reactive oxygen species (ROS) production seem to be the most important indirect pathways of oxidative stress induction by Cd. However, the induction of antioxidant MT [165,166] and activation of GSH synthesis [179,181] occur very early in response to Cd exposure, and these effects need to be overcome for the oxidative stress to ensue. The interplay of these pro- and antioxidative processes appears to be relevant for apoptosis-related Cd carcinogenesis.

Apoptosis is a frequent result of Cd exposure in cell cultures. Both caspase-dependent and caspase-independent mechanisms were reported

[182,183], with oxidative stress as a likely common origin of the process [184]. This concept is supported by antiapoptotic effects of antioxidants in Cd exposure [185]. On the other hand, Cd has been frequently reported to inhibit apoptosis induced by other toxins, thereby serving as a cocarcinogen [186,187]. One way to explain this apparent contradiction was provided by the observation that Cd exposure of RWPE-1 prostate cell cultures resulted in the selection of a subset of cells, which were apoptosis resistant due to the elevation of MT content [188]. The prevention of apoptosis is considered to facilitate accumulation of DNA lesions in surviving cells, leading to malignant transformation [176]. What is very important, individual elements of these overall mechanisms may be enhanced or suppressed in response of various cell types to Cd exposure. For example, testicular toxicity of Cd in various strains of mice was reported to be independent of the relative MT contents [189].

Low-level (submicromolar) Cd exposures result in alterations in gene expression patterns, which are clearly cell type specific [176]. Oxidative stress and ROS production are implicated in many of these phenomena, including overexpression of proto-oncogenes, such as *c-fos, c-jun*, and others [190–192], and inhibition of expression of tumor suppressors, such as *p53* [188]. More research is required to elucidate the cause–effect patterns involving these phenomena.

DNA repair inhibition emerges as a major molecular mechanism in Cd carcinogenesis, explaining the apparent contradiction between weak mutagenicity and strong cocarcinogenicity of Cd. There are four major DNA repair systems in mammalian cells: mismatch repair (MMR), nucleotide excision repair (NER), base excision repair (BER), and recombinational repair [193]. Cd(II) was reported to affect the first three [180,194,195]. The relevance of DNA repair inhibition in carcinogenesis due to a chronic exposure to Cd is supported by very low, noncytotoxic Cd(II) levels, at which DNA repair inhibition is observed. There is sufficient evidence to assume that Cd(II) ions interfere with repair systems on the level of individual proteins involved, rather than at a DNA lesion site.

With respect to BER, Cd(II) inhibited repair of DNA oxidative damage products [196,197]. The mechanism of this activity includes inhibition of several BER proteins, such as OGG1, which repairs 8-oxoguanine lesions [198] or PARP, which orchestrates single strand break repair [199]. The action on OGG1 appears to be indirect, via Sp1 transcription factor, while that on PARP may be direct. Cd(II) ions inhibit the first step of the NER system, the incision of the DNA lesion. Therefore, the XPA protein, an NER repair complex initiator was proposed to be the prime Cd toxicity target [200]. The MMR inhibition by Cd(II) also involves a direct interaction with the repair complex, resulting in the decrease of ATP consumption by MSH6 protein, observed in human cell cultures [201,202].

The above data for NER and BER are consistent with a concept of zinc fingers (ZFs) in DNA repair proteins as targets for carcinogenic Cd(II) ions, as many of the toxic effects described above could be reversed by an administration of Zn(II) ions. Section 4.3 presents molecular evidence for this idea in more detail. Zn(II) administration did not, however, reverse the inhibition of MHS6 exerted by Cd(II) ions, suggesting that the MMR pathway of Cd toxicology involves oxygen, rather than sulfur-binding sites.

4.1.3. Effects of Cd(II) on cellular junctions

While Cd primarily damages kidney, the metal is also known to readily assault vascular endothelium [203]. The focal point of Cd toxicity toward these two targets is the interaction of the Cd(II) ions with cell adhesion molecules, which form cell–cell or cell–matrix junctions. In this respect, the most important junctions include adhering junctions and tight junctions [zonula occludens (ZO)] [204].

Adhering junction is a complex of transmembrane proteins—cadherins, whose intracellular domains form links with catenin scaffolding proteins, which, in turn, are physically linked with cellular skeleton proteins. Cadherins are single-span transmembrane proteins, responsible for calcium-dependent cell–cell adhesion. They can transfer information intracellularly through α- and β-catenins and the actin skeleton [205]. β-catenin has a double function, it is both a structural protein and a transcription factor. It participates in the Wnt signaling pathway (controlling embryogenesis and involved in human carcinogenesis) via TCF/LEF proteins [205,206]. β-catenin trans-activates genes stimulating cell proliferation (like *c-myc*) and also genes protecting from apoptosis (e.g., *Abcb1*) [206] and therefore may be involved in the malignant transformation.

Tight junctions comprise occludins, claudines, JAMs (junctional adhesion molecules), and ZO proteins. They form a complex serving as a semipermeable barrier to the paracellular transport of ions, solutes, water, and cells (e.g., leukocytes). Tight junctions provide a barrier dividing the apical domains of plasma membranes from their basolateral parts [207].

It has been reported that in vascular and kidney epithelium Cd disrupts the cadherin-dependent cell junctions. It is believed that Cd(II) binds at the Ca(II)-binding domain, thereby disorganizing the whole adhering junction complex. The molecular details of this instance of calcium/Cd antagonism are not known. This action has a twofold effect: not only the cellular attachment loosens, but also the β-catenin molecule translocates to the nucleus where it exerts its gene-regulatory properties [204,206]. In kidney, the disruption of cellular junctions takes place both in the proximal tubule and in vasculature [204]. It has been also reported that expression of the endothelium-specific claudin-5 in tight junctions was irregular and diminished in the glomeruli and small blood vessels of the kidneys from

Cd-treated rats [204]. Therefore, Cd(II) clearly influences at least two types of cell–cell junctions.

Due to its junction disrupting properties, Cd exerts a direct antiangiogenic effect on vascular epithelium by redistributing vascular E-cadherin from cell–cell contacts and disabling the migration and tube formation of endothelial cells [208]. This fact leads to the suggestion that under certain conditions, Cd may have an anticarcinogenic effect by preventing formation of blood vessels feeding the growing tumor [203,208].

Cd toxicity to other organs may also be attributed to the Cd capacity to disrupt cell–cell junctions in the vascular endothelium. For example, in lungs the earliest stages of Cd-induced pulmonary injury involve the disruption of the alveolar septum and the leakage of fluid and solutes into the alveoli. This observation is in accordance with the fact that Cd, via disruption of cellular junctions, increases the endothelial permeability [203].

4.2. Molecular mechanisms of nickel toxicity

The studies of molecular mechanisms in Ni toxicology are virtually limited to two major Ni-dependent pathologies: allergy and carcinogenesis. Current views on these mechanisms are presented in respective sections below.

4.2.1. Molecular mechanisms in nickel allergy

Ni allergy is a T-cell-controlled disease [209]. The allergic reaction is a result of skin surface penetration by Ni, which results in the induction of cellular immune response. In this chapter we focus on those molecular events of Ni allergy that involve Ni(II) ions directly. Other important molecular aspects of immune system response to Ni exposure have been reviewed recently [210,211].

The allergenic potential of a Ni-containing material depends on its ability to deliver Ni(II) ions. The oxidation of metallic Ni to Ni(II) occurs in human sweat with a sufficient rate to elicit allergic reaction, while NiO particles, which do not dissolve in sweat, are not allergenic [130,131,212]. The translocation of Ni through the outer layers of skin occurs in the form of Ni(II) ions, most likely bound to proteins. Human serum albumin (HSA) is considered as a likely main Ni(II) shuttle, due to its high abundance and mobility in skin [213]. This protein contains a specific Ni(II) binding site at its Asp–Ala–His– N-terminal sequence [214–216]. Recently, another skin protein, filaggrin (FLG), has been implicated in Ni(II) binding in the skin. This large protein is necessary for the process of skin cornification, which provides a barrier preventing epidermal water loss and penetration by infectious agents, toxins, and allergens [217]. A decrease of expression or

loss-of-function mutations in FLG gene are seen in a large proportion of atopic dermatitis individuals, including those suffering from Ni allergy. In addition to a general barrier function, FLG is considered to provide Ni(II)-specific defense by chelating Ni(II) ions [218,219]. A role of recently discovered FLG2 in Ni allergy remains to be investigated [220].

Upon skin penetration, Ni(II) ions induce hyperreactivity by activating human leucocyte antigen (HLA)-restricted, Ni-specific T cells. There is evidence for two concurrent mechanisms of initiation of immune response by Ni(II) [221]. Some T cells can react to HLA-associated peptidic determinants which include bound Ni(II). This mechanism is similar to the standard presentation of organic haptens, except for the fact that Ni(II) ions do not form strong, covalent bonds with presenting peptides. Instead, much more labile coordination bonds are formed. Another mechanism requires a permanent presence of surplus Ni(II) in the medium for activation, independent of peptides presented. These cells seem to be activated by Ni(II) complexation at TCR–MHC (T cell receptor–major histocompatibility complex) contact sites, which add strength to the TCR–MHC binding. HSA is a likely, but confirmed only *in vitro*, donor of Ni(II) to such complexes [213,221]. Histidine residues in surface peptides have been implicated in Ni(II) binding in these more or less putative complexes [221–223].

Despite these developments, the chemical nature of Ni(II) interactions with T cells remains largely unknown. The allergic cross-reactivity between Ni(II) and Pd(II) has been noted [224,225]. This fact suggests that active Ni(II) complexes are square-planar, rather than octahedral, because Pd(II) complexes are always square-planar [10]. Very recently, it was demonstrated that $NiSO_4$ triggers monocyte activation in a way that includes changes of cell surface thiols [226]. A hypothetical Ni(II)–thiol complex would also be square-planar [227]. Furthermore, experiments in mice suggested that Ni(II) compounds can activate T cells, but are unable to prime the naïve ones. The latter effect could be obtained by using preformed Ni(III) or Ni(IV) peptide complexes or by coadministration of Ni(II) with H_2O_2 [228,229]. All these pieces of evidence point at the involvement of redox active planar Ni(II) species in the mechanism of Ni allergy [177,230].

The ability of some metal ions to hydrolyze peptides was mentioned as potentially contributing to abnormal antigen processing, and thereby eliciting allergic response. However, no data were presented in support of this idea [231]. In this context, it is very interesting to note that Ni(II) ions are able to hydrolyze specific His-containing sequences, *in vitro* as well as intracellularly, yielding redox-active square-planar Ni(II) complexes [232–235]. Another interesting line of research stems from the epidemiological observation that a prolonged childhood contact with Ni-releasing orthodontic braces prior to ear piercing decreases incidence of Ni allergy.

Reversing this order of events, however, provides no protection [236,237]. Once sensitized, a patient can develop skin symptoms upon oral challenge with Ni(II) compounds [238]. The dose-dependent development of oral tolerance to Ni(II) was confirmed recently in an animal study, which showed that only mice challenged with $NiCl_2$ orally had specific Ni(II)-reactive regulatory T cells [239]. These data suggest the presence of specific chelation of Ni(II) somewhere in the digestive tract that results in a "safe" presentation of Ni(II) to the immune system. One can clearly state that despite significant progress, very much remains to be discovered with respect to molecular mechanisms in early stages of Ni allergy. Such knowledge is prerequisite for the development of Ni allergy medication.

4.2.2. Molecular mechanisms in nickel carcinogenesis

As presented above, Ni carcinogenicity depends on the water solubility of its compound. Insoluble, particulate Ni(II) compounds are stronger carcinogens than soluble compounds in both epidemiological and experimental animal studies. However, there is abundant evidence that soluble Ni(II) is the actual ultimate carcinogen for both types of compounds (for review, see [54,133,177,240]). The difference in health hazards is primarily due to the resistance of insoluble compounds to clearance from the site of exposure in the body. For example, NiO yields Ni lung burdens with persistence up to 1000-fold higher than $NiSO_4$ [241]. Furthermore, particles of Ni(II) compounds of dimensions smaller than 5 μm can cross the cell membrane by phagocytosis, delivering very high amounts of Ni in the vicinity of cell nucleus [242–244]. The toxicity of Ni delivered this way depends on the efficiency of mobilization of Ni(II) ions by dissolution in lysosomes [243–246]. A very recent study demonstrated higher toxicity of NiO nanoparticles, compared to both fine (micrometer size) NiO particles and soluble $NiCl_2$ in cell lines [247]. This property can be assigned to a combination of efficient particle delivery with fast intracellular dissolution of small particles. By the way, this finding is the early sign of an emerging problem of nanoparticle toxicity.

Another, much slower way of delivering Ni(II) intracellularly is through DMT-1, which exhibits a broad metal ion specificity, and participates in Cd(II) transport as well [36,248,249]. This transport mode yields substantial amounts of cytosolic Ni(II), but particulate Ni(II) compounds, dissolved intracellularly were found to deliver a higher proportion of Ni(II) into the cell nucleus [243,245]. A nonspecific diffusion through the cell membrane was also proposed [250]. The latter mechanism, however, seems to be less likely *in vivo*, except for the digestive tract.

Many molecular mechanisms were proposed for Ni(II) carcinogenesis, and the relative importance of these mechanisms is far from being understood. Ni(II) has been considered to be a source of ROS in the cell nucleus,

with concomitant procarcinogenic DNA damage [177,251]. Indeed, the pattern of DNA damage in cells exposed to Ni(II) resembles that of ionizing radiation, which suggests the involvement of Ni(II)-generated ROS [252]. Even more importantly, G → T transversions, mutations typical for oxidative damage, were found in both experimental renal tumors induced by Ni_3S_2, and in human lung cancers associated with Ni exposure [253,254]. However, the mutagenicity of Ni(II) compounds is very low in many experimental systems, at odds with their high ability to induce neoplastic transformation [240,255]. Several concepts were raised to overcome this apparent discrepancy. Cell line studies provided more or less stringent evidence for epigenetic mechanisms of Ni carcinogenesis. A unifying epigenetic concept has been proposed recently, which combines several hitherto separate molecular tracks [240]. Ni(II) exposure leads to alterations of acetylation, methylation, and ubiquitylation of core histones, which may be associated with silencing of tumor suppressor and other cell cycle control genes [256–261]. Ni(II) ions are also able to damage histone H2A directly, by hydrolytic truncation of the C-terminal H2A octapeptide [234]. The presence of such truncated H2A in cultured cells resulted in an altered pattern of expression of cancer-related genes [262].

Ni(II) ions disturb intracellular redox control by depleting cellular stores of glutathione and ascorbate [263–267]. The latter event leads to the accumulation of Fe(III) in the cells. Finally, Ni(II)-exposed cells suffer from hypoxia, which is common to fast-growing tumors [268,269]. The latter state facilitates selection of neoplastic phenotype that can escape apoptosis. This preconditioning may be combined with a weak, but present mutagenic ability of Ni(II) to complete carcinogenic transformation [240].

An order of these events may also be different for specific carcinogens. For example, Ni_3S_2 dissolution is biphasic. The first, rapid phase is associated with high redox activity and may lead to the DNA damage, while the second, slow phase of Ni(II) release may elicit epigenetic damage [270].

The above phenomena result from exposures of cells to high levels of intracellular Ni(II), most likely to be induced by phagocytosis of Ni sulfides or oxide. However, low, noncytotoxic Ni(II) levels may also cause DNA damage and neoplastic transformation. At low concentrations, Ni(II) ions strongly enhance mutagenicity of other carcinogens, by inhibiting DNA repair [193]. Such synergy of Ni(II) with mutagenic carcinogens, including UV irradiation, *N*-methyl-*N*-nitrosourea and benzo[*a*]pyrene was demonstrated in cell line experiments [271–273]. Ni(II) was demonstrated to inhibit the XPA protein, which enables the formation of the NER complex [274]. This cocarcinogenic mechanism can also very well explain the discrepancy between the low mutagenicity and the high carcinogenicity of Ni(II) compounds.

It seems that exposure to Ni(II) can induce many concurrent intracellular processes. Their relative relevance is likely to depend strongly on the type of tissue and cells affected. This general notion was formulated previously in the context of various strains of mice [270]. It is also valid on the most elementary molecular level. For example, the ability of Ni(II) to deplete GSH depended strongly on the cell line type [263–266]. Also, the efficiency of the direct attack of Ni(II) on histone H2A was cell type specific [234]. To elucidate these and other basic mechanisms of Ni(II) interactions inside the cell one needs to find out about molecular forms of its presence. Taking into account the intracellular abundance of potential low- and high-molecular-weight ligands for Ni(II), which can be estimated as higher than 20 mM, hypothetical free Ni^{2+} aqua ions may only exist temporarily at the moment of dissolution of a particle. Studies using molecular models, aided by species distribution calculations suggest that essential metabolites, ATP and histidine, as well as histones may bind the majority of Ni(II) ions in the cell nucleus [232,233,275–278]. These data indicate another direction of future research, linking basic metabolism of particular cell types with their susceptibility to Ni(II)-induced carcinogenesis. A clear protective effect of Mg(II) ions and other essential divalent metals against Ni_3S_2 carcinogenesis seems to fall into the same category [133,279].

4.3. Interactions with zinc fingers—a common target for cadmium and nickel

ZF domains are one of the most abundant families of protein motifs in the eukaryotic genome, comprising at least 3% of identified human proteins [280]. Their functions include the binding and recognition of nucleic acids and formation of multiprotein complexes [281,282]. Typical ZF domains contain one or two Zn(II) ions bonded tetrahedrally in Cys_2His_2, Cys_3His, or Cys_4 environments, and ZF proteins contain from one to more than 20 individual ZF units [283]. Zn(II) does not participate in interactions of ZF, but secures their structure, so that zinc release results in the loss of the ZF function [284]. ZF are targets for oxidizing agents, and cellular toxicity of reactive oxygen and nitrogen species is attributed in part to oxidation of zinc-binding thiol groups in ZF [284,285]. ZF were also proposed to be targeted by toxic metals, including Ni(II) and Cd(II). This issue is particularly interesting, because it provides a unifying mechanistic concept for carcinogenesis related to DNA repair inhibition [286]. Indeed, several DNA repair proteins, which are susceptible to inhibition by carcinogenic metals, contain ZF domains [194,286]. ZF is a dual target for a toxic metal ion, because its function can be compromised by metal–metal substitution as well as by metal-catalyzed oxidation of zinc-binding thiols. Ni(II) ions

form weaker complexes with all kinds of ZF than Zn(II) ions [227,287–289]. Nevertheless, they were demonstrated to substitute for Zn(II) in Cys_4 and Cys_2His_2 ZF at a sufficient molar excess [227,290]. This substitution results in an alteration of ZF structure, because of the nontetrahedral geometry of the binding site, imposed by the Ni(II) ion [227,287,288]. Moreover, Ni(II) ions were shown to facilitate disulfide bridge formation and zinc release from XPAzf, a ZF peptide derived from the XPA DNA repair protein [227]. The relative affinity of Cd(II) ions to ZF versus Zn(II) ions increases with the number of Cys residues in the ZF-binding site [291]. It is lower for Cys_2His_2 ZF [289–293]. On the other hand, Cys_4 ZF preferentially bind Cd(II) ions [287,294]. The binding in the latter ZF is nearly isostructural, as demonstrated for XPAzf [295,296]. Oppositely to the Ni(II) finger, Cd(II)-substituted XPAzf was much more resistant to oxidation than the parent Zn(II) complex [294]. These facts suggest that the ZF-based mechanisms of Ni and Cd toxicity may be different. Ni(II) ions can assault ZF domains directly, or indirectly by eliciting oxidative damage. Cd(II) ions can impair physiological redox control of ZF activity, by protecting it when inhibition would be desired, for example, in gene transcription regulation [284].

The yet unsolved issue of the molecular mechanism of Cd(II) xenoestrogenicity is also related to ZF interactions. The estrogen-mimicking activity of Cd(II) ions, mentioned in Section 3.1.2, appears to be largely due to their direct interaction with the the α-subtype of estrogen receptor (ERα). Its DNA-binding domain (DBD) and ligand-binding domain (LBD) are two potential binding sites for Cd(II). DBD is a dimeric ZF structure, and its apo-form was demonstrated to reconstitute in the presence of Cd(II) ions. The resulting complex retained DNA-binding properties of the native domain [297]. However, a Zn(II)/Cd(II) competition was not studied. LBD contains four Cys residues which were not seen to form disulfide bonds in crystal structures [298]. The issue of Cd(II) binding to these cysteines remains however, to be elucidated [299–301]. Notably, the Zn(II) ions were found not to bind to LBD, but the Ni(II) ions were found to do so with a high affinity [299].

5. Summary

Toxic properties of Cd and Ni are usually discussed separately, due to their obvious differences in chemical properties (such as ionic radii), preferred geometries of complexes with bioligands, and redox properties. However, the awareness of health hazards related to exposure to their compounds appears to be generally low. Therefore, we chose to describe these two elements together, in one chapter. Nevertheless, as described

above, Cd and Ni share some toxicologically relevant features. They are increasingly present in the human environment due to their joint technological usage, such as Ni–Cd batteries. They are coemitted in fly ash generated in coal power plants and municipal waste incinerators and are simultaneously present in the tobacco smoke. As a result, they share the respiratory route of human exposure. The main difference between exposures to Cd and Ni is due to the different levels at which toxic effects are induced. The lower presence of Cd in the earth's crust corresponds to its higher toxicity, compared to Ni.

Further similarities between Cd and Ni can be noticed in their fate in the human body. Both Cd(II) and Ni(II) ions are taken up in the digestive tract via DMT-1, distributed in the blood by albumin and finally delivered to liver. A crucial difference in toxic properties between Cd(II) and Ni(II) ions results from the ability of Cd(II) (and inability of Ni(II)) to induce MT synthesis in hepatocytes. This difference is probably due to the distinct geometric requirements of thiolate complexes: Cd(II) readily forms a tetrahedral structure, while Ni(II) strongly prefers a square-planar geometry of the complex. The long term accumulation of Cd within the human body and Cd nephrotoxicity appear to be the distant consequence of this difference in its geometric requirements. In contrast, some data, reviewed above, seem to indicate that the preference of Ni(II) to form planar complexes containing sulfur atoms may be partially responsible for the Ni allergy. Despite these differences, both Cd(II) and Ni(II) were shown to deplete intracellular glutathione and elicit oxidative stress, which is likely relevant in their carcinogenesis.

DNA repair inhibition is a yet another common area of Cd and Ni toxicity. Subcellular and molecular studies indicate that both these metals may actually target the same ZF domains in repair complex components. However, specific mechanisms of this interference differ on the molecular level, as Ni(II) destroys ZF structures, while Cd(II) appears to stabilize them, in comparison to the native Zn(II) ion.

The above presented data provide a reason for research on the effects of joint exposures to Cd(II) and Ni(II). The combination of analogies and discrepancies of their molecular properties, discussed briefly above, makes them potentially synergic toxins, properties of which need to be investigated in order to provide a better protection for humans exposed.

Acknowledgement

We thank Dr A. Bonna of IBB PAS for critical reading of the manuscript.

REFERENCES

[1] P.W. Durbin, S. Lauriston, Taylor Lecture: The quest for therapeutic actinide chelators, Health Phys. 95 (2008) 465–492.
[2] G.D. Howells, D.J.A. Brown, K. Sadler, Effects of acidity, calcium, and aluminum on fish survival and productivity—a review, J. Sci. Food Agric. 34 (1983) 559–570.
[3] D.W. Schindler, Effects of acid rain on freshwater ecosystems, Science 239 (1988) 149–157.
[4] L. Alessio, M. Campagna, R. Lucchini, From lead to manganese through mercury: Mythology, science, and lessons for prevention, Am. J. Ind. Med. 50 (2007) 779–787.
[5] J. Schwartz, Low-level lead exposure and children's IQ: A meta-analysis and search for a threshold, Environment 65 (1994) 42–55.
[6] L. Magos, T.W. Clarkson, Overview of the clinical toxicity of mercury, Ann. Clin. Biochem. 43 (2006) 257–268.
[7] D. Seyferth, The rise and fall of tetraethyllead. 2, Organometallics 22 (2003) 5154–5178.
[8] R.F. Edlich, C.L. Cross, C.A. Wack, W.B. Long, III, A.T. Newkirk, The food and drug administration agrees to classify mercury fillings, J. Environ. Pathol. Toxicol. Oncol. 27 (2008) 303–305.
[9] S. Trümpler, W. Lohmann, B. Meermann, W. Buscher, M. Sperling, U. Karst, Interaction of thimerosal with proteins—ethylmercury adduct formation of human serum albumin and β-lactoglobulin A, Metallomics 1 (2009) 87–91.
[10] F.A. Cotton, G. Wilkinson, C.A. Murillo, M. Bochmann, Advanced Inorganic Chemistry, (sixth ed.), Wiley, New York, 1999.
[11] A. Frenkel, A. Vairavamurthy, M. Newville, A study of the coordination environment in aqueous cadmium-thiol complexes by EXAFS spectroscopy: Experimental vs theoretical standards, J. Synchrotron Rad. 8 (2001) 669–671.
[12] R.G. Pearson, Hard and soft acids and bases, J. Am. Chem. Soc. 85 (1963) 3533–3539.
[13] B.A. Krizek, D.L. Merkle, J.M. Berg, Ligand variation and metal ion binding specificity in zinc finger peptide, Inorg. Chem. 32 (1993) 937–940.
[14] S.B. Mulrooney, R.P. Hausinger, Nickel uptake and utilization by microorganisms, FEMS Microbiol. Rev. 27 (2003) 239–261.
[15] D.W. Margerum, S.L. Anliker, Nickel(III) Chemistry and Properties of the Peptide Complexes of Ni(II) and Ni(III), in: J.R. Lancaster, Jr (Ed.), Bioinorganic Chemistry of Nickel, VCH Publishers, Weinheim, New York, 1988, pp. 29–51.
[16] W. Bal, M.I. Djuran, D.W. Margerum, E.T. Gray, Jr, M.A. Mazid, R.T. Tom, E. Nieboer, P.J. Sadler, Dioxygen-induced decarboxylation and hydroxylation of [Ni^{II}(Glycyl-Glycyl-L-Histidine)] occurs via Ni^{III}: X-ray crystal structure of [Ni^{II}(Glycyl-Glycyl-α-hydroxy-D,L-Histamine)]3H_2O, J. Chem. Soc. Chem. Commun. (1994) 1889–1890.
[17] C.L. Coyle, E.I. Stiefel, The coordination chemistry of nickel: An introductory survey, in: J.R. Lancaster, Jr (Ed.), Bioinorganic Chemistry of Nickel, VCH Publishers, Weinheim, New York, 1988, pp. 1–28.
[18] Mindat.org—the mineral and locality database, http://www.mindat.org/min-3040.html
[19] B.R. Singh, M.J. McLaughlin, Cadmium in soils and plants, in: M.J. McLaughlin, B.R. Singh (Eds.), Developments in Plant and Soil Sciences, Kluwer Academic Publishers, Dordrecht, 1999, pp. 257–268.
[20] T.W. Lane, F.M.M. Morel, A biological function for cadmium in marine diatoms, Proc. Natl. Acad. Sci. U. S. A. 97 (2000) 4627–4631.
[21] F.M.M. Morel, The co-evolution of phytoplankton and trace element cycles in the oceans, Geobiology 6 (2008) 318–324.
[22] J. Wang, H. Ban, X. Teng, H. Wang, K. Ladwig, Chemosphere 64 (2006) 1892–1898.

[23] A. Baba, A. Kaya, Leaching characteristics of solid wastes from thermal power plants of western Turkey and comparison of toxicity methodologies, J. Environ. Manage. 73 (2004) 199–207.
[24] M. Takaoka, Y. Kuramoto, N. Takeda, T. Fujiwara, Estimation of species of zinc, lead, copper and cadmium in fly ash by a sequential chemical extraction method, Proc. JSCE 685 (2001) 79–90.
[25] M.C. Camerani, A. Somogyi, B. Vekemans, S. Ansell, A.S. Simionovici, B.M. Steenari, I. Panas, Determination of the Cd-bearing phases in municipal solid waste and biomass single fly ash particles using SR-microXRF spectroscopy, Anal. Chem. 79 (2007) 6496–6506.
[26] M.C. Camerani Pinzani, S. Ansell, A. Somogyi, B.M. Steenari, O. Lindqvist, Micro-extended X-ray absorption fine structure studies of cadmium speciation within single municipal solid waste fly ash particles, Anal. Chem. 76 (2004) 1596–1602.
[27] M.C. Pinzani, A. Somogyi, A.S. Simionovici, S. Ansell, B.M. Steenari, O. Lindqvist, Direct determination of cadmium speciation in municipal solid waste fly ashes by synchrotron radiation induced mu-X-ray fluorescence and mu-X-ray absorption spectroscopy, Environ. Sci. Technol. 36 (2002) 3165–3169.
[28] C.H. Williams, D.J. David, The effect of superphosphate on the cadmium content of soils and plants, Aust. J. Soil Res. 11 (1973) 43–56.
[29] A. Zaniewicz-Bajkowska, R. Rosa, J. Franczuk, E. Kosterna, Direct and secondary effect of liming and organic fertilization on cadmium content in soil and in vegetables, Plant Soil Environ. 53 (2007) 473–481.
[30] K. Rustemeier, R. Stabbert, H.J. Haussmann, E. Roemer, E.L. Carmines, Evaluation of the potential effects of ingredients added to cigarettes. Part 2: Chemical composition of mainstream smoke. Food Chem. Toxicol. 40 (2002) 93–104.
[31] A. Mutti, M. Corradi, M. Goldoni, M.V. Vettori, A. Bernard, P. Apostoli, Exhaled metallic elements and serum pneumoproteins in asymptomatic smokers and patients with COPD or asthma, Chest 129 (2006) 1288–1297.
[32] K.S. Min, N. Iwata, N. Tetsutikawahara, S. Onosaka, K. Tanaka, Effect of hemolytic and iron-deficiency anemia on intestinal absorption and tissue accumulation of cadmium, Toxicol. Lett. 179 (2008) 48–52.
[33] L. Nasreddine, D. Parent-Massin, Food contamination by metals and pesticides in the European Union. Should we worry? Toxicol. Lett. 127 (2002) 29–41.
[34] P.G. Reeves, R.L. Chaney, Bioavailability as an issue in risk assessment and management of food cadmium: A review, Sci. Total Environ. 398 (2008) 13–19.
[35] M. Vahter, M. Berglund, B. Nermell, A. Åkesson, Bioavailability of cadmium from shellfish and mixed diet in women, Toxicol. Appl. Pharmacol. 136 (1996) 332–341.
[36] T. Suzuki, K. Momoi, M. Hosoyamada, M. Kimura, T. Shibasaki, Normal cadmium uptake in microcytic anemia mk/mk mice suggests that DMT1 is not the only cadmium transporter in vivo, Toxicol. Appl. Pharmacol. 227 (2008) 462–467.
[37] ATSDR, Cadmium toxicity—case studies in environmental medicine, Agency for Toxic Substances and Disease Registry, U.S. Department of Health and Human Services, Atlanta, GA, 2008.
[38] Y. Suwazono, T. Kido, H. Nakagawa, M. Nishijo, R. Honda, E. Kobayashi, M. Dochi, K. Nogawa, Biological half-life of cadmium in the urine of inhabitants after cessation of cadmium exposure, Biomarkers 14 (2009) 77–81.
[39] M.P. Waalkes, Cadmium carcinogenesis, Mutat. Res. 533 (2003) 107–120.
[40] M. Trzcinka-Ochocka, M. Jakubowski, G. Razniewska, T. Halatek, A. Gazewski, The effects of environmental cadmium exposure on kidney function: The possible influence of age, Environ. Res. 95 (2004) 143–150.
[41] SARA Group, Sudbury soils study, Metals health environment, www.sudburysoils-study.com

[42] D.L. Eskew, R.M. Welch, E.E. Cary, Nickel: An essential micronutrient for legumes and possibly all higher plants, Science 222 (1983) 621–623.
[43] A. Sirko, R. Brodzik, Plant ureases: Roles and regulation, Acta Biochim. Polon. 47 (2000) 1189–1195.
[44] F.H. Nielson, Nickel, in: W. Mertz (Ed.), Trace Elements Inhuman and Animal Nutrition, vol. 1, fifth ed., Academic Press, San Diego, 1987, pp. 245–273.
[45] F.W. Sunderman, Jr, S.M. Hopfer, K.R. Sweeney, Nickel absorption and kinetics in human volunteers, Proc. Soc. Exp. Biol. Med. 191 (1989) 5–11.
[46] S.E. Horak, F.W. Sunderman, Jr, Fecal nickel excretion by healthy adults, Clin. Chem. 19 (1972) 429–430.
[47] D.R. Myron, T.J. Zimmermann, T.R. Shuler, Intake of nickel and vanadium by humans, Am. J. Clin. Nutr. 31 (1978) 527–531.
[48] A. Tossavainen, M. Nurminen, P. Mutanen, S. Tola, Application of mathematical modelling for assessing the biological halftimes of chromium and nickel in field studies, Br. J. Ind. Med. 37 (1980) 285–291.
[49] M. Anke, L. Angelow, M. Glei, M. Müller, H. Illing, The biological importance of nickel in the food chain, Fresenius J. Anal. Chem. 352 (1995) 92–96.
[50] F.W. Sunderman, Jr, R.M. Maenza, P.R. Alpass, J.M. Mitchell, I. Damjanov, P.J. Goldblatt, Carcinogenicity of nickel subsulfide in Fischer rats and Syrian hamsters after administration by various routes, Adv. Exp. Med. Biol. 91 (1977) 57–67.
[51] W. Torjussen, I. Anderson, Nickel concentrations in nasal mucosa, plasma, and urine in active and retired nickel workers, Ann. Clin. Lab. Sci. 9 (1979) 289–298.
[52] D.C. Muir, N. Jadon, J.A. Julian, R.S. Roberts, Cancer of the respiratory tract in nickel sinter plant workers: Effect of removal from sinter plant exposure, Occup. Environ. Med. 51 (1994) 19–22.
[53] K.B. Svenes, I. Andersen, Distribution of nickel in lungs from former nickel workers, Int. Arch. Occup. Environ. Health 71 (1998) 424–428.
[54] E. Denkhaus, K. Salnikow, Nickel essentiality, toxicity, and carcinogenicity, Crit. Rev. Oncol. Hematol. 42 (2002) 35–56.
[55] E.D. Segal, S.J. Shon, L.S. Tompkins, Characterization of Helicobacter pylori urease mutants, Infect. Immunol. 60 (1992) 1883–1889.
[56] A.J. Ghio, R. Silbajoris, J.L. Carson, J.M. Samet, Biologic effects of oil fly ash, Environ. Health Perspect. 110 (Suppl. 1) 200289–94.
[57] K.C. Galbreath, R.L. Schulz, D.L. Toman, C.M. Nyberg, F.E. Huggins, G.P. Huffman, E.J. Zillioux, Nickel and sulfur speciation of residual oil fly ashes from two electric utility steam-generating units, J. Air Waste Manage. Assoc. 55 (2005) 309–318.
[58] B.J. Bennett, Environmental nickel pathways to man, in: F.W. Sunderman, Jr (Ed.), Nickel in the Human Environment, International Agency for Research on Cancer, Lyon, 1994, pp. 487–495.
[59] K. Brigden, D. Santillo, Heavy metal and metalloid content of fly ash collected from the Sual, Mauban and Masinloc coal-fired power plants in the Philippines, Greenpeace Research Laboratories Technical Note 7/2002, www.greenpeace.to/publications/philflyash.pdf
[60] A. Profumo, G. Spini, L. Cucca, M. Pesavento, Determination of inorganic nickel compounds in the particulate matter of emissions and workplace air by selective sequential dissolutions, Talanta 61 (2003) 465–472.
[61] S. Pattanaik, F.E. Huggins, G.P. Huffman, W.P. Linak, C.A. Miller, XAFS studies of nickel and sulfur speciation in residual oil fly-ash particulate matters (ROFA PM), Environ. Sci. Technol. 41 (2007) 1104–1110.
[62] E. Soco, J. Kalembkiewicz, Investigations of chemical fraction of Co and Ni in industrial fly ash and mobility of metals in environmental conditions, Chemosphere 67 (2007) 359–364.

[63] U.P. Kodavanti, R. Hauser, D.C. Christiani, Z.H. Meng, J. McGee, A. Ledbetter, J. Richards, D.L. Cost, Pulmonary responses to oil fly ash particles in the rat differ by virtue of their specific soluble metals, Toxicol. Sci. 43 (1998) 204–212.
[64] A.K. Prahalad, J.M. Soukup, J. Inmon, R. Willis, A.J. Ghio, S. Becker, J.E. Gallagher, Ambient air particles: Effects on cellular oxidant radical generation in relation to particulate elemental chemistry, Toxicol. Appl. Pharmacol. 158 (1999) 81–91.
[65] A.K. Prahalad, J. Inmon, A.J. Ghio, J.E. Gallagher, Enhancement of 2′-deoxyguanosine hydroxylation and DNA damage by coal and oil fly ash in relation to particulate metal content and availability, Chem. Res. Toxicol. 13 (2000) 1011–1019.
[66] D.L. Costa, J.R. Lehmann, D. Winsett, J. Richards, A.D. Ledbetter, K.L. Dreher, Comparative pulmonary toxicological assessment of oil combustion particles following inhalation or instillation exposure, Toxicol. Sci. 91 (2006) 237–246.
[67] M.E. Klein-Patel, G. Diamond, M. Boniotto, S. Saad, L.K. Ryan, Inhibition of beta-defensin gene expression in airway epithelial cells by low doses of residual oil fly ash is mediated by vanadium, Toxicol. Sci. 92 (2006) 115–125.
[68] A. Di Pietro, G. Visalli, F. Munaò, B. Baluce, S. La Maestra, P. Primerano, F. Corigliano, S. De Flora, Oxidative damage in human epithelial alveolar cells exposed in vitro to oil fly ash transition metals, Int. J. Hyg. Environ. Health 212 (2009) 196–208.
[69] R.A. Goyer, M.G. Cherian, Renal effects of metals, in: R.A. Goyer, C.D. Klaassen, M.D. Waalkes (Eds.), Metal Toxicology, Academic Press, San Diego, 1995, pp. 389–412.
[70] K. Iwata, H. Saito, M.. Moriyama, A. Nakano, Renal tubular function after reduction of environmental cadmium exposure: A ten-year follow-up, Arch. Environ. Health 48 (1993) 157–163.
[71] Y. Ando, E. Shibata, F. Tsuchiyama, S. Sakai, Elevated urinary cadmium concentrations in a patient with acute cadmium pneumonitis, Scand. J. Work Environ. Health 22 (1996) 150–153.
[72] T. Gordon, Respiratory System, in: R.A. Goyer, C.D. Klaassen, M.D. Waalkes (Eds.), Metal Toxicology, Academic Press, San Diego, 1995, pp. 237–263.
[73] J.A. Thomas, Gonadal-specific metal toxicology, in: R.A. Goyer, C.D. Klaassen, M.D. Waalkes (Eds.), Metal Toxicology, Academic Press, San Diego, 1995, pp. 413–446.
[74] IARC, Cadmium and certain cadmium compounds, in: World Health Organization, (Eds.), IARC Monographs on the Evaluation the Carcinogenic Risk of Chemicals to Humans, Beryllium Cadmium, Mercury and Exposures in the Glass Manufacturing Industry, vol. 58, International Agency for Research on Cancer, Lyon, 1993, pp. 120–136.
[75] M.C. Henson, P.J. Chedrese, Endocrine disruption by cadmium, a common environmental toxicant with paradoxical effects on reproduction, Exp. Biol. Med. 229 (2004) 383–392.
[76] M.H. Bhattacharyya, E.K. Silbergeld, E. Jeffery, A.K. Wilson, L. Watson, Metal-induced osteotoxicities, in: R.A. Goyer, C.D. Klaassen, M.D. Waalkes (Eds.), Metal Toxicology, Academic Press, San Diego, 1995, pp. 465–510.
[77] G.F. Nordberg, Historical perspectives on cadmium toxicology, Toxicol. Appl. Pharmacol. 238 (2009) 192–200.
[78] K. Arisawa, A. Nakano, H. Saito, X.-J. Liu, M. Yokoo, M. Soda, T. Koba, T. Takahashi, K. Kinoshita, Mortality and cancer incidence among a population previously exposed to environmental cadmium, Int. Arch. Occup. Environ. Health 74 (2001) 255–262.
[79] H.C. Gonick, Nephrotoxicity of cadmium and lead, Indian J. Med. Res. 128 (2008) 335–352.

[80] A. Bernard, A. Goret, H. Roels, J.P. Buchet, R. Lauwerys, Experimental confirmation in rats of the mixed type proteinuria observed in workers exposed to cadmium. Toxicology 10 (1978) 369–375.
[81] H. Roels, A. Bernard, J.P. Buchet, A. Goret, R. Lauwerys, D.R. Chettle, T.C. Harvey, I.A. Haddad, Critical concentration of cadmium in renal cortex and urine, Lancet 1 (8109) (1979) 221.
[82] A.M. Bernard, R.R. Lauwery, Dose-reponse relations between urinary cadmium and tubular proteinuria in adult workers, Am. J. Ind. Med. 31 (1997) 116–118.
[83] S. Satarug, M.R. Moore, Adverse health effects of chronic exposure to low level cadmium in foodstuffs and cigarette smoke, Environ. Health Perspect. 112 (2004) 1099–1103.
[84] K.J. Ellis, W.D. Morgan, I. Zanzi, S. Yasumura, D. Vartsky, S.H. Cohn, *In vivo* measurement of critical level of kidney cadmium: Dose effect studies in cadmium smelter workers, Am. J. Ind. Med. 1 (1980) 339–348.
[85] J.R. Edwards, W.C. Prozialeck, Cadmium, diabetes and chronic kidney disease, Toxicol. Appl. Pharmacol. 238 (2009), 289–293.
[86] E.R. Siu, D.D. Mruk, C.S. Porto, Y. Cheng, Cadmium-induced testicular injury, Toxicol. Appl. Pharmacol. 238 (2009) 240–249.
[87] J. Thompson, J. Bannigan, Cadmium: Toxic effects on the reproductive system and the embryo, Reprod. Toxicol. 25 (2008) 304–315.
[88] M. Takiguchi, S. Yoshihara, New aspects of cadmium as endocrine disruptor, Environ. Sci. 13 (2006) 107–116.
[89] Y. Zang, S. Odwin-DaCosta, J.D. Yager, Effects of cadmium on estrogen receptor mediated signaling and estrogen induced DNA synthesis in T47D human breast cancer cells, Toxicol. Lett. 184 (2009) 134–138.
[90] R.A. Pauwels, A.S. Buist, P.M. Calverley, C.R. Jenkins, S.S. Hurd, GOLD Scientific Committee. Global strategy for the diagnosis, management, and prevention of chronic obstructive pulmonary disease. NHLBI/WHO Global Initiative for Chronic Obstructive Lung Disease (GOLD) Workshop summary, Am. J. Respir. Crit. Care 163 (2001) 1256–1276.
[91] A. Mutti, M. Corradi, M. Goldoni, M.V. Vettori, A. Bernard, P. Apostoli, Exhaled metallic elements and serum pneumoproteins in asymptomatic smokers and patients with COPD or asthma, Chest 129 (2006) 1288–1297.
[92] S. Weinmann, W.M. Vollmer, V. Breen, M. Heumann, E. Hnizdo, J. Villnave, B. Doney, M. Graziani, M.A. McBurnie, A.S. Buist, COPD and occupational exposures: A case-control study, J. Occup. Environ. Med. 50 (2008) 561–569.
[93] D.M. Mannino, F. Holguin, H.M. Greves, A. Savage-Brown, A.L. Stock, R.L. Jones, Urinary cadmium levels predict lower lung function in current and former smokers: Data from the Third National Health and Nutrition Examination Survey, Thorax 59 (2004) 194–198.
[94] B.J. Lampe, S.K. Park, T. Robins, B. Mukherjee, A.A. Litonjua, C. Amarasiriwardena, M. Weisskopf, D. Sparrow, H. Hu, Association between 24-hour urinary cadmium and pulmonary function among community-exposed men: The VA Normative Aging Study. Environ. Health Perspect. 116 (2008) 1226–1230.
[95] http://www-cie.iarc.fr/monoeval/grlist.html
[96] M.P. Waalkes, Cadmium carcinogenesis, Mutat. Res. 533 (2003) 107–120.
[97] J. Huff, R.M. Lunn, M.P. Waalkes, L. Tomatis, P.F. Infante, Cadmium-induced cancers in animals and in humans, Int. J. Occup. Environ. Health 13 (2007) 202–212.
[98] J. Siemiatycki, R. Dewar, L. Nadon, M. Gerin, Occupational risk factors for bladder cancer: Results from a case control study in Montreal, Quebec, Canada, Am. J. Epidemiol. 140 (1994) 1061–1080.

[99] E. Kellen, M. Zeegers, E.D. Hond, F. Buntinx, Blood cadmium may be associated with bladder carcinogenesis; the Belgian case control study on bladder cancer, Cancer Detect. Prev. 31 (2007) 77–82.
[100] C. Murta-Nascimento, B.J. Schmitz-Dräger, M.P. Zeegers, G. Steineck, M. Kogevinas, F.X. Real, N. Malats, Epidemiology of urinary bladder cancer: From tumor development to patient's death, World J. Urol. 25 (2007) 285–295.
[101] C. Samanic, M. Kogevinas, M. Dosemeci, N. Malats, F.X. Real, M. Garcia-Closas, C. Serra, A. Carrato, R. García-Closas, M. Sala, J. Lloreta, A. Tardón, N. Rothman, D.T. Silverman, Smoking and bladder cancer in Spain: Effects of tobacco type, timing, environmental tobacco smoke, and gender, Cancer Epidemiol. Biomarkers Prev. 15 (2006) 1348–1354.
[102] D.A. Sens, S. Park, V. Gurel, M.A. Sens, S.H. Garrett, S. Somji, Inorganic, cadmium- and arsenite-induced malignant transformation of human bladder urothelial cells, Toxicol. Sci. 79 (2004) 56–63.
[103] M.E. Parent, J. Siemiatycki, Occupation and prostate cancer, Epidemiol. Rev. 23 (2001) 138–143.
[104] L. Terracio, M. Nachtigal, Oncogenicity of rat prostate cells transformed in vitro with cadmium chloride, Arch. Toxicol. 61 (1988) 450–456.
[105] M.P. Waalkes, S. Rehm, Cadmium and prostate cancer, J. Toxicol. Environ. Health 43 (1994) 251–269.
[106] W.E. Achanzar, B.A. Diwan, S.T. Quader, M.M. Webber, M.P. Waalkes, Cadmium-induced malignant transformation of human prostate epithelial cells, Cancer Res. 61 (2001) 455–458.
[107] J.-D. Lee, S.-M. Wu, L.-Y. Lu, Y.-T. Yang, S.-Y. Jeng, Cadmium concentration and metallothionein expression in prostate cancer and benign prostatic hyperplasia of humans, J. Formos. Med. Assoc. 108 (2009) 554–559
[108] G.G. Schwartz, I.M. Reis, Is cadmium a cause of human pancreatic cancer? Cancer Epidemiol. Biomarkers Prev. 9 (2000) 139–145.
[109] A.M. Kriegel, A.S. Soliman, Q. Zhang, N. El-Ghawalby, F. Ezzat, A. Soultan, M. Abdel-Wahab, O. Fathy, G. Ebidi, N. Bassiouni, S.R. Hamilton, J.L. Abbruzzese, M.R. Lacey, D.A. Blake, Serum cadmium levels in pancreatic cancer patients from the East Nile Delta Region of Egypt, Environ. Health. Perspect. 113 (2005) 113–119.
[110] American Cancer Society, Cancer Facts and Figures, American Cancer Society, Atlanta, GA, www.cancer.org/downloads/STT/CAFF2005f4PWSecured.pdf, 2005.
[111] B. Pesch, J. Haerting, U. Ranft, A. Klimpel, B. Oelschlagel, W. Schill, Occupational risk factors for renal cell carcinoma: Agent-specific results from a case-control study in Germany. MURC Study Group. Multicenter urothelial and renal cancer study. Int. J. Epidemiol. 29 (2000) 1014–1024.
[112] J. Hu, Y. Mao, K. White, Canadian Cancer Registries Epidemiology Research Group, Renal cell carcinoma and occupational exposure in Canada, Occup. Med. 52 (2002) 157–164.
[113] S. Pacini, T. Punzi, G. Morucci, M. Gulisano, M. Ruggiero, A paradox of cadmium: A carcinogen that impairs the capability of human breast cancer cells to induce angiogenesis, J. Environ. Pathol. Toxicol. Oncol. 28 (2009) 85–88.
[114] C. Byrne, S.D. Divekar, G.B. Storchan, D.A. Parodi, M.B. Martin, Cadmium—a metallohormone? Toxicol. Appl. Pharmacol. 238 (2009) 266–271.
[115] A. Akesson, B. Julin, A. Wolk, Long-term dietary cadmium intake and postmenopausal endometrial cancer incidence: A population-based prospective cohort study, Cancer Res. 68 (2008) 6435–6441.
[116] T. Shirakawa, Y. Kusaka, N. Fujimura, M. Kato, S. Heki, K. Morimoto, Hard metal asthma: Cross immunological and respiratory reactivity between cobalt and nickel? Thorax 45 (1990) 267–271.

[117] V.P. Chashschin, G.P. Artunina, T. Norseth, Congenital defects, abortion and other health effects in nickel refinery workers, Sci. Total Environ. 148 (1994) 287–291.
[118] A. Vaktskjold, L.V. Talykova, V.P. Chashchin, J.Ø. Odland, E. Nieboer, Spontaneous abortions among nickel-exposed female refinery workers, Int. J. Environ. Health Res. 18 (2008) 99–115.
[119] L. Mond, K. Langer, F. Quincke, Action of carbon monoxide on nickel, J. Chem. Soc. 57 (1890) 749–753.
[120] F.W. Sunderman, J.F. Kincaid, Nickel poisoning: II. Studies on patients suffering from acute exposure to vapors of nickel carbonyl, J. Am Med. Assoc. 155 (1954) 889–894.
[121] Z. Shi, Nickel carbonyl: Toxicity and human health, Sci. Total Environ. 148 (1994) 293–298.
[122] F.W. Sunderman, Jr, B. Dingle, S.M. Hopfer, T. Swift, Acute nickel toxicity in electroplating workers who accidently ingested a solution of nickel sulfate and nickel chloride, Am. J. Ind. Med. 14 (1988) 257–266.
[123] H.A. Krob, A.B. Fleischer, Jr, R. D'Agostino, Jr, C.L. Haverstock, S Feldman, Prevalence and relevance of contact dermatitis allergens: A meta-analysis of 15 years of published T.R.U.E. test data, J. Am. Acad. Dermatol. 51 (2004) 349–353.
[124] W. Uter, A. Pfahlberg, O. Gefeller, J. Geier, A. Schnuch, Risk factors for contact allergy to nickel—results of a multifactorial analysis, Contact Derm. 48 (2003) 33–38.
[125] J.P. Thyssen, P. Jensen, J.D. Johansen, T. Menné, Contact dermatitis caused by nickel release from hair clasps purchased in a country covered by the EU Nickel Directive. Contact Derm. 60 (2009) 180–181.
[126] COMMISSION DIRECTIVE 2004/96/EC of 27 September 2004 amending Council Directive 76/769/EEC as regards restrictions on the marketing and use of nickel for piercing post assemblies for the purpose of adapting its Annex I to technical progress. Official J. Eur. Union L 301/51 (2004).
[127] S.E. Jacob, J.N. Moennich, B.A. McKean, M.J. Zirwas, J.S. Taylor, Nickel allergy in the United States: A public health issue in need of a "nickel directive", J. Am. Acad. Dermatol. 60 (2009) 1067–1069.
[128] R.L. Rietschel, J.F. Fowler, E.M. Warshaw, D. Belsito, V.A. DeLeo, H.I. Maibach, J.G. Marks, C.G. Mathias, M. Pratt, D. Sasseville, F.J. Storrs, J.S. Taylor, K.A. Zug, Detection of nickel sensitivity has increased in North American patch-test patients, Dermatitis 19 (2008) 16–19.
[129] S.E. Jacob, B. Brod, G.H. Crawford, Clinically relevant patch test reactions in children—a United States based study, Pediatr. Dermatol. 25 (2008) 520–527.
[130] F.O. Nestle, H. Speidel, M.O. Speidel, High nickel release from1- and 2-euro coins, Nature 419 (2002) 132.
[131] C. Lidén, L. Skare, M. Vahter, Release of nickel from coins and deposition onto skin from coin handling—comparing euro coins and SEK, Contact Derm. 59 (2008) 31–37.
[132] International Agency for Research on Cancer, IARC Monographs on the Evaluation of Carcinogenic Risks to Humans, vol. 49, Chromium, Nickel and Welding, IARC Scientific Publications, Lyon, 1990, pp. 257–445.
[133] K.S. Kasprzak, F.W. Sunderman, Jr, K. Salnikow, Nickel carcinogenesis, Mutat. Res. 533 (2003) 67–97.
[134] E.W. Baader, Berufkrebs, Neu. Ergeb. Geb. Krebskrankh. 1 (1937) 104–128.
[135] R. Doll, Cancer of the lung and nose in nickel workers, Br. J. Ind. Med. 15 (1958) 217–223.
[136] R. Doll, Report of the International Committee on Nickel Carcinogenesis in Man, Scand. J. Work. Environ. Health 16 (1990) 9–82.

[137] T.K. Grimsrud, S.R. Berge, J.I. Martinsen, A. Andersen, Lung cancer incidence among Norwegian nickel-refinery workers, 1953–2000, J. Environ. Monit. 5 (2003) 190–197.
[138] F.W. Sunderman, Jr, L.G. Morgan, A. Andersen, D. Ashley, F.A. Forouhar, Histopathology of sinonasal and lung cancers in nickel refinery workers, Ann. Clin. Lab. Sci. 19 (1989) 44–50.
[139] M. Lippmann, D.B. Yeates, R.E. Albert, Deposition, retention, and clearance of inhaled particles, Br. J. Ind. Med. 37 (1980) 337–362.
[140] K.S. Kasprzak, P. Gabryel, K. Jarczewska, Carcinogenicity of nickel(II) hydroxides and nickel(II) sulfate in Wistar rats and its relation to the in vitro dissolution rates, Carcinogenesis 4 (1983) 275–279.
[141] M. Shibata, K. Izumi, N. Sano, A. Akagi, H. Otsuka, Induction of soft tissue tumours in F344 rats by subcutaneous, intramuscular, intra-articular, and retroperitoneal injection of nickel sulphide (Ni_3S_2), J. Pathol. 157 (1989) 263–274.
[142] G.D. Stoner, M.B. Shimkin, M.C. Troxell, T.L. Thompson, L.S. Terry, Test for carcinogenicity of metallic compounds by the pulmonary tumor response in strain A mice, Cancer Res. 36 (1976) 1744–1747.
[143] K.S. Kasprzak, B.A. Diwan, N. Konishi, M. Misra, J.M. Rice, Initiation by nickel acetate and promotion by sodium barbital of renal cortical epithelial tumors in male F344 rats, Carcinogenesis 11 (1990) 647–652.
[144] B.A. Diwan, K.S. Kasprzak, J.M. Rice, Transplacental carcinogenic effects of nickel (II) acetate in the renal cortex, Carcinogenesis 13 (1992) 1351–1357.
[145] G.R. Bunin, K. Noller, P. Rose, E. Smith, Carcinogenesis, in: M. Paul (Ed.), Occupational and Environmental Reproductive Hazards: A Guide for Clinicians, Williams & Wilkins, Baltimore, MD, 1992, pp. 76–88.
[146] F.W. Sunderman, Jr, Carcinogenicity of metal alloys in orthopedic prostheses: Clinical and experimental studies, Fundam. Appl. Toxicol. 13 (1989) 205–216.
[147] D.B. McGregor, R.A. Baan, C. Partensky, J.M. Rice, J.D. Wilbourn, Evaluation of the carcinogenic risks to humans associated with surgical implants and other foreign bodies—a report of an IARC Monographs Programme Meeting, Eur. J. Cancer 36 (2000) 307–313.
[148] H.-J. Raithel, K.H. Schaller, A. Reith, K.B. Svenes, H. Valentin, Investigations on the quantitative determination of nickel and chromium in human lung tissue, Int. Arch. Occup. Environ. Healh. 60 (1988) 55–66.
[149] H.-J. Raithel, K.H. Schaller, T. Kraus, G. Lehnert, Biomonitoring of nickel and chromium in human pulmonary tissue, Int. Arch. Occup. Environ. Health 65 (1993) S197–S200.
[150] K. Hughes, M.E. Meek, R. Newhook, P.K.L. Chan, Speciation and health risk assessment of metals: Evaluation of effects associated with forms present in the environment, Regul. Toxicol. Pharmacol. 22 (1995) 213–220.
[151] W. Goumakos, J.P. Laussac, B. Sarkar, Binding of cadmium(II) and zinc(II) to human and dog serum albumins: An equilibrium dialysis and 113Cd-NMR study, Biochem. Cell Biol. 69 (1991) 809–820.
[152] P.J. Sadler, J.H. Viles, ^{1}H and ^{113}Cd NMR investigations of Cd^{2+} and Zn^{2+} binding sites on serum albumin: Competition with Ca^{2+}, Ni^{2+}, Cu^{2+}, and Zn^{2+}, Inorg. Chem. 35 (1996) 4490–4496.
[153] W.R. Harris, L.J. Madsen, Equilibrium studies on the binding of cadmium(II) to human serum transferring, Biochemistry 27 (1988) 284–288.
[154] B.J. Scott, A.R. Bradwell, Identification of the serum binding proteins for iron, zinc, cadmium, nickel, and calcium, Clin. Chem. 29 (1983) 629–633.
[155] K.T. Suzuki, S. Kawahara, H. Sunaga, E. Kobayashi, N. Shimojo, Discriminative uptake of metals by the liver and its relation to induction of metallothionein by cadmium, copper and zinc, Comp. Biochem. Physiol. C. 95 (1990) 279–284.

[156] W. Kadima, D.L. Rabenstein, A quantitative study of the complexation of cadmium in hemolyzed human erythrocytes by 1H NMR spectroscopy, J. Inorg. Biochem. 40 (1990) 141–149.
[157] A. Krężel, W. Bal, The coordination chemistry of glutathione, Acta Biochim. Polon. 46 (1999) 567–580.
[158] S. Prévéral, L. Gayet, C. Moldes, J. Hoffmann, S. Mounicou, A. Gruet, F. Reynaud, R. Lobinski, J.M. Verbavatz, A. Vavasseur, C. Forestier, A common highly conserved cadmium detoxification mechanism from bacteria to humans: Heavy metal tolerance conferred by the ATP-binding cassette (ABC) transporter SpHMT1 requires glutathione but not metal-chelating phytochelatin peptides, J. Biol. Chem. 284 (2009) 4936–4943.
[159] M.G. Cherian, Chelation of cadmium without increased renal cadmium deposition, Environ. Health Perspect. 54 (1984) 243–248.
[160] W. Maret, Y. Li, Coordination dynamics of zinc in proteins, Chem. Rev., in press, 109 (2009) 4682–4707.
[161] V. Lalioti, G. Muruais, Y. Tsuchiya, D. Pulido, I.V. Sandoval, Molecular mechanisms of copper homeostasis, Front. Biosci. 14 (2009) 4878–4903.
[162] A. Krężel, W. Maret, Dual nanomolar and picomolar Zn(II) binding properties of metallothionein, J. Am. Chem. Soc. 129 (2007) 10911–10921.
[163] D.A. Fowle, M.J. Stillman, Comparison of the structures of the metal-thiolate binding site in Zn(II)-, Cd(II)-, and Hg(II)-metallothioneins using molecular modeling techniques, J. Biomol. Struct. Dyn. 14 (1997) 393–406.
[164] G. Henkel, B. Krebs, Metallothioneins: Zinc, cadmium, mercury, and copper thiolates and selenolates mimicking protein active site features—structural aspects and biological implications, Chem. Rev. 104 (2004) 801–824.
[165] C.D. Klaassen, J. Liu, Induction of metallothionein as an adaptive mechanism affecting the magnitude and progression of toxicological injury, Environ. Health Perspect. 106 (Suppl. 1) (1998) 297–300.
[166] C.D. Klaassen, J. Liu, B.A. Diwan, Metallothionein protection of cadmium toxicity, Toxicol. Appl. Pharmacol. 238 (2009) 215–220.
[167] B.A. Hart, R.J. Potts, R.D. Watkin, Cadmium adaptation in the lung—a double-edged sword? Toxicology 160 (2001) 65–70.
[168] M.P. Waalkes, J. Liu, Metallothionein in inorganic carcinogenesis, in: A. Sigel, H. Sigel, R.K.O. Sigel (Eds.), Met. Ions Life Sci. 5 (2009) 399–412.
[169] J. Liu, M.L. Cheng, Q. Yang, K.R. Shan, J. Shen, Y. Zhou, X. Zhang, A.L. Dill, M.P. Waalkes, Blood metallothionein transcript as a biomarker for metal sensitivity: Low blood metallothionein transcripts in arsenicosis patients from Guizhou, China, Environ. Health Perspect. 115 (2007) 1101–1106.
[170] N. Miura, Individual susceptibility to cadmium toxicity and metallothionein gene polymorphisms: With references to current status of occupational cadmium exposure, Ind. Health 47 (2009) 487–494.
[171] C.D. Klaassen, J. Liu, S. Choudhuri, Metallothionein: An intracellular protein to protect against cadmium toxicity, Annu. Rev. Pharmacol. Toxicol. 39 (1999) 267–294.
[172] H.M. Chan, L.-F. Zhu, D. Grant, R.A. Goyer, G.M. Cherian, Nephrotoxicity in rats following liver transplantation from cadmium exposed rats, Toxicol. Appl. Pharmacol. 123 (1993) 89–96.
[173] W.C. Prozialeck, D.R. Wellington, P.C. Lamar, Comparison of the cytotoxic effects of cadmium chloride and cadmium-metallothionein in LLC-PK1 cells, Life Sci. 53 (1993) 337–342.
[174] J. Liu, Y. Liu, C.D. Klaassen, Nephrotoxicity of $CdCl_2$ and Cd-metallothionein in cultured rat kidney proximal tubules and LLC-PK1 cells, Toxicol. Appl. Pharmacol. 128 (1994) 264–270.

[175] J. Liu, Y. Liu, S.S. Habeebu, C.D. Klaassen, Susceptibility of MT-null mice to chronic $CdCl_2$-induced nephrotoxicity indicates that renal injury is not mediated by the CdMT complex, Toxicol. Sci. 46 (1998) 197–203.
[176] P. Joseph, Mechanisms of cadmium carcinogenesis, Toxicol. Appl. Pharmacol. 238 (2009) 272–279.
[177] W. Bal, K.S. Kasprzak, Induction of oxidative DNA damage by carcinogenic metals, Toxicol. Lett. 127 (2002) 55–62.
[178] M.V. Mikhailova, N.A. Littlefield, B.S. Hass, L.A. Poirier, M.W. Chou, Cadmium-induced 8-hydroxydeoxyguanosine formation, DNA strand breaks and antioxidant enzyme activities in lymphoblastoid cells, Cancer Lett. 115 (1997) 141–148.
[179] J. Liu, W. Qu, M.B. Kadiiska, Role of oxidative stress in cadmium toxicity and carcinogenesis, Toxicol. Appl. Pharmacol. 238 (2009) 209–214.
[180] G. Bertin, D. Averbeck, Cadmium: Cellular effects, modifications of biomolecules, modulation of DNA repair and genotoxic consequences (a review), Biochimie 88 (2006) 1549–1559.
[181] J.D. Eneman, R.J. Potts, M. Osier, G.S. Shukla, C.H. Lee, J.F. Chiu, B.A. Hart, Suppressed oxidant-induced apoptosis in cadmium adapted alveolar epithelial cells and its potential involvement in cadmium carcinogenesis, Toxicology 147 (2000) 215–228.
[182] M. Kondoh, S. Araragi, K. Sato, M. Higashimoto, M. Takiguchi, M. Sato, Cadmium induces apoptosis partly via caspase-9 activation in HL-60 cells, Toxicology 170 (2002) 111–117.
[183] C.M. Shih, W.C. Ko, J.S. Wu, Y.H. Wei, L.F. Wang, E.E. Chang, T.Y. Lo, H.H. Cheng, C.T. Chen, Mediating of caspase-independent apoptosis by cadmium through the mitochondria-ROS pathway in MRC-5 fibroblasts, J. Cell. Biochem. 91 (2004) 384–397.
[184] J. Kim, R.P. Sharma, Cadmium-induced apoptosis in murine macrophages is antagonized by antioxidants and caspase inhibitors, J. Toxicol. Environ. Health 69 (2006) 1181–1201.
[185] W. Watjen, D. Beyersmann, Cadmium-induced apoptosis in C6 glioma cells: Influence of oxidative stress, BioMetals 17 (2004) 65–78.
[186] W.E. Achanzar, M.M. Webber, M.P. Waalkes, Altered apoptotic gene expression and acquired apoptotic resistance in cadmium-transformed human prostate epithelial cells, Prostate 52 (2002) 236–244.
[187] J.J. Mukherjee, S.K. Gupta, S. Kumar, Inhibition of benzopyrene diol epoxide induced apoptosis by cadmium(II) is AP-1-independent: Role of extracelluler signal related kinase, Chem.-Biol. Interact. 172 (2008) 72–80.
[188] W.E. Achanzar, K.B. Achanzar, J.G. Lewis, M.M. Webber, M.P. Waalkes, Cadmium induces c-myc, p53, and c-jun expression in normal human prostate epithelial cells as a prelude to apoptosis, Toxicol. Appl. Pharmacol. 164 (2000) 291–300.
[189] J. Liu, C. Corton, D.J. Dix, Y. Liu, M.P. Waalkes, C.D. Klaassen, Genetic background but not metallothionein phenotype dictates sensitivity to cadmium-induced testicular injury in mice, Toxicol. Appl. Pharmacol. 176 (2001) 1–9.
[190] P. Joseph, T.K. Muchnok, M.L. Klishis, J.R. Roberts, J.M. Antonini, W.Z. Whong, T. Ong, Cadmium-induced cell transformation and tumorigenesis are associated with transcriptional activation of c-fos, c-jun, and c-myc proto-oncogenes: Role of cellular calcium and reactive oxygen species, Toxicol. Sci. 61 (2001) 295–303.
[191] P. Joseph, Y.X. Lei, W.Z. Whong, T. Ong, Oncogenic potential of mouse translation elongation factor-1 delta, a novel cadmium-responsive proto-oncogene, J. Biol. Chem. 277 (2002) 6131–6136.

[192] P. Joseph, Y.X. Lei, T. Ong, Up-regulation of expression of translation factors-a novel molecular mechanism for cadmium carcinogenesis, Mol. Cell. Biochem. 255 (2004) 93–101.
[193] J.H. Hoeijmakers, Genome maintenance mechanisms for preventing cancer, Nature 411 (2001) 366–374.
[194] D. Beyersmann, A. Hartwig, Carcinogenic metal compounds: Recent insight into molecular and cellular mechanisms, Arch Toxicol. 82 (2008) 493–512.
[195] A. Hartwig, T. Schwerdtle, Interactions by carcinogenic metal compounds with DNA repair systems: Toxicological implications, Toxicol. Lett. 127 (2002) 47–54.
[196] H. Dally, A. Hartwig, Induction and repair inhibition of oxidative DNA damage by nickel(II) and cadmium(II) in mammalian cells, Carcinogenesis 18 (1997) 1021–1026.
[197] T. Fatur, M. Tusek, I. Falnoga, J. Scancar, T.T. Lach, M. Filipic, Cadmium inhibits repair of UV-, methyl methanesulfonate- and N-methyl-N-nitrosothiourea-induced DNA damage in Chinese hamster ovary cells, Mutat. Res. 529 (2003) 109–116.
[198] R.D. Watkin, T. Nawrot, R.J. Potts, B.A. Hart, Mechanisms regulating the cadmium-mediated suppression of Sp1 transcription factor activity in alveolar epithelial cells, Toxicology 184 (2003) 157–178.
[199] A. Hartwig, M. Asmuss, H. Blessing, S. Hoffmann, G. Jahnke, S. Khandelwal, A. Pelzer, A. Burkle, Interference by toxic metal ions with zinc-dependent proteins involved in maintaining genomic stability, Food Chem. Toxicol. 40 (2002) 1179–1184.
[200] M. Asmuss, L.H.F. Mullenders, A. Elker, A. Hartwig, Differential effects of toxic metal compounds on the activities of Fpg and XPA, two zinc finger proteins involved in DNA repair, Carcinogenesis 21 (2000) 2097–2104.
[201] A. Lutzen, S.E. Liberti, L.J. Rasmussen, Cadmium inhibits human DNA mismatch repair in vivo, Biochem. Biophys. Res. Commun. 321 (2004) 21–25.
[202] A.B. Clark, T.A. Kunkel, Cadmium inhibits the functions of eukaryotic MutS complexes, J. Biol. Chem. 279 (2004) 53903–53906.
[203] W.C. Prozialeck, J.R. Edwards, J.M. Woods, The vascular endothelium as a target of cadmium toxicity, Life Sci. 79 (2006) 1493–1506.
[204] W.C. Prozialeck, J.R. Edwards, Cell adhesion molecules in chemically-induced renal injury, Pharmacol. Ther. 114 (2007) 74–93.
[205] B.D. Angst, C. Marcozzi, A.I. Magee, The cadherin superfamily: Diversity in form and function, J. Cell Sci. 114 (2001) 629–641.
[206] F. Thévenod, N.A. Wolff, U. Bork, W.-K. Lee, M. Abouhamed, Cadmium induces nuclear translocation of β-catenin and increases expression of *c-myc* and *Abcb1a* in kidney proximal tubule cells, Biometals 20 (2007) 807–820.
[207] H. Chiba, M. Osani, M. Murata, T. Kojima, N. Sawada, Transmembrane proteins of tight junctions, Biochim. Biophys. Acta 1778 (2008) 558–600.
[208] J.M. Woods, M. Leone, K. Klosowska, P.C. Lamar, T.J. Shankovsky, W.C. Prozialeck, Direct antiangiogenic actions of cadmium on human vascular endothelial cells, Toxicol. In Vitro 22 (2008) 643–651.
[209] G. Girolomoni, S. Sebastiani, C. Albanesi, A. Cavani, T-cell subpopulations in the development of atopic and contact allergy, Curr. Opin. Immunol. 13 (2001) 733–737.
[210] A. Cavani, Breaking tolerance to nickel, Toxicology 209 (2005) 119–121.
[211] R. Kornik, K.A. Zug, Nickel, Dermatitis 19 (2008) 3–8.
[212] E. Czarnobilska, K. Obtułowicz, K. Wsołek, J. Piętowska, R. Śpiewak, Mechanisms of nickel allergy, Przegl. Lek. 64 (2007) 502–505.
[213] H.-J. Thierse, C. Moulon, Y. Allespach, B. Zimmermann, A. Doetze, S. Kuppig, D. Wild, F. Herberg, H.U. Weltzien, Metal-protein complex-mediated transport and delivery of Ni^{2+} to TCR/MHC contact sites in nickel-specific human T cell activation, J. Immunol. 172 (2004) 1926–1934.

[214] P.J. Sadler, A. Tucker, J.H. Viles, Involvement of a lysine residue in the N-terminal Ni^{2+} and Cu^{2+} binding site of serum albumins. Comparison with Co^{2+}, Cd^{2+} and Al^{3+}, Eur. J. Biochem. 220 (1994) 193–200.
[215] W. Bal, J. Christodoulou, P.J. Sadler, A. Tucker, Multi metal binding site of serum albumin, J. Inorg. Biochem. 70 (1998) 33–39.
[216] M. Sokołowska, A. Krężel, M. Dyba, Z. Szewczuk, W. Bal, Short peptides are not reliable models of thermodynamic and kinetic properties of the N-terminal metal binding site in serum albumin, Eur. J. Biochem. 269 (2002) 1323–1331.
[217] C. Giwercman, A. Lerbaek, H. Bisgaard, T. Menné, Classification of atopic hand eczema and the filaggrin mutation, Contact Derm. 59 (2008) 257–260.
[218] J.P. Thyssen, B.C. Carlsen, T. Menné, Nickel sensitization, hand eczema, and loss-of-function mutations in the filaggrin gene, Dermatitis 19 (2008) 303–307.
[219] N. Novak, H. Baurecht, T. Schäfer, E. Rodriguez, S. Wagenpfeil, N. Klopp, J. Heinrich, H. Behrendt, J. Ring, E. Wichmann, T. Illig, S. Weidinger, Loss-of-function mutations in the filaggrin gene and allergic contact sensitization to nickel, J. Invest. Dermatol. 128 (2008) 1430–1435.
[220] Z. Wu, B. Hansmann, U. Meyer-Hoffert, R. Gläser, J.-M. Schröder, Molecular identification and expression analysis of filaggrin-2, a member of the S100 fused-type protein family, PLoS ONE 4 (2009) e5227. doi:10.1371/journal.pone.0005227
[221] H.-J. Thierse, K. Gamerdinger, C. Junkes, N. Guerreiro, H.U. Weltzien, T cell receptor (TCR) interaction with haptens: Metal ions as non-classical haptens, Toxicology 209 (2005) 101–107.
[222] P. Romagnoli, A.M. Labhardt, F. Sinigaglia, Selective interaction of Ni with an MHC-bound peptide, EMBO J. 10 (1991) 1303–1306.
[223] L. Lu, J. Vollmer, C. Moulon, H.U. Weltzien, P. Marrack, J. Kappler, Components of the ligand for a Ni^{++} reactive human T cell clone, J. Exp. Med. 197 (2003) 567–574.
[224] V. Bordignon, F. Palamara, P. Cordiali-Fei, A. Vento, A. Aiello, M. Picardo, F. Ensoli, A. Cristaudo, Nickel, palladium and rhodium induced IFN-gamma and IL-10 production as assessed by in vitro ELISpot-analysis in contact dermatitis patients, BMC Immunol. 9 (2008) 19 (http://www.biomedcentral.com/1471-2172/9/19).
[225] M. Hindsén, A. Spirén, M. Bruze, Cross-reactivity between nickel and palladium demonstrated by systemic administration of nickel, Contact Derm. 53 (2005) 2–8.
[226] M. Hirota, M. Suzuki, S. Hagino, S. Kagatani, Y. Sasaki, S. Aiba, H. Itagaki, Modification of cell-surface thiols elicits activation of human monocytic cell line THP-1: Possible involvement in effect of haptens 2,4-dinitrochlorobenzene and nickel sulfate, J. Toxicol. Sci. 34 (2009) 139–150.
[227] W. Bal, T. Schwerdtle, A. Hartwig, Mechanism of nickel assault on the zinc finger of DNA repair protein XPA, Chem. Res. Toxicol. 16 (2003) 242–248.
[228] S. Artik, C. von Vultée, E. Gleichmann, T. Schwarz, P. Griem, Nickel allergy in mice: Enhanced sensitization capacity of nickel at higher oxidation states, J. Immunol. 163 (1999) 1143–1152.
[229] S. Artik, K. Haarhuis, X. Wu, J. Begerow, E. Gleichmann, High frequency of anergic T cells with persistent suppressor activity, J. Immunol. 167 (2001) 6794–6803.
[230] K.S. Kasprzak, W. Bal, A.A. Karaczyn, The role of chromatin damage in nickel-induced carcinogenesis. Review of recent developments, J. Environ. Monit. 5 (2003) 1–6.
[231] H.-C. Schuppe, A.C. Rönnau, S. von Schmiedeberg, T. Ruzicka, E. Gleichmann, P. Griem, Immunomodulation by heavy metal compounds, Clin. Dermatol. 16 (1998) 149–157.
[232] W. Bal, J. Lukszo, K. Białkowski, K.S. Kasprzak, Interactions of nickel(II) with histones: Interactions of Ni(II) with CH_3CO-Thr-Glu-Ser-His-His-Lys-NH_2, a peptide modeling the potential metal binding site in the "C-tail" region of histone H2A, Chem. Res. Toxicol. 11 (1998) 1014–1023.

[233] W. Bal, R. Liang, J. Lukszo, S.-H. Lee, M. Dizdaroglu, K.S. Kasprzak, Ni(II) specifically cleaves the C-terminal tail of the major variant of histone H2A and forms an oxidative damage-mediating complex with the cleaved octapeptide, Chem. Res. Toxicol. 13 (2000) 616–624.
[234] A.A. Karaczyn, W. Bal, S.L. North, R.M. Bare, V.M. Hoang, R.J. Fisher, K.S. Kasprzak, The octapeptidic end of the C-terminal tail of histone H2A is cleaved-off in cells exposed to carcinogenic Ni(II), Chem. Res. Toxicol. 16 (2003) 1555–1559.
[235] A. Krężel, M. Mylonas, E. Kopera, W. Bal, Sequence-specific Ni(II)-dependent peptide bond hydrolysis in a peptide containing threonine and histidine residues, Acta Biochim. Polon. 53 (2006) 721–727.
[236] I.M.W. Van Hoogstraten, K.E. Andersen, B.M.E. Von Blomberg, D. Boden, D.P. Bruynzeel, D. Burrows, J.G. Camarasa, A. Dooms-Goossens, G. Kraal, A. Lahti, T. Menné, R.J.G. Rycroft, S. Shaw, D. Todd, K.J.J. Vreeburg, J.D. Wilkinson, R.J. Scheper, Reduced frequency of nickel allergy upon oral nickel contact at an early age. Clin. Exp. Immunol. 85 (1991) 441–445.
[237] H. Kerosuo, A. Kullaa, E. Kerosuo, L. Kanerva, A. Hensten Pettersen, Nickel allergy in adolescents in relation to orthodontic treatment and piercing of ears, Am. J. Orthod. Dentofacial Orthop. 109 (1996) 148–154.
[238] C.S. Jensen, T. Menné, J.D. Johansen, Systemic contact dermatitis after oral exposure to nickel: A review with a modified meta-analysis, Contact Derm. 54 (2006) 79–86.
[239] X. Wu, K. Roelofs-Haarhuis, J. Zhang, M. Nowak, L. Layland, E. Jermann, E. Gleichmann, Dose dependence of oral tolerance to nickel, Int. Immunol. 19 (2007) 965–975.
[240] K. Salnikow, A. Zhitkovich, Genetic and epigenetic mechanisms in metal carcinogenesis and cocarcinogenesis: Nickel, arsenic, chromium, Chem. Res Toxicol. 21 (2008) 28–44.
[241] J.K. Dunnick, M.R. Elwell, A.E. Radovsky, J.M. Benson, F.F. Hahn, K.J. Nikula, E.B. Barr, C.H. Hobbs, Comparative carcinogenic effects of nickel subsulfide, nickel oxide, or nickel sulfate hexahydrate chronic exposures in the lung, Cancer Res. 55 (1995) 5251–5256.
[242] M. Costa, H.H. Mollenhauer, Carcinogenic activity of particulate nickel compounds is proportional to their cellular uptake, Science 209 (1980) 515–517.
[243] M. Costa, J. Simmons-Hansen, C.W. Bedrossian, J. Bonura, R.M. Caprioli, Phagocytosis, cellular distribution, and carcinogenic activity of particulate nickel compounds in tissue culture, Cancer Res. 41 (1981) 2868–2876.
[244] R.M. Evans, P.J. Davies, M. Costa, Video time-lapse microscopy of phagocytosis and intracellular fate of crystalline nickel sulfide particles in cultured mammalian cells, Cancer Res. 42 (1982) 2729–2735.
[245] G.G. Fletcher, F.E. Rosetto, J.D. Turnbull, E. Nieboer, Toxicity, uptake, and mutagenicity of particulate and soluble nickel compounds, Environ. Health Perspect. 102 (Suppl. 3) (1994) 69–79.
[246] A. Longstaff, A.I.T. Walker, R. Jackh, Nickel oxide, potential carcinogenicity—a review and further evidence, in: F.W. Sunderman (Ed.), Nickel in the Human Environment, vol. 53, IARC Scientific Publications, Lyon 1984, pp. 235–244.
[247] M. Horie, K. Nishio, K. Fujita, H. Kato, A. Nakamura, S. Kinugasa, S. Endoh, A. Miyauchi, K. Yamamoto, H. Murayama, E. Niki, H. Iwahashi, Y. Yoshida, J. Nakanishi, Ultrafine NiO particles induce cytotoxicity in vitro by cellular uptake and subsequent Ni(II) release, Chem. Res. Toxicol. 22 (2009) 1415–1426.
[248] J. Tallkvist, H. Tjalve, Transport of nickel across monolayers of human intestinal Caco-2 cells, Toxicol. Appl. Pharmacol. 151 (1998) 117–122.
[249] M. Knopfel, G. Schulthess, F. Funk, H. Hauser, Characterization of an integral protein of the brush border membrane mediating the transport of divalent metal ions, Biophys. J. 79 (2000) 874–884.

[250] E.C. Foulkes, D.M. McMullen, On the mechanism of nickel absorption in the rat jejunum, Toxicology 38 (1986) 35–42.
[251] K.S. Kasprzak, Possible role of oxidative damage in metal-induced carcinogenesis, Cancer Invest. 13 (1995) 411–430.
[252] L.K. Tkeshelashvili, T.M. Reid, T.J. McBride, L.A. Loeb, Nickel induces a signature mutation for oxygen free radical damage, Cancer Res. 53 (1993) 4172–4174.
[253] K.G. Higinbotham, J.M. Rice, B.A. Diwan, K.S. Kasprzak, C.D. Reed, A.O. Perantoni, GGT to GTT transversions in codon 12 of the K-ras oncogene in rat renal sarcomas induced with nickel subsulfide or nickel subsulfide/iron are consistent with oxidative damage to DNA, Cancer Res. 52 (1992) 4747–4751.
[254] L.C. Harty, D.G. Guinee, Jr, W.D. Travis, W.P. Bennett, J. Jett, T.V. Coby, H. Tazelaar, V. Trastek, P. Pairolero, L.A. Liotta, C.C. Harris, N.E. Caporaso, p53 mutations and occupational exposures in a surgical series of lung cancers, Cancer Epidemiol. Biomark. Prev. 5 (1996) 997–1003.
[255] A. Arita, M. Costa, Epigenetics in metal carcinogenesis: Nickel, arsenic, chromium and cadmium, Metallomics 1 (2009) 222–228.
[256] F. Golebiowski, K.S. Kasprzak, Inhibition of core histones acetylation by carcinogenic nickel(II), Mol. Cell. Biochem. 279 (2005) 133–139.
[257] A.A. Karaczyn, F. Golebiowski, K.S. Kasprzak, Truncation, deamidation, and oxidation of histone H2B in cells cultured with nickel(II), Chem. Res. Toxicol. 18 (2005) 1934–1942.
[258] A.A. Karaczyn, F. Golebiowski, K.S. Kasprzak, Ni(II) affects ubiquitination of core histones H2B and H2A, Exp. Cell. Res. 312 (2006) 3252–3259.
[259] L. Broday, W. Peng, M.H. Kuo, K. Salnikow, M. Zoroddu, M. Costa, Nickel compounds are novel inhibitors of histone H4 acetylation, Cancer Res. 60 (2000) 238–241.
[260] H. Chen, Q. Ke, T. Kluz, Y. Yan, M. Costa, M. Nickel ions increase histone H3 lysine 9 dimethylation and induce transgene silencing, Mol. Cell. Biol. 26 (2006) 3728–3737.
[261] Q. Ke, T. Davidson, H. Chen, T. Kluz, M. Costa, Alterations of histone modifications and transgene silencing by nickel chloride, Carcinogenesis 27 (2006) 1481–1488.
[262] A.A. Karaczyn, R.Y.S. Cheng, G.S. Buzard, J. Hartley, D. Esposito, K.S. Kasprzak, Truncation of histone H2A's C-terminal tail, as is typical for Ni(II)-assisted specific peptide bond hydrolysis, has gene expression altering effects, Ann. Clin. Lab. Sci. 39 (2009) 251–262.
[263] W. Li, Y. Zhao, I.N. Chou, Alterations in cytoskeletal protein sulfhydryls and cellular glutathione in cultured cells exposed to cadmium and nickel ions, Toxicology 77 (1993) 65–79.
[264] S. Lynn, F.H. Yew, J.-W. Hwang, M.-J. Tseng, K.Y. Jan, Glutathione can rescue the inhibitory effects of nickel on DNA ligation and repair synthesis, Carcinogenesis 15 (1994) 2811–2816.
[265] W. Li, Y. Zhao, I.N. Chou, Mg^{2+} antagonism on Ni^{2+}-induced changes in microtubule assembly and cellular thiol homeostasis, Toxicol. Appl. Pharmacol. 136 (1996) 101–111.
[266] K. Salnikow, M. Gao, V. Voitkun, X. Huang, M. Costa, Altered oxidative stress responses in nickel-resistant mammalian cells, Cancer Res. 54 (1994) 6407–6412.
[267] K. Salnikow, K.S. Kasprzak, Ascorbate depletion: A critical step in nickel carcinogenesis, Environ. Health Perspect. 113 (2005) 577–584.
[268] K. Salnikow, T. Davidson, Q. Zhang, L.C. Chen, W. Su, M. Costa, The involvement of hypoxia-inducible transcription factor-1-dependent pathway in nickel carcinogenesis, Cancer Res. 63 (2003) 3524–3530.
[269] M. Kaczmarek, R.E. Cachau, I.A. Topol, K.S. Kasprzak, A. Ghio, K. Salnikow, Metal ions-stimulated iron oxidation in hydroxylases facilitates stabilization of HIF-1 alpha protein, Toxicol. Sci. 107 (2009) 394–403.

[270] R.E. Rodriguez, M. Misra, B.A. Diwan, C.W. Riggs, K.S. Kasprzak, Relative susceptibilities of C57BL/6, (C57BL/6 × C3H/He)F1, and C3H/He mice to acute toxicity and carcinogenicity of nickel subsulfide, Toxicology 107 (1996) 131–140.
[271] A. Hartwig, L.H.F. Mullenders, R. Schlepegrell, U. Kasten, D. Beyersmann, Nickel (II) interferes with the incision step in nucleotide excision repair in mammalian cells. Cancer Res. 54 (1994) 4045–4051.
[272] F. Iwitzki, R. Schlepegrell, U. Eichhorn, B. Kaina, D. Beyersmann, A. Hartwig, Nickel(II) inhibits the repair of O6-methylguanine in mammalian cells, Arch. Toxicol. 72 (1998) 681–689.
[273] T. Schwerdtle, A. Seidel, A. Hartwig, Effect of soluble and particulate nickel compounds on the formation and repair of stable benzo[a]pyrene DNA adducts in human lung cells, Carcinogenesis 23 (2002) 47–53.
[274] M. Asmuss, L.H.F. Mullenders, A. Elker, A. Hartwig, Differential effects of toxic metal compounds on the activities of Fpg and XPA, two zinc finger proteins involved in DNA repair, Carcinogenesis 21 (2000) 2097–2104.
[275] W. Bal, M. Jeżowska-Bojczuk, J. Lukszo, K.S. Kasprzak, Interactions of nickel(II) with histones. Stability and solution structure of complexes with CH_3CO-Cys-Ala-Ile-His-NH_2, a putative metal binding sequence of histone H3, Chem. Res. Toxicol. 8 (1995) 683–692.
[276] W. Bal, J. Lukszo, K.S. Kasprzak, Interactions of nickel(II) with histones: Enhancement of 2′-deoxyguanosine oxidation by Ni(II) complexes with CH_3CO-Cys-Ala-Ile-His-NH_2, a putative metal binding sequence of histone H3, Chem. Res. Toxicol. 9 (1996) 435–440.
[277] W. Bal, V. Karantza, E.N. Moudrianakis, K.S. Kasprzak, Interactions of nickel(II) with the histone core tetramer in vitro, Arch. Biochem. Biophys. 364 (1999) 161–166.
[278] A. Krężel, W. Szczepanik, M. Sokołowska, M. Jeżowska-Bojczuk, W. Bal, Correlations between complexation modes and redox activities of Ni(II)-GSH complexes, Chem. Res. Toxicol. 16 (2003) 855–864.
[279] K.S. Kasprzak, J.M. Ward, L.A. Poirier, D.A. Reichardt, A.C. Denn III, C.W. Reynolds, Nickel–magnesium interactions in carcinogenesis: Dose–effects and involvement natural killer cells, Carcinogenesis 8 (1987) 1005–1011.
[280] W. Maret, Cellular zinc and redox states converge in the metallothionein/thionein pair, J. Nutr. 133 (2003) 1460S–1462S.
[281] J.P. Mackay, M. Crossley, Zinc fingers are sticking together, Trends Biochem. Sci. 23 (1998) 1–4.
[282] J.H. Laity, B.M. Lee, P.E. Wright, Zinc finger proteins: New insights into structural and functional diversity, Curr. Opin. Struct. Biol. 11 (2001) 39–46.
[283] W. Maret, Zinc and sulfur: A critical biological partnership, Biochemistry 43 (2004) 3301–3309.
[284] A. Witkiewicz-Kucharczyk, W. Bal, Damage of zinc fingers in DNA repair proteins, a novel molecular mechanism in carcinogenesis, Toxicol. Lett. 162 (2006) 29–42.
[285] K.-D. Kröncke, L.-O. Klotz, Zinc fingers as biologic redox switches? Antioxid. Redox Signal. 11 (2009) 1015–1027.
[286] A. Hartwig, Zinc finger proteins as potential targets for toxic metal ions: Differential effects on structure and function, Antioxid. Redox Signal. 3 (2001) 625–634.
[287] B.A. Krizek, J.M. Berg, Complexes of zinc finger peptides with Ni^{2+} and Fe^{2+}, Inorg. Chem. 31 (1992) 2984–2986.
[288] M.C. Posewitz, D.E. Wilcox, Properties of the Sp1 zinc finger 3 peptide: Coordination chemistry, redox reactions, and metal binding competition with metallothionein, Chem. Res. Toxicol. 8 (1995) 1020–1028.

[289] G.S. Makowski, F.W. Sunderman, Jr, The interactions of zinc, nickel and cadmium with Xenopus transcription factor IIIA, assessed by equilibrium dialysis, J. Inorg. Biochem. 48 (1992) 107–119.
[290] G.S. Makowski, S.-M. Lin, S.M. Brennan, H.M. Smilowitz, S.M. Hopfer, F.W. Sunderman, Jr, Detection of two Zn-finger proteins of Xenopus laevis, TFIIIA, and p43, by probing western blots of ovary cytosol with $^{65}Zn^{2+}$, $^{63}Ni^{2+}$, or $^{109}Cd^{2+}$, Biol. Trace Elem. Res. 29 (1991) 93–109.
[291] B.A. Krizek, D.L. Merkle, J.M. Berg, Ligand variation and metal ion binding specificity in zinc finger peptides, Inorg. Chem. 32 (1993) 937–940.
[292] D. Krepkiy, F.H. Försterling, D.H. Petering, Interaction of Cd^{2+} with Zn finger of transcription factor IIIA: Structures and binding to cognate DNA, Chem. Res. Toxicol. 17 (2004) 863–870.
[293] M. Huang, D. Krepkiy, W. Hu, D.H. Petering, Zn-, Cd-, and Pb-transcription factor IIIA: Properties, DNA binding and comparison with TFIIIA-finger 3 metal complexes, J. Inorg. Biochem. 98 (2004) 775–785.
[294] E. Kopera, T. Schwerdtle, A. Hartwig, W. Bal, Co(II) and Cd(II) substitute for Zn (II) in the zinc finger derived from the DNA repair protein XPA, demonstrating a variety of potential mechanisms of toxicity, Chem. Res. Toxicol. 17 (2004) 1452–1458.
[295] G.W. Buchko, N.J. Hess, M.A. Kennedy, Human nucleotide excision repair protein XPA: Summary of EXAFS studies on the Zn(II), Co(II) and Cd(II) associated minimal DNA-binding domain, Protein Pept. Lett. 7 (2000) 49–56.
[296] G.W. Buchko, N.J. Hess, M.A. Kennedy, Cadmium mutagenicity and human nucleotide excision repair protein XPA: CD, EXAFS and 1H/15N-NMR spectroscopic studies on the zinc(II)- and cadmium(II)-associated minimal DNA-binding domain (M98-F219), Carcinogenesis 21 (2000) 1051–1057.
[297] P.F. Predki, B. Sarkar, Effect of replacement of "zinc finger" zinc on estrogen receptor DNA interactions, J. Biol. Chem. 267 (1992) 5842–5846.
[298] L. Nagy, J.W.R. Schwabe, Mechanism of the nuclear receptor molecular switch, Trends Biochem. Sci. 29 (2004) 317–324.
[299] M.B. Martin, R. Reiter, T. Pham, Y.R. Avellanet, J. Camara, M. Lahm., E. Pentecost, K. Pratap, B.A. Gilmore, S. Diverkar, R.S. Dagata, J.L. Bull, A. Stoica, Estrogen-like activity of metals in Mcf-7 breast cancer cells, Endocrinology 144 (2003) 2425–2436.
[300] A. Stoica, B.S. Katzenellenbogen, M.B. Martin, Activation of estrogen receptor α by the heavy metal cadmium, Mol. Endocrinol. 14 (2000) 545–553.
[301] V.J. Nesatyy, B.V. Rutishauser, R.I. Eggen, M.J. Suter, Identification of the estrogen receptor Cd-binding sites by chemical modification, Analyst 130 (2005) 1087–1097.

CHAPTER 4

FATE OF DNA SUGAR RADICALS

Amanda C. Bryant-Friedrich*

Contents

1. INTRODUCTION

Oxidative damage to nucleic acids occurs at the nucleobase and at the sugar-phosphate backbone. While base damage dominates in frequency, the attack of oxidants at sugars in the nucleic acid backbone often leads to strand breaks which ultimately leave gaps or nicks that carry modified or

Department of Medicinal and Biological Chemistry, College of Pharmacy, University of Toledo, Toledo, OH, USA

* Corresponding author. Tel.:419-530-1940
Email address: abryant9@utnet.utoledo.edu

Advances in Molecular Toxicology, Volume 4
ISSN 1872-0854, DOI 10.1016/S1872-0854(10)04004-X

"dirty" ends. When the damage is focused on the 2′-deoxyribose component of DNA, hydrogen atoms are abstracted from one of the five unique carbons of the pentose ring to deliver a highly reactive radical intermediate. Due to the fact that each radical is chemically unique, the majority of degradation products formed from each intermediate are characteristic of the radical that preceded it [1–3] (Figure 1). The level of oxygen present, the amount of reducing equivalents available, and the extracellular pH all influence the nature and distribution of products formed [4]. These parameters must all be taken into consideration when the outcome of *in vivo* oxidative damage to DNA is to be predicted.

Another important factor, which should be considered when attempting to make such predictions, is the identity of the oxidant. One of the most significant species to consider when discussing DNA oxidants is the hydroxyl radical. This reactive oxygen species is produced endogenously through cellular metabolism, at higher levels under conditions of oxidative stress, as a part of chronic inflammation and as a major outcome of the exposure of cells to ionizing radiation. The hydroxyl radical is small, highly diffusible, extremely reactive, and capable of hydrogen atom abstraction at any position of 2′-deoxyribose. When it has completed this task, it loses its oxidizing abilities. Other entities of significance to toxicology that participate in nucleic acid oxidation are much more complex and may have the capacity to carry out other reactions with DNA radicals in addition to oxidation. These include, but are not limited to, pharmaceutical agents and environmental toxins. Many of these compounds are not rendered inactive through reduction and have the ability to participate in oxidation, conjugation, or electron transfer processes with radical intermediates. These conversions can influence the ultimate fate of the initially formed sugar radical in DNA.

It is clear however that irrespective of the oxidant, the initial reactive intermediate formed upon abstraction of a hydrogen atom from the 2′-deoxyribose moiety of a nucleotide is a sugar radical. From a chemical perspective, these are all carbon-centered radicals whose reactivity is highly influenced by, among other factors, α- and β-substitution. The C1′-radical (**1**) is a *N*-glycosyl radical whose reactivity may be sequence dependent due to its direct attachment to the nucleobase; however, this has yet to be fully demonstrated. The C2′- and C4′-radicals (**2**, **4**) are both β-phosphatoxyalkyl species, one of which (**4**) has been demonstrated to easily undergo β-elimination leading to prompt strand breaks [5]. Radical **4** is chemically distinct from the analogous C2′-radical (**2**) due to the fact that it is also an α-oxy radical whereas the C2′-radical is not α-oxy but β-glycosidic. The remaining reactive intermediates, the C3′- and C5′-radicals (**3**, **5**), are both α-phosphatoxyalkyl radicals with **3** being tertiary and **5** being secondary and in very close proximity to the nucleobase. Even though each of the 2′-deoxyribose radicals in DNA is

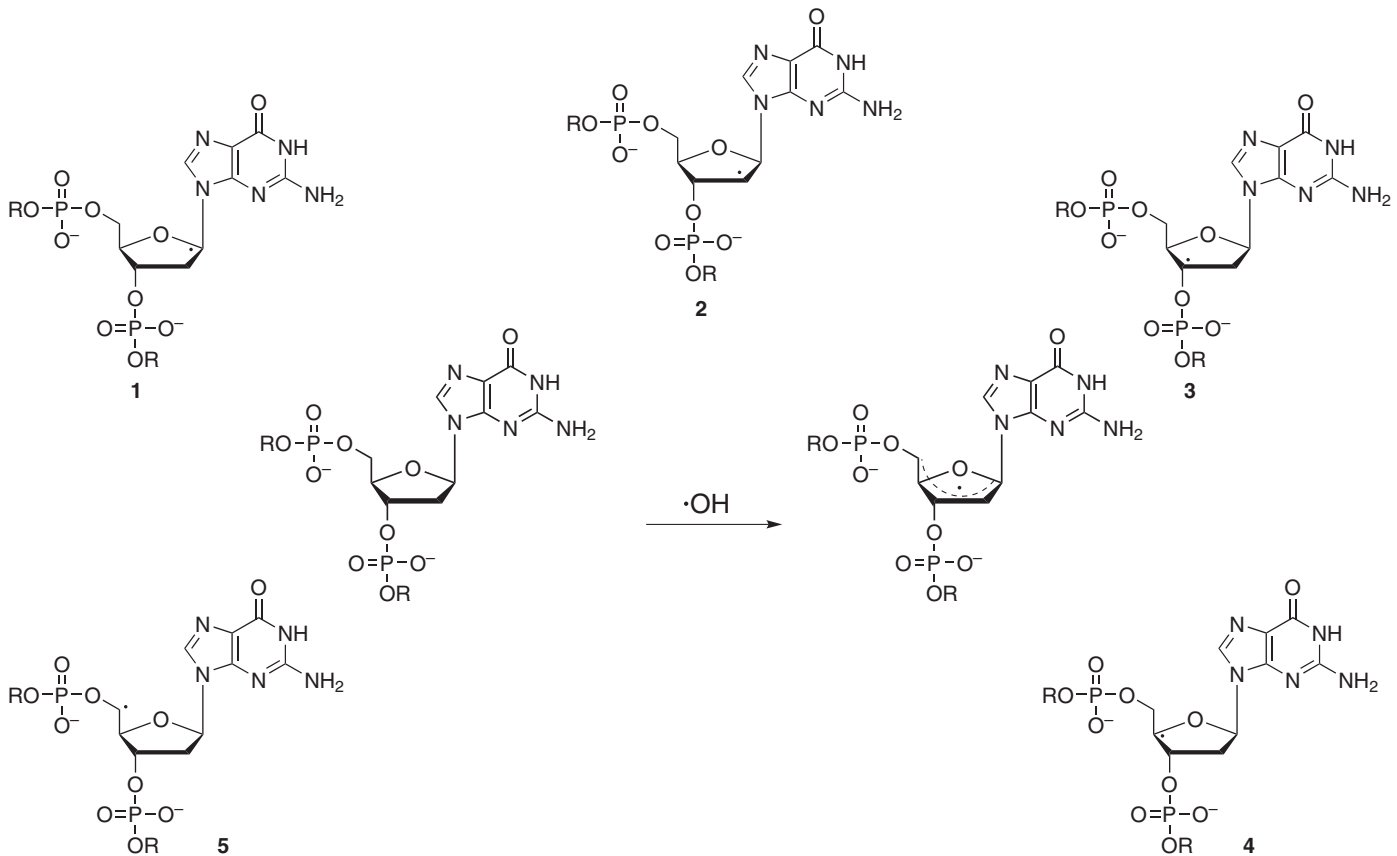

Figure 1 2′-Deoxyribose radicals in DNA.

chemically distinct, some generalities remain as follows: (1) In the absence of oxygen or at very low oxygen concentrations, the initially formed radicals are subject to reduction by cellular thiols. (2) Each of these radicals reacts with oxygen at or near diffusion-controlled rates delivering peroxyl radicals, which are also subject to reduction by the same cellular thiols.

Extensive studies have been performed that have significantly increased our understanding of the mechanism and fate of the oxidative damage of nucleic acids. The majority of these studies have employed systems which photochemically generate radical intermediates, site specifically, in nucleic acids at defined locations, making the determination of the fate of the radical intermediate less ambiguous [6,7]. These systems revealed their value in the elucidation of oxidative mechanisms in simple DNA systems and DNA–protein complexes [8]. This is significant considering the fact that oxidative damage to DNA, within cells, occurs when proteins are attempting to protect DNA from mechanical and chemical assault or carrying out their duties during replication, transcription, repair, etc. In any case, proteins are in close proximity, altering the structure of DNA frequently and its environment dramatically. Alterations in DNA structure can lead to intramolecular hydrogen atom abstraction events and the formation of DNA damage products not seen in normal B-form DNA [9]. In addition, the ability of oxygen to reach radical sites may be limited, making aerobic degradation a less likely pathway. The same may be true of reducing equivalents that are not found within the bound protein. These factors can significantly alter the mechanism and fate of oxidative damage in DNA as compared to that found in the noncomplexed nucleic acid.

Another factor, which may significantly alter the outcome of oxidative damage mechanisms, is the cellular environment in which the sugar radical is formed. When DNA is present at sites of disease such as in the tumor microenvironment, normal physiological conditions can be significantly altered. It has long been known that in the tumor microenvironment, the availability of oxygen and reducing equivalents is cyclic and the pH of the extracellular compartment is low [10]. As mentioned above, sugar radicals react with oxygen, when available, to deliver peroxyl radicals, which undergo reaction with reducing agents. When reducing equivalents are not in abundance, peroxyl radicals can find other sources of hydrogen atoms through intra- or interstrand hydrogen atom abstraction in DNA or the release of superoxide. When hydroperoxides are produced, they may participate in rearrangements or degradation pathways, which are strongly dependent upon pH. The outcome of these rearrangements is the formation of strand breaks, which form nicks or gaps in DNA, which in turn possess modified ends. These modified ends may be released as small molecules if not repaired. The genotoxicity of oxidative damage depends to some degree on the reactivity of these small molecules. Their reactivity toward the nucleobases of DNA can cause the formation of DNA adducts which may be mutagenic.

2. The C1′-Radical

The C1′-radical (**1**) is an *N*-glycosyl radical that is trapped by a hydrogen atom from one of two faces of the sugar to deliver the distinctly different isomeric nucleosides **6** and **7**. When reduction by thiols occurs from the α-face, repair of the initially formed radical delivers the β-nucleoside **6**. Repair from the β-face leads to "pseudorepair" and formation of α-nucleoside **7** (Scheme 1).

When DNA was exposed to gamma radiation under anoxic conditions, α-adenosine was determined to be a primary damage product [11]. In ssDNA and dsDNA of the same sequence, Greenberg *et al.* demonstrated through the site-specific generation of 2-deoxyuridin-1-yl (**1**), using a photocleavable radical precursor that both α- and β-2-deoxyuridine derivatives are obtained upon reduction with β-mercaptoethanol (BME), with the natural nucleoside dominating (4:1 ssDNA, 6:1 dsDNA, and 3:2 in the monomer) [12]. With rates of trapping of $\sim 1.8 \pm 0.6 \times 10^6$ M^{-1} s^{-1} in dsDNA and $< 4 \times 10^6$ M^{-1} s^{-1} in ssDNA, this reduction, which leads to chemical repair as well as a premutagenic lesion, can compete with oxygen trapping.

In addition to reduction products, the C1′-radical, under anaerobic conditions, is also responsible for the creation of small amounts of the 2-deoxyribonolactone lesion (**9**, Scheme 2). This lesion, which is the hallmark of C1′-oxidation, is produced in greater abundance in the presence of oxygen [13,14]. Various aspects of the generation and fate of **1** have been extensively reviewed elsewhere and will not be covered here [5,6]; however, a few points are relevant to this review. One significant point about **1** that makes it different from several of the other sugar radicals is the reactivity of the hydroperoxide formed upon oxygen trapping. Through competition experiments it was determined that peroxyl radical **14** undergoes release of superoxide at a rate that inhibits the formation of the corresponding hydroperoxide. Upon the release of superoxide from **14**,

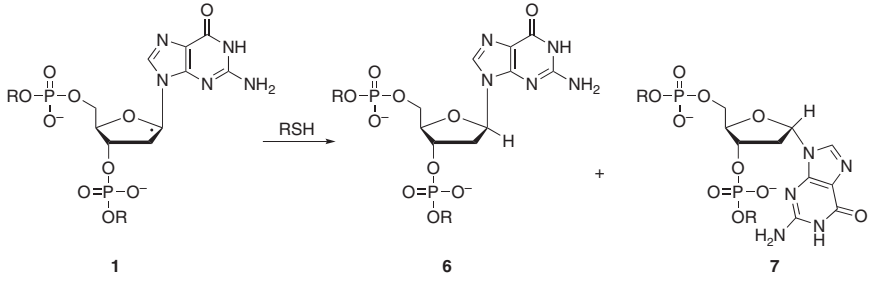

Scheme 1

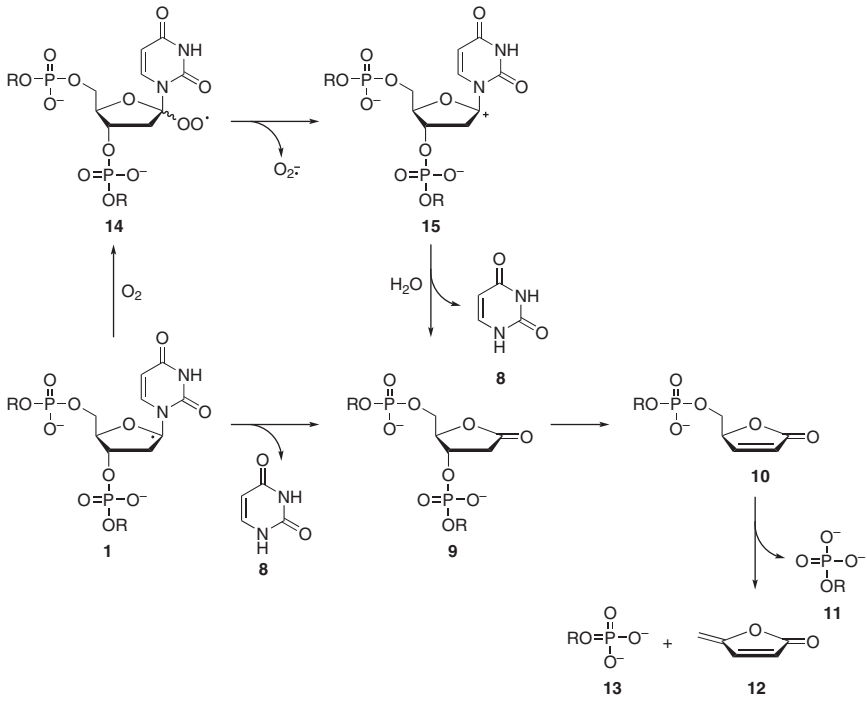

Scheme 2

a carbocation forms, which subsequently reacts with surrounding water to deliver ribonolactone **9** [15]. Under physiological conditions of temperature and pH, **9** has a half-life of ~20 h in ssDNA and 32–54 h in dsDNA depending upon the opposing base [16]. This makes the formation of strand breaks resulting from the ribonolactone lesion a very slow process. In cases where enzymatic repair is hindered, strand breaks may occur through β-elimination producing a Michael acceptor, which is in turn reactive toward nitrogen and sulfur nucleophiles [15,17]. Lesion **10** can undergo a second elimination which releases a small sugar-derived fragment, 5-methylene-2-furanone (**12**). This small molecule is a strong electrophile, which has the capacity to react with a variety of cellular nucleophiles.

3. The C2′-Radical

C2′-oxidation occurs through the abstraction of either the 2′α- or β-H of a 2′-deoxyribose moiety in DNA. Radical intermediate **2** has been generated by γ-radiolysis of DNA [18] and through the abstraction of

either of the 2′-hydrogens by the photochemically generated 5-uridinyl radical [8]. As this reactive intermediate is a β-phosphatoxyalkyl radical, it is expected that rapid β-phosphate elimination occurs under anoxic conditions to deliver a highly reactive radical cation that participates in electron transfer processes. To date this aspect of the reactivity of the C2′-radical has not been fully validated. Reduction of **2** by cellular thiols from either face of the nucleoside delivers the same substrate, so issues of stereochemical scrambling do not exist with this reactive intermediate.

Through trapping of the C2′-radical with oxygen, isomeric α,β-2′-peroxyl radicals are formed (Scheme 3). The ratio of these radicals and/or their degradation products is strongly influenced by the geometry of the sugar at the time of radical generation. This has been proven by analysis of the decomposition products observed to result from **2** when it is formed under conditions that promote the stabilization of DNA in different conformations [8]. For example, as noted in Scheme 3, when **2** is generated in Z-form DNA, the primary product is ribonucleotide **17** [19,20]. When the same radical is generated in B-form DNA, the major products of degradation are formed through base release, with concomitant formation of an erythrose abasic site **18**. Lesion **18** is stable with a half-life of 3 h in 0.1 M NaOH at 37 °C [21].

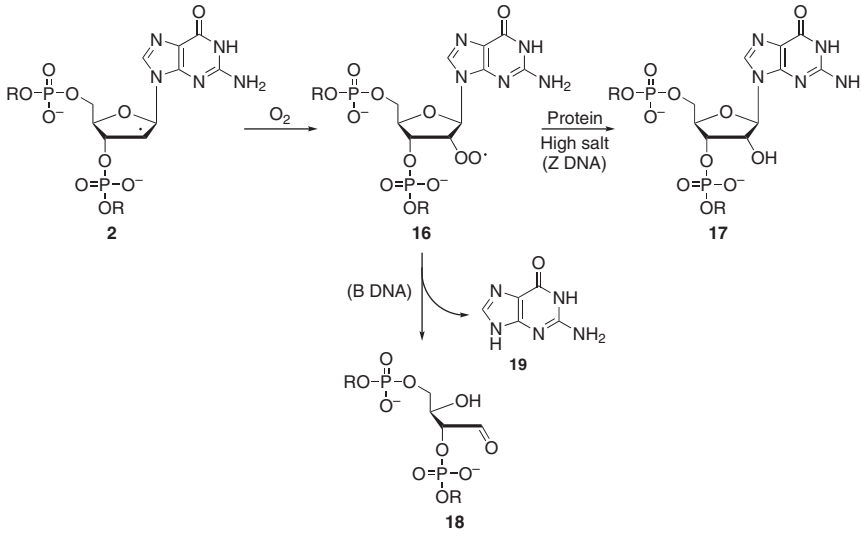

Scheme 3

4. The C3′-Radical

Formal hydrogen atom abstraction at the C3′-carbon of 2′-deoxyribose in DNA produces the α-phosphatoxyalkyl radical **3** (Scheme 4). The decomposition of **3** has been investigated through its site-specific generation using a photocleavable radical precursor [22]. It was determined using this system that when oxygen concentration is low or oxygen is absent altogether, spontaneous strand scission is the result. Barton reported similar results upon the generation of **3**, using Rh-phenanthrenequinone diimine complexes [23,24].

In our laboratory we have shown that in the presence of thiols, strand breaks compete with radical reduction [25], resulting in the chemical repair of the nucleoside delivering the natural 2′-deoxyribose moiety or "pseudorepair" to 2-deoxyxylose containing oligomers. When **3** is generated in the presence of physiological concentrations of glutathione (GSH) [~6 mM], a 1:1 ratio of oligomers **6** and **20** is obtained. DNA oligomers containing 2-deoxyxylose-derived nucleosides have been shown to significantly destabilize DNA duplexes [26] in an additive fashion [27,28].

Under aerobic conditions, trapping of **3** also occurs from both faces of the nucleoside forming isomeric nucleoside peroxyl radicals **21a** and **b** (Scheme 5). We determined, through extensive chromatographic and mass spectral analysis, that the major products observed in the degradation of **3** under aerobic conditions are **13** and **11** [29]. These products are likely the result of the formation and subsequent degradation of 3′-oxonucleoside **23**. In addition to **23**, several other lesions were also observed, which can be traced back to intramolecular hydrogen atom abstraction events at the

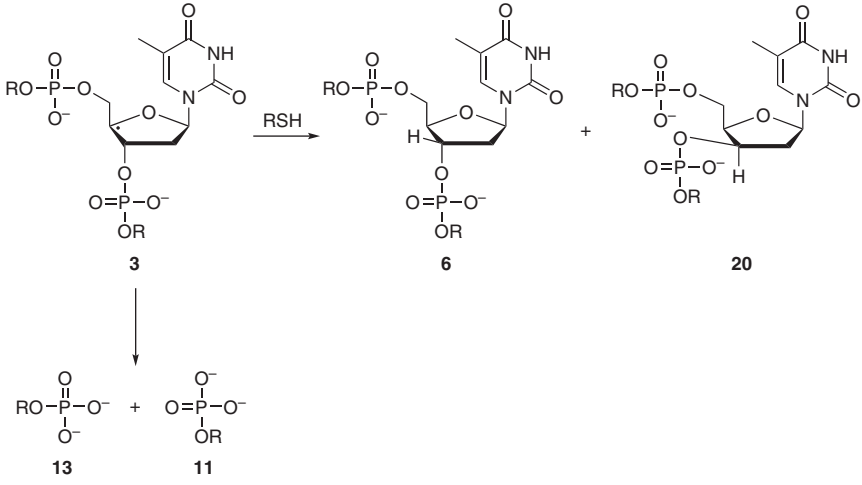

Scheme 4

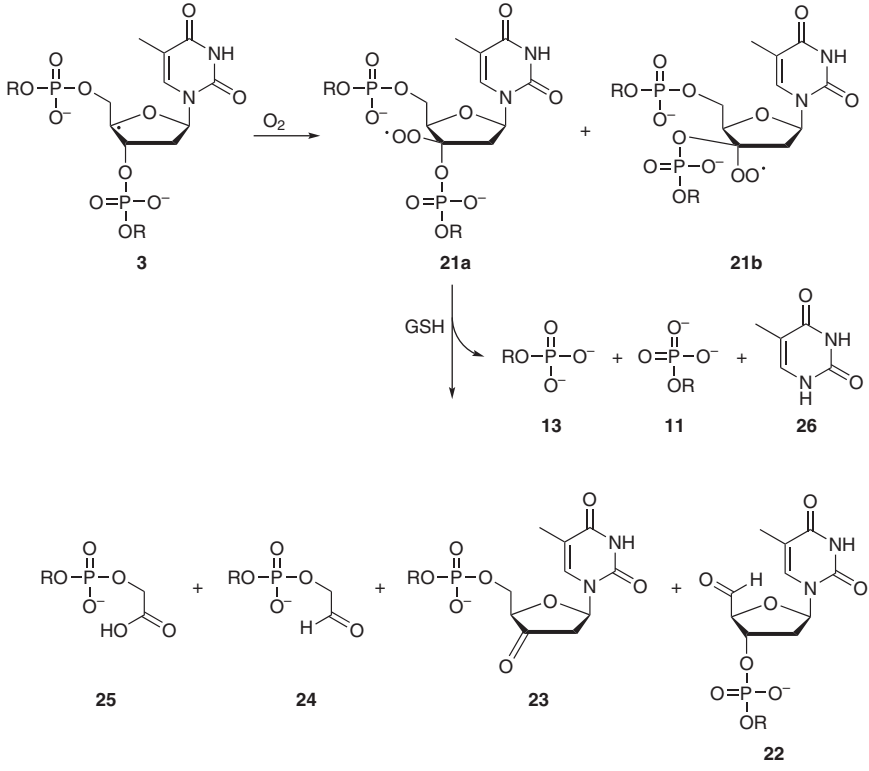

Scheme 5

C4′- and C5′-positions within the same oligonucleotide strand in ssDNA. These outcomes indicate the decreased reactivity of **21a** and **b** toward GSH. Without reduction, the peroxyl radicals can undergo other reactions such as superoxide release or intramolecular hydrogen atom abstraction to produce **22, 23**, and **25**. Compound **24** is the expected product of the aerobic degradation of **3**. Superoxide release from **21a** or **b** would result in cation formation, which upon solvolysis delivers lesion **23**. This is a plausible but yet to be confirmed mechanism for the formation of these products.

5. The C4′-Radical

The C4′-radical is fascinating in that it is β-phosphatoxyalkyl (relative to two phosphate groups). This unique position in the sugar moiety of DNA is reflected in the complexity of its degradation pathway. Under conditions of limited oxygen availability, spontaneous strand breaks occur upon

C4′-oxidation via β-phosphate elimination to generate a highly reactive radical cation (Scheme 6) [30]. Thiol trapping competes with this process to chemically repair/"pseudorepair" the radical, delivering the natural nucleoside **6** and the unnatural 2-deoxy-*R*-L-*threo*-pentofuranosyl nucleoside isomer **27** (Scheme 7) [30]. In ssDNA, chemical repair is nonselective, producing **6** and **27** in equal quantities. When the DNA is double stranded, reduction is much more selective, chemically repairing the radical to its natural state in an 8:1 ratio.

Another lesion which has been shown to form as a result of C4′-oxidation is **30** (Scheme 8). The lesion, a 2-deoxypentos-4-ulose derivative, results from the oxidation of the initially formed radical and ultimately leads to the loss of the nucleobase. The stability of the subsequent lesion was found to be comparatively low having a half-life of 8–26 h at physiological pH and temperature [31,32].

At physiological concentrations of oxygen and reducing equivalents, reduction is only a minor competitor with isomeric peroxyl radical production. These radicals are then converted to hydroperoxides which rearrange to the C4′-associated 3′-phosphoglycolate (3′-PG) residue (**25**) [33] and base propenal (**32**) [34] (Scheme 9). The phosphoglycolate lesion is highly stable and is formed as a result of the oxidation of DNA by ionizing radiation, bleomycin, and peroxynitrite, among others.

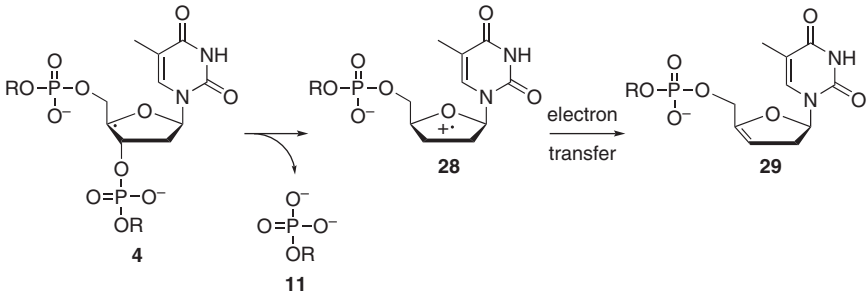

Scheme 6

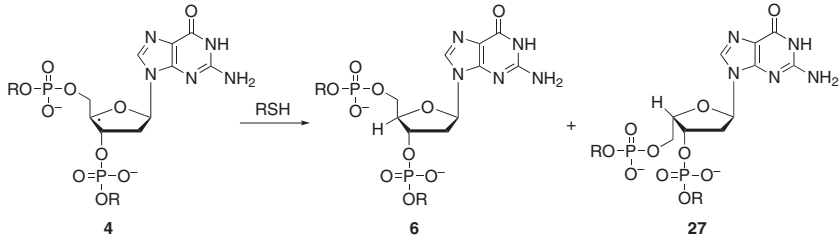

Scheme 7

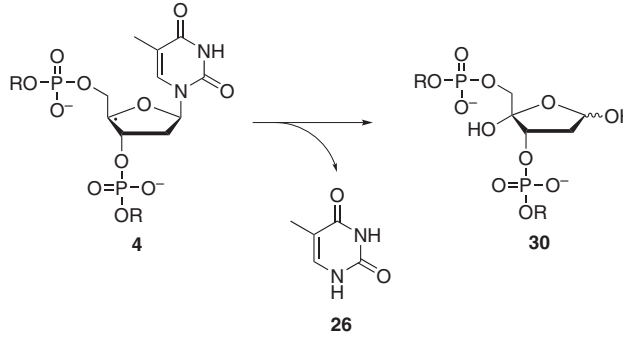

Scheme 8

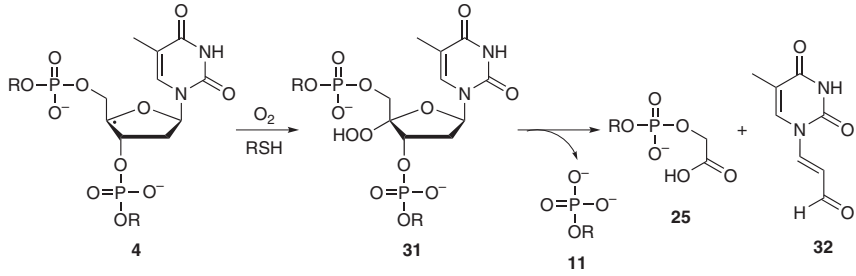

Scheme 9

6. The C5′-Radical

Finally, the position of the C5′-radical (**5**) relative to the nucleobase of DNA renders its reactivity toward the heterocyclic nucleic acid moieties very distinct as compared to the four other positions. When oxygen is low and the number of reducing equivalents is minimal, this radical whether generated from pro-R or pro-S hydrogen atom abstraction results in cyclization at the C8 of purine bases to deliver the bulky cycloA and cycloG adducts (**33** and **34**) shown in Scheme 10 [35]. Due to the formation of two damage sites, that is, at the sugar and the base in the same nucleotide, the formation of **33** and/or **34** in a DNA oligomer is considered to be a tandem lesion. The rate constant for this cyclization has been determined to be 1.0×10^6 and 1.6×10^5, respectively, for dA and dG indicating that trapping by GSH at physiological concentrations likely competes with cyclization. In nucleoside monomers, the rate of trapping of **5** by cysteine and GSH was found to be 2.1×10^7 and 4.9×10^7, respectively [36]. The rate of trapping in DNA oligomers however remains to be evaluated.

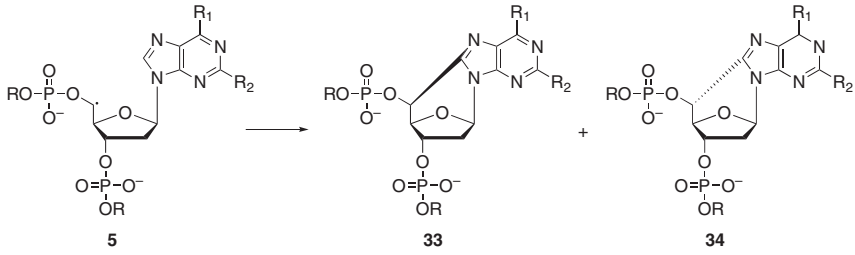

Scheme 10

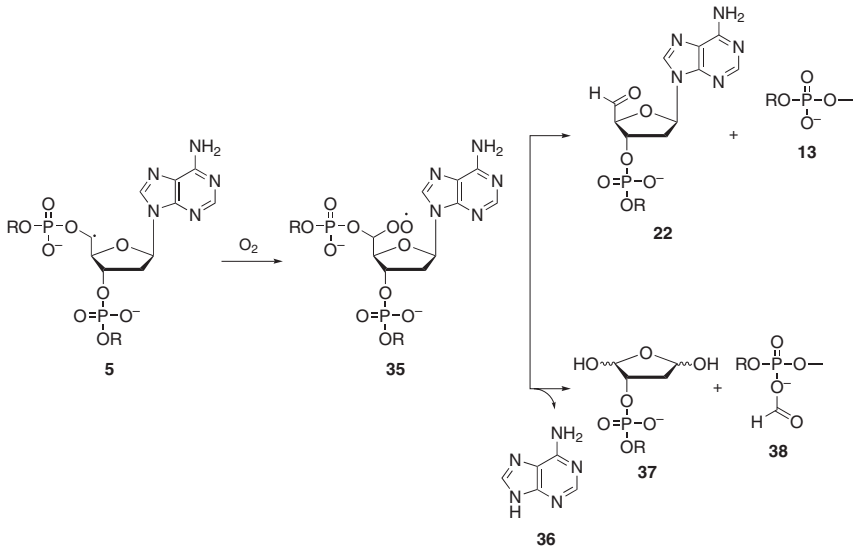

Scheme 11

Reaction of **5** with oxygen, as is the case with all other sugar radicals, is at diffusion-controlled rates ($\sim 2 \times 10^9$). The resulting peroxyl radical (**35**) has been postulated to decompose via two different pathways, delivering either a 5′-aldehyde **22** [37] or a 5′-(2-phosphoryl-1,4-dioxobutane) (**37**) [38,39] residue at the point of radical formation (Scheme 11). In the case of strand breaks, which result in 5′-aldehyde formation, the 5′-oligomer carries a 3′-phosphate (**13**), while 5′-(2-phosphoryl-1,4-dioxobutane) (**37**)-associated breaks carry a formyl modification (**38**) on the 5′-oligomer. These differences in product distribution often depend upon the nature of the oxidant. For example, it has been observed that in the presence of manganese porphyrin compounds [1] (oligonucleotides) under anaerobic

conditions, the production of the aldehyde lesion predominates. Also, in the presence of oxygen, the 5′-aldehyde is the predominant lesion [1].

Oxidative damage of DNA involves a highly complex set of events, which only begins with the attack of a reactive oxidant. When the 2-deoxy-ribose moieties of DNA are the target of cellular oxidants, sugar radicals are formed which undergo chemical "repair/isomerization" with cellular thiols or react with oxygen. When the latter ensues, lesions result in the form of base loss or formation of gaps and nicks, which are associated with modified ends that may or may not be repaired within the time span of their lifetimes. Even when strand breaks do not result, these lesions can cause distortion in the DNA helix. A great deal of the biological effects observed as a result of lesion formation such as the inhibition of gene expression, interference with transcription and mutagenesis can be related to this feature. In the next sections we will explore the consequences of sugar-derived oxidatively generated DNA lesions.

7. The Fate of Anaerobic Radical Damage Products

Normal human cells experience oxygen levels at or near arterial levels (~100 mm Hg) to average tissue levels (~40 mm Hg). In the microenvironment of a tumor, this can change drastically dropping to anoxic levels (<0.1% O_2) [40]. In such situations, anaerobic damage pathways dominate due to the lack of available oxygen for radical trapping. In addition, this hypoxic environment is also believed to make changes in the proteome, which lead to elevated levels of H-donors in the form of GSH and protein thiols. It is under these conditions that the substrates in Figure 2 are likely to form.

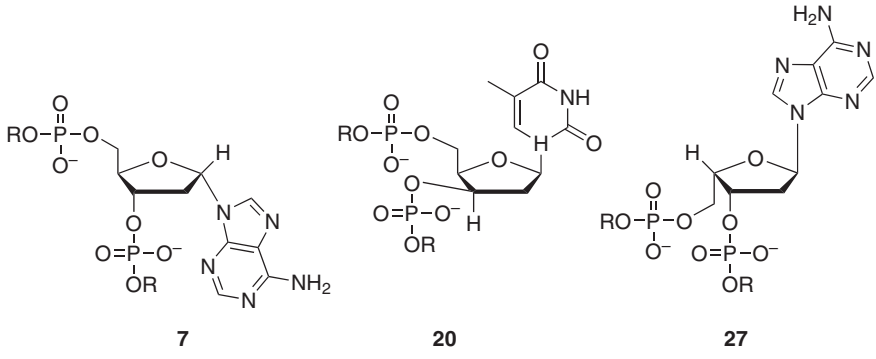

Figure 2 "Inverted" nucleic acids in DNA.

8. "Inverted" Nucleic Acids

α-Deoxyribonucleotides have not been extensively studied with the exception of α-adenosine. As mentioned above, when DNA was exposed to gamma radiation under anoxic conditions, α-2-deoxyadenosine was determined to be a primary damage product. This modified nucleoside was also found to be promutagenic [41]. Oligomers containing **7** block replication moderately and generate single nucleotide deletions *in vivo*. In addition to the incorporation of the correct nucleoside opposite the lesion, dC and dA are also incorporated [42]. In M13 vectors, exclusively single nucleotide deletions are observed [43]. α-2-Deoxyadenosine is repaired by the nucleotide excision repair pathway and found not to be a substrate for base excision repair glycosylases [44–46]. Human Ape1 incises duplex DNA at both α-dA and α-dT in a glycosylase independent manner, creating a nick at the 5′-side of the base leaving proper ends for DNA synthesis, a 3′-hydroxyl and a 5′-phosphate terminus.

The formation of α-deoxynucleosides is strongly dependent upon the existence of hypoxic conditions. It has been postulated that the confinement of oxidative metabolism to the mitochondria of eukaryotic cells [47,48], along with the presence of a repair pathway for α-nucleosides, indicates a possible biological significance of these lesions. The structural consequences of the formation of **7** and related substrates have been evaluated through thermal denaturation [49] and NMR solution studies [50]. In 9-mer duplexes it was determined that inversion of configuration at the glycosidic carbon of a single dA does not disturb stacking of the nucleobase in the DNA helix or pairing with the conical T. This stability appears to be sequence dependent, however, as decamer duplexes containing α-dA exhibited slightly lower stability [48]. NMR studies reveal the presence of a wide minor groove in duplexes containing α-dA similar to that seen in duplexes containing abasic residues [51,52]. As these lesions are recognized and repaired by human Ape1, the same enzyme responsible for the repair of abasic sites, it is believed that this structural feature plays a role in damage recognition of α-nucleosides.

Nucleic acids with inversion of configuration at the C3′- and C4′-positions have received limited attention. The majority of the investigations into **20** (Scheme 4) have centered on the change in sugar pucker exerted on the nucleoside by the altered configuration at C3′. This altered configuration was considered advantageous for use of these substrates in antisense technology [53]. It has been determined by several groups through thermal denaturation experiments that the incorporation of a single xylo nucleoside (e.g., **20**) into a DNA duplex has a significant destabilizing effect [26–28]. The reduction product of the 4'-radical, a threo nucleic acid, **27** (Scheme 6), was shown to transiently block DNA pol I (Klenow fragment) on

damaged templates [54]. Stereochemical inversion at the 4′-position of the sugar did not impair base pairing; however, polymerization was still interrupted. These studies indicate that backbone distortions created by such conformation changes may have an effect on DNA replication. Studies remain to be performed to determine the level of occurrence of all three of these lesions under physiological conditions.

9. 8,5-Cyclopurine-2-Deoxynucleosides

An excellent review by Dizdaroglu appeared recently concerning the formation and repair of 8,5-cyclopurine-2-deoxynucleosides [35]. Several of these damage lesions were found to form in cells exposed to ionizing radiation [55] as well as in the DNA of primary keratinocytes and fibroblasts obtained from XP complementation group C (XP-C) patients, who have been exposed to low doses of ionizing radiation [56]. In addition, the S isomer of 8,5-cyclo-2-deoxyadenosine (**33**) was found to be significantly elevated in the stroma of women, between the ages of 32–46, whose incidence of breast cancer is significantly higher. The presence of cyclopurine lesions in diseases in which cancer incidence is higher indicates its role in mutagenesis and carcinogenesis. These lesions are repaired by the nucleotide excision repair pathway; however, when this fails, their accumulation leads to transcriptional mutagenesis and carcinogenesis. Lesion **33** was found to block transcription and DNA polymerases including the bypass polymerase η [35]. As is the case with the "inverted" nucleosides discussed above, lesions **33** and **34** have an excessively distorting effect on the structure of the DNA helix. Local distortion is seen at **33** and **34**, with increased bond lengths from C2′ to C5′ due to the formation of the covalent bond between the sugar and the base [57]. This causes the sugar pucker and the bond angles at this nucleoside to diverge significantly from those of a normal 2-deoxyadenosine [58]. The required rotation of the base around the *N*-glycosidic bond to form the covalent bond with the C5′ weakens hydrogen bonding at the adenosine causing helix distortion [59]. This combination of structural abnormalities can have a significant impact on the processing of these lesions [60].

10. The Fate of Aerobic Damage Products

When sugar radicals are generated in DNA, without the interception of reducing agents, the result is often a single-strand break. In the presence of oxygen, nucleic acid peroxyl radicals result. It is the fate of these peroxyl radicals that becomes of interest when investigating the toxic outcomes of

oxidative damage to DNA under aerobic conditions. It has been shown that, at least in the case of the C1′-[14] and likely the C3′-peroxyl radicals [29], superoxide is released to generate a carbocation, which dictates some of the products derived from the original radical. Due to the high reactivity of peroxyl radicals, transfer of damage to the bases or other sugars within close proximity in the same nucleic acid strand through hydrogen atom abstraction is also observed causing tandem and cluster lesion formation. This type of damage is believed to be particularly difficult for DNA repair systems to reverse [61,62]. Radical degradation usually occurs with base loss and is often accompanied with strand cleavage. When strand breaks occur, oligonucleotide fragments are produced which are terminated with small highly oxygenated and often electrophilic fragments. These breaks form at high rates or very slowly depending upon the originating radical. We will look at the fate of the lesions, which are formed upon aerobic degradation of sugar radicals.

10.1. Strand breaks

When the sugar moiety of DNA degrades via a peroxyl radical, oxygen atoms are incorporated either from molecular oxygen found in the cell or from water molecules found in the aqueous environment. This leads normally to the formation of modified end groups that are electrophilic. These lesions are usually part of nicks in the nucleic acid strand because the original sugar is not completely degraded and the phosphate group of either one or both unmodified nucleotides at the damage site is maintained. From the point of view of repair, this is a rather complicated single-strand break to repair, depending upon the modifying group. These chemically diverse functional groups block the work of DNA polymerases and ligases as these enzymes require a 5′-phosphate and a 3′-hydroxyl functionality for gap filling and ligation. Due to their electrophilic nature, they can react with the side chains of amino acids or nucleobases to form protein–DNA or DNA–DNA cross-links. If repair is slow or inefficient, several of these lesions can also hydrolyze, delivering small electrophilic sugar fragments which themselves react with the nucleobases and side chains of amino acids. The consequences of formation of several of these fragments will be discussed below.

11. 3′-Phosphate (3′-P)

Many agents, which oxidatively damage DNA, generate breaks in the nucleic acid strand leaving behind phosphate groups on both the 3′- and 5′-oligomers. As mentioned above, the removal of the 3′-phosphate is required for repair of the strand break while the 5′-phosphate is needed by ligases. Cells conveniently possess an enzyme, which has 3′-phosphatase activity to remove the 3′-phosphate group and convert it to the required

3′-hydroxyl terminus. This enzyme, in humans, polynucleotide kinase (hPNK), also possesses 5′-kinase activity to facilitate the introduction of a 5′-phosphate moiety at DNA strand breaks when it is required for repair [63]. Interestingly, many damaging agents as well as repair pathways involved in the formation of breaks with 3′-phosphate termini; therefore, PNKs become a vital part of the repair of single-strand breaks in DNA.

12. 3′-Phosphoglycolaldehyde

The complex mixture of oxidation products generated through 3′-oxidation under aerobic conditions in ssDNA is not unique. Many of the reactive intermediates formed during the process of oxidative damage degrade via several pathways leading to several modified oligonucleotide products, nucleobases, and sugar fragments. The C3′-radical is a key example. One of the products derived through this process is 3′-phosphoglycolaldehyde (3′-PGA). Due to the complex mixture of products obtained from this radical species, it cannot be stated with certainty; however mechanistically, it can be assumed that a gap is created upon 3′-PGA formation accompanied by a 5′-phosphate residue. To date there have been no systematic studies reported on the repair of **24** in human systems. Demple and coworkers used the 3′-PGA fragment as a model system to determine the enzymes in yeast [64] and *Escherichia coli* [65] responsible for the removal of modified end groups such as **24** and **25** (see below). The same synthetically obtained oligonucleotides were used for the identification of 3′-esterases in human cells [66]. Two class II AP endonucleases and repair diesterases were determined to convert these 3′-PGA-containing oligomers to 3′-OH-terminated oligonucleotides. These are class II AP endonucleases, endonuclease IV from *E. coli* and Apn1 from *Saccharomyces Cerevisiae*, and exonuclease III from *E. coli* and Apn2 from *S. cerevisiae* as well as Ape1 from humans. Ape1 has, however, a very low level of 3′-phosphatase activity.

In the purification of human Ape1 from HeLa cells, Demple *et al.* used the above assay to determine enzyme activity by monitoring the release of radioactively labeled 2-phosphoglycolaldehyde [67]. Interestingly, over a decade later Dedon and coworkers determined that 2-phosphoglycolaldehyde (**39**) reacts with dG and DNA to form the diastereomeric 1,N^2-glyoxal adducts of dG, 3-(2-deoxy-β-D-*erythro*-pentofuransyl)-6,7-dihydro-6,7-dihydroxyimidazo-[1,2-*a*]purine-9(3H)-one (**41**) [68] (Scheme 12). This DNA adduct is also a product of the direct action of the known mutagen glyoxal [69,70]. The reaction was determined to occur much slower than that of dG with glyoxal; however, it is not clear if changes in cellular conditions such as those found in the tumor microenvironment may change this reactivity. Through sensitive and specific analytical techniques, Dedon *et al.* were able to detect the formation of **39** in isolated DNA and cells exposed to ionizing radiation [71,72].

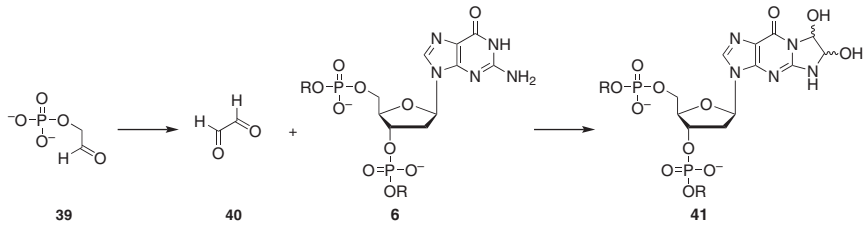

39 40 6 41

Scheme 12

13. 3′-Phosphoglycolate

When a single nucleotide gap is created in a DNA strand upon C4′-oxidation under aerobic conditions through ionizing radiation or the action of one of several pharmaceutical agents, it carries a 3′-PG end group (**25**) and a 5′-phosphate residue. The 5′-residue is required for further processing by polymerases and ligases; however, the 3′-PG residue must be trimmed to give the necessary 3′-hydroxyl. This can be accomplished by the base excision repair (BER) enzyme APE-1 at single-strand breaks [73,74]; more recently, it was also reported that this lesion can be processed by the single strand break (SSB) repair enzyme aprataxin [75]. 3′-PG at double-strand breaks has been discovered to present a much more complex picture. Because 3′-PG has been found to be a primary lesion formed in cells exposed to ionizing radiation, it is logical to assume that it will be formed at sites of double-strand breaks and complex lesions. In addition, the formation of 3′-PG as a product of the highly complex mixture of 3′-oxidation products makes the elucidation of its repair outside simple strand breaks important. Enzymes outside BER have been identified to process **25** in several cases of double-strand breaks; however, the nature of the break and sequence context appear to have quite an effect on lesion repair. The enzymes that have been identified to be involved are human tyrosyl-DNA phosphodiesterase (hTdp1) [76] and Artemis nuclease along with DNA-dependent protein kinase [77]. There is no true consensus on the mechanism of repair of this lesion and further studies are warranted.

14. 3′-Ketone

The 3′-keto- or 3′-oxo-nucleoside-terminated oligomer **23** is one component of the complex mixture of damage fragments generated upon 3′-oxidation under aerobic conditions in ssDNA (Scheme 13). Preliminary

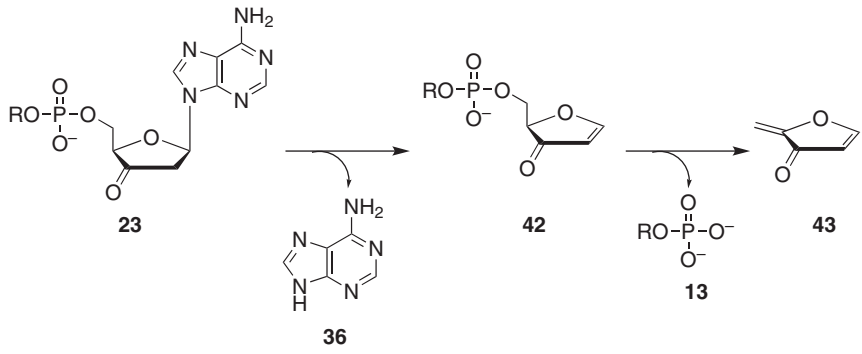

Scheme 13

results from our laboratory indicate, just as proposed by Stubbe several decades ago [78], that this compound is also the determining intermediate in the anaerobic degradation of the 3′-radical. In addition to the formation of **23** as the direct result of 3′-oxidation, both the Sugiyama and Greenberg groups have observed this labile fragment as the result of 5-uridinyl radical formation [79,80]. Work of Sugiyama indicates that **23** is relatively unstable in water at 0 °C with a half-life of 48 h. This suggests that under physiological conditions of pH and temperature, the lesion is expected to possess considerable instability. Lesion **23** decomposes by the elimination of the nucleobase to deliver unsaturated ketone **42**, which undergoes a second elimination of a 3′-phosphate to yield furanone **43**. There have been no studies on the repair of this lesion either *in vivo* or *in vitro*.

15. 5′-Aldehyde

The 5′-aldehyde (5′A), produced by 5′-oxidation under aerobic conditions, represents a strand break, which does not carry a 5′-phosphate; however the nucleobase remains intact. To the knowledge of the author, the repair pathway of **22** is not known. It has been demonstrated that **22** degrades through liberation of a 5′-phosphorylated oligomer (**11**) to give an unsaturated substrate (**44**), which undergoes aromatization via base elimination to form furfural [81,82] (**45**, Scheme 14). It has been further shown that **45** reacts with adenine residues in DNA to generate the N^6-furfuryladenine adduct [83]. This adduct undergoes deglycosidation to deliver an abasic site (**46**) and kinetin (**47**) (Scheme 15). Compound **47** is an experimental chemotherapeutic as well as a kinase inhibitor and induces redifferentiation in human leukemia cells [84].

The 5′-(2-phosphoryl-1,4-dioxobutane) lesion, which is also a product of 5′-oxidation, is a biselectrophile that was shown through independent

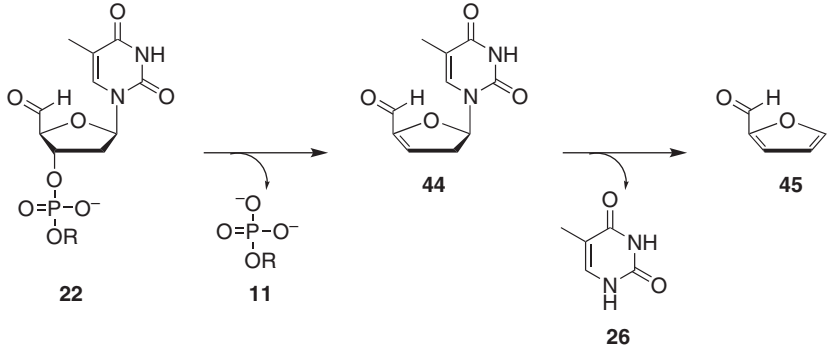

Scheme 14

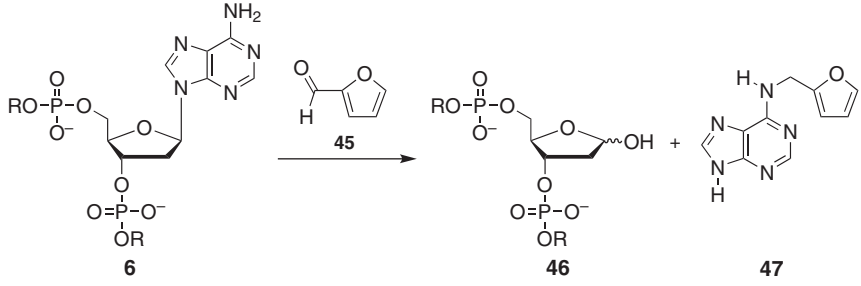

Scheme 15

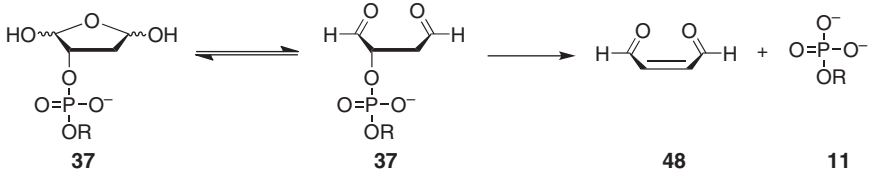

Scheme 16

generation of the lesion via photochemical means to form DNA–DNA cross-links [85]. Two structures in equilibrium constitute the lesion, a cyclic and an open chain form, and can undergo β-elimination of a 5′-phosphorylated oligomer to give cis-2-butene-1,4-dial (**48**), a known metabolite of furan (Scheme 16) [86]. This metabolite also forms adducts with DNA bases offering another avenue of endogenous oxidative damage.

16. Oxidatively Generated Abasic Lesions

Several degradation pathways of sugar radicals in DNA do not lead to prompt strand breaks. Instead, the lesions that are generated constitute relatively stable oligonucleotides, which are devoid of the respective nucleobases due to base elimination. These lesions include the ribonolactone lesion **9**, the erythrose abasic site **18**, and the 2-deoxypentos-4-ulose abasic site **30** (Figure 3). Due to the extensive coverage of the consequences of the formation of **9** in other reviews, it will not be discussed here [5,6]. The erythrose abasic site **18** was described by the Greenberg group to observe the "A-rule" in primer extension studies, showing preference for insertion of dA opposite the damage lesion when the Klenow fragment is employed [87]. These findings indicate that this abasic site behaves with great similarity to the traditional abasic lesions formed by spontaneous base loss in DNA. While 4′-lesion **30** also adheres to the "A-rule," it induces three-nucleotide deletions under SOS conditions [88]. This was attributed to structural differences in the abasic site, which are not found in related lesions. These data represent examples of a larger body of work involving a variety of abasic sites. The results indicate that structural variations at abasic sites can affect the interactions of these lesions with DNA polymerases. This is significant in that this information can provide insight into the means by which polymerases handle each of these structurally distinct lesions. In the case of 2′-lesion **18**, it was shown that both Endo IV and Exo III are capable of its processing, however, much less efficiently than other abasic lesions [87]. Lesion **18** is also not a substrate for Exo II, while **30** is effectively processed by this type II repair enzyme [89]. Lesion **30** is a substrate for Endo III and IV as well as Exo III. One of the most interesting cluster lesions seen to date arises from the cross-link formed between lesion **30** and dA or dC in the opposing strand. This lesion exists in a dioxo form, which readily undergoes elimination when catalyzed by a nearby adenine or other available bases. The resulting alkene then forms an adduct with the above-mentioned nucleobases creating a nick and a cross-link at adjacent sites [90].

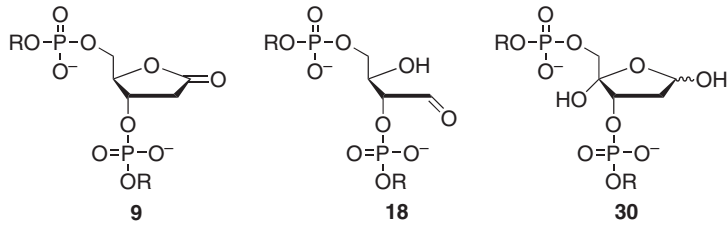

Figure 3 Oxidatively generated abasic lesions.

This lesion is handled by the nucleotide excision repair pathway and appears to result in the generation of double-strand breaks when repaired by UvrABC [91].

17. Adducts Derived from 2′-Deoxyribose Damage Lesions

Several DNA adducts which are derived from oxidatively generated sugar fragments have been introduced heretofore during this discussion. These include the experimental chemotherapeutic, kinetin (**47**), and the 1, N^2-glyoxal adducts of dG, 3-(2-deoxy-β-D-*erythro*-pentofuransyl)-6,7-dihydro-6,7-dihydroxyimidazo-[1,2-*a*]purine-9(3H)-one (**41**). These adducts are the result of the formation of the reactive electrophiles furfural (**45**) and glyoxal (**40**) formed via the C5′- and C3′-radicals, respectively [36,37,68,83] (Figure 4). Even though these small molecules are reactive, they selectively form adducts with specific nucleobases with greater prevalence. In the case of furfural, adenine adducts are formed exclusively [92] and with glyoxal (**40**), guanine is the primary target [69]. Nucleic acid adducts formed from oxidative damage products are an aspect of the genotoxicity of oxidative damage to DNA, which has been considered

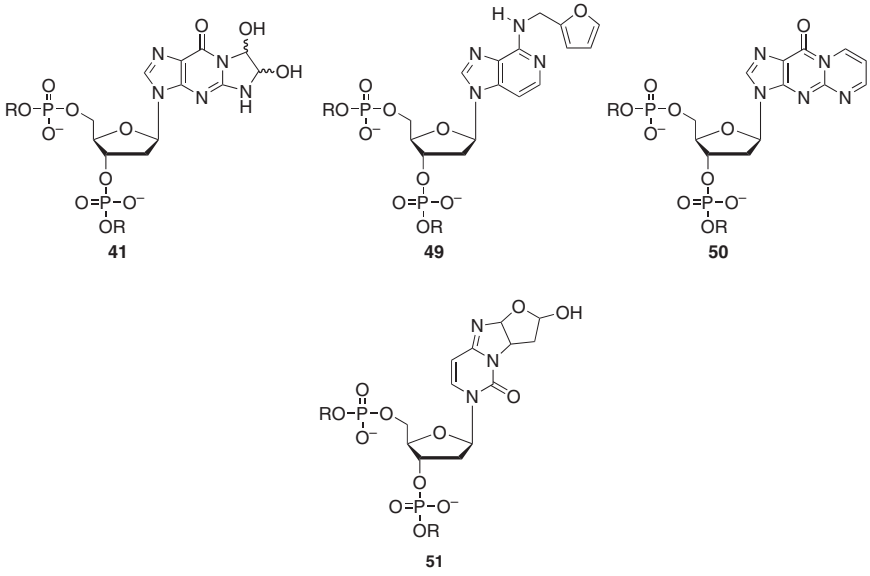

Figure 4 DNA adducts derived from 2′-deoxyribose oxidation.

only marginally in the role that oxidative stress plays in disease development.

Another significant adduct which belongs to this group is the pyrimido [1,2-*a*]purin-10-(3*H*)one nucleoside (M_1G) (**50**) derived from deoxyguanosine. This adduct results from the conjugation of dG by the base propenals (**32**) which are formed during C4′-radical decomposition [34]. Base propenals are mutagenic, a property that is likely related to their ability to form DNA adducts [93]. The actual mechanism of formation is not known; however, M_1G, which is also formed from a prevalent product of lipid peroxidation, namely malondialdehyde [94], is believed to be a significant contributor to the effects of oxidative damage. Additionally, base adducts have been identified which are the result of the adduction of dC, dA, and dG by a second 5′-oxidation product, cis-1,4-butenedial (**48**) [95,96]. These adducts were identified in varying amounts in DNA exposed to agents from various classes capable of 2′-deoxyribose oxidation. In addition to these adducts, this lesion has also demonstrated its ability to form interstrand DNA cross-links [97].

Several other DNA damage lesions have demonstrated reactivity toward simple nitrogen and sulfur nucleophiles. In the case of ribonolactone lesion **9**, both Sheppard [15] and Greenberg [16] showed that the secondary amines piperidine and dimethylethylene-diamine as well as the thiol BME react with the β-elimination product of the lactone to give relatively stable adducts. Even though this type of reactivity toward the nucleobases of DNA has not been demonstrated to date, it is not definite that these types of reactions do not occur. In addition, the cross-linking, which is manifested through the interaction of several of these lesions with repair proteins, indicates the willingness of these substrates to participate in conjugation reactions under physiological conditions [98]. Lesion **43** has also been shown to react readily with sulfur nucleophiles [99]. Initial experiments in our laboratory indicate that lactone **43** reacts readily with dC to deliver several adducts. The 1,4-dicarbonyl-containing lesion **30** resulting from C4′-oxidation also reacts readily with simple amines [100].

18. Summary

The catalog of DNA damage lesions which result from the oxidation of the 2′-deoxyribose moiety in DNA is large and steadily growing as we continue to utilize traditional and developing techniques to ponder old questions and to tackle new ones. With the identification of the lesions, which arise from sugar oxidation, we can now begin to understand their participation in further chemical reactions, their repair pathways, and their toxicity. We have only begun to scratch to surface of the complex pathways

by which these events may affect the interactions of DNA damage lesions with the enzymes responsible for their processing or the adduction of the same to form cross-links and protein adducts. Even though we have answered many questions about the formation of radicals in DNA by oxidants, issues still remain in this arena. The effect of sequence on the outcome of lesion formation or the effect of protein binding on the fate of the radical remains to be more thoroughly investigated.

REFERENCES

[1] W.K. Pogozelski, T.D. Tullius, Oxidative strand scission of nucleic acids: Routes initiated by hydrogen abstraction from the sugar moiety, Chem. Rev. 98 (1998) 1089–1108.
[2] P.C. Dedon, The chemical toxicology of 2-deoxyribose oxidation in DNA, Chem. Res. Toxicol. 21 (2008) 206–219.
[3] C.V. Sonntag, Free-Radical-Induced DNA Damage and Its Repair: A Chemical Perspective, Springer, New York, 2006.
[4] R.S. Bindra, P.M. Glazer, Genetic instability and the tumor microenvironment: Towards the concept of microenvironment-induced mutagenesis, Mutat. Res. 569 (2005) 75–85.
[5] B. Giese, X. Beyrich-Graf, P. Erdmann, M. Petretta, U. Schwitter, The chemistry of single-stranded 4′-DNA radicals: Influence of the radical precursor on anaerobic and aerobic strand cleavage, Chem. Biol. 2 (1995) 367–375.
[6] M.M. Greenberg, Elucidating DNA damage and repair processes by independently generating reactive and metastable intermediates, Org. Biomol. Chem. 5 (2007) 18–30.
[7] M.M. Greenberg, Investigating nucleic acid damage processes via independent generation of reactive intermediates, Chem. Res. Toxicol. 11 (1998) 1235–1248.
[8] X. Peng, Y.Z. Pigli, P.A. Rice, M.M. Greenberg, Protein binding has a large effect on radical mediated DNA damage, J. Am. Chem. Soc. 130 (2008) 12890–12891.
[9] Y. Xu, H. Sugiyama, Photochemical approach to probing different DNA structures, Angew. Chem. Intl. Ed. 45 (2006) 1354–1362.
[10] P. Vaupel, Tumor microenvironmental physiology and its implications for radiation oncology, Semin. Radiat. Oncol. 14 (2004) 198–206.
[11] K.B. Lesiak, K.T. Wheeler, Formation of α-deoxyadenosine in polydeoxynucleotides exposed to ionizing radiation under anoxic conditions, Radiat. Res. 121 (1990) 328–337.
[12] J.-T. Hwang, M.M. Greenberg, Kinetics and stereoselectivity of thiol trapping of deoxyuridin-1′-yl in biopolymers and their relationship to the formation of premutagenic α-deoxynucleotides, J. Am. Chem. Soc. 121 (1999) 4311–4315.
[13] C. Tronche, B.K. Goodman, M.M. Greenberg, DNA damage induced via independent generation of the radical resulting from formal hydrogen atom abstraction from the C1′-position of a nucleotide, Chem. Biol. 5 (1998) 263–271.
[14] B.K. Goodman, M.M. Greenberg, Independent generation and reactivity of 2′-deoxyurid-1′-yl, J. Org. Chem. 61 (1996) 2–3.
[15] K.A.Tallman, C.Tronche, D.J. Yoo, M.M. Greenberg, Release of superoxide from nucleoside peroxyl radicals, a double-edged sword? J. Am. Chem. Soc. 120 (1998) 4903–4909.

[16] Y. Zheng, T.L. Sheppard, Half-life and DNA strand scission products of 2-deoxyribonolactone oxidative DNA damage lesions, Chem. Res. Toxicol. 17 (2004) 197–207.
[17] J.-T. Hwang, K.A. Tallman, M.M. Greenberg, The reactivity of the 2-deoxyribonolactone lesion in single-stranded DNA and its implications in reaction mechanisms of DNA damage and repair, Nucleic Acids Res. 72 (1999) 3805–3810.
[18] M. Dizdaroglu, D. Schulte-Frohlinde, C. von Sonntag, γ-Radiolyses of DNA in oxygenated aqueous solution. Structure of an alkali-labile site, Z. Naturforsch. C 32 (1977) 1021–1022.
[19] K. Kawai, I. Saito, H. Sugiyama, Conformation-dependent photochemistry of 5-halouracil-containing DNA: Stereospecific 2′-alpha-hydroxylation of deoxyribose in Z-form DNA, J. Am. Chem. Soc. 121 (1999) 1391–1392.
[20] T. Oyoshi, K. Kawai, H. Sugiyama, Efficient C2′α-hydroxylation of deoxyribose in protein-induced Z-Form DNA, J. Am. Chem. Soc. 125 (2003) 1526–1531.
[21] J. Kim, Y.N. Weledji, M.M. Greenberg, Independent generation and characterization of a C2′-oxidized abasic site in chemically synthesized oligonucleotides, J. Org. Chem. 69 (2004) 6100–6104.
[22] S. Körner, A. Bryant-Friedrich, B. Giese, C-3′-Branched thymidines as precursors for the selective generation of C-3′-nucleoside radicals, J. Org. Chem. 64 (1999) 1559–1564.
[23] J. Brunner, J.K. Barton, Site-specific DNA photocleavage by rhodium intercalators analyzed by MALDI-TOF mass spectrometry, J. Am. Chem. Soc. 128 (2006) 6772–6773.
[24] A. Sitlani, E.C. Long, A.M. Pyle, J.K. Barton, DNA photocleavage by phenanthrenequinone diimine complexes of rhodium(III): Shape-selective recognition and reaction, J. Am. Chem. Soc. 114 (1992) 2303–2312.
[25] A.C. Bryant-Friedrich, Generation of a C-3′-thymidinyl radical in single-stranded oligonucleotides under anaerobic conditions, Org. Lett. 6 (2004) 2329–2332.
[26] G. Lahoud, J. Fancher, S. Grosu, B. Cavanaugh, A. Bryant-Friedrich, Automated synthesis, characterization, and structural analysis of oligonucleotide C-3′-radical precursors, Bioorg. Med. Chem. 14 (2006) 2581–2588.
[27] N.E. Poopeiko, B.M. Dahl, J. Wengel, xylo-Configured oligonucleotides (XNA, xylo nucleic acids): Synthesis and hybridization studies, Nucleosides Nucleotides Nucleic Acids 22 (2003) 1147–1149.
[28] A. Schoeppe, H.-J. Hinz, H. Rosemeyer, F. Seela, Xylose-DNA: Comparison of the thermodynamic stability of oligo(2′-deoxyxylonucleotide) and oligo(2′-deoxyribonucleotide) duplexes, Eur. J. Biochem. 239 (1996) 33–41.
[29] G.A. Lahoud, A.L. Hitt, A.C. Bryant-Friedrich, Aerobic fate of the C-3′-thymidinyl radical in single-stranded DNA, Chem. Res. Toxicol. 19 (2006) 1630–1636.
[30] B. Giese, A. Dussy, E. Meggers, M. Petretta, U. Schwitter, Conformation, lifetime and repair of 4′-DNA radicals, J. Am. Chem. Soc. 119 (1997) 11130–11131.
[31] J. Chen, J. Stubbe, Synthesis and characterization of oligonucleotides containing a 4′-keto abasic site, Biochemistry 43 (2004) 5278–5286.
[32] J. Kim, J.M. Gil, M.M. Greenberg, Synthesis and characterization of oligonucleotides containing the C4′-oxidized abasic site produced by bleomycin and other DNA damaging agents, Angew. Chem. Int. Ed. 42 (2003) 5882–5885.
[33] P.C. Dedon, S.R. Tannenbaum, Reactive nitrogen species in the chemical biology of inflammation, Arch. Biochem. Biophys. 423 (2004) 12–22.
[34] X. Zhou, K. Taghizadeh, P.C. Dedon, Chemical and biological evidence for base propenals as the major source of the endogenous M_1dG adduct in cellular DNA, J. Biol. Chem. 280 (2005) 25377–25382.
[35] P. Jaruga, M. Dizdaroglu, 8,5-Cyclopurine-2-deoxynucleosides in DNA: Mechanisms of formation, measurement, repair and biological effects, DNA Repair 7 (2008) 1413–1425.

[36] F. Boussicault, P. Kaloudis, C. Caminal, Q.G. Mulazzani, C. Chatgilialoglu, The fate of C5′ radicals of purine nucleosides under oxidative conditions, J. Am. Chem. Soc. 130 (2008) 8377–8385.
[37] P.C. Dedon, I.H. Goldberg, Free-radical mechanisms involved in the formation of sequence-dependent bistranded DNA lesions by the antitumor antibiotics bleomycin, neocarzinostatin, and calicheamicin, Chem. Res. Toxicol. 5 (1992) 311–332.
[38] B. Chen, T. Bohnert, X. Zhou, P.C. Dedon, 5′-(2-phosphoryl-1,4-dioxobutane) as a product of 5′-oxidation of deoxyribose in DNA: Elimination as trans-1,4-dioxo-2-butene and approaches to analysis, Chem. Res. Toxicol. 17 (2004) 1406–1413.
[39] H. Kawabata, H. Takeshita, T. Fujiwara, H. Sugiyama, T. Matsuura, I. Saito, Chemistry of neocarzinostatin-mediated degradation of d(GCATGC). Mechanism of spontaneous thymine release, Tetrahedron Lett. 30 (1989) 4263–4266.
[40] S.J. Lunt, N. Chaudary, R.P. Hill, The tumor microenvironment and metastatic disease, Clin. Exp. Metastasis 26 (2009) 19–34.
[41] K.B. Lesiak, K.T. Wheeler, Formation of α-deoxyadenosine in polydeoxynucleotides exposed to ionizing radiation under anoxic conditions, Radiat. Res. 121 (1990) 328–337.
[42] H. Ide, T. Yamaoka, Y. Kimura, Replication of DNA templates containing the alpha-anomer of deoxyadenosine, a major adenine lesion produced by hydroxyl radicals, Biochemistry 33 (1994) 7127–7133.
[43] H. Shimizu, R. Yagi, Y. Kimura, K. Makino, H. Terato, Y. Ohyama, H. Ide, Replication bypass and mutagenic effect of α-deoxyadenosine site-specifically incorporated into single-stranded vectors, Nucleic Acids Res. 25 (1997) 597–603.
[44] H. Ide, K. Tedzuka, H. Shimzu, Y. Kimura, A.A. Purmal, S.S. Wallace, Y.W. Kow, α-Deoxyadenosine, a major anoxic radiolysis product of adenine in DNA, is a substrate for Escherichia coli endonuclease IV, Biochemistry 33 (1994) 7842–7847.
[45] A.A. Ishchenko, H. Ide, D. Ramotar, G. Nevinsky, M. Saparbaev, α-Anomeric deoxynucleotides, anoxic products of ionizing radiation, are substrates for the endonuclease IV-type AP endonucleases, Biochemistry 43 (2004) 15210–15216.
[46] L. Gros, A.A. Ishchenko, H. Ide, R.H. Elder, M.K. Saparbaev, The major human AP endonuclease (Ape1) is involved in the nucleotide incision repair pathway, Nucleic Acids Res. 32 (2004) 73–81.
[47] T. Lindahl, Instability and decay of the primary structure of DNA, Nature 362 (1993) 709–715.
[48] H. Joenje, Genetic toxicology of oxygen, Mutat. Res. 219 (1989) 193–208.
[49] H. Ide, H. Shimizu, Y. Kimura, S. Sakamoto, K. Makino, M. Glackin, S. Wallace, H. Nakamuta, M. Sasaki, N. Sugimoto, Influence of α-deoxyadenosine on the stability and structue of DNA. Thermodynamic and molecular mechanics studies, Biochemistry 34 (1995) 6947–6955.
[50] J.M. Aramini, S.H. Cleaver, R.T. Pon, R.P. Cunningham, M.W.Germann, Solution structure of a DNA duplex containing an α-anomeric adenosine: Insights into substrate recognition by endonuclease IV, J. Mol. Biol. 338 (2004) 77–91.
[51] C.D. Mol, D.J. Hosfield, J.A. Tainer, Abasic site recognition by two apurinic/apyrimidinic endonuclease families in DNA base excision repair: The 3′ ends justify the means, Mutat. Res. 460 (2000) 211–229.
[52] C.D. Mol, T. Izumi, S. Mitra, J.A. Tainer, DNA-bound structures and mutants reveal abasic DNA binding by APE1 and DNA repair coordination [corrected], Nature 403 (2000) 451–456.
[53] N.E. Poopeiko, M. Juhl, B. Vester, M.D. Sorensen, J. Wengel, xylo-Configured oligonucleotides (XNA, xylo nucleic acid): Synthesis of conformationally restricted

derivatives and hybridization towards DNA and RNA complements, Bioorg. Med. Chem. Lett. 13 (2003) 2285–2290.
[54] M.T. Hess, U. Schwitter, M. Petretta, B. Giese, H. Naegeli, DNA synthesis arrest at C4′-modified deoxyribose residues, Biochemistry 36 (1997) 2332–2337.
[55] M. Dizdaroglu, M.L. Dirksen, H.X. Jiang, J.H. Robbins, Ionizing-radiation-induced damage in the DNA of cultured human cells. Identification of 8,5′-cyclo-2′-deoxyguanosine, Biochem. J. 241 (1987) 929–932.
[56] M. D′Errico, E. Parlanti, M. Teson, A. Calcagnile, P. Jaruga, G. Zambuno, M. Stefanini, M. Dizdaroglu, E. Dogliotti, New functions of XPC in the protection of human skin cells from oxidative damage, Oncogene 25 (2006) 4305–4315.
[57] G.I. Girnbaum, M. Cygler, L. Dudycz, R. Stolarski, D. Shugar, Comparison of solid state and solution conformation of R and S epimers of 8,5′-cycloadenosine and their relevance to some enzymatic reaction, Biochemistry 20 (1981) 3294–3301.
[58] T.P. Haromy, J. Raleigh, M. Sundaralingam, Enzyme-bound conformations of nucleotide substrates. X-ray structure and absolute configuration of 8,5′-cycloadenosine monohydrate, Biochemistry 19 (1980) 1718–1722.
[59] K. Miaskiewicz, J.H. Miller, A.F. Fuciarelli, Theoretical analysis of DNA intrastrand cross linking by formation of 8,5′-cyclodeoxyadenosine, Nucleic Acids Res. 23 (1995) 515–521.
[60] C. Marietta, P.J. Brooks, Transcriptional bypass of bulky DNA lesions causes new mutant RNA transcripts in human cells, EMBO Rep. 8 (2007) 388–393.
[61] L.J. Eccles, M.E. Lomax, P. O′Neill, Hierarchy of lesion processing governs the repair, double-strand break formation and mutability of three-lesion clustered DNA damage, Nucleic Acids Res. 38 (2010) 1123–1134. December 3 [epub ahead of print].
[62] B. Paap, D.M. Wilson, III, B.M. Sutherland, Human abasic endonuclease action on multilesion abasic clusters: Implications for radiation-induced biological damage, Nucleic Acids Res. 36 (2008) 2717–2727.
[63] N.K. Bernstein, F. Karimi-Busheri, A. Rasouli-Nia, R. Mani, G. Dianov, J.N. Glover, M. Weinfeld, Polynucleotide kinase as a potential target for enhancing cytotoxicity by ionizing radiation and topoisomerase I inhibitors, Anticancer Agents Med. Chem. 8 (2008) 358–367.
[64] A.W. Johnson, B. Demple, Yeast DNA 3′-repair diesterase is the major cellular apurinic/apyrimidinic endonuclease: Substrate specificity and kinetics, J. Biol. Chem. 263 (1988) 18017–18022.
[65] C. Bernelot-Moens, B. Demple, Multiple DNA repair activities for 3′-deoxyribose fragments in Escherichia coli, Nucleic Acids Res. 17 (1989) 587–600.
[66] D.M.Wilson, III, M. Takeshita, A.P. Grollman, B. Demple, Incision activity of human apurinic endonuclease (Ape) at abasic site analogs in DNA, J. Biol. Chem. 270 (1995) 16002–16007.
[67] B. Demple, A. Johnson, D. Fung, Exonuclease III and endonuclease IV remove 3′ blocks from DNA synthesis primers in H_2O_2-damaged Escherichia coli, Proc. Natl. Acad. Sci. U. S. A. 83 (1986) 7731–7735.
[68] M. Awada, P.C. Dedon, Formation of the 1,*N*2-glyoxal adduct of deoxyguanosine by phosphoglycolaldehyde, a product of 3′-deoxyribose oxidation in DNA, Chem. Res. Toxicol. 14 (2001) 1247–1253.
[69] H. Kasai, N. Iwamoto-Tanaka, S. Fukada, DNA modifications by the mutagen glyoxal: Adduction to G and C, deamination of C and GC and GA cross-linking, Carcinogenesis 19 (1998) 1459–1465.
[70] R. Olsen, P. Molander, S. Ovrebo, D.G. Ellingsen, S. Thorud, Y. Thomassen, E. Lundanes, T. Greibrokk, J. Backman, R. Sjoholm, L. Kronberg, Reaction of glyoxal with 2′-deoxyguanosine, 2′-deoxyadenosine, 2′-deoxycytidine, cytidine, thymidine,

and calf thymus DNA: Identification of DNA adducts, Chem. Res. Toxicol. 18 (2005) 730–739.
[71] C. Collins, M.M. Awada, X. Zhou, P.C. Dedon, Analysis of 3′-phosphoglycolaldehyde residues in oxidized DNA by gas chromatography/negative chemical ionization/mass spectrometry, Chem. Res. Toxicol. 16 (2003) 1560–1566.
[72] C. Collins, X. Zhou, R. Wang, M.C. Barth, T. Jiang, J.A. Coderre, P.C. Dedon, Differential oxidation of deoxyribose in DNA by gamma and alpha-particle radiation, Radiat. Res. 163 (2005) 654–662.
[73] J.L. Parsons, I.I. Dianova, G.L. Dianov, APE1 is the major 3′-phosphoglycolate activity in human cell extracts, Nucleic Acids Res. 32 (2004) 3531–3536.
[74] T.A. Winters, W.D. Henner, P.S. Russell, A. McCullough, T.J. Jorgensen, Removal of 3′-phosphoglycolate from DNA strand-break damage in an oligonucleotide substrate by recombinant human apurinic/apyrimidinic endonuclease 1, Nucleic Acids Res. 22 (1994) 1866–1873.
[75] T. Takahashi, M. Tada, S. Igarashi, A. Koyama, H. Date, A.Yokoseki, A. Shiga, Y. Yoshida, S. Tsuji, M. Nishizawa, O. Onodera, Aprataxin, causative gene product for EAOH/AOA1, repairs DNA single-strand breaks with damaged 3′-phosphate and 3′-phosphoglycolate ends, Nucleic Acids Res. 35 (2007) 3797–3809.
[76] T. Zhou, K. Akopiants, S. Mohapatra, P.S. Lin, K. Valerie, D.A. Ramsden, S.P. Lees-Miller, L.F. Povirk, Tyrosyl-DNA phosphodiesterase and the repair of 3′-phosphoglycolate-terminated DNA double-strand breaks, DNA Repair (Amst) 8 (2009) 901–911.
[77] L.F. Povirk, T. Zhou, R. Zhou, M.J. Cowan, S.M. Yannone, Processing of 3′-phosphoglycolate-terminated DNA double strand breaks by Artemis nuclease, DNA Repair (Amst) 282 (2007) 3547–3558.
[78] J. Stubbe, J.W. Kozarich, Mechanisms of bleomycin-induced DNA degradation, Chem. Rev. 87 (1987) 1107–1136.
[79] H. Sugiyama, K. Fujimoto, I. Saito, Stereospecific 1,2-hydride shift in ribonolactone formation in the photoreaction of 2′-iododeoxyuridine, J. Am. Chem. Soc. 117 (1995) 2945–2946.
[80] G.P. Cook, M.M. Greenberg, A novel mechanims for the formation of direct strand breaks upon anaerobic photolysis of duplex DNA containing 5-bromodeoxyuridine, J. Am. Chem. Soc. 118 (1996) 10025–10030.
[81] A. Angeloff, I. Dubey, G. Pratviel, J. Bernadou, B. Meunier, Characterization of a 5′-aldehyde terminus resulting from the oxidative attack at C5′ of a 2-deoxyribose on DNA, Chem. Res. Toxicol. 14 (2001) 1413–1420.
[82] G. Pratviel, M. Pitie, J. Bernadou, B. Meunier, Furfural as a marker of DNA cleavage by hydroxylation at the 5′ carbon of deoxyribose, Angew. Chem. Int. Ed. 30 (1991) 702–704.
[83] J. Barciszewski, G.E. Siboska, B.O. Pedersen, B.F.C. Clark, S.I.S. Rattan, A mechanism for the in vivo formation of *N*6-furfuryladenine, kinetin, as a secondary oxidative damage product of DNA, FEBS Lett. 414 (1997) 457–460.
[84] C.M. Cabello, W.B. Bair, III, S. Ley, S.D. Lamore, S. Azimian, G.T. Wondrak, The experimental chemotherapeutic *N*6-furfuryladenosine (kinetin-riboside) induces rapid ATP depletion, genotoxic stress, and CDKN1A(p21) upregulation in human cancer cell lines, Biochem. Pharmacol. 77 (2009) 1125–1138.
[85] L. Guan, M.M. Greenberg, DNA interstrand cross-link formation by the 1,4-dioxobutane abasic lesion, J. Am. Chem. Soc. 131 (2009) 15225–15231.
[86] L.J. Chen, S.S. Hecht, L.A. Peterson, Identification of cis-2-butene-1,4-dial as a microsomal metabolite of furan, Chem. Res. Toxicol. 8 (1995) 903–906.
[87] M.M. Greenberg, Y.N. Weledji, K.M. Kroeger, J. Kim, In vitro replication and repair of DNA containing a C2′-oxidized abasic site, Biochemistry 43 (2004) 15217–15222.

[88] K.M. Kroeger, J. Kim, M.F. Goodman, M.M. Greenberg, Replication of an oxidized abasic site in Escherichia coli by a dNTP-stabilized misalignment mechanism that reads upstream and downstream nucleotides, Biochemistry 45 (2006) 5048–5056.
[89] M.M. Greenberg, Y.N. Weledji, J. Kim, B.C. Bales, Repair of oxidized abasic sites by exonuclease III, endonuclease IV, and endonuclease III, Biochemistry 43 (2004) 8178–8183.
[90] J.T. Sczepanski, A.C. Jacobs, A. Majumdar, M.M. Greenberg, Scope and mechanism of interstrand cross-link formation by the C4′-oxidized abasic site, J. Am. Chem. Soc. 131 (2009) 11132–11139.
[91] J.T. Sczepanski, A.C. Jacobs, B. Van Houten, M.M. Greenberg, Double-strand break formation during nucleotide excision repair of a DNA interstrand cross-link, Biochemistry 48 (2009) 7565–7567.
[92] S.M. Hadi, R.A. Shahabuddin, Specificity of the interaction of furfural with DNA, Mutat. Res. 225 (1989) 101–106.
[93] J.P. Plastaras, P.C. Dedon, L.J. Marnett, Effects of DNA structure on oxopropenylation by the endogenous mutagens malondialdehyde and base propenal, Biochemistry 41 (2002) 5033–5042.
[94] A.K. Basu, S.M. O′Hara, P. Valladier, K. Stone, O. Mols, L.J. Marnett, Identification of adducts formed by reaction of guanine nucleosides with malondialdehyde and structurally related aldehydes, Chem. Res. Toxicol. 1 (1988) 53–59.
[95] B. Chen, C.C. Vu, M.C. Byrns, P.C. Dedon, L.A. Peterson, Formation of 1,4-dioxo-2-butene-derived adducts of 2′-deoxyadenosine and 2′-deoxycytidine in oxidized DNA, Chem. Res. Toxicol. 19 (2006) 982–985.
[96] M.C. Byrns, C.C. Vu, J.W. Neidigh, J.L. Abad, R.A. Jones, L. Peterson, Detection of DNA adducts derived from the reactive metabolite of furan, cis-2-butene-1,4-dial, Chem. Res. Toxicol. 19 (2006) 414–420.
[97] L. Guan, M.M. Greenberg, DNA interstrand cross-link formation by the 1,4-dioxobutane abasic lesion, J. Am. Chem. Soc. 131 (2009) 15225–15231.
[98] M. Hashimoto, M.M. Greenberg, Y.W. Kow, J.T. Hwang, R.P. Cunningham, The 2-deoxyribonolactone lesion produced in DNA by neocarzinostatin and other damaging agents forms cross-links with the base-excision repair enzyme endonuclease III, J. Am. Chem. Soc. 123 (2001) 3161–3162.
[99] G. Harris, M. Ator, J. Stubbe, Mechanism of inactivation of Escherichia coli and Lactobacillus leichmannii ribonucleotide reductases by 2′-chloro-2′-deoxynucleotides: Evidence for generation of 2-methylene-3(2H)-furanone, Biochemistry 23 (1984) 5214–5225.
[100] M. Aso, K. Usui, M. Fukuda, Y. Kakihara, T. Goromaru, H. Suemune, Photochemical generation of C4′-oxidized abasic site containing oligodeoxynucleotide and its efficient amine modification, Org. Lett. 8 (2006) 3183–3186.

CHAPTER 5

Nitric Oxide and Redox Inflammation in Cancer

Robert Cheng, Sharon Glynn, Wilmarie Flores-Santana, Christopher Switzer, Lisa Ridnour, *and* David A. Wink*

Contents

Radiation Biology Branch, National Cancer Institute, National Institutes of Health, Bethesda, MD, USA

* Corresponding author. Tel.: (301) 496 7511; Fax: (301) 480 2238
Email address: wink@mail.nih.gov

Advances in Molecular Toxicology, Volume 4

ISSN 1872-0854, DOI 10.1016/S1872-0854(10)04005-1

1. Introduction

Since the discovery of nitric oxide's (NO) role in vasodilation (which was mistakenly considered as a direct effect of acetylcholine at that time) in the early 1980s by Furchgott and coworkers [1], NO has demonstrated involvement in nearly every aspect of tumor biology [2–4]. In tumor cells, NO can increase proliferation, adhesion, and migration. Moreover, NO promotes angiogenesis and regulates the activity of different matrix proteins [5]. Chronic elevated expressions of proinflammatory biomarkers [i.e., cyclooxygenase (COX)-2] in a number of cancers have shown its influence on tumor progression and represent mechanisms and pathways that are deleterious to the patient. Although the biological responses to NO are multifaceted and appear contradictory at times, the concentration-dependent responses clarify discrepancies and point to a simpler model. Therefore, many of the dichotomous responses to NO can be explained in terms of its concentration and duration profiles. Many of the differential cellular responses may be simply a function of the concentration (dose) and duration of exposure, so that distinct biological responses result from specific incremental NO levels. NO is a diffusible gas whose biological concentration is determined partly by its distance from the point of synthesis and partly by the cellular redox environment as discussed below.

There are three major isoforms of nitric oxide synthase (NOS) which are responsible for the conversion of arginine to citrulline and NO [6]. The constitutive forms NOS1 and NOS3 regulate physiological functions and are calcium dependent. However, NOS3 (or eNOS) can be phosphorylated, becoming calcium independent providing a low flux of prolonged NO at nanomolar concentrations. This is important in processes such as angiogenesis (blood vessel formation). The inducible NOS, NOS2 (or iNOS) is generally associated with inflammation [7]. Though it can be expressed constitutively in lung and kidney regulating some physiological functions [8,9], it is primarily related to inflammation where this isoform has received much attention with respect to cancer [2,10]. Despite these vast differences in behavior, the effector molecule NO and its related chemistry play critical roles in every tissue, in both physiological and pathophysiological processes. The diversity of this biological activity is due to its unique chemistry [2,11].

2. Direct and Indirect Effects of the Chemistry of NO

The chemistry involved with the chemical biology of NO occurs in two different types of reactions, direct and indirect [12]. The direct reactions are where NO directly reacts with biological target molecules, including metals and highly reactive radicals (Figures 1 and 2). In contrast, the indirect effects require that NO reacts with oxygen or superoxide to generate reactive nitrogen species (RNS), which subsequently react with different biomacromolecules and alter their downstream functions. The indirect mechanism can be further subdivided into nitrosative and oxidative stress [13]. Nitrosative stress implies the addition of a nitrosonium [NO^+] equivalent to a thiol or secondary amine or hydroxyl groups. Reactive

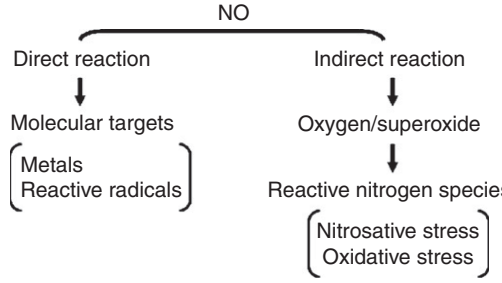

Figure 1 Direct and indirect reactions of NO.

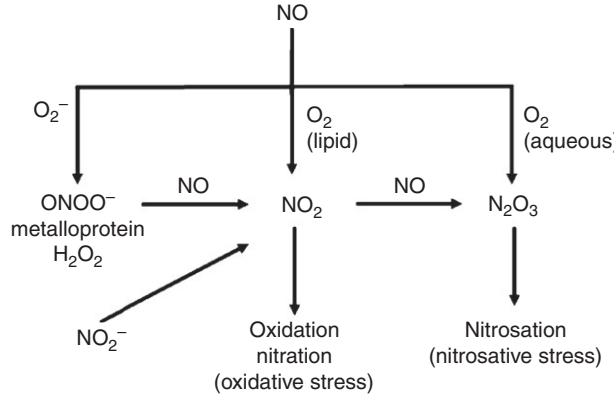

Figure 2 The chemistry of direct and indirect reactions of NO.

oxygen species (ROS) (OH radical, O_2^-) such as those produced by the Fenton reaction are most often associated with oxidative stress. N_2O_3 is the primary initiator of nitrosative stress and can generate nitrosamines as well as *S*-nitrosothiols. Though $ONOO^-$ is a powerful oxidant, it is rapidly converted to NO_2 which is the primary oxidant and can lead to lipid oxidation and create products such as 4-hydroxynonenal that can alter DNA, as well as induce signal transduction cascades [14,15]. However, the chemistry of NO_2 and other oxidants formed from peroxynitrite are extremely limited in the presence of NO due to their near-diffusion-controlled reaction with NO [16]. Thus, it was anticipated that high NO levels such as those experienced by an activated macrophage or hepatocyte would lead to nitrosative or oxidative stress.

3. The Chemistry of Nitric Oxides and Reactive Nitrogen and Oxygen Species

The primary determinant for the role of NO, the ROS, and the RNS are their chemical components and the surrounding redox environment. Interactions of ROS and NO could result in a number of RNS that can affect different biological pathways. The predominant result of ROS and NO is the rapid conversion of NO to nitrite/nitrate which represents a mechanism to reduce the bioavailability of NO [eqs. (1–9)]. However, the interaction of NO and O_2 produces the reactive species $ONOO^-$ suggesting potential powerful oxidants may form [eqs. (3 and 4)]. Conversely, O_2^- quenches peroxynitrite-mediated oxidation and nitration indicating that direct peroxynitrite chemistry has a limited role (10) [17,18].

$$\mathrm{NO} \rightarrow \text{reacts with biological target} \tag{1}$$

$$\mathrm{NO} + \mathrm{O_2^-} \rightarrow \mathrm{ONOO^-} \tag{2}$$

$$\mathrm{ONOO^-} + \mathrm{CO_2} \rightarrow \mathrm{CO_2ONOO^-} \tag{3}$$

$$\mathrm{CO_2} - \mathrm{OONO^-} \rightarrow [\mathrm{CO_3} \cdots \mathrm{NO_2}]^- \tag{4}$$

$$[\mathrm{CO_3} \cdots \mathrm{NO_2}]^- \rightarrow \text{oxidants} \rightarrow \mathrm{NO_3^-} + \mathrm{CO_2} \tag{5}$$

$$\mathrm{NO} + [\mathrm{CO_3} \cdots \mathrm{NO_2}]^- \rightarrow \mathrm{NO_2} + \mathrm{CO_3^{2-}} \tag{6}$$

$$NO_2 + NO \rightarrow N_2O_3 \quad (7)$$

$$N_2O_3 \rightarrow \text{nitrosation} \quad (8)$$

$$N_2O_3 + H_2O \rightarrow 2HNO_2 \quad (9)$$

$$2O_2^- + [CO_3 \cdots NO_2]^- \rightarrow NO_2^- + CO_3^{2-} \quad (10)$$

However, NO_2 generated from this reaction can oxidize and nitrate substrates as well as nitrosate proteins via N_2O_3 [eqs. (6–9)] [19,20]. NO_2 and N_2O_3 induce heme oxygenase (HO)-1 and IL-8 in monocytes [21] implying that RNS has anti-inflammatory properties and stimulates proliferation. Nitrosation by N_2O_3 can activate latent TGFβ [22] which downregulates type 2 inflammation. Despite the potential deleterious effects of RNS, the biological signaling has been adapted to these reactive intermediates that are utilized as feedback mechanisms to downregulate the inflammatory response, promote wound healing, and restore tissue. The RNS-mediated cellular responses indicate that there are biological alarm systems as well as feedback loops that are important in understanding NO response *in vivo*.

4. Nitric Oxide and Inflammation

Inflammation is associated with numerous cancers at every stage of the disease [7]. Moreover, one third of all cancers are thought to have arisen from previous inflammatory conditions [23] while inflammation is proposed to drive some cancers to more aggressive phenotypes [2]. Two key mediators of inflammation, NOS2 and COX-2, are associated with cancer progression and poor prognosis in several tumor types [10, 24]. Inflammation can be classified into acute and chronic. Though the temporal profiles differ, there are common mechanisms though with different timescales and amplitudes of the biological response. One of the best examples of the acute inflammation response is the major tissue restoration processes that occur after ischemia reperfusion injury, while classic examples of chronic inflammation include ulcerative colitis [25] or neurological degeneration diseases such as Alzheimer's disease [26]. In the case of cancer, it has been likened to a wound that does not heal [27–29] (Figure 3). Solid tumors utilize aspects of both acute and chronic inflammation.

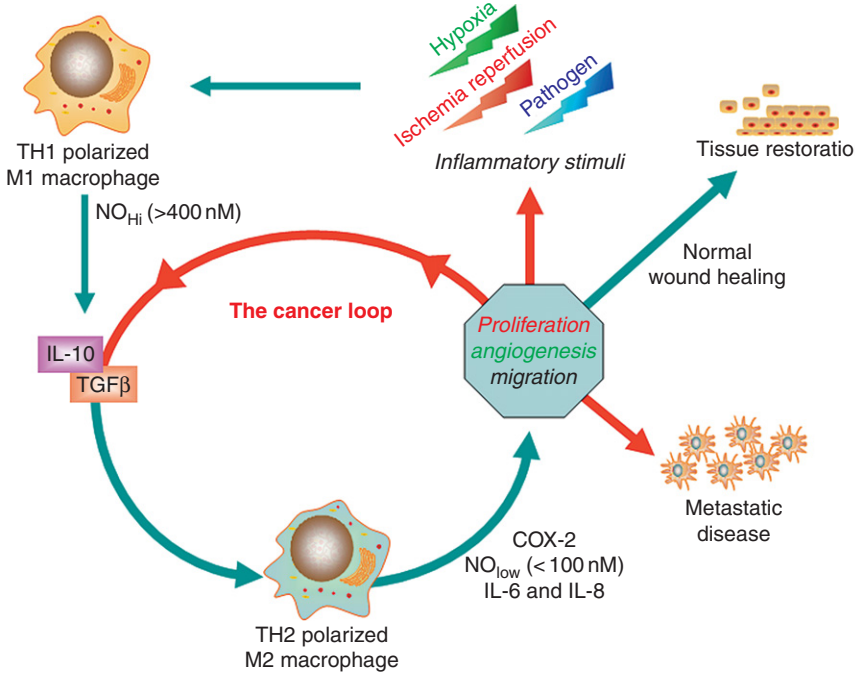

Figure 3 NO and inflammation. Inflammation is associated with numerous cancers at every stage of the disease and is proposed to drive some cancers to more aggressive phenotypes. Unlike pathogen infection or ischemia reperfusion, cancer-related inflammation can initiate a cancer loop (red arrows) and keep the TH1-polarized M1 macrophage at bay, thus preventing the M1 to M2 transformation. Such cancer loop would evade the normal wound healing initiation and benefit cancer growth.

5. The Two Faces of NO in Cancer

NO and inflammation have been associated with increased genotoxicity and tumor progression as well as antitumor activity. In the early 1980s it was found that nitrite increased in ill human patients [30]. Both *in vitro* and *in vivo* assays exhibited increased levels of nitrosamines during inflammation [31,32]. In addition, it was shown that NO and resulting intermediates could increase genotoxicity by inhibiting DNA repair [33]. These studies bridged the gaps between NOS, inflammation, and cancer.

In the mid-1990s, two studies overexpressing NOS2 in colon tumor cells showed increased tumorigenicity and aggressiveness while increased NOS2 expression in melanoma showed decreases in these two attributes [34–39]. These findings indicated that NOS, NO, and RNS are playing multiple roles that could result in different phenotypes.

6. Inflammatory Molecules, NOS2, and COX-2 in Patient Outcome

Although NOS2 correlates with good prognosis in ovarian [40] and lung cancers [41], epidemiological studies suggest that elevated NOS is associated with poor prognosis in other cancers [42–45]. Many studies suggest that elevated NOS2 is linked to poorer prognosis in breast [46], colon [3], gastric [47–49], esophageal [50], prostate [51], melanoma [52,53], cervical [43], squamous cell carcinoma [54], hepatocellular carcinoma [55], and leukemia [56] cancers. These studies often concluded that there is a link to the inflammation biomarkers. These findings suggest that NOS2 and COX-2 play a role in chronic inflammation in the resistance to conventional cancer treatment that leads to a more aggressive phenotype.

7. Mechanism of NO in Cancer

Not only it is a multifactorial disease, cancer is also a multifaceted disease that progresses in different stages over decades. It is not a single disease but rather over 256 different types, which share the common characteristic of uncontrolled growth, that is, tissue that has lost normal growth control. These diseases are further complicated for even when they share similar genotypes, they may have different prognoses. For example, breast cancer can be characterized into several types. One distinction is the estrogen status or the presence of estrogen receptor (ER)α, which can be further divided into five distinct subtypes which give different prognoses [57]. Another difficulty in curing cancer is that there are subpopulations of cells within a solid tumor that escape conventional treatment and have developed resistance that leads to the failure of therapy. This illustrates the complexity of this disease and since there is no magic bullet, there is an urge to devise multi-pathway therapies that target different mechanisms in addition to the cytotoxic agents. In addition, there is a need for developing personalized treatment for individual patients. It is becoming clear from whole genome transcript profiling that there are numerous subpopulations of patients that respond differently to various treatments within the same category of cancer. This has become possible with the advent of gene therapy and metabolomic methodologies. Hopefully, the findings from these new approaches will bring hope to those patients with poor prognostic indications.

8. Hypoxia as the Driving Factor of Inflammation

There are two main types of cancer, the ascites tumor, which include the hemopoietic cancers such as leukemia and lymphoma, and the solid tumors which are [57] commonly known by their organ of origin. Tumor staging is reflective of the severity of the disease and is measured by the degree of invasiveness/metastasis. In general, if the tumor spreads to organs such as the brain, liver, lung, or bone, it will dramatically lower the 2-, 5-, and 10-year survival rate. The tumor environment is unique and often amorphous with poorly structured cell architecture and vascular supply, which is due to rapidly growing tumor cells and extensive recruitment of leukocytes and endothelial cells. The poor and inconsistent blood flow within a tumor leads to cellular heterogeneity and an uneven distribution of nutrients and oxygen leads to areas of hypoxia, a low oxygen concentration status [58]. Hypoxia within a solid tumor would alter the physiology of cells of the stressed regions which leads to increase in growth factors that promote angiogenesis as well as factors that drive processes involved with metastasis, such as epithelial mesenchymal transitions (EMTs) and matrix reorganization through increases in matrix metalloproteinase (MMP) activities. Solid tumors with regions of greater than 35% hypoxia lead to poor outcomes no matter what treatment is received [59]. This indicates that hypoxia is a major driving force behind patients with poor outcomes.

9. Hypoxia and Wound Healing

Hypoxic conditions will fluctuate due to inconsistent blood flow. Unlike normal tissue where the unidirectional flow from the arterial to venule side of the circulation through the capillaries, tumor blood flow can be retrograde with backflow and erratic patterns (Figure 4) [58]. This leads to areas of hypoxia similar to the condition caused by ischemia reperfusion injury (the loss of blood flow and low oxygen followed by restoration of the blood flow), which leads to stroke and myocardiac infarction. This dramatic fluctuation in oxygen levels with regions of hypoxia would cause cell injury [58,60,61]. This injury leads to a cascade of immune responses similar to tissue ischemia or wound healing. There is a burst of macrophage infiltration with other immune cells. This would initiate the Th1 response

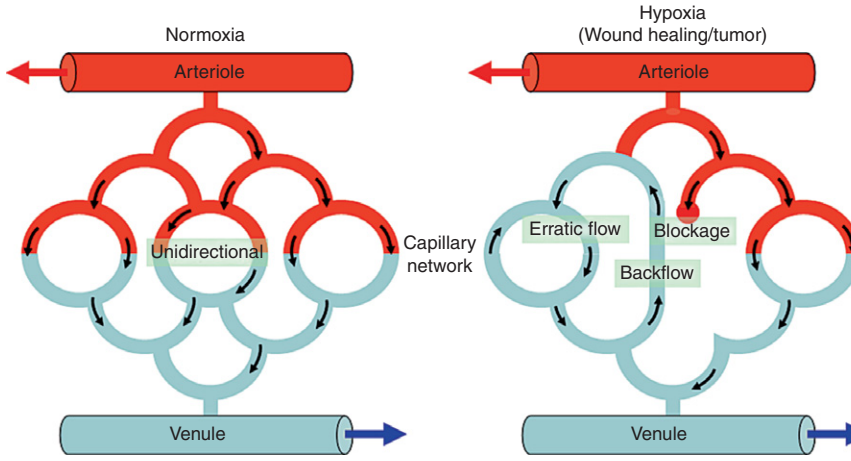

Figure 4 Hypoxia and normoxia. A normal capillary network would only allow unidirectional blood flow from arteriole to venule. In the case of wound healing or cancer, blood flow patterns at the lesion can be erratic due to damaged capillary network.

(Figure 5). In normal wound healing this process eradicates infection in the wound and triggers a conversion to M2 macrophage or alternative polarization, which increases the immunosuppression and is followed by a tissue restoration response. In tumors, there is as much as 40% leukocyte infiltration and particularly the monocytes with other fibroblasts. Cancer can be termed as "the wound that does not heal" [27–29].

In the normal wound healing process, the innate immune response involving neutrophils and macrophages utilizes redox molecules such as ROS and NO to eradicate pathogens. If the innate immune response fails, there is an increase in the adaptive immune response and orchestrating this response can also include reactive species. Upon eradication of infection, the macrophages will become polarized to facilitate the cleanup and tissue restoration processes [26,62,63]. In cancer, macrophages are chronically polarized and remain in M2 state without resolution; thus, tumors are constantly undergoing these ischemia reperfusion events that lead to the stimulation of injury wound healing processes. One of these is EMT, where cells change to become more mobile as well as an increase in factors that stimulate proliferation. This is essential to restore normal tissue; however, in tumors these processes lead to cells migrating from the lesion to the neighboring stroma and eventual entry into the blood and lymph. These processes lead to metastatic disease and result in higher staged tumors and a poor survival outcome [64,65]. Thus, the driving forces are essentially coming from the failure of normal inflammatory and tissue restoration

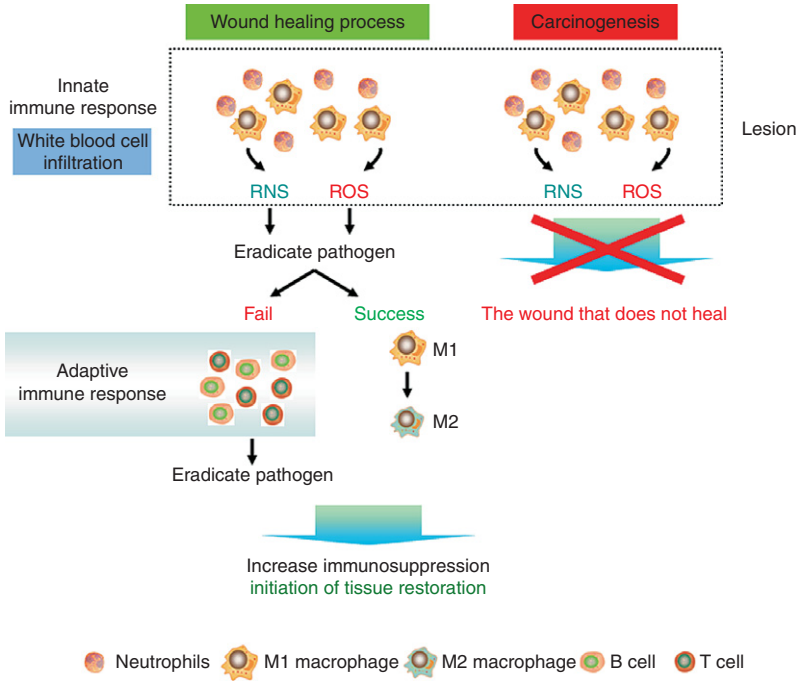

Figure 5 A wound that does not heal. An injury can lead to a cascade of immune responses similar to tissue ischemia or wound healing. First is a burst of macrophage and other immune cells' infiltration. This would initiate the Th1 response, the polarized M1 macrophage will transform into M2 macrophage if they successfully removed the pathogen. Adaptive immune response will respond if the innate immune response failed to eradicate the pathogen. Once the pathogen is eliminated, an increase in immunosuppression and initiation of tissue restoration occurs. During carcinogenesis, the cancer cells is not eradicated by the body's immune system, thus the lesion would like "a wound that never heals."

responses. There are several factors that contribute to this: one is the genetic and epigenetic changes that occur in the tumor cells that are reprogrammed to rapid uncontrolled growth, this causes poor architecture in blood flow and escape from the immune surveillance system. Another factor is the increase of hypoxia regions in tumors and that triggers the chronic injury and inflammatory responses along with the increase of tissue restoration factors.

10. Tissue Restoration and Nitric Oxide

In the events such as ischemia reperfusion and wound healing, redox molecules play critical roles in not only the eradication of pathogens and tumors but also in cellular, immune, and physiological processes.

Endogenously produced redox molecules include NO, ROS and RNS, arachidonic acid metabolites, carbon monoxide (CO), and hydrogen sulfide (H_2S). These molecules all play roles in the normal regulation of physiological function such as cardiovascular homeostasis and even neurological function as well as being part of the tissue restoration response [66–68]. ROS are formed from the reduction of oxygen to superoxide and peroxide. Through the reaction with metal centers (heme and nonheme) there is production of powerful oxidants that if unchecked, lead to the oxidation of proteins, lipids, and DNA, which is referred to as oxidative stress. Peroxide and hypochlorous acid (HOCl) are used in the innate immune response to sterilize the area of injury. The primary source of ROS is NOX, which reduces oxygen through the heme site through an outer-sphere electron transfer reaction. There are five isoforms of NOX where NOX-2 is associated with the innate immune system and oxidative burst [69]. This isoform can generate 1 nmol min^{-1} 10^{-6} cells of superoxide which rapidly dismutates to peroxide [70]. In contrast, the other isoforms produce much lower superoxide/peroxide within the cell and regulate critical cellular processes. The superoxide and peroxide mediate the biological outcomes through reactions with metals to produce oxidants resulting in oxidation, particularly of thiols. The latter has emerged as a large biomedical field and thiols are critical molecular targets for ROS and RNS.

More recently discovered endogenously formed redox molecules are CO and H_2S [66,71,72]. CO is produced by HO-1, which catalyzes the degradation of heme to generate bilirubin, iron, and CO. CO is an immune suppressor which is able to downregulate the innate inflammatory response. Also, CO is able to stimulate processes such as angiogenesis and inhalation of CO has been utilized to treat shock and other forms of trauma [71]. H_2S has been discovered in a variety of tissues in concentrations as high as 100 μM in the central nervous system [66]. It is reported to be derived from the cystathionine γ-lyase and cystathionine β synthase, two enzymes involved in the conversion of methionine to cysteine. It has been reported that H_2S regulates circadian rhythms, neuron signal transmission, and modulation of the blood flow [66,73].

11. NO and Macrophages

Macrophages are not only an important component of the immune system but also act as a major source of NO. Macrophages generate NO derivatives such as nitrosamines that were early indicators that nitrosative environment is endogenously generated [74,75] Macrophages perform a wide variety of functions from fighting bacteria and suppressing tumor growth to coordinating the resolution of tissue repair and restoration

processes. In 1990, the Fe–NO electron paramagnetic resonance (EPR) signal was discovered, and it was demonstrated that dinitrosoiron complexes were formed during the inflammation process [76]. These diverse properties in the cardiovascular and immune response suggested that NO was a multifunctional molecule. Macrophages can generate a number of different levels of NO that serve different purposes [77]. For instance, endothelial nitric oxide synthase (eNOS) stimulation of guanylate cyclase in nonactivated macrophages is required to fully activate lipopolysaccharide (LPS)-induced iNOS in activated macrophages [78]. Interestingly, the amount of NO produced from activated macrophages is dependent upon the manner by which they are stimulated. When IFNγ pretreated macrophages are activated by TNFα or IL-1β, the amount of NO generated in solution is approximately 10 times less than when they are stimulated with IFNγ + LPS (PIPC and Listeria) even though there is only a modest difference in NOS activity [77,79]. Moreover, the amount of NO-mediated nitrosation from TNFα or IL-1β stimulation was 30 times less than when stimulated with LPS or PIPC [77]. This suggests that NO generated from cytokine stimulation leads to considerably lower NO concentrations in the surrounding environment than those agents that activate through the toll-like receptors. These data revealed that murine macrophages are capable of producing wide ranges of NO concentrations depending on the source of stimulus.

12. Nitric Oxide Levels Determine Effects

The paradoxical nature of NO biological effects can be explained in terms of concentration and temporal response. Characterizing steady-state concentration of NO is particularly important when assessing its effects at the cellular level [80,81]. Distinct signaling pathways are elicited in response to distinct fluxes of NO. For example, 50 nM of sustained NO is associated with increased cGMP-mediated ERK phosphorylation, where intermediate sustained concentrations (>100 nM) lead to hypoxia-inducible factor (HIF)-1α stabilization, and high sustained concentrations of NO (>300 nM) increase p53-P(ser-15), which persists even after NO drops below these concentrations [summarized in [80] (Figure 6)]. These phenotypic responses favor a pro-growth and anti-apoptotic paradigm at steady-state NO levels at or below 100 nM. However, the prosurvival effects of NO are lost at concentrations above 400 nM, which is signified by increases in phosphorylation and acetylation of p53 and the induction of p53 tumor suppressor activity [82]. Other proteins, including MKP-1, a phosphatase that regulates pERK, also increases at or above 400 nM steady-state NO [83,84]. This signaling profile was mimicked by activated macrophages co-cultured with MCF-7 cells at varying ratios

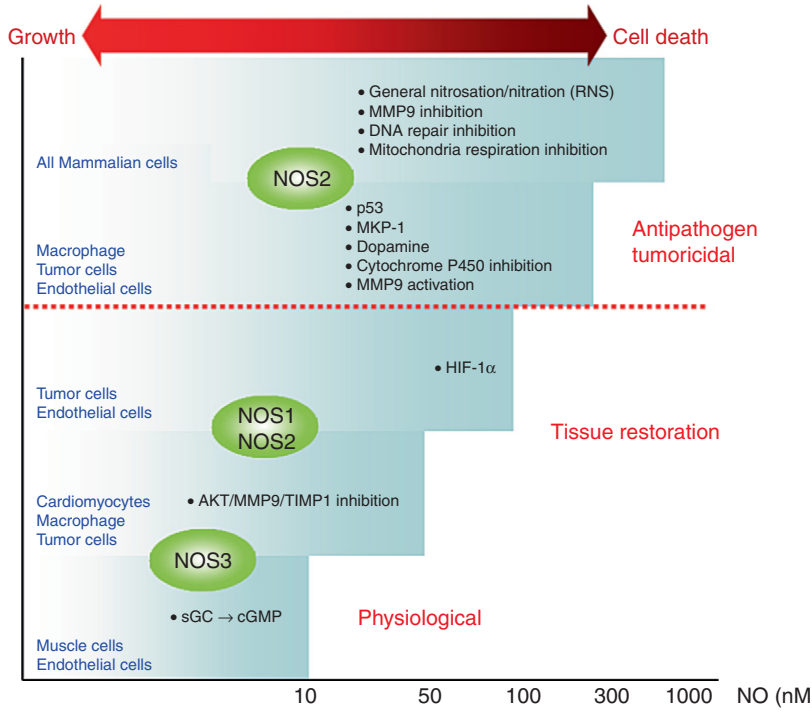

Figure 6 NO levels determine effects. The molecular levels of NO determine its effects to the surrounding cells. Low levels (<10 nM) of NO are required to maintain physiological function in muscle and endothelial cells. Fifty nanometres of sustained NO is associated with increased cGMP-mediated ERK phosphorylation, where intermediate sustained concentrations (>100 nM) lead to HIF-1α stabilization, and high sustained concentrations of NO (>300 nM) increase p53-P(ser-15), which persisted even after NO drops below these concentrations.

[85]. Interestingly, high levels which mediate the tumorcidial activity in leukemic cells requires wild-type p53 [86]. Indeed, tumor phagocyte density and aberrant p53 expression correlated significantly with the phosphorylation of Akt at ser-473 in human breast cancer tissue [87]. Similarly, co-localization of p53-P-(ser-15) and iNOS protein expression in human samples of ulcerative colitis indicate that NO causes a p53 pathway activation in humans [82]. Therefore, some aspect of NO as tumoricidal agent or promoting of cancer depends on p53 status.

Another important aspect in signaling involves the temporal properties of NO. Though NO is short lived, the sustained NO flux generated by NOS can vary in duration from seconds to days. NO-mediated HIF-1α stabilization correlates directly with concentration and time [80]. While pERK increases immediately in response to NO, it also transiently decreases despite the maintenance of steady-state NO levels. Moreover,

NO-induced p53 phosphorylation remains stably elevated even after the dissipation of steady-state NO. Thus, signaling responses to NO are temporally and spatially defined [80].

13. Fluxes of NO in cells and *in vivo*

Although NO elicits many unique cellular responses *in vitro*, the question remains: are these NO concentrations and conditions actually achievable *in vivo*? Several studies have looked at *in vivo* concentrations of NO under different biological conditions by different methods [88,89]. One method to address this question is to compare the cellular response to NO generated from NO-donor compounds with responses from NO generated from NOS. Correlating these two different sources of NO provides an approximation of the *in vivo* NO concentrations necessary to elicit specific cellular responses. Using this "molecular signature" approach for various concentration levels of NO, a picture of the redox environment under specific biological conditions can be ascertained. Previous studies using MCF-7 cells co-cultured with activated NO-producing ANA-1 murine macrophages show increases in the phosphorylation of Akt, and p53 as well as stabilization of HIF-1α as discussed above [82,85,87]. Increases in the macrophage to tumor cell ratio led to a proportional increase in the measured NO in bulk solution which increased Akt then HIF-1α and then p53 at the highest macrophage concentration [85,87]. As discussed above, when NO donors were employed for NO delivery, the concentration of NO necessary to induce p53 phosphorylation was >400 nM while with the macrophage and tumor cell co-culture the level was only >160 nM [85]. This discrepancy can be rectified by considering that NO generated from NO donors is uniformly distributed throughout the media, whereas, the enzymatic production of NO from macrophage generates a concentration gradient emanating from the point of origin. Therefore the close proximity of the macrophages and the tumor cell indicate that a much higher local NO concentration than 160 nM and the local flux is 400 nM [85,86,90], the minimum amount of NO necessary to cause p53 phosphorylation [85].

14. Nitric oxide, Cancer, and p53

Under inflammatory conditions, several studies have shown an increase in both p53 and NOS2 expression [82]. Furthermore, over 60% of cancers are reported to have a disruption in their p53 signaling [91]. As discussed below, there is an important relationship between p53 and NO. It has been shown that p53 can directly inhibit NOS2 activity by binding and

decreasing its activity [92]. But when there is a high level of NO, the p53 phosphorylation and acetylation are increased [82]. This finding has important consequences for apoptotic and DNA repair mechanisms. In p53 mutated or p53 null cells, there is dysregulation in cell cycle. p53 mutated cells are far less susceptible to apoptosis and this leads to a higher rate of mutation, and increased survival. On the other hand, the leukemic cells that were p53 wild type that are influenced by macrophage-derived NO were more likely to undergo apoptosis [86]. This is borne out in the p53–/– and NOS2–/– animals, which have a dramatic increase in leukemia [93]. Therefore, NO ability for tumorigenicity and DNA repair are influenced by the p53 status.

15. The Paradigm of NO/cGMP and its Inhibitor TSP-1

In 2005, we showed that low (<2 nM) steady-state NO mediated 50% suppression of the antiangiogenic factor thrombospondin-1 (TSP-1) in endothelial cells, which was both cGMP and ERK dependent, and inhibited by the exogenous TSP-1. MKP-1 phosphatase expression levels were elevated when NO concentrations increased to ~100 nM. At the same time, there is a decrease in phosphorylated ERK and subsequently incremental increases in TSP-1 levels were observed. Hence, we identified an important cross-talk relationship between proangiogenic NO and antiangiogenic TSP-1 [84]. These molecules are mutually antagonistic and provide a critical balance in many processes related to inflammation and wound healing. TSP-1 is a large glycoprotein secreted by various cells under stress conditions such as those found in ischemic injury. This protein engages several cell surface receptors through which it elicits different effects on cells in the cardiovascular and immune systems. One of the major functions of this protein pertains to its inhibitory affects of adhesion, motility, growth, and survival of endothelial cells [94,95]. In addition to regulating endothelial cell growth, TSP-1 also regulates T cells, monocytes, and macrophage differentiation, and therefore has critical functions during innate and adaptive immunity [96,97].

This cross-talk relationship was then extended to demonstrate dramatically improved tissue survival in skin flap, hind-limb ischemia, and radiation injury models. A protective response was observed in TSP-1 null mice exposed to ischemic injury, suggesting improved NO vascular response in the absence of systemic TSP-1 [98]. Moreover, when the TSP-1 null mouse was exposed to an NO donor, nearly complete tissue preservation following ischemic injury can be observed. TSP-1 null mice also demonstrated an enhanced protection against soft tissue radiation

injury [99]. These results demonstrate the *in vivo* existence of NO/TSP-1 cross talk; reduction of endogenous TSP-1 would increase NO-mediated vascular response culminating in dramatically improved wound healing following ischemic injury. NO/TSP-1 antagonism is mediated by CD47 cell surface receptor, and affects NO/cGMP signaling. During ischemia, NO donors provide abatement of numerous mechanisms that increase flow and reduce leukocyte recruitment of neutrophils and macrophages, which are M1 polarized. In addition to increase blood flow, NO also induces an antiapoptotic response in the cell. Thus, reduction of TSP-1 increases the bioavailability and efficacy of the protective effects of NO. However, ischemic injury results in increased TSP1 expression that effectively blocks the beneficial activity of NO. Thus, agents that either suppress TSP1 or prevent its interaction with CD47 would dramatically improve survival of fixed ischemic injuries as well as ischemia/reperfusion injury [100,101].

16. Role of NO in Matrix Reorganization and Angiogenesis

Tumor angiogenesis, growth, and metastasis all require matrix degradation and remodeling to facilitate cell migration and neovascularization processes. Three major groups of proteases that regulate angiogenesis are MMPs, cathepsin cysteine proteases, and serine proteases. Among the MMPs, MT1-MMP, MMP-2, and MMP-9 are considered the most important regulators of angiogenesis in many diseases including cancer [102,103]. We have shown NO regulation of MMP-9 in murine macrophages, which involved cGMP/pERK-mediated suppression of TIMP-1 [104]. In addition, higher NO concentrations such as those present in activated macrophages would suppress MMP-9 activity, due to the nitrosation of the enzyme, and provides a unique mechanism for regulation of this zymogen. Importantly, NO activation of MMP-9 in macrophage-conditioned media stimulated vascular cell migration in a muscle explant angiogenesis assay, which was inhibited by the silencing of macrophage MMP-9 protein translation prior to NO exposure. It was further shown that exogenous TSP-1 blocked both NO-mediated MMP activation and TIMP-1 suppression. Thus, TSP-1 suppresses NO-mediated angiogenic responses in both macrophage and endothelial cell models.

Following injury, macrophages are recruited into the wounded tissue bed during the initial stage of inflammation. A previous report has shown that TSP-1 overexpression in human melanoma cells increases ROS production and M1 differentiated macrophage recruitment in tumor xenografts. This observation demonstrates a role of TSP-1 in antitumor

immunity and therefore suggests a selection which favors the loss of TSP-1 during cancer progression [97]. During Th1/Th2 transition of wound response, NO will scavenge ROS as well as suppress TSP-1, which suggests that NO donors could decrease M1 polarization and trigger M2 resolution phase and tissue restoration. We believe this concept will prove to be important in chronic inflammation as it is associated with the progression and cancer therapy, and will provide new opportunities in drug development.

17. Nitric Oxide and Matrix Metalloproteinases

MMPs are important mediators of inflammation, angiogenesis, wound response, and carcinogenesis [102,103,105,106]. MMPs are tightly regulated, primarily at the levels of transcription and posttranslation and are targeted by ROS and RNS at both these levels [107–109]. While contradictory results have been reported with respect to redox regulation of MMPs, the ability of ROS and RNS to biphasically regulate MMP activity has been reported and suggests a critical role of these species in the spatial and temporal regulation of MMPs during matrix remodeling [110–112]. Toward this end, the biphasic and dose-dependent regulation of matrilysin (MMP-7) by HOCl, initially demonstrated by Peppin and Weiss [110] involved oxidation of the cysteine switch at low HOCl concentrations that mediated activation of the zymogen [111]. Higher HOCl concentrations inactivated the enzyme by chlorination/oxidation of adjacent tryptophan–glycine residues within the catalytic domain, leading to structural modifications that impeded substrate binding at the active site cleft [113,114]. The physiologic relevance of oxidant-mediated MMP inactivation was later demonstrated using gp91phox knockouts in a murine model of emphysema [115]. Macrophage-derived NO has also been shown to biphasically modulate the activity of MMPs. A recent report demonstrated both biological and chemical mechanisms of MMP activation by macrophage-derived NO [112]. MMP activity (MMP-9, -1, and -13) secreted from macrophages increased in response to low steady-state NO levels (~50 nM) via cGMP-mediated suppression of the endogenous tissue inhibitor of metalloproteinase-1 (TIMP-1) [112]. Exposure of purified latent MMP-9 to exogenous NO demonstrated a concentration-dependent activation ($\geq$500 nM) and inactivation ($>1\,\mu M$) of the enzyme, which occurred at higher NO flux. These chemical reactions occurred at concentrations similar to that of activated macrophages. Interestingly, inactivation of TIMP-1 by HOCl has also been

reported, again suggesting multiple mechanisms for oxidant regulation of MMPs during matrix remodeling [116]. In an epithelial wound model, low NO levels similarly increased MMP-9 mRNA, which translated to enhanced enzymatic activity [117]. Together, these results suggest that NO regulation of MMP-9 secreted from macrophages may occur chemically by RNS-mediated protein modification or biologically through sGC-dependent modulation of the MMP-9/TIMP-1 balance.

18. Potential Agents that Modulate NO

Certain agents provide an opportunity for reversing pathways that involve NO. The first and most obvious are NOS inhibitors. The second is not as obvious and involves the use of NO donors. The third is targeting pathway nodes downstream. All have advantages and disadvantages where NOS inhibitors can reduce blood flow from tumor, while NO donors can reduce blood pressure. Targeting a single pathway can also be problematic in that cancer progression and metastasis always involve numerous complimentary pathways. Nonetheless, cytotoxic agents, surgical approaches, and radiation therapy are still essential procedures and therapies beyond this will be complimentary to these effects.

While NO has multiple roles in carcinogenesis, NO donors or NOS inhibitors can affect conventional therapy such as radiation and chemotherapy. A limiting factor in radiation treatment of solid tumors is low oxygen *in vivo*. In 1957 Howard Flanders demonstrated radiosensitization of *Escherichia coli*, grown under hypoxic conditions, by O_2 and NO [118]. Several decades later it was found that NO performs nearly as well as O_2 in the radiosensitization of hypoxic mammalian cells [119].

In vivo, local administration of NO donors prior to radiation would enhance tumor blood flow and oxygenation, resulting in a modest radiosensitization of the tumor [120] or sensitize tumor cells to chemotherapeutic compounds with particular alkylating agents [121]. NO donors also sensitize tumor cells to cisplatin and melphalan toxicities which persisted for several hours after NO treatment [122,123]. Similarly, iNOS gene therapy in combination with an inducible promoter also caused tumor radiosensitization *in vivo* [124] while eNOS knockout animals showed decreased sensitization [125]. Interestingly, NOS inhibition also enhances radiation response of animal xenografts if given post-irradiation by modulation of the tumor's wound response [126]. These studies further indicate the temporal importance of NO modulation in tumor outcome.

19. Conclusion

Compelling evidence that a significant number of diseases and conditions have features of altered NO metabolism that may be expected to affect biological properties, such as inflammation, wound healing, and carcinogenesis have been reviewed here. Over the years, NO has firmly been established as a potent redox molecule, influencing a myriad of physiological and pathophysiological processes through various pathways and reactions. Connecting and understanding the alterations in NO metabolism observed in different diseases or conditions would be the main challenge in the NO arena.

A deeper understanding of the biochemical pathways that dictate NO availability and levels will also be required in order to optimize the beneficial functions of NO, while limiting the formation of more damaging RNS or triggering untoward pathways. Lastly, more in-depth investigations between NO and inflammation will no doubt benefit our understanding of the carcinogenesis (and other diseases) process and may shine a light on how to cure the "the wound that does not heal."

REFERENCES

[1] R.F. Furchgott, J.V. Zawadzki, The obligatory role of endothelial cells in the relaxation of arterial smooth muscle by acetylcholine, Nature 288 (1980) 373–376.
[2] D.A. Wink, L.A. Ridnour, S.P. Hussain, C.C. Harris, The reemergence of nitric oxide and cancer, Nitric Oxide 19 (2008) 65–67.
[3] J.E. Goodman, L.J. Hofseth, S.P. Hussain, C.C. Harris, Nitric Oxide and p53 in cancer-prone chronic inflammation and oxyradical overload disease, Environ. Mol. Mutagen. 44 (2004) 3–9.
[4] D.A. Wink, Y. Vodovotz, J. Laval, F. Laval, M.W. Dewhirst, J.B. Mitchell, The multifaceted roles of nitric oxide in cancer, Carcinogenesis 19 (1998) 711–721.
[5] L.A. Ridnour, D.D. Thomas, S. Donzelli, M.G. Espey, D.D. Roberts, D.A. Wink, J.S. Isenberg, The biphasic nature of nitric oxide responses in tumor biology, Antioxid. Redox. Signal 8 (2006) 1329–1337.
[6] D.J. Stuehr, Structure-function aspects in the nitric oxide synthases, Annu. Rev. Pharmacol. Toxicol. 37 (1997) 339–359.
[7] S.P. Hussain, C.C. Harris, Inflammation and cancer: an ancient link with novel potentials, Int. J. Cancer 121 (2007) 2373–2380.
[8] F.H. Guo, H.R. De Raeve, T.W. Rice, D.J. Stuehr, F.B. Thunnissen, S.C. Erzurum, Continuous nitric oxide synthesis by inducible nitric oxide synthase in normal human airway epithelium in vivo, Proc. Natl. Acad. Sci. U. S. A. 92 (1995) 7809–7813.
[9] S. Ito, O.A. Carretero, K. Abe, Role of nitric oxide in the control of glomerular microcirculation, Clin. Exp. Pharmacol. Physiol. 24 (1997) 578–581.
[10] S. Ekmekcioglu, C.H. Tang, E.A. Grimm, NO news is not necessarily good news in cancer, Curr. Cancer Drug Targets 5 (2005) 103–115.

[11] D.A. Wink, J.B. Mitchell, Nitric oxide and cancer: An introduction, Free Radic. Biol. Med. 34 (2003) 951–954.
[12] D.A. Wink, I. Hanbauer, M.B. Grisham, F. Laval, R.W. Nims, J. Laval, J. Cook, R. Pacelli, J. Liebmann, M. Krishna, P.C. Ford, J.B. Mitchell, The chemical biology of NO. Insights into regulation, protective and toxic mechanisms of nitric oxide, Curr. Top. Cell. Regul. 34 (1996) 159–187.
[13] D.A. Wink, J.B. Mitchell, Chemical biology of nitric oxide: Insights into regulatory, cytotoxic, and cytoprotective mechanisms of nitric oxide, Free Radic. Biol. Med. 25 (1998) 434–456.
[14] S.D. Cline, J.N. Riggins, S. Tornaletti, L.J. Marnett, P.C. Hanawalt, Malondialdehyde adducts in DNA arrest transcription by T7 RNA polymerase and mammalian RNA polymerase II, Proc. Natl. Acad. Sci. U. S. A. 101 (2004) 7275–7280.
[15] J.D. West, C. Ji, S.T. Duncan, V. Amarnath, C. Schneider, C.J. Rizzo, A.R. Brash, L.J. Marnett, Induction of apoptosis in colorectal carcinoma cells treated with 4-hydroxy-2-nonenal and structurally related aldehydic products of lipid peroxidation, Chem. Res. Toxicol. 17 (2004) 453–462.
[16] L.A. Ridnour, D.D. Thomas, D. Mancardi, M.G. Espey, K.M. Miranda, N. Paolocci, M. Feelisch, J. Fukuto, D.A. Wink, The chemistry of nitrosative stress induced by nitric oxide and reactive nitrogen oxide species. Putting perspective on stressful biological situations, Biol. Chem. 385 (2004) 1–10.
[17] D.A. Wink, J.A. Cook, S. Kim, Y. Vodovotz, R. Pacelli, M.C. Kirshna, A. Russo, J.B. Mitchell, D. Jourd'heuil, A.M. Miles, M.B. Grisham, Superoxide modulates the oxidation and nitrosation of thiols by nitric oxide derived reactive intermediates, J. Biol. Chem. 272 (1997) 11147–11151.
[18] D. Jourd'heuil, K.M. Miranda, S.M. Kim, M.G. Espey, Y. Vodovotz, S. Laroux, C.T. Mai, A.M. Miles, M.B. Grisham, D.A. Wink, The oxidative and nitrosative chemistry of the nitric oxide/superoxide reaction in the presence of bicarbonate, Arch. Biochem. Biophys. 365 (1999) 92–100.
[19] M.G. Espey, S. Xavier, D.D. Thomas, K.M. Miranda, D.A. Wink, Direct real-time evaluation of nitration with green fluorescent protein in solution and within human cells reveals the impact of nitrogen dioxide vs. peroxynitrite mechanisms, Proc. Natl. Acad. Sci. U. S. A. 99 (2002) 3481–3486.
[20] M.G. Espey, D.D. Thomas, K.M. Miranda, D.A. Wink, Focusing of nitric oxide mediated nitrosation and oxidative nitrosylation as a consequence of reaction with superoxide, Proc. Natl. Acad. Sci. U. S. A. 99 (2002) 11127–11132.
[21] K. Turpaev, C. Bouton, J.C. Drapier, Nitric oxide-derived nitrosating species and gene expression in human monocytic cells, Biochemistry 43 (2004) 10844–10850.
[22] Y. Vodovotz, L. Chesler, H. Chong, S.J. Kim, J.T. Simpson, W. DeGraff, G.W. Cox, A.B. Roberts, D.A. Wink, M.H. Barcellos-Hoff, Regulation of transforming growth factor beta1 by nitric oxide, Cancer Res. 59 (1999) 2142–2149.
[23] B.N. Ames, L.S. Gold, W.C. Willett, The causes and prevention of cancer, Proc. Natl. Acad. Sci. U. S. A. 92 (1995) 5258–5265.
[24] M.E. Turini, R.N. DuBois, Cyclooxygenase-2: A therapeutic target, Annu. Rev. Med. 53 (2002) 35–57.
[25] S.P. Hussain, P. Amstad, K. Raja, S. Ambs, M. Nagashima, W.P. Bennett, P.G. Shields, A.J. Ham, J.A. Swenberg, A.J. Marrogi, C.C. Harris, Increased p53 mutation load in noncancerous colon tissue from ulcerative colitis: A cancer-prone chronic inflammatory disease, Cancer Res. 60 (2000) 3333–3337.
[26] C.A. Colton, Heterogeneity of microglial activation in the innate immune response in the brain, J. Neuroimmune Pharmacol. 4 (2009) 399–418.
[27] E.Y. Lin, J.W. Pollard, Macrophages: Modulators of breast cancer progression, Novartis Found. Symp. 256 (2004) 158–168; discussion 168–172, 259–269.

[28] S.O. Hofer, G. Molema, R.A. Hermens, H.J. Wanebo, J.S. Reichner, H.J. Hoekstra, The effect of surgical wounding on tumour development, Eur. J. Surg. Oncol. 25 (1999) 231–243.
[29] J. Riss, C. Khanna, S. Koo, G.V. Chandramouli, H.H. Yang, Y. Hu, D.E. Kleiner, A. Rosenwald, C.F. Schaefer, S.A. Ben-Sasson, L. Yang, J. Powell, D.W. Kane, R.A. Star, O. Aprelikova, K. Bauer, J.R. Vasselli, J.K. Maranchie, K.W. Kohn, K.H. Buetow, W.M. Linehan, J.N. Weinstein, M.P. Lee, R.D. Klausner, J.C. Barrett, Cancers as wounds that do not heal: Differences and similarities between renal regeneration/repair and renal cell carcinoma, Cancer Res. 66 (2006) 7216–7224.
[30] L.C. Green, K. Ruiz de Luzuriaga, D.A. Wagner, W. Rand, N. Istfan, V.R. Young, S.R. Tannenbaum, Nitrate biosynthesis in man, Proc. Natl. Acad. Sci. U. S. A. 78 (1981) 7764–7768.
[31] J.S. Wishnok, S.R. Tannenbaum, W.G. Stillwell, J.A. Glogowski, C.D. Leaf, Urinary markers for exposures to alkylating or nitrosating agents, Environ. Health Perspect. 99 (1993) 155–159.
[32] R.H. Liu, J.R. Jacob, B.D. Tennant, J.H. Hotchkiss, Nitrite and nitrosamine synthesis by hepatocytes isloated from normal woodchucks (Marmota monax) and woodchucks chronically infected with woochuck hepatitis virus, Cancer Res. 52 (1992) 4139–4143.
[33] F. Laval, D.A. Wink, J. Laval, "A discussion of mechanisms of NO genotoxicty. Implication of inhibtion of DNA repair proteins, Rev. Physiol. Biochem. Pharmacol. 131 (1996) 175–191.
[34] D.C. Jenkins, I.G. Charles, L.L. Thomsen, D.W. Moss, L.S. Holmes, S.A. Baylis, P. Rhodes, K. Westmore, P.C. Emson, S. Moncada, Roles of nitric oxide in tumor growth, Proc. Natl. Acad. Sci. U. S. A. 92 (1995) 4392–4396.
[35] D.C. Jenkins, I.G. Charles, S.A. Baylis, R. Lelchuk, M.W. Radomski, S. Moncada, Human colon cancer cell lines show a diverse pattern of nitric oxide synthase gene expression and nitric oxide generation, Br. J. Cancer 70 (1994) 847–849.
[36] L.L. Thomsen, F.G. Lawton, R.G. Knowles, J.E. Beesley, V. Riveros-Moreno, and S. Moncada, Nitric oxide synthase activity in human gynecological cancer, Cancer Res. 54 (1994) 1352–1354.
[37] L.L. Thomsen, D.W. Miles, L. Happerfield, L.G. Bobrow, R.G. Knowles, S. Moncada, Nitric oxide synthase activity in human breast cancer, Br. J. Cancer 72 (1995) 41–44.
[38] K. Xie, Z. Dong, I.J. Fidler, Activation of nitric oxide synthase gene for inhibition of cancer metastasis, J. Leukoc. Biol. 59 (1996) 797–803.
[39] K. Xie, S. Huang, Z. Dong, S.H. Juang, M. Gutman, e.Q.W. Xi, C. Nathan, I.J. Fidler, Transfection with the inducible nitric oxide synthase gene suppresses tumorigenicity and abrogates metastasis by K-1735 murine melanoma cells. J. Exp. Med. 181 (1995) 1333–1343.
[40] M.A. Anttila, K. Voutilainen, S. Merivalo, S. Saarikoski, V.M. Kosma, Prognostic significance of iNOS in epithelial ovarian cancer, Gynecol. Oncol. 105 (2007) 97–103.
[41] A. Puhakka, V. Kinnula, U. Napankangas, M. Saily, P. Koistinen, P. Paakko, Y. Soini, High expression of nitric oxide synthases is a favorable prognostic sign in non-small cell lung carcinoma, APMIS 111 (2003) 1137–1146.
[42] K.M. Lee, J.Y. Choi, J.E. Lee, D.Y. Noh, S.H. Ahn, W. Han, K.Y. Yoo, R.B. Hayes, D. Kang, Genetic polymorphisms of NOS3 are associated with the risk of invasive breast cancer with lymph node involvement, Breast Cancer Res. Treat. 106 (2007) 433–438.
[43] H.H. Chen, W.C. Su, C.Y. Chou, H.R. Guo, S.Y. Ho, J. Que, W.Y. Lee, Increased expression of nitric oxide synthase and cyclooxygenase-2 is associated with poor

survival in cervical cancer treated with radiotherapy, Int. J. Radiat. Oncol. Biol. Phys. 63 (2005) 1093–1100.
[44] N. Tanriover, M.O. Ulu, C. Isler, H. Durak, B. Oz, M. Uzan, Z. Akar, Neuronal nitric oxide synthase expression in glial tumors: Correlation with malignancy and tumor proliferation, Neurol. Res. 30 (2008) 940–944.
[45] L. Wang, G.G. Shi, J.C. Yao, W. Gong, D. Wei, T.T. Wu, J.A. Ajani, S. Huang, K. Xie, Expression of endothelial nitric oxide synthase correlates with the angiogenic phenotype of and predicts poor prognosis in human gastric cancer, Gastric Cancer 8 (2005) 18–28.
[46] A.S. Bulut, E. Erden, S.D. Sak, H. Doruk, N. Kursun, D. Dincol, Significance of inducible nitric oxide synthase expression in benign and malignant breast epithelium: An immunohistochemical study of 151 cases, Virchows Arch 447 (2005) 24–30.
[47] L.G. Li, H.M. Xu, Inducible nitric oxide synthase, nitrotyrosine and apoptosis in gastric adenocarcinomas and their correlation with a poor survival, World J. Gastroenterol. 11 (2005) 2539–2544.
[48] J. Shen, R.T. Wang, L.W. Wang, Y.C. Xu, X.R. Wang, A novel genetic polymorphism of inducible nitric oxide synthase is associated with an increased risk of gastric cancer, World J. Gastroenterol. 10 (2004) 3278–3283.
[49] C.N. Chen, F.J. Hsieh, Y.M. Cheng, K.J. Chang, P.H. Lee, Expression of inducible nitric oxide synthase and cyclooxygenase-2 in angiogenesis and clinical outcome of human gastric cancer, J. Surg. Oncol. 94 (2006) 226–233.
[50] M. Matsumoto, M. Furihata, A. Kurabayashi, K. Araki, S. Sasaguri, Y. Ohtsuki, Association between inducible nitric oxide synthase expression and p53 status in human esophageal squamous cell carcinoma, Oncology 64 (2003) 90–96.
[51] S.H. Aaltoma, P.K. Lipponen, V.M. Kosma, Inducible nitric oxide synthase (iNOS) expression and its prognostic value in prostate cancer, Anticancer Res. 21 (2001) 3101–3106.
[52] S. Ekmekcioglu, J. Ellerhorst, C.M. Smid, V.G. Prieto, M. Munsell, A.C. Buzaid, E.A. Grimm, Inducible nitric oxide synthase and nitrotyrosine in human metastatic melanoma tumors correlate with poor survival, Clin. Cancer Res. 6 (2000) 4768–4775.
[53] S. Ekmekcioglu, J.A. Ellerhorst, V.G. Prieto, M.M. Johnson, L.D. Broemeling, E.A. Grimm, Tumor iNOS predicts poor survival for stage III melanoma patients, Int. J. Cancer 119 (2006) 861–866.
[54] H. Shigyo, S. Nonaka, A. Katada, N. Bandoh, T. Ogino, A. Katayama, M. Takahara, T. Hayashi, Y. Harabuchi, Inducible nitric oxide synthase expression in various laryngeal lesions in relation to carcinogenesis, angiogenesis, and patients' prognosis, Acta Otolaryngol. 127 (2007) 970–979.
[55] M.H. Sun, X.C. Han, M.K. Jia, W.D. Jiang, M. Wang, H. Zhang, G. Han, Y. Jiang, Expressions of inducible nitric oxide synthase and matrix metalloproteinase-9 and their effects on angiogenesis and progression of hepatocellular carcinoma, World J. Gastroenterol. 11 (2005) 5931–5937.
[56] M.C. Levesque, Y. Chen, B.E. Beasley, C.W. O'Loughlin, J.P. Gockerman, J.O. Moore, J.B. Weinberg, Chronic lymphocytic leukemia cell CD38 expression and inducible nitric oxide synthase expression are associated with serum IL-4 levels, Leuk. Res. 30 (2006) 24–28.
[57] J.D. Brenton, L.A. Carey, A.A. Ahmed, C. Caldas, Molecular classification and molecular forecasting of breast cancer: Ready for clinical application? J. Clin. Oncol. 23 (2005) 7350–7360.
[58] S.A. Paul, J.W. Simons, N.J. Mabjeesh, HIF at the crossroads between ischemia and carcinogenesis. J. Cell Physiol. 200 (2004) 20–30.

[59] D.M. Brizel, G.S. Sibley, L.R. Prosnitz, R.L. Scher, M. Dewhirst, Tumor hypoxia adversely affects the prognosis of carcinoma of the head and neck, Int. J. Radiat. Oncol. Biol. Phys. 38 (1997) 285–289.
[60] K.S. Siveen, G. Kuttan, Role of macrophages in tumour progression, Immunol. Lett. 123 (2009) 97–102.
[61] J.I. Arias, M.A. Aller, F. Sanchez-Patan, J. Arias, Inflammation and cancer: Is trophism the link? Surg. Oncol. 15 (2006) 235–242.
[62] C.A. Colton, D.M. Wilcock, Assessing activation states in microglia, CNS Neurol. Disord. Drug Targets (2009). Oct 7. [Epub ahead of print].
[63] F.O. Martinez, A. Sica, A. Mantovani, M. Locati, Macrophage activation and polarization, Front. Biosci. 13 (2008) 453–461.
[64] K. Hall, S. Ran, Regulation of tumor angiogenesis by the local environment, Front. Biosci. 15 (2010) 195–212.
[65] R. Kalluri, EMT: When epithelial cells decide to become mesenchymal-like cells. J. Clin. Invest. 119 (2009) 1417–1419.
[66] C.W. Leffler, H. Parfenova, J.H. Jaggar, R. Wang, Carbon monoxide and hydrogen sulfide: Gaseous messengers in cerebrovascular circulation, J. Appl. Physiol. 100 (2006) 1065–1076.
[67] A. Schwentker, Y. Vodovotz, R. Weller, T.R. Billiar, Nitric oxide and wound repair: role of cytokines? Nitric Oxide 7 (2002) 1–10.
[68] A.M. Malkinson, Role of inflammation in mouse lung tumorigenesis: A review, Exp. Lung. Res. 31 (2005) 57–82.
[69] P.V. Vignais, The superoxide-generating NADPH oxidase: Structural aspects and activation mechanism, Cell Mol. Life Sci. 59 (2002) 1428–1459.
[70] A.M. Miles, M. Gibson, M. Krishna, J.C. Cook, R. Pacelli, D.A. Wink, M.B. Grisham, Effects of superoxide on nitric oxide-dependent N-nitrosation reactions, Free Radic. Res. 233 (1995) 379–390.
[71] D. Morse, A.M. Choi, Heme oxygenase-1: The "emerging molecule" has arrived, Am. J. Respir. Cell Mol. Biol. 27 (2002) 8–16.
[72] M. Bhatia, Hydrogen sulfide as a vasodilator, IUBMB Life 57 (2005) 603–606.
[73] D. Mancardi, C. Penna, A. Merlino, P. Del Soldato, D.A. Wink, P. Pagliaro, Physiological and pharmacological features of the novel gasotransmitter: Hydrogen sulfide, Biochim. Biophys. Acta (2009). Acta 1787(7) (2009) 864–872. [Epub 2009 Mar 13].
[74] M.A. Marletta, Mammalian synthesis of nitrite, nitrate, nitric oxide and N-nitrosating agents, Chem. Res. Toxicol. 1 (1988) 249–257.
[75] R.H. Liu, J.H. Hotchkiss, Potential genotoxicity of chronically elevated nitric oxide: A review, Mutat. Res. 339 (1995) 73–89.
[76] J.R. Lancaster, J.B. Hibbs, EPR demonstration of iron-nitrosyl complex formation by cytotoxic activated macrophages, Proc. Natl. Acad. Sci. U. S. A. 87 (1990) 1223–1227.
[77] M.G. Espey, K.M. Miranda, R.M. Pluta, D.A. Wink, Nitrosative capacity of macrophages is dependent on nitric-oxide synthase induction signals, J. Biol. Chem. 275 (2000) 11341–11347.
[78] L. Connelly, A.T. Jacobs, M. Palacios-Callender, S. Moncada, A.J. Hobbs, Macrophage endothelial nitric-oxide synthase autoregulates cellular activation and pro-inflammatory protein expression, J. Biol. Chem. 278 (2003) 26480–26487.
[79] R. Ogawa, R. Pacelli, M.G. Espey, K.M. Miranda, N. Friedman, S.M. Kim, G. Cox, J.B. Mitchell, D.A. Wink, A. Russo, Comparison of control of Listeria by nitric oxide redox chemistry from murine macrophages and NO donors: Insights into listeriocidal activity of oxidative and nitrosative stress, Free Radic. Biol. Med. 30 (2001) 268–276.

[80] D.D. Thomas, L.A. Ridnour, J.S. Isenberg, W. Flores-Santana, C.H. Switzer, S. Donzelli, P. Hussain, C. Vecoli, N. Paolocci, S. Ambs, C.A. Colton, C.C. Harris, D.D. Roberts, D.A. Wink, The chemical biology of nitric oxide: implications in cellular signaling, Free Radic. Biol. Med. 45 (2008) 18–31.
[81] L.A. Ridnour, D.D. Thomas, C. Switzer, W. Flores-Santana, J.S. Isenberg, S. Ambs, D.D. Roberts, D.A. Wink, Molecular mechanisms for discrete nitric oxide levels in cancer, Nitric Oxide 19 (2008) 73–76.
[82] L.J. Hofseth, S. Saito, S.P. Hussain, M.G. Espey, K.M. Miranda, Y. Araki, C. Jhappan, Y. Higashimoto, P. He, S.P. Linke, M.M. Quezado, I. Zurer, V. Rotter, D.A. Wink, E. Appella, C.C. Harris, Nitric oxide-induced cellular stress and p53 activation in chronic inflammation, Proc. Natl. Acad. Sci. U. S. A. 100 (2003) 143–148.
[83] S. Pervin, R. Singh, W.A. Freije, G. Chaudhuri, MKP-1-induced dephosphorylation of extracellular signal-regulated kinase is essential for triggering nitric oxide-induced apoptosis in human breast cancer cell lines: Implications in breast cancer, Cancer Res. 63 (2003) 8853–8860.
[84] L.A. Ridnour, J.S. Isenberg, M.G. Espey, D.D. Thomas, D.D. Roberts, D.A. Wink, Nitric oxide regulates angiogenesis through a functional switch involving thrombospondin-1, Proc. Natl. Acad. Sci. U. S. A. 102 (2005) 13147–13152.
[85] D.D. Thomas, M.G. Espey, L.A. Ridnour, L.J. Hofseth, D. Mancardi, C.C. Harris, D.A. Wink, Hypoxic inducible factor 1alpha, extracellular signal-regulated kinase, and p53 are regulated by distinct threshold concentrations of nitric oxide, Proc. Natl. Acad. Sci. U. S. A. 101 (2004) 8894–8899.
[86] C. Wang, L.J. Trudel, G.N. Wogan, W.M. Deen, Thresholds of nitric oxide-mediated toxicity in human lymphoblastoid cells, Chem. Res. Toxicol. 16 (2003) 1004–1013.
[87] R.L. Prueitt, B.J. Boersma, T.M. Howe, J.E. Goodman, D.D. Thomas, L. Ying, C.M. Pfiester, H.G. Yfantis, J.R. Cottrell, D.H. Lee, A.T. Remaley, L.J. Hofseth, D.A. Wink, S. Ambs, Inflammation and IGF-I activate the Akt pathway in breast cancer, Int. J. Cancer 120 (2007) 796–805.
[88] X. Zhang, Real time and in vivo monitoring of nitric oxide by electrochemical sensors—from dream to reality, Front. Biosci. 9 (2004) 3434–3446.
[89] M.M. Tarpey, D.A. Wink, M.B. Grisham, Methods for detection of reactive metabolites of oxygen and nitrogen: In vitro and in vivo considerations, Am. J. Physiol. Regul. Integr. Comp. Physiol. 286 (2004) R431–R444.
[90] M. Laurent, M. Lepoivre, J.P. Tenu, Kinetic modelling of the nitric oxide gradient generated in vitro by adherent cells expressing inducible nitric oxide synthase, Biochem. J. 314 (1996) 109–113.
[91] M.S. Colman, C.A. Afshari, J.C. Barrett, Regulation of p53 stability and activity in response to genotoxic stress, Mutat. Res. 462 (2000) 179–188.
[92] K. Forrester, S. Ambs, S.E. Lupold, R.B. Kapust, E.A. Spillare, W.C. Weinberg, E. Felley-Bosco, X.W. Wang, D.A. Geller, E. Tzeng, T. Billiar, C.C. Harris, Nitric oxide-induced p53 accumulation and regulation of inducible nitric oxide synthase expression by wild-type p53, Proc. Natl. Acad. Sci. U. S. A. 93 (1996) 2442–2447.
[93] S.P. Hussain, P. He, J. Subleski, L.J. Hofseth, G.E. Trivers, L. Mechanic, A.B. Hofseth, M. Bernard, J. Schwank, G. Nguyen, E. Mathe, D. Djurickovic, D. Haines, J. Weiss, T. Back, E. Gruys, V.E. Laubach, R.H. Wiltrout, C.C. Harris, Nitric oxide is a key component in inflammation-accelerated tumorigenesis, Cancer Res. 68 (2008) 7130–7136.
[94] G. Taraboletti, D. Roberts, L.A. Liotta, R. Giavazzi, Platelet thrombospondin modulates endothelial cell adhesion, motility, and growth: A potential angiogenesis regulatory factor, J. Cell. Biol. 111 (1990) 765–772.

[95] N. Guo, H.C. Krutzsch, J.K. Inman, D.D. Roberts, Thrombospondin 1 and type I repeat peptides of thrombospondin 1 specifically induce apoptosis of endothelial cells, Cancer Res. 57 (1997) 1735–1742.
[96] Z. Li, M.J. Calzada, J.M. Sipes, J.A. Cashel, H.C. Krutzsch, D.S. Annis, D.F. Mosher, D.D. Roberts, Interactions of thrombospondins with alpha4beta1 integrin and CD47 differentially modulate T cell behavior, J. Cell. Biol. 157 (2002) 509–519.
[97] G. Martin-Manso, S. Galli, L.A. Ridnour, M. Tsokos, D.A. Wink, D.D. Roberts, Thrombospondin 1 promotes tumor macrophage recruitment and enhances tumor cell cytotoxicity of differentiated U937 cells, Cancer Res. 68 (2008) 7090–7099.
[98] J.S. Isenberg, F. Hyodo, K. Matsumoto, M.J. Romeo, M. Abu-Asab, M. Tsokos, P. Kuppusamy, D.A. Wink, M.C. Krishna, D.D. Roberts, Thrombospondin-1 limits ischemic tissue survival by inhibiting nitric oxide-mediated vascular smooth muscle relaxation, Blood 109 (2007) 1945–1952.
[99] J.S. Isenberg, J.B. Maxhimer, F. Hyodo, M.L. Pendrak, L.A. Ridnour, W.G. DeGraff, M. Tsokos, D.A. Wink, D.D. Roberts, Thrombospondin-1 and CD47 limit cell and tissue survival of radiation injury, Am. J. Pathol. 173 (2008) 1100–1112.
[100] J.S. Isenberg, F. Hyodo, L.K. Pappan, M. Abu-Asab, M. Tsokos, M.C. Krishna, W.A. Frazier, D.D. Roberts, Blocking thrombospondin-1/CD47 signaling alleviates deleterious effects of aging on tissue responses to ischemia, Arterioscler. Thromb. Vasc. Biol. 27 (2007) 2582–2588.
[101] J.S. Isenberg, L.K. Pappan, M.J. Romeo, M. Abu-Asab, M. Tsokos, D.A. Wink, W.A. Frazier, D.D. Roberts, Blockade of thrombospondin-1-CD47 interactions prevents necrosis of full thickness skin grafts, Ann. Surg. 247 (2008) 180–190.
[102] M.D. Sternlicht, Z. Werb, How matrix metalloproteinases regulate cell behavior, Annu. Rev. Cell. Dev. Biol. 17 (2001) 463–516.
[103] C. Chang, Z. Werb, The many faces of metalloproteases: Cell growth, invasion, angiogenesis and metastasis, Trends Cell. Biol. 11 (2001) S37–S43.
[104] L.A. Ridnour, A.N. Windhausen, J.S. Isenberg, N. Yeung, D.D. Thomas, M.P. Vitek, D.D. Roberts, D.A. Wink, Nitric oxide regulates matrix metalloproteinase-9 activity by guanylyl-cyclase-dependent and -independent pathways, Proc. Natl. Acad. Sci. U. S. A. 104(43) (2007) 16898–16903. [Epub 2007 Oct 17].
[105] L.M. Coussens, Z. Werb, Inflammation and cancer, Nature 420 (2002) 860–867.
[106] W.C. Parks, Matrix metalloproteinases in repair, Wound Repair Regen. 7 (1999) 423–432.
[107] T. Okamoto, T. Akuta, F. Tamura, D.V.A. van, T. Akaike, Molecular mechanism for activation and regulation of matrix metalloproteinases during bacterial infections and respiratory inflammation, Biol. Chem. 385 (2004) 997–1006.
[108] K.K. Nelson, J.A. Melendez, Mitochondrial redox control of matrix metalloproteinases, Free Radic. Biol. Med. 37 (2004) 768–784.
[109] D.A. Siwik, W.S. Colucci, Regulation of matrix metalloproteinases by cytokines and reactive oxygen/nitrogen species in the myocardium, Heart Fail. Rev. 9 (2004) 43–51.
[110] G.J. Peppin, S.J. Weiss, Activation of the endogenous metalloproteinase, gelatinase, by triggered human neutrophils, Proc. Natl. Acad. Sci. U. S. A. 83 (1986) 4322–4326.
[111] X. Fu, S.Y. Kassim, W.C. Parks, J.W. Heinecke, Hypochlorous acid oxygenates the cysteine switch domain of pro-matrilysin (MMP-7). A mechanism for matrix metalloproteinase activation and atherosclerotic plaque rupture by myeloperoxidase, J. Biol. Chem. 276 (2001) 41279–41287.
[112] L.A. Ridnour, A.N. Windhausen, J.S. Isenberg, N. Yeung, D.D. Thomas, M.P. Vitek, D.D. Roberts, D.A. Wink, Nitric oxide regulates matrix metalloproteinase-9

activity by guanylyl-cyclase-dependent and -independent pathways, Proc. Natl. Acad. Sci. U. S. A. 104 (2007) 16898–16903.
[113] X. Fu, S.Y. Kassim, W.C. Parks, J.W. Heinecke, Hypochlorous acid generated by myeloperoxidase modifies adjacent tryptophan and glycine residues in the catalytic domain of matrix metalloproteinase-7 (matrilysin): An oxidative mechanism for restraining proteolytic activity during inflammation, J. Biol. Chem. 278 (2003) 28403–28409.
[114] X. Fu, J.L. Kao, C. Bergt, S.Y. Kassim, N.P. Huq, A. d'Avignon, W.C. Parks, R.P. Mecham, J.W. Heinecke, Oxidative cross-linking of tryptophan to glycine restrains matrix metalloproteinase activity: Specific structural motifs control protein oxidation, J. Biol. Chem. 279 (2004) 6209–6212.
[115] S.Y. Kassim, X. Fu, W.C. Liles, S.D. Shapiro, W.C. Parks, J.W. Heinecke, NADPH oxidase restrains the matrix metalloproteinase activity of macrophages, J. Biol. Chem. 280 (2005) 30201–30205.
[116] Y. Wang, H. Rosen, D.K. Madtes, B. Shao, T.R. Martin, J.W. Heinecke, X. Fu, Myeloperoxidase Inactivates TIMP-1 by Oxidizing Its N-terminal Cysteine Residue: An oxidative mechanism for regulating proteolysis during inflammation, J. Biol. Chem. 282 (2007) 31826–31834.
[117] P.F. Bove, U.V. Wesley, A.K. Greul, M. Hristova, W.R. Dostmann, d.V.A. van, Nitric oxide promotes airway epithelial wound repair through enhanced activation of MMP-9, Am. J. Respir. Cell. Mol. Biol. 36 (2007) 138–146.
[118] P. Howard-Flanders, Effect of nitric oxide on the radiosensitivity of bacteria. Nature 180 (1957) 1191–1192.
[119] J.B. Mitchell, D.A. Wink, W. DeGraff, J. Gamson, L.K. Keefer, M.C. Krishna, Hypoxic mammalian cell radiosensitization by nitric oxide, Cancer Res. 53 (1993) 5845–5848.
[120] P.J. Wood, I.J. Stratford, G.E. Adams, C. Szabo, C. Thiemermann, J.R. Vane, Modification of energy metabolism and radiation response of a murine tumour by changes in nitric oxide availability, Biochem. Biophys. Res. Commun. 192 (1993) 505–510.
[121] F. Laval, D.A. Wink, Inhibition by nitric oxide of the repair protein O6-methylguanin-DNA-methyltransferase, Carcinogenesis 15 (1994) 443–447.
[122] J.A. Cook, M.C. Krishna, R. Pacelli, W. DeGraff, J. Liebmann, A. Russo, J.B. Mitchell, D.A. Wink, Nitric oxide enhancement of melphalan-induced cytotoxicity, Br. J. Cancer 76 (1997) 325–334.
[123] D.A. Wink, J.A. Cook, D. Christodoulou, M.C. Krishna, R. Pacelli, S. Kim, W. DeGraff, J. Gamson, Y. Vodovotz, A. Russo, J.B. Mitchell, Nitric oxide and some nitric oxide donor compounds enhance the cytotoxicity of cisplatin, Nitric Oxide 1 (1997) 88–94.
[124] T. Cook, Z. Wang, S. Alber, K. Liu, S.C. Watkins, Y. Vodovotz, T.R. Billiar, D. Blumberg, Nitric oxide and ionizing radiation synergistically promote apoptosis and growth inhibition of cancer by activating p53, Cancer Res. 64 (2004) 8015–8021.
[125] B.F. Jordan, P. Sonveaux, O. Feron, V. Gregoire, N. Beghein, C. Dessy, B. Gallez, Nitric oxide as a radiosensitizer: Evidence for an intrinsic role in addition to its effect on oxygen delivery and consumption. Int. J. Cancer 109 (2004) 768–773.
[126] F. Li, P. Sonveaux, Z.N. Rabbani, S. Liu, B. Yan, Q. Huang, Z. Vujaskovic, M.W. Dewhirst, C.Y. Li, Regulation of HIF-1alpha stability through S-nitrosylation, Mol. Cell. 26 (2007) 63–74.

CHAPTER 6

Redox Chemistry of Biological Thiols

Péter Nagy* *and* Christine C. Winterbourn

Contents

1. Introduction

Sulfur is the second chalcogen after oxygen in the periodic table. It has 16 protons and an electron configuration of $1s^2\ 2s^2\ 2p^6\ 3s^2\ 3p^4$. Sulfur has six valence electrons and a vacant 3d orbital, which allows it to exist in a wide range of oxidation states (from −2 to +6). Thus it has strong electron-donating and electron-accepting properties and an extraordinary reactivity

Department of Pathology, University of Otago Christchurch, Christchurch, New Zealand

* Corresponding author. Tel.: +64 3 364 0567; Fax: +64 3 364 0009
Email address: peter.nagy@otago.ac.nz

Advances in Molecular Toxicology, Volume 4
ISSN 1872-0854, DOI 10.1016/S1872-0854(10)04006-3

compared to oxygen or nitrogen. The thiol functional group (–SH also called a sulfhydryl group), where the sulfur atom is in its lowest oxidation state, is the functional group of the amino acid cysteine. Due to the soft nature of sulfur and its low oxidation state in the sulfhydryl group, thiols are very strong nucleophiles and susceptible to oxidation. Cysteine residues in proteins have important physiological functions. They provide covalent cross-linking of proteins and protein subunits, represent the redox active functional group of many different enzyme active sites, act as nucleophiles in proteases and phosphatases, have an integral role in redox signaling and have oxidant-scavenging function in antioxidant peptides and proteins [1–5]. Many of these physiological properties are mediated by the promiscuous redox chemistry of cysteine. However, the underlying chemical mechanisms whereby thiol oxidation mediates biological events, albeit extensively studied, are still not fully understood [6]. This chapter emphasizes the importance of a rigorous chemical approach to gain insight into the biology of thiols.

Most endogenously generated oxidants show preferential reactivity toward sulfhydryl groups. We mainly focus on two-electron oxidations of thiols but also shed light on radical-mediated reactions. We demonstrate the importance of the oxidizing and electrophilic properties of the oxidant as well as the nucleophilicity of the sulfur center in these reactions. The ionizability of the sulfhydryl group is a major determining factor in its nucleophilic character. We summarize the chemistry of microscopic and macroscopic acid dissociation equilibria of cysteine and glutathione and emphasize the importance and challenges of measuring protein sulfhydryl pK_a values. Although most studies focus on the initial step of cysteine oxidation, it is now realized that this initiates an array of subsequent events. These reaction cascades play important roles in redox-mediated cellular functions and may determine the outcome of the initial stimulus. Therefore, it is fundamental to understand the chemistry of the intermediates and products of these reactions, which is the focus of this contribution. We also highlight the physiological importance and the redox properties of hydrogen sulfide (H_2S), a newly recognized signaling molecule that can be seen from the chemical point of view as the smallest thiol.

2. Redox Reactions of Thiols with Two-Electron Oxidants

Aerobic organisms produce large amounts of reactive oxidants often referred to as reactive oxygen species (ROS). Oxidant production is mostly considered to be a "side effect" of respiration or an immune response to pathogenic invasion. Overproduction of these oxidants *in vivo* is associated with many inflammatory diseases, cancer, and aging, representing the toxic

nature of these species. Therefore, aerobic organisms produce an array of antioxidants to prevent oxidant-mediated cellular damage. However, mounting evidence suggests that intentional oxidant production is involved, via redox signaling, in the regulation of cellular events in metabolism, cell proliferation, and apoptosis [7].

Cysteine residues efficiently scavenge both one- and two-electron oxidants and they are major players in antioxidant defense and signal transduction. The bimolecular oxidation of thiols by ROS generates reactive sulfur-centered intermediates. Two-electron oxidants generate sulfenic acids (either directly or indirectly, see the later sections) and thiyl radicals are formed in reactions with radical species. Due to their high reactivity both species are short lived. Sulfenic acids initiate two-electron redox cascades and thiyl radicals are precursors of short radical chain reactions in biological systems. We are focusing on two-electron redox reactions and their products and only mention some interesting aspects of the radical-mediated pathways. We discuss the initial oxidation reactions of thiols with the most studied two-electron oxidants hydrogen peroxide (H_2O_2), peroxynitrite, the hypohalous acids, and hypothiocyanous acid.

2.1. Hydrogen peroxide

H_2O_2 is produced in large quantities *in vivo*. It is generated for example directly by peroxisomal enzymes (e.g., D-amino acid oxidase or uric acid oxidase) or indirectly in the mitochondria via the disproportionation of superoxide ($O_2^{\bullet -}$). H_2O_2 is a strong oxidant. However, its redox reactions with nucleophiles in many cases have a high activation barrier and therefore, although thermodynamically favored, are quite sluggish. Thiols are among the few nonmetallic biomolecules that can reduce H_2O_2 efficiently. These reactions produce a sulfenic acid intermediate. The rate of sulfenic acid formation is highly dependent on the pK_a of the sulfhydryl group (see Section 3). It can vary significantly based on the microenvironment of the thiol with the apparent second-order rate constants at pH 7 being anywhere between 1 and $10^7\,M^{-1}\,s^{-1}$. An unusual example is the peroxiredoxin (Prx) family, which to date represent the highest reactivity thiols with H_2O_2 ($k_{eff} = 10^7\,M^{-1}\,s^{-1}$ at pH 7) [8–11]. The underlying chemical reasons for this high reactivity are not clear, but cannot be explained solely by the low pK_a of their peroxidative cysteine thiol group.

There have been extensive efforts to study the redox signaling function of H_2O_2 via its reactions with thiol proteins. A number of key enzymes, including Prxs, protein tyrosine phosphatases (PTPs, e.g., PTP1B), the dual-specificity phosphatase Cdc25B, and the glycolytic glyceraldehyde-3-phosphate dehydrogenase (GAPDH), all have reactive cysteines in their

active site and have been identified as critical targets of H_2O_2. A common feature of these proteins is that they exhibit relatively large reactivity with H_2O_2 compared to glutathione (with second-order rate constants at pH ~ 7.4: $k^{GSH} = 0.89\,M^{-1}\,s^{-1}$, $k^{PTP1B} = 20\,M^{-1}\,s^{-1}$, $k^{Cdc25B} = 160\,M^{-1}\,s^{-1}$, $k^{GAPDH} \sim 500\,M^{-1}\,s^{-1}$). Based on simple kinetic considerations, the initial site of H_2O_2 attack in complex biological systems will not only depend on the reactivity but also on the relative concentrations of the different thiols in the cellular compartment where H_2O_2 is generated. In a recent review article, we have attempted to model the partitioning of H_2O_2 between the above-mentioned thiol proteins and GSH, using published intracellular thiol concentrations (in a typical mammalian cell) and their reactivities with H_2O_2 assuming a homogenous system (see Figure 1) [5]. Due to its high reactivity with H_2O_2 ($k^{GPx1} = 3 \times 10^7\,M^{-1}\,s^{-1}$) we have also included the selenoprotein glutathione peroxidase (GPx1) in the model.

The most important conclusions that can be drawn from this exercise are as follows:

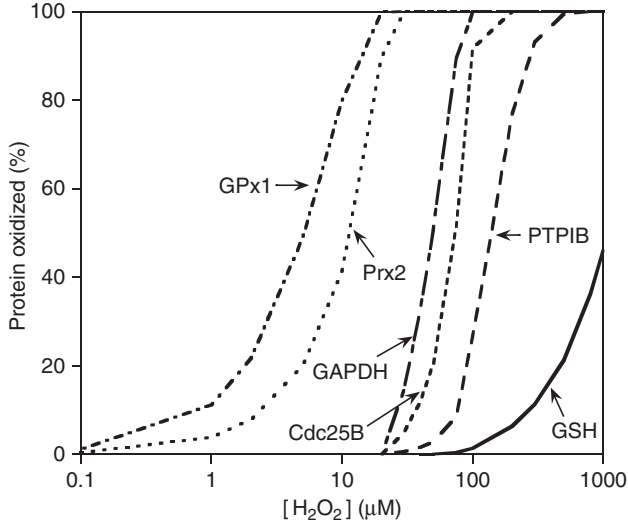

Figure 1 Simulation of oxidation of thiol proteins and GSH in a mixture treated with increasing concentrations of H_2O_2. Simulations of the kinetic traces were carried out using Mathematica 5.2. The simultaneous differential equations that represent the rate laws of the competing reactions were solved numerically using the Euler–Cauchy method. The time increments were chosen to be less than one-tenth the inverse of the largest rate constant to ensure that the Euler–Cauchy method provided acceptable accuracy. In the model, previously published second-order rate constants and cytoplasmic protein concentrations were used in the absence of target recycling. Figure was adapted from Winterbourn and Hampton [5].

- Despite its very high abundance in the cytosol, reduced glutathione (GSH) competes very poorly for H_2O_2.
- Owing to their large reactivity and local concentration, Prxs are favored targets of H_2O_2.
- Gpx1 and Prx consume virtually all H_2O_2 until they are fully oxidized. If they are efficiently recycled other proteins should be minimally modified by H_2O_2.
- Based on the model, GAPDH and PTPs, despite their low pK_a values, would only start reacting when Prxs are consumed. This inability to efficiently compete for H_2O_2 is somewhat against experimental observations, but perhaps tells us that their oxidation is a result of either secondary events rather than direct bimolecular reactions with H_2O_2 or colocalization with the oxidant source.

We would like to emphasize that cells are nonhomogenous systems, which represent the greatest limitation for such kinetic modeling.

2.2. Hypo(pseudo)halous acids

Hypohalous acids (HOX; X = Cl, Br, I) and hypothiocyanous acid (HOSCN) are produced by heme peroxidase-catalyzed oxidation of halogens and thiocyanate by H_2O_2.

The relative oxidant strength of HOX are HOCl > HOBr >> HOI ~ HOSCN [12]. Their pK_a values are 4.85 for HOSCN [13], 7.59 for HOCl [14], 8.59 for HOBr [15], and 10.4 for HOI [16]. Therefore at physiological pH (7.4) HOI and HOBr are protonated, HOCl is partially protonated and HOSCN is completely deprotonated. This is important, because these oxidants react with thiols in an electrophilic–nucleophilic reaction where they serve as the electrophile. In these reactions the electrophile accepts an electron pair (they are Lewis acids) donated by the nucleophile. Therefore, due to columbic effect, the protonated forms of the oxidants are usually 3–5 orders of magnitude more reactive than the deprotonated forms [13,15,17–20]. All of them react preferentially with thiols under physiological conditions [13,21–24]. The oxidizing and electrophilic nature of these species as well as their pK_a all contribute to their reactivity with sulfhydryls. The pH-independent second-order rate constants of the reactions of HOCl, HOBr, and HOSCN with thiols are very similar at ~$10^9\,M^{-1}\,s^{-1}$ [13,19,25]. However, due to the large difference in their pK_a values their reactions at pH 7 exhibit very different apparent second-order rate constants [for GSH: HOBr ($6 \times 10^8\,M^{-1}\,s^{-1}$) [26] > HOCl ($2 \times 10^7\,M^{-1}\,s^{-1}$) [24] >> HOSCN ($8 \times 10^4\,M^{-1}\,s^{-1}$) [13]].

The bimolecular reactions of HOX with thiols proceed via X^+ transfer to give a sulfenyl-(pseudo)halide. The initial formation of sulfenyl-

thiocyanates was observed directly in the reaction of thiols with HOSCN [27–30] but the formation of sulfenyl-chloride and sulfenyl-bromide was only observed indirectly by kinetic analysis because they hydrolyze very rapidly to give a sulfenic acid [19].

HOX can interconvert via their reactions with halides and SCN^-. In line with their oxidizing strength HOCl reacts with Br^-, I^-, and SCN^- but HOBr only reacts with I^- and SCN^-. The low abundance of I^- in physiological fluids and cells and the slow reactivity of HOCl with Br^- suggest a minor role for these reactions. However, HOCl and HOBr react with SCN^- very rapidly to generate HOSCN and these reactions are likely to occur *in vivo* [20,31]. They were shown to be important when predicting the partitioning of HOX in a physiological milieu, because in contrast to HOCl and HOBr, which are indiscriminant and react with a variety of functional groups [21,32], HOSCN is specific to thiols [13,23]. The hydrolysis product of HOSCN, thiocarbamate *S*-oxide, also reacts with thiols in a similar way. Sulfenyl-thiocarbamate is formed in the initial reaction, which then reacts with another thiol to give the disulfide and thiocarbamate [33,34].

HOCl and HOBr also react with amine residues in a highly favorable reaction to give haloamines (e.g., [35,36]). Haloamines are also reactive oxidants, and are more specific to thiols than HOCl or HOBr. They are generated *in vivo*, for example, in the phagosomal space and surroundings of neutrophil white blood cells [37,38]. Their membrane permeability and reactivity with thiols vary depending on their size, structure, and other functional groups [21,39]. For example, ammonia–chloramine and glycine–chloramine can readily pass through cell membranes and directly oxidize thiol proteins [40], but taurine–chloramine is membrane impermeable and can only act extracellularly [41–43].

2.3. Peroxynitrous acid/peroxynitrite

Peroxynitrous acid (ONOOH) is a strong two-electron oxidant that is generated in the diffusion controlled reaction of $O_2^{\bullet -}$ and nitrogen monoxide (NO; also called nitric oxide) [44]. Since NO is relatively long lived compared to $O_2^{\bullet -}$, the sites of ONOOH formation *in vivo* are associated with $O_2^{\bullet -}$ production.

ONOOH is very unstable in aqueous media and decomposes via different reaction pathways which can give secondary thiol-reactive species. It can isomerize to nitrate, it can decompose via radical-mediated pathways to eventually produce oxygen and nitrite in a 1:2 molar ratio [45–49] and based on a recent study its disproportionation yields peroxynitrate and nitrite [50]. ONOOH can be stabilized at high pH, because its deprotonated form $ONOO^-$ is relatively long lived. Its pK_a is around 6.5–6.8, depending on the buffer and ionic strength of the solution [51].

Peroxynitrite reacts rapidly with thiols, predominantly via two-electron oxidation. However, thiol oxidation can in some cases compete with the decomposition of ONOOH, and result in radical-mediated thiol oxidation pathways [52]. These reactions were proposed to proceed via $NO_2^{\bullet}$ or $OH^{\bullet}$. The decomposition of ONOOH is facilitated by bicarbonate. This produces carbonate radicals that also react with thiols preferentially. The reactivity of ONOOH with different thiols has not been investigated systematically, but the major two-electron oxidation pathways are clearly pH [53,54] and thiol pK_a dependent [55]. Prxs exhibit high reactivity with ONOOH ($k_{eff} = \sim 10^5$–$10^7\ M^{-1}\ s^{-1}$ at pH 7) compared to typical rate constants with other thiols, and are proposed to be specific ONOOH scavengers *in vivo* [56–59].

3. Acid–Base Equilibria of Thiols

The protonation state of the sulfhydryl group has a marked effect on its reactivity with oxidizing agents. In general, the thiolate form is a much better nucleophile than the thiol and exhibits larger reactivity with electrophilic oxidants. In addition, based on the linear free energy relationship theory (described by the Bronsted equation) the pH-independent second-order rate constants for the reaction of the oxidant with the thiolate are linearly correlated with the pK_a of the thiol [60,61]. In other words when the thiol is deprotonated at any given pH the rate of the reaction will increase with the pK_a of the thiol, representing an opposite pK_a effect. Therefore, it is essential to understand speciation in aqueous solution when investigating the redox reactions of thiols. We attempt to summarize the most important aspects of thiol protonation equilibria in aqueous solution and give examples how to calculate the concentrations of the thiolate derivatives.

3.1. Macroscopic and microscopic acid dissociation constants

Even the amino acid cysteine has three ionizable functional groups and hence is considered a polyprotic acid. For a biprotic acid the following equilibria establishes the speciation of the different macroscopic protonation states of a molecule.

$$LH_2 \overset{K_{a1}}{\rightleftharpoons} LH^- \overset{K_{a2}}{\rightleftharpoons} L^{2-}$$

K_{a1} and K_{a2} are macroscopic acid dissociation constants. When L^{2-} has only one protonation site, consecutive protonation equilibria are well described by K_{a1} and K_{a2}, such as in the case of H_2S where $K_{a1} = 6.76$ and $K_{a2} = 19.2$ [62]. However, when L^{2-} has two different protonation sites, from the statistical point of view, the proton in the first reaction can

bind either of the sites representing two structurally different protonation isomers, also called microspecies. Therefore LH^- in this case represents a mixture of two protonation isomers and is called a macrospecies. In some cases the macroscopic constants are well separated, due to drastic differences in the proton affinity of the different functional groups. In this extreme case, one of the protonation isomers is in large excess at any given pH. The macroscopic dissociation constants therefore represent protonation equilibria of particular functional groups and the speciation of microspecies. In most cases, however, the protonation of a particular functional group affects the proton affinity of the neighboring group. Binding a proton (even though to a different functional site) increases the total charge of the molecule usually resulting in a decrease in proton affinity (this is particularly true in the case of small molecules).

Conventional titration methods (such as pH–potentiometric or UV–vis spectophotometric titration) determine the overall protonation states of a molecule and therefore result in macroscopic pK_a values. Microscopic pK_a values are relatively hard to determine. Special techniques that can determine microspeciation have to be used. However, in most cases the protonation of a functional group has an effect on the spectroscopic properties of the other functional groups (due to the same reason why they have an effect on each other's pK_a values). For example, when nuclear magnetic resonance (NMR) spectroscopy is used to study microspeciation, protonation (at any site) results in a decrease in overall electron density of the molecule and therefore the nucleus of interest senses a different electronic environment. This causes a difference in the chemical shift of this particular species, the parameter that is used in the pH-dependent spectral series [63]. Therefore corrections, using assumptions, are necessary to calculate the contribution of the protonation of the functional group of interest to the observed change in the chemical shift. The same is true for other spectroscopic techniques such as Raman, IR, or UV–vis spectroscopies. The microscopic acid dissociation constants of cysteine and GSH were widely studied by a plethora of different techniques. Each of these techniques uses its own assumptions, but the results are in reasonable agreement. It is, however, very challenging to obtain pK_a values for macromolecules, such as larger peptides or proteins that are important to understand fundamental biological events like cell signaling. In the next sections we discuss these issues using cysteine and GSH as examples.

3.2. Cysteine

Cysteine is a triprotic acid with three ionizable functional groups including a carboxylic acid, an amino, and a sulfhydryl group (Scheme 1). The three macroscopic pK_a values were determined by Brooks *et al.* in 1937 to be: 1.71, 8.33, and 10.78 at 25°C and close to zero ionic strength [64]. It is

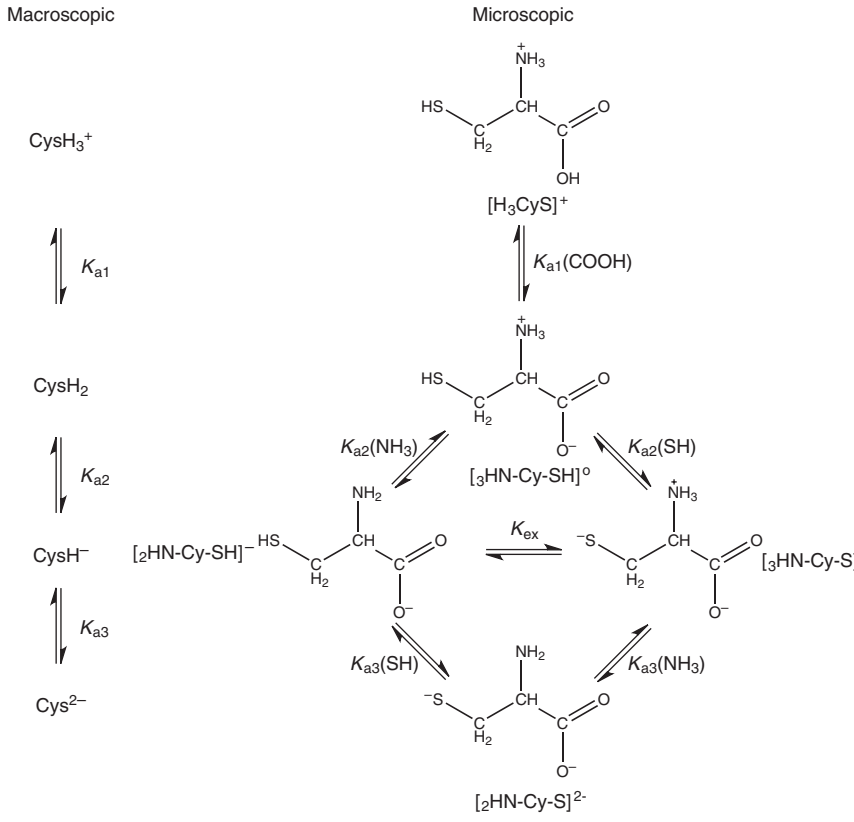

Scheme 1 Macroscopic and microscopic acid–base equilibria of cysteine.

generally accepted that the first macroscopic pK_a of cysteine represents the acid–base equilibria of the carboxylic acid group. Therefore the carboxylate group at pH > 3 is fully ionized. However, the second and third macroscopic pK_a values were the subject of a large debate in the 1950s through to the 1970s. Initially, Cohn and Edsall assigned the dissociation of the second proton to the ammonium group and the third to the sulfhydryl group [65], whereas Calvin suggested the opposite [66]. Even 10–15 years later different textbooks assigned the two macroscopic pK_a values to different functional groups [67,68]. Edsall was the first to suggest that since the intrinsic proton affinities of nitrogen and sulfur are very similar, the two pK_a values should represent mixed equilibrium constants. They and others (even almost 30 years later) have tried to evaluate the microscopic pK_a values by derivatizing each group separately and measuring the pK_a value of the other [69,70]. However, this approach eliminates the potential effects of

intramolecular H-bonding and intermolecular H-bonding with water molecules [71]. The microscopic pK_a values (see Scheme 1) of cysteine were first determined in the classical work of Benesch and Benesch [72]. They used UV–vis spectrophotometric titration to follow the ionization of the sulfhydryl group at 230–240 nm and assumed that the two cysteine thiolate derivatives ($[_2$HN-Cy-S$]^{2-}$ and $[_3$HN-Cy-S$]^-$ in Scheme 1) had similar extinction coefficients in this wavelength range.

In 1956 De Deken suggested that the shift in the absorption maximum in the Benesch and Benesch study was due to a H-bonding interaction between the sulfur and nitrogen centers and suggested that the biprotonated cysteine represents one microspecies (see Scheme 2) [73].

Later, Edsall revisited the problem using Raman spectroscopy utilizing the strong S–H stretching frequency at 2580 cm^{-1} [74,75]. He elegantly showed that if the H-bonding intermediate exists at all, it must have a very low (undetectable) steady-state concentration [76]. An equilibrium between $[_2$HN-Cy-SH$]^-$ and $[_3$HN-Cy-S$]^-$ (K_{ex}) should also exist and the reaction most probably proceeds by entropy reduction facilitated intramolecular H^+ transfer, where a low steady-state concentration of the above suggested intermediate is feasible. Edsall's microscopic pK_a values agreed well with those reported by Benesch and Benesch (see Table 1) in spite of differences in ionic strengths between the two studies (Table 1). Others have remeasured the microscopic pK_a values for cysteine using different methods and in most cases the obtained values were relatively close (see Table 1).

It is interesting to note that the four microspecies form a thermodynamic cycle and therefore are interrelated [see box, eq. (1)]. They also relate to the macroscopic pK_a values [eqs. (2 and 3)]. Also, $[_2$HN-Cy-SH$]^-$ and $[_3$HN-Cy-S$]^-$ are protonation isomers and their ratio is independent of the pH and total concentration of cysteine [eq. (4)]. Therefore if one of the microscopic pK_a values can be measured, it is enough to establish all the others.

From the kinetics point of view, it is important to use microscopic rather than macroscopic pK_a values, because the reactivity of the cysteine thiol will be more affected by the ionization state of the sulfhydryl group than the

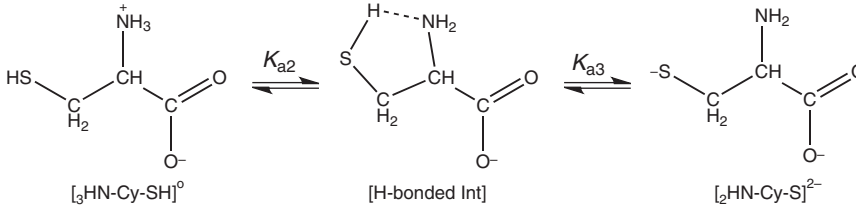

Scheme 2 Acid–base equilibria of cysteine via a H-bonded intermediate protonation state as proposed by De Deken *et al.* [73].

Table 1 Reported microscopic acid dissociation constants for cysteine

pK_{a2}(SH)	pK_{a2}(NH_3)	pK_{a3}(SH)	pK_{a3}(NH_3)	Ionic strength	Temperature (°C)	Method	Ref.
8.53	8.86	10.03	10.36	[phosphate] = [borate] = 0.02 M	23	Spectrophotometry	[72]
8.50	8.85	10.00	10.35	$[CySH]_{tot}$ = 1.0 M	25	Raman specroscopy	[74]
8.21	8.65	9.56	10.0	I = 1.0 M (KCl)	30	Spectrophotometry	[77]
8.4	8.85	9.6	10.05	I = 0.5 M (KCl),	25	Spectrophotometry	[78]
> 8.72				0M	25	Kinetics	[79]
8.58	8.69	10.16	10.27	H_2O	25	Estimated based on macroscopic pK_a values for *S*-methyl and *S*-ethyl-Cys	[80]
8.66	8. 99	10.84	10.51	H_2O	12	Estimated based on	[81]
8.66	8.60	10.45	10.51	H_2O	25	macroscopic pK_a	
8.66	8.25	10.10	10.51	H_2O	37	values	

macroscopic protonation state of the whole molecule. The extent of the deprotonation of an individual site can be given by protonation functions. The protonation functions of the sulfhydryl group can be calculated using the microscopic pK_a values based on eq. (5). One can also define a function that relates to the deprotonation of the sulfhydryl group ($F^{(SH)}$) using microscopic pK_a values, which results in the speciation of the cysteine derivatives with protonated and unprotonated sulfhydryl groups and ignores the protonation state of the ammonium group [eqs. (6 and 7)]. It should be noted that although this function represent the kinetics of thiols with oxidants far better than the macroscopic pK_a values, the protonation of the amino groups could also have an effect on the reactivity of the sulfur [82,83] and therefore different rate constants should be assigned to each microspecies when possible.

$$K_{a2}(NH_3) \cdot K_{a3}(SH) = K_{a2}(SH) \cdot K_{a3}(NH_3) \tag{1}$$

$$K_{a2} = K_{a3}(NH_3) + K_{a3}(SH) \tag{2}$$

$$K_{a2} \cdot K_{a3} = K_{a2}(NH_3) \cdot K_{a3}(SH) = K_{a2}(SH) \cdot K_{a3}(NH_3) \tag{3}$$

$$\frac{\left[{}_3\text{HN-Cy-S}\right]^-}{\left[{}_2\text{HN-Cy-SH}\right]^-} = \frac{K_{a2}(SH)[H^+]\left[{}_3\text{HN-Cy-SH}\right]^0}{K_{a2}(NH_3)[H^+]\left[{}_3\text{HN-Cy-SH}\right]^0} = \frac{K_{a2}(SH)}{K_{a2}(NH_3)} \tag{4}$$

$$\begin{aligned}\alpha(SH) &= \frac{\left[{}_3\text{HN-Cy-S}\right]^- + \left[{}_2\text{HN-Cy-S}\right]^{2-}}{[\text{Cys}]_{tot}} \\ &= \frac{K_{a2}(SH)/[H^+] + K_{a2}(SH)K_{a3}(NH_3)/[H^+]^2}{1 + (K_{a2}(SH) + K_{a2}(NH_3))/[H^+] + K_{a2}(SH)K_{a3}(NH_3)/[H^+]^2} \\ &= \frac{K_{a2}(SH)/[H^+] + K_{a2}K_{a3}/[H^+]^2}{1 + K_{a2}/[H^+] + K_{a2}K_{a3}/[H^+]^2}\end{aligned} \tag{5}$$

$$\begin{aligned}\text{CySH} \rightleftharpoons \text{CyS}^- + H^+, \quad F^{(SH)} &= \frac{[\text{CyS}^-][H^+]}{[\text{CySH}]} \\ &= \frac{\left(\left[{}_3\text{HN-Cy-S}\right]^- + \left[{}_2\text{HN-Cy-S}\right]^{2-}\right)[H^+]}{\left(\left[{}_3\text{HN-Cy-SH}\right]^0 + \left[{}_2\text{HN-Cy-SH}\right]^-\right)}\end{aligned} \tag{6}$$

$$F^{(SH)} = \frac{\alpha(SH)[H^+]}{1 - \alpha(SH)} = \frac{K_{a2}(SH)[H^+] + K_{a2}(SH)K_{a3}(NH_3)}{[H^+] + K_{a2}(NH_3)} \tag{7}$$

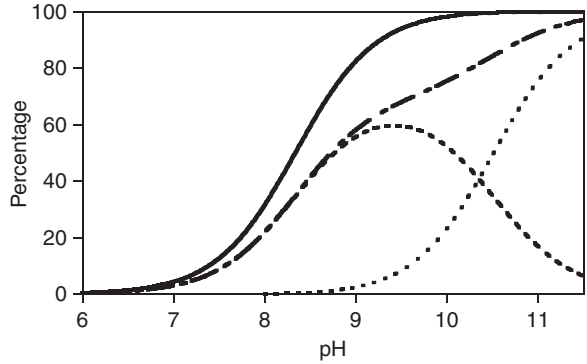

Figure 2 Differences in thiolate distribution using microscopic or macroscopic K_a values. Thiolate concentrations calculated assuming that the macroscopic pK_{a2} (solid line) or pK_{a3} (dotted line) represent the sulfhydryl group and using the microscopic pK_a values (dot dashed line) determined by Elson *et al.* [74]. The dashed and dotted lines show the distribution of the microspecies $[_3HN\text{-}Cy\text{-}S]^-$ and $[_2HN\text{-}Cy\text{-}S]^{2-}$, respectively, and the dot–dashed line was obtained by summation of $[_3HN\text{-}Cy\text{-}S]^-$ and $[_2HN\text{-}Cy\text{-}S]^{2-}$.

Figure 2 represents the marked differences in speciation when macroscopic or microscopic pK_a values are used.

3.3. Reduced glutathione

GSH is a tripeptide (γ-Glu–Cys–Gly). It has two carboxylic acid, an amino and a sulfhydryl functional groups. Rabenstein has shown that the two carboxylic acid groups are protonated simultaneously in the pH < 6 region, well separated from the ammonium and sulfhydryl groups, which protonate in the pH > 7 region [84,85]. He has shown that GSH acts as a biprotic acid in both regions (see Scheme 3).

Values determined for the physiologically more important microscopic pK_a values for the ammonium and sulfhydryl groups of GSH are shown in Table 2.

3.4. Proteins

The measurement of thiol pK_a values of particular protein cysteines is highly desirable to predict or explain reactivities or enzymatic function. The most extensively used methods include NMR spectroscopy [87–89], spectrophotometric titration at 240 nm (the absorbance maximum of thiolate) for example, [90], and changes in rates of reactions with electrophiles. There are several complications associated with each method which include the following:

– In most proteins there are more than one Cys residues and in many cases spectrophotometric and kinetic pK_a measurements cannot

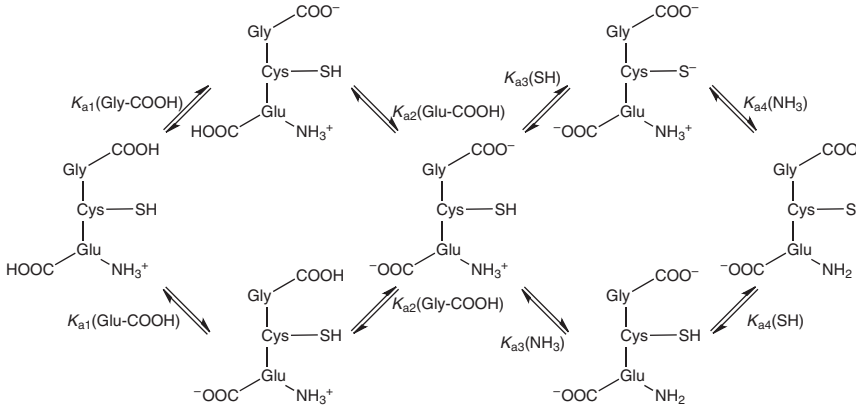

Scheme 3 Microscopic acid–base equilibria of reduced glutathione.

differentiate between them. One way to overcome this problem is site directed mutagenesis, although even point mutations may result in significant conformational changes and alter the pK_a values of interest. A recent study reported an elegant liquid chromatography/mass spectrometry (LC/MS) method where quenching the reaction of cysteine residues with an iodoacetamide-based reagent at different time points is followed by tryptic digestion and peptide mapping, which allows to follow alkylation of each cysteine residues separately [91].

- pK_a measurement by NMR spectroscopy is challenging because of overlapping signals and line-broadening problems. Changes in chemical shifts are usually not specific to one functional group (see Section 3.1).
- Accessibility to the active site can affect kinetic measurements by alkylating agents such as iodoacetate or iodoacetamide [92].

Moreover, in light of the complexity of measuring the pK_a values for cysteine or glutathione it is not hard to imagine that there are further challenges in the complex systems of proteins. We would like to draw attention on the 2 orders of magnitude difference in the K_a values of the sulfhydryl group of free cysteine when the ammonium group is protonated or deprotonated (see Table 1). Likewise in proteins, neighboring charged, aromatic, or H-bond donor or acceptor functional groups will have a pronounced effect on the thiol pK_a, especially at buried active sites. In fact, these interactions are used in protein pK_a simulation methods (e.g., [93]). Furthermore, all experimental methods to measure pK_a values include pH titration and most proteins are known to undergo conformational changes as the pH is varied. Therefore, changing the pH could not

Table 2 Reported microscopic acid dissociation constants for the ammonium and sulfhydryl groups of reduced glutathione

pK_{a2}(SH)	pK_{a2}(NH_3)	pK_{a3}(SH)	pK_{a3}(NH_3)	Ionic strength	Temperature (°C)	Method	Ref.
8.93	9.13	9.28	9.08	$I = 0.2$–0.55 M	25	NMR specroscopy	[84]
8.72	9.47	8.72	9.47	$I = 1$ M (KCl)	30	Spectrophotometry	[77]
8.72	9.28	8.72	9.28	N/A reported to have negligible effect	25	Kinetics	[86]

only perturb the charge and protonation state of the thiol and the neighboring functional groups, but also their distances from each other. It is therefore hard (if not impossible) to evaluate the contribution of the protonation/deprotonation of one particular functional group in a pH titration data set of a protein. However, this complex network is exactly what causes the extraordinary reactivity and specificity of protein thiols compared to small molecules. Therefore from the functional point of view, it is more important to understand how the pH affects the reactivity of the protein thiol and draw general conclusions based on the ionizability of its sulfhydryl group, than strictly assigning its acid dissociation constant. Therefore the meaning of protein pK_a is slightly different than the strict chemical definition used for small molecule pK_a.

4. Closed-Shell[1] Sulfur Species Generated in Thiol Redox Reactions

Sulfenic acids are typically formed in the two-electron oxidation reactions of thiols and can engage in various inter and intramolecular redox reactions to give derivatives with sulfur centers having higher or lower oxidation states. The most common biologically relevant derivatives are depicted on Figure 3. A reaction scheme demonstrating some of the possible pathways for their interconversion is shown in Scheme 4.

Studying the chemistry of these reactions is challenging because most of the derivatives are short lived and do not exhibit distinct spectroscopic properties. However recent studies involving chemical trapping and kinetic analysis have identified most of the intermediates on small thiols or proteins and are currently the focus of many biochemical investigations.

4.1. Sulfenic acid

Sulfenic acids are produced by the reactions of a thiol with two-electron oxidants [3,94–97]. They can alternatively be generated via the hydrolysis of sulfenyl-halides, sulfenyl-thiocyanate [19,29,98–100] or thiosulfinate esters [82,83,101,102], or in radical-mediated reactions (see the later sections).

Sulfenic acids are usually short-lived transient species [103], and in the presence of thiols they are rapidly consumed to form disulfides. A lower limit for the second-order rate constant of the reaction of cysteine sulfenic acid with cysteine thiolate at pH 7 was estimated to be $10^5\ M^{-1}\ s^{-1}$ [19]. In

[1] Closed shell molecules have only doubly occupied or empty molecular orbitals and no unpaired electrons.

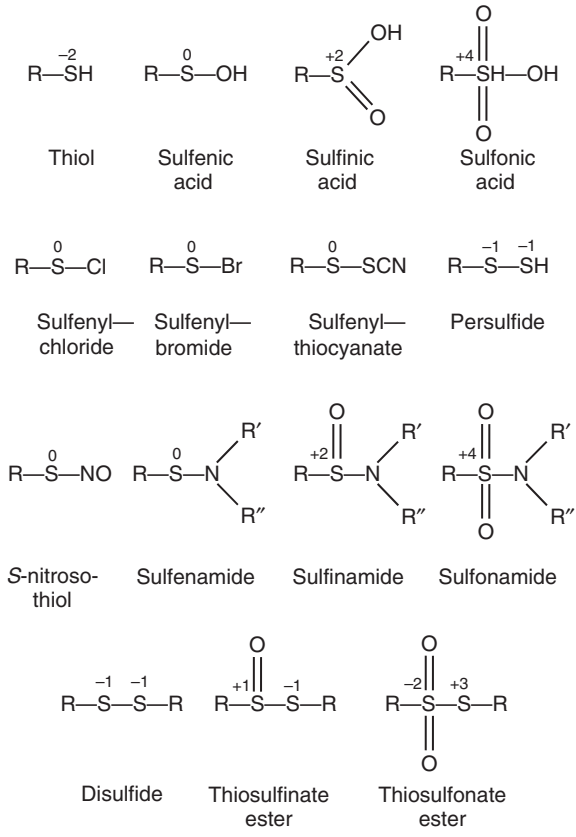

Figure 3 Most common thiol oxidation products and intermediates observed in biological systems. Numbers, above sulfur represent the oxidation state of the sulfur atoms.

contrast, the rates of the reactions of sulfenic acid on human serum albumin (HSA–SOH) with low-molecular-weight thiols are surprisingly slow with second-order rate constants in the range of 2–100 $M^{-1}s^{-1}$ [104]. This could be due to the fact that Cys34 of HSA is located in a partially solvent-protected hydrophobic cleft. This could also be the reason for the large stability of HSA–SOH (after 2 h incubation less than 15% decomposition was observed) in the absence of nucleophiles (other that H_2O or OH^-) at neutral pH [105]. These reactions are, however, rapid enough to ensure a short lifetime of HSA–SOH under physiologic conditions, suggested by the fact that 25% of HSA circulates in blood as a mixed disulfide with low-molecular-weight thiols [106].

Condensation of two sulfenic acids to give a thiosulfinate ester [19,107] or disproportionation to a sulfinic acid and a thiol (P. Nagy , unpublished results) can compete to some extent with disulfide formation even at a

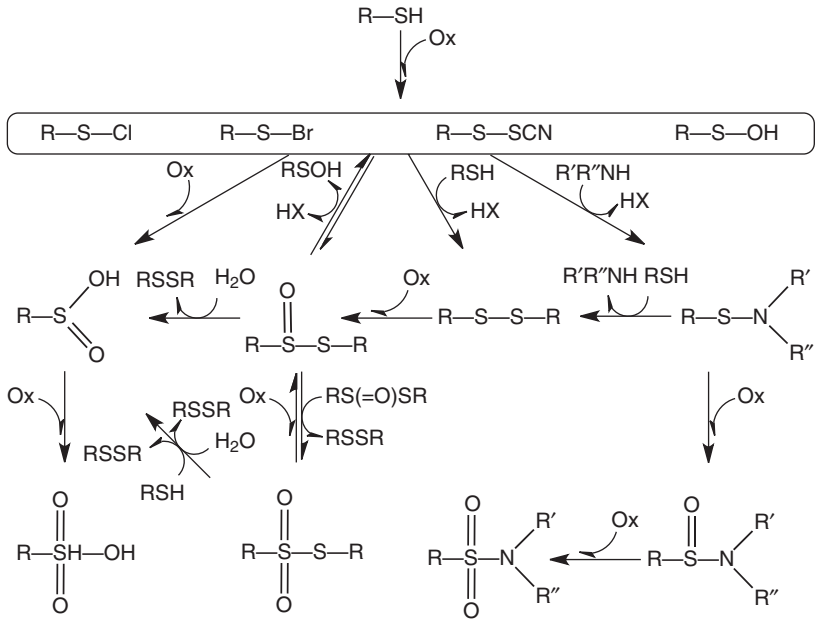

Scheme 4 Two-electron redox cascade of biologically common Cys derivatives. X = Cl, Br, SCN, or OH.

>10-fold excess of thiol over sulfenic acid [19]. The contributions of these reaction pathways are dependent on the pH, pK_a of the sulfenic acid and the surrounding thiols, and the relative thiol and steady-state sulfenic acid concentrations. The rates of the disproportionation and condensation reactions are expected to peak close to the pK_a of the sulfenic acid. The rational for this is that one sulfenic acid serves as the electrophile and the other as the nucleophile in these reactions and at the pK_a of the sulfenic acid the deprotonated and protonated isoforms (representing the best nucleophile and electrophile, respectively) are present at equal concentrations. Due to their high reactivity, measuring the pK_a for a sulfenic acid is complicated and as far as we are aware there is only one study that estimated a range of 6–10 for the pK_a value for a cysteine sulfenic acid [19]. The steady-state sulfenic acid concentration largely affects the rate of the condensation and disproportionation reactions because the rate laws of these reactions exhibit second-order dependency on it. It is determined by the relative rates of the initial oxidation step (which produces sulfenic acid) and the reaction of the sulfenic acid with extra thiol (which consumes sulfenic acid). Therefore the oxidative properties of the primary oxidant and its relative concentration affect the extent of the self-reactions compared to disulfide formation. The mechanisms of sulfenic acid disproportionation and condensation reactions have

not been studied in detail and are not well understood. However, it is clear that the redox potential and pK_a of the sulfenic acid as well as the pH and the nature of the primary oxidant have a major effect on these reactions.

Sulfenic acids can also be further oxidized [19,108]. These reactions occur in competition with the reaction of the sulfenic acid with another thiol molecule. Sulfenic acid overoxidation can be detrimental to protein function. However, solvent-exposed protein sulfenic acids are expected to react rapidly with abundant low-molecular-weight thiols such as glutathione. This is recognized as a mechanism for protecting protein thiols from overoxidation (see Section 4.2).

Sulfenic acids also react with amines and amides in both inter- and intramolecular reactions to form sulfenamides, sulfinamides, or sulfonamides (see Section 4.5) [109–112]. Other reactions, such as the reaction of a thiosulfinate ester or a disulfide with the sulfenic acid can theoretically happen, but these reactions have not been observed to date [19,83]. Their relevance is even less likely in a complex biological system, where other nonsulfur-derived electrophiles and nucleophiles will join the competition for sulfenic acids and further complicate their chemistry (these reactions are not discussed here).

Sulfenic acid formation on proteins is now well recognized. Initially long-lived sulfenic acids were detected on proteins such as HSA [105], NADPH peroxidase [113,114], glutathione reductase (GR), 1-Cys Prxs [115,116], and methionine sulfoxide reductase [117]. In these proteins the sulfenic acids are stabilized from disulfide formation due to conjugation, H-bonding, or steric hindrance [118–123]. They have been characterized by NMR, MS, chemical trapping, or even single-crystal X-ray diffraction (reviewed in [97]). Evidence for intermediate sulfenic acid formation in 2-Cys Prxs [124], OhrR [125], cysteine-based proteases (Cathepsin B and L and SUMO proteases) [126,127], and PTPs [128] were also obtained recently by means of chemical trapping and kinetics (reviewed in [2]). The potential of Cys–sulfenic acids as regulatory switches for the activation and deactivation of tyrosine phosphatases is now widely accepted [111,112]. Carroll's group has developed dimedone analogs that specifically react with sulfenic acids, which allow study of thiol oxidation in cellular systems. For example, azidodimedone was utilized in human tumor cell lines to confirm 14 known proteins that are modified by sulfenic acid formation as well as identify almost 200 new potential candidates that are involved in wide ranging cellular functions [129]. Antibodies that recognize dimedone-labeled proteins [130] will have further application for probing sulfenic acid formation in pathological conditions. An important recent study suggests that sulfenic acids represent a major posttranslational modification of periplasmic Cys residues in *Escherichia coli*. The same work discovered that two thioredoxin (Trx)-like proteins DsbG and DsbC are responsible for maintaining thiol homeostasis via reducing sulfenic acids on proteins with single functional cysteine residues [131].

4.2. Disulfide

Disulfides are relatively stable products of thiol oxidation and have important roles in the secondary, tertiary, and quaternary structures of proteins. Folding of newly synthesized polypeptides is accompanied by enzyme-catalyzed disulfide bond formation. Briefly, in the endoplasmic reticulum protein oxidation is mediated by protein disulfide isomerases via their intramolecular redox active Cys–x–x–Cys disulfide bonds and in the mitochondrial intermembrane space the Mia40 enzyme is responsible for oxidation of the incoming proteins via its Cys–Pro–Cys motif (reviewed in [132]). It was thought for a long time that once formed structural disulfide bonds are stable and inert entities in a physiological milieu. However, a number of proteins contain disulfide bonds that can be reduced enzymatically, suggesting a much more dynamic situation. This process has been shown to be involved in activation of a number of regulatory proteins, including thrombospondin, cell surface receptors, and tissue factor (reviewed in [133]).

Disulfide formation is a common outcome of oxidative stress. Sulfenic acids, sulfenyl-halides, and sulfenyl-thiocyanates on proteins or small molecules, are generally intermediates and are rapidly quenched by reacting with an additional thiol to form disulfides. Nitrosothiols and sulfenamides also react slowly with thiols to give disulfides. Higher oxidation states such as thiosulfinate or thiosulfonate esters can convert to disulfides by reduction or hydrolysis. Radical-mediated thiol oxidation can lead to disulfides (see the later sections). For proteins with vicinal thiols, the product is an intramolecular disulfide. For other protein thiols, the favored reaction of the oxidized intermediate is with the GSH present at high intracellular concentrations to form a glutathionylated protein. Protein glutathionylation is thought to be important as a mechanism for protecting functional protein thiols under oxidative stress. Although this can render the protein inactive, removal of the glutathione can restore activity. Reversible protein glutathionylation is also being increasingly recognized as a regulatory mechanism in signal transduction.

Formation of disulfides on redox-active thiols is a dynamic and reversible process. Trx and glutaredoxin, together with Trx reductase and GR, are largely responsible for intracellular disulfide reduction. These enzymes themselves function via reversible inter- and intramolecular thiol–disulfide (or seleno–sulfide) cycles [134–137]. Disulfides also undergo exchange reactions. Spontaneous thiol–disulfide exchange is relatively slow; the order of magnitude of their second-order rate constants at pH 7 is ~10^{-3} $M^{-1}\,s^{-1}$ [138]. It proceeds via nucleophilic attack of the thiolate on the more electrophilic sulfur centers in the disulfide bond. Therefore both the thermodynamic and kinetic properties of these reactions will largely depend on the corresponding thiol pK_a values and redox potentials. These reactions are used to determine protein redox potentials and pK_a values (reviewed in

[139]). Uncatalyzed exchange reactions are too slow to have a major impact in a dynamic cellular environment. However, enzyme-catalyzed exchange reactions, catalyzed primarily by glutaredoxin and Trx, play an important role not only in reversing oxidation but in regulating protein glutathionylation and redox-sensitive signaling pathways (reviewed in [140]).

Thiols are thought to act as intracellular redox buffers and the redox potentials of the GSH/GSSG, Trx_{red}/Trx_{ox} and cysteine/cystine couples provide a useful measure of cellular oxidative stress. Interestingly, these couples are not in equilibrium but are insulated kinetically. In other words, as a result of marked differences in thiol oxidation and disulfide reduction rates (*vis-à-vis* catalyzed and noncatalyzed events) the redox status of the cell is controlled kinetically rather than thermodynamically, representing a dynamic nonequilibrium steady-state system [141,142].

4.3. Thiosulfinate and thiosulfonate ester

Thiosulfinate esters are formed in the condensation reaction of two sulfenic acids or via oxidation of disulfides [19,82,83,101,143–145]. They are also an intermediate in the reduction of sulfinic acids via ATP-dependent sulfiredoxin (Srx)-catalyzed pathways (see the next section) [146–148].

Thiosulfinate esters are reactive species. They react further with thiols to give a sulfenic acid and a disulfide [83,149,150] or in the absence of thiols undergo hydrolysis. Hydrolysis can proceed via a number of pathways, with the contribution of each largely depending on the conditions [82]. All eventually yield disulfide and sulfinic acid in a 1:1 ratio, but the nature of the intermediates could be different.

Disproportionation of aromatic thiosulfinate esters was reported to give a thiosulfonate ester and a disulfide [102,151–153]. Thiosulfonate esters can alternatively be intermediates in the hydrolysis of thiosulfinate esters [82]. While cysteine thiosulfonate ester reacts rapidly with cysteine to give a disulfide and a sulfinic acid [82], the thiosulfonate ester of glutathione is quite stable even in the presence of excess GSH [154]. The biological importance of these species has not been explored.

Thiosulfinate esters on the other hand are biologically relevant. They are intermediates in the enzymatic reduction of Prx sulfinic acid residues by Srx (see Section 4.4). The natural products allicin and leinamycin are thiosulfinate esters. These species were reported to have antibacterial, antineoplastic, antifungal, antithrombic, hepatoprotective, and cholesterol-lowering [155–159] properties. Most of these properties are mediated via their reactions with thiols. Oxidation of GSH by singlet oxygen or H_2O_2 has been reported to give substantial formation of the thiosulfinate ester (GS(=O)SG) [160,161]. Singlet oxygen was also shown to oxidize GSSG to form GS(=O)SG [162,163]. Due to its reactivity with thiols a

recent study proposed GS(=O)SG to be a primary glutathionylating species *in vivo* [164]. Furthermore, enzymatic oxidation of disulfides by cytochrome P-450 can lead to thiosulfinate ester formation in rat and human liver microsomes, which provide evidence for the catalytic formation of these species in complex biological systems [165–167].

4.4. Sulfinic and sulfonic acid

Two-electron oxidants can react with sulfenic acids to give sulfinic acids or sulfonic acids, which are much less reactive species. They can also be formed in disproportionation reactions of sulfenic acids or in hydrolysis and redox reactions of oxi-disulfide derivatives. In the cysteine dioxygenase (CDO) pathway of cysteine metabolisms CDO oxidizes free cysteine to cysteine sulfinic acid, which eventually breaks down to taurine or pyruvate and sulfate [168].

Sulfinic acids are far less reactive than sulfenic acids or thiosulfinate esters and ~5% of cellular protein cysteine residues has been estimated to be in this oxidation state [169]. The sulfinic acid functional group has a pK_a value at around 2, and is always deprotonated under physiological conditions. This would explain why sulfinic acids mainly act as soft nucleophiles despite having two largely electron-withdrawing oxygens attached to the sulfur center. Importantly, sulfinic acids cannot be reduced by thiols.

Recently, sulfinic acid formation on Prxs has received considerable interest [170–173]. The reactive thiol in these proteins reacts with peroxides to form a sulfenic acid intermediate. This sulfenic acid then reacts with another Cys (either on the same or on an adjacent subunit) to form a disulfide. The sulfenic acid can alternatively react with another peroxide to give a sulfinic acid and thus inactivate the protein (this phenomenon is commonly called hyperoxidation). However, an ATP-driven sulfinic acid reducing enzyme called Srx is able to reverse this process [174,175]. Two groups have studied the mechanism of Srx-mediated Prx sulfinic acid reduction [146–148]. They propose slightly different pathways but agree on the involvement of a mixed protein thiosulfinate ester intermediate. The reaction takes Prx back to its reduced form, but it is very slow compared to the Trx-mediated disulfide reduction. Prx hyperoxidation is proposed to have a role in cellular signaling as a redox switch (reviewed in [2]).

Sulfinic acids can be further oxidized by strong oxidizing agents such as HOX, H_2O_2, or ONOOH to give sulfonic acids. These are believed to truly represent dead-end oxidation products, because no biological pathway has been discovered to date for sulfonic acid reduction. This posttranslational modification on an active site cysteine may irreversibly inhibit enzyme function. Chae *et al*. have shown that sulfonic acid formation on

Prx activates a "super-chaperone" activity that may be induced during oxidative stress [176]. They have also discovered a protective mechanism against irreversible overoxidation by acetylation of the N-terminal amino group [177]. When formed on an N-terminal cysteine residue (such as GTPase-activating proteins) the sulfonic acid group can also be a marker for ubiquitin-dependent protein degradation [178–180].

4.5. Sulfenamide, sulfinamide, and sulfonamide

The discovery of a sulfenamide intermediate in the oxidation of the catalytic cysteine of PTP1B drew attention to this type of posttranslational modification [111,112]. The PTP1B sulfenamide is formed via electrophilic attack of the catalytic Cys sulfenic acid residue on the adjacent main chain amide nitrogen to form a five-membered sulfenamide ring (also called sulfenyl amide). It is proposed to protect the catalytic cysteine from overoxidation during oxidative stress. Sulfenamide formation is accompanied by conformational changes in the active site, which retards substrate binding. Importantly, this cyclic sulfenamide can further react with thiols, for example, GSH, thus allowing reversible redox-regulated enzyme inhibition. Formation of five-membered isothiazolidinone rings, analogous to the sulfenamide in PTP1B, requires high energy, which can be associated with the breakage of the S–O bond [181]. However by enhancing the electrophilicity of the sulfenic acid sulfur or the nucleophilicity of the amide nitrogen (e.g., via H-bonding between the amide oxygen and His214 in PTP1B) the reaction can be so favorable as to proceed even in the presence of thiols. Sulfenamide, sulfinamide, and sulfonamide formation in peptides by hypochlorous acid has been demonstrated and proposed as a potential pathway for myeloperoxidase-mediated cross-linking of low-density lipoproteins [109]. HOCl-mediated oxidation of the neutrophil cytoplasmic protein S100A8 also results in sulfinamide formation via intramolecular as well as intermolecular cross linking. These sulfinamides are stable and form via a sulfenic acid intermediate that was chemically trapped in the presence of dimedone [110].

The reaction of GSH with HOCl or HOBr results in the formation of a stable sulfonamide derivative with a nine-membered ring structure [154,182,183]. Glutathione sulfonamide has an intramolecular covalent bond between its γ-glutamyl ammonium nitrogen and its Cys sulfur and is proposed to form via a sulfenamide intermediate. Glutathione sulfonamide is formed in cellular systems and it is stable under physiological conditions [182–184]. It forms when the oxidants are generated by myeloperoxidase or neutrophils and it is specific to HOCl or HOBr-initiated two-electron redox reactions of GSH. This makes it an important biomarker for neutrophil-mediated oxidative damage in clinical samples [185].

5. Radical-Mediated Chain Reactions Involving Thiols

Free radicals are highly reactive species, with one or more unpaired electrons on an open-shell configuration. Radical-mediated acute or cumulative tissue injury is associated with many diseases including inflammatory and neurodegenerative diseases, atherosclerosis, cancer, and aging. The most extensively studied endogenously generated free radicals include the hydroxyl radical ($OH^{\bullet}$), $O_2^{\bullet-}$, NO, nitrogen dioxide ($NO_2^{\bullet}$), and tyrosyl radical. They all react with thiols and eventually produce similar closed-shell intermediates and products as the two-electron oxidants (see Scheme 5). The reaction of $OH^{\bullet}$ is diffusion controlled at pH 7 [186], but most other radicals react more slowly.

Tyrosyl radicals together with $NO_2^{\bullet}$ can be produced by peroxidase-catalyzed reactions. Protein tyrosyl radicals also participate in the catalytic cycle of some enzymes such as ribonucleotide reductase. Hydroxyl radical ($OH^{\bullet}$) is produced by splitting water by ionizing radiation or by transition metal ion-catalyzed homolytic cleavage of the O–O bond in H_2O_2 (called Fenton or Fenton-like reactions). It is the most reactive and indiscriminant radical produced by living organisms. $O_2^{\bullet-}$ represents the most abundant radical in biology. It is primarily generated during respiration via the

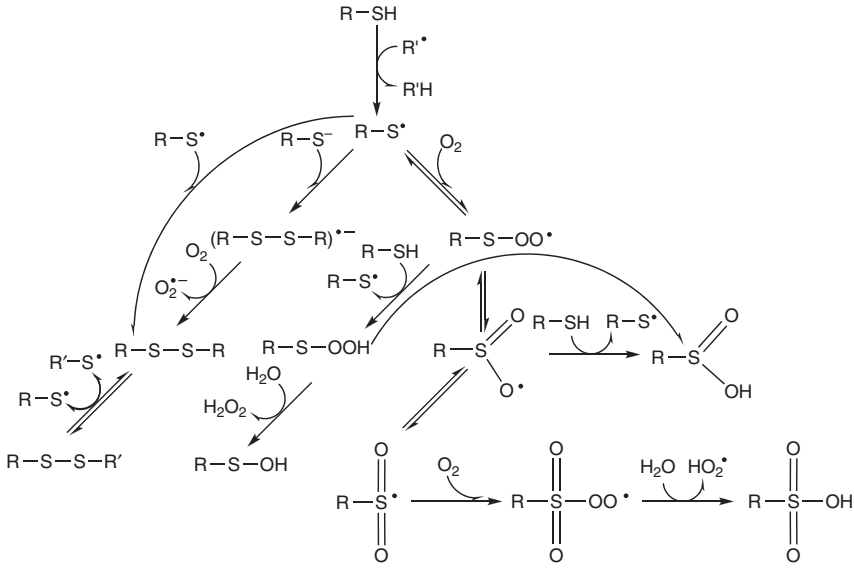

Scheme 5 One-electron reaction cascade of common biological Cys-derived radicals. Reviewed in [189].

accidental leakage of electrons from the mitochondrial electron transport chain or by the Nox (NADPH oxidase) family of enzymes. NO is produced *in vivo* by neuronal, inducible, or endothelial NO synthases during the oxidation of L-arginine to L-citrulline. Its cell regulatory role is mainly attributed to its interaction with guanylate cyclase but its reactions with protein thiols to form, among others, nitrosothiol intermediate species are increasingly recognized as major contributors to its signaling function [187]. The chemistry of nitrosothiol formation and degradation is a subject of a heated debate. Several pathways including one- and two-electron redox reactions are proposed and reviewed elsewhere [188].

Most radicals react with thiols to generate the highly reactive thiyl radical [186]. Thiyl radicals can combine to give a closed-shell disulfide with a second-order rate constant of $2k = 1.5 \times 10^9\,M^{-1}\,s^{-1}$ for GSH [190]. This reaction, albeit fast, is likely to be minor in a physiological environment, because thiyl radicals are highly reactive with other more abundant species. The two most favorable reactions of thiyl radicals under biological conditions are (1) with molecular oxygen ($k \sim 10^8$–$10^9\,M^{-1}\,s^{-1}$) to give a thiyl peroxyl radical ($RSOO^{\bullet}$) or (2) with another thiol ($>10^9\,M^{-1}\,s^{-1}$) to give a disulfide radical anion ($RSSR^{\bullet-}$). The latter reaction proceeds via the deprotonated thiolate; therefore, the apparent rate of this reaction will be dependent on the pK_a and concentration of the thiol. In contrast to the oxidizing thiyl radical, $RSSR^{\bullet-}$ is a very powerful reductant. It predominantly reacts with molecular oxygen ($k = 5 \times 10^9\,M^{-1}\,s^{-1}$ for GSH) to give $O_2^{\bullet-}$ and RSSR. $RSOO^{\bullet}$ can be reduced to a thiyl hydroperoxide (RSOOH) via hydrogen abstraction, which was suggested to be a possible intermediate in the formation of sulfenic, sulfinic, and sulfonic acids [94,95,191]. Alternatively $RSOO^{\bullet}$ can react with another thiol molecule to give a sulfenic acid and a sulfinyl radical. The latter can also be reduced to sulfenic acid after hydrogen abstraction [52,192]. The isomerization of $RSOO^{\bullet}$ to the sulfonyl radical ($RSO_2^{\bullet}$) is thermodynamically favored [193]. $RSO_2^{\bullet}$ can be reduced to a sulfinic acid or react further with oxygen to give the sulfonyl peroxyl radical ($RSO_2OO^{\bullet}$) [193]. $RSO_2OO^{\bullet}$ ultimately converts to a sulfonic acid [194].

From a biological point of view, the reaction of thiyl radicals with oxygen is proposed to have a minor role compared to the reaction with another thiolate in the presence of millimolar glutathione concentrations at pH 6–8, representative of a cellular environment [195]. As GSH was shown to play an important role in scavenging oxidizing radicals, the subsequent conversion of these radicals to $O_2^{\bullet-}$ via $RSSR^{\bullet-}$, to be destroyed by superoxide dismutase represent an intriguing intracellular radical sink [196–200]. This hypothesis was corroborated by rigorous physical chemical calculations of the energetics of all possible reactions [201]. It is important to mention that ascorbate competes for the thiyl radical with glutathione representing another radical sink mechanism which is discussed elsewhere [202].

$$O_2^{\bullet-} + GSH \longrightarrow (GS{-}{-}{-}O_2H)^{\bullet-} \longrightarrow GSO^{\bullet} + OH^-$$

$$GSO^{\bullet} + GSH \longrightarrow GSOH + GS^{\bullet}$$

$$GSOH + GSH \longrightarrow GSSG + H_2O$$

$$GS^{\bullet} + GS^- \rightleftharpoons GSSG^{\bullet-}$$

$$GSSG^{\bullet-} + O_2 \longrightarrow GSSG + O_2^{\bullet-}$$

$$2O_2^{\bullet-} + 2H^+ \longrightarrow O_2 + H_2O_2$$

Scheme 6 Short radical chain reactions initiated by the reaction of $O_2^{\bullet-}$ with GSH [197].

The rate of the reaction of $O_2^{\bullet-}$ with thiols is relatively slow (the second-order rate constant is only around 10–1000 $M^{-1}s^{-1}$ [197,200,203–205], but the large concentration of thiols makes it feasable under physiological conditions. The reactions comprise a short chain that consumes oxygen and regenerates $O_2^{\bullet-}$ (see Scheme 6) [197]. The chain reaction eventually yields 90% GSSG and 10% GSO_3H, representing the partitioning of the preformed thiyl radical between another thiolate and oxygen, respectively.

6. Hydrogen Sulfide

An emerging signaling molecule, H_2S, from the chemical point of view can be seen as the smallest thiol. It represents a sulfhydryl group with only one extra hydrogen attached to it. Initial reports on the biology of H_2S were focused on its toxicity, mainly via its inhibitory effect on cytochrome *c* oxidase [206]. However, it is now clear that H_2S is formed physiologically in mammalian tissue by the pyridoxal phosphate-dependent enzymes, cystathione gamma lyase and cystathione beta synthetase, that are involved in the transsulfuration pathways of cysteine metabolism [207]. The discovery of the *in vivo* generation of H_2S resulted in a sharp increase of studies to assess its physiological function. Following on from NO and carbon monoxide (CO), it is also identified as a physiological gasotransmitter. A large body of literature has accumulated on the signaling properties of NO and CO and the role of H_2S as a signaling molecule is also increasingly recognized [208,209]. As with NO and CO it has vasorelaxant properties, but unlike NO or CO it acts via opening K_{ATP} channels [210,211]. It induces suspended animation in mice by decreasing oxygen consumption and drastic reduction of metabolic rate [212] and increases thermotolerance and lifespan in *Caenorhabditis elegans* [213]. Its medical and therapeutic potential is attracting considerable interest [214]. The protective role of H_2S in cardiovascular disease was reported recently by several research groups [209,215–217]. Lefer and colleagues showed that direct injection of H_2S into the heart protects against

inflammatory events and ischemia reperfusion injury [216]. Evidence that H_2S is indeed a physiologic vasorelaxant arose from the hypertension seen in cystathione γ lyase knockout mice [211].

However, the physiological effects of H_2S are controversial. Conflicting reports suggest pro- [218] and anti-inflammatory [219], pro- [220] and antiapoptotic [221], and pro- [222] and antioxidant [223] effects of H_2S. This is perhaps the result of the diverse physiological chemistry of H_2S that has not been fully explored. Future studies to understand the underlying chemical mechanisms of the interactions of H_2S with biological molecules (some proposed major pathways are outlined in Figure 4) are needed to explain controversial physiological observations.

H_2S reacts rapidly with two-electron oxidants. As the smallest thiol, its redox chemistry exhibits similarities to that of cysteine. A major difference is that whereas the highest common oxidation state of sulfur for cysteine derivatives is +4 in sulfonic acids, sulfite (SO_3^{2-}, which is the sulfonic acid analog of H_2S) can be easily oxidized to sulfate (SO_4^{2-}) [224,225] in which the oxidation state of the sulfur center is +6. H_2S reacts rapidly with ONOOH, H_2O_2, lipid peroxides, and HOCl ([226–228] and P. Nagy, unpublished results). Its oxidation can lead to the formation of polysulfides HS_x^- ($x = 2$–8), thiosulfate ($S_2O_3^{2-}$), tetrathionate ($S_4O_6^{2-}$), SO_3^{2-}, and SO_4^{2-}. Similar to cysteine thiol oxidation products, these species also interconvert [229,230]. The kinetics of H_2S oxidation reactions have not been widely studied except for its relatively slow reaction with H_2O_2 [231,232]. The bimolecular reaction is proposed to give a sulfenic acid analog HSOH. It is also proposed to be a short-lived intermediate (that

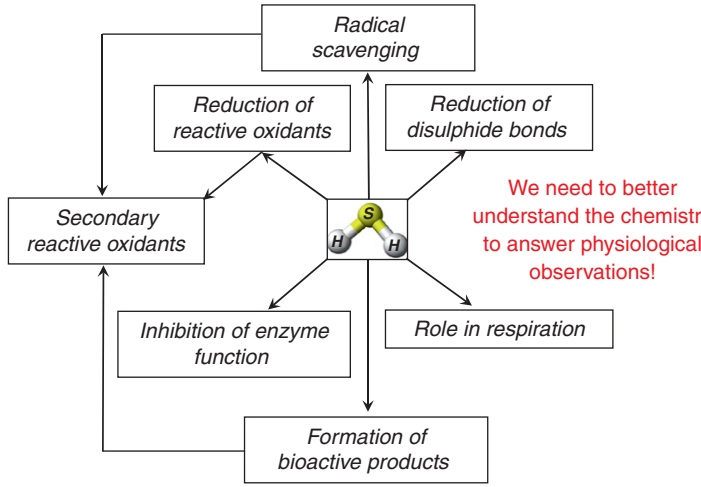

Figure 4 Proposed molecular mechanisms for the interactions of H_2S with biological molecules.

has never been observed experimentally) and similar to cysteine sulfenic acids another SH^- and H_2O_2 can compete for HSOH to give polysulfides or polythionates (oxysulfur species), respectively.

7. Conclusions

The chemical properties of sulfur make it very reactive in biological systems. Cysteine residues are primary targets of endogenous oxidants that are generated in large quantities especially under inflammatory conditions. Thiols engage in two-electron oxidation reactions and they are also efficient scavengers of radical species. The rates of these reactions are largely dependent on the chemical properties of the oxidant as well as the thiol. The nucleophilic character of thiols is probably the most important factor that determines reactivity. This property is reflected in thiol ionizability and therefore the acid dissociation constants of sulfhydryl groups provide invaluable information in kinetic studies. Using the rate constants obtained from kinetic investigations in modeling potential cellular targets of different oxidants provide a very powerful tool for cell biologists.

Most studies are focused on the initial oxidation step. However, it is now clear that these primary reactions generate reactive intermediates, which initiate a cascade of redox events. The mechanisms of these reactions are not well understood. Nevertheless, their importance in determining the final outcome of the oxidative stimuli is more appreciated and warrants further investigation.

Recent improvements in proteomic, kinetic, and imaging techniques to detect cysteine posttranslational modifications and previously undetected intermediate species has resulted in an explosion of publications on redox mediated cellular events via thiol oxidation. To be able to gain further insight into the functional significance and regulation of these phenomena, it is essential to undertake a multidisciplinary approach, which includes mechanistic studies using rigorous chemical analysis.

The recent discovery that H_2S exerts its signaling properties via interacting with protein thiols to form persulfides opens up a new aspect of thiol biochemistry [233]. This further complicates the redox chemistry of thiols and sets the stage for systematic chemical and biochemical studies.

REFERENCES

[1] P. Nagy, J.D. Becker, R.C. Mallo, M.T. Ashby, The Jekyll and Hyde roles of cysteine derivatives during oxidative stress, New Biocides Dev. Comb. Approach Chem. Microbiol. 967 (2007) 193–212.

[2] L.B. Poole, K.J. Nelson, Discovering mechanisms of signaling-mediated cysteine oxidation, Curr. Opin. Chem. Biol. 12 (2008) 18–24.

[3] K.G. Reddie, K.S. Carroll, Expanding the functional diversity of proteins through cysteine oxidation, Curr. Opin. Chem. Biol. 12 (2008) 746–754.
[4] C.C. Winterbourn, Reconciling the chemistry and biology of reactive oxygen species, Nat. Chem. Biol. 4 (2008) 278–286.
[5] C.C. Winterbourn, M.B. Hampton, Thiol chemistry and specificity in redox signaling, Free Radic. Biol. Med. 45 (2008) 549–561.
[6] A. Yarnell, Cysteine oxidation, Chem Eng. News 87 (2009) 38–40.
[7] R.J. Soberman, The expanding network of redox signaling: New observations, complexities, and perspectives, J. Clin. Invest. 111 (2003) 571–574.
[8] A.G. Cox, A.V. Peskin, L.N. Paton, C.C. Winterbourn, M.B. Hampton, Redox potential and peroxide reactivity of human peroxiredoxin 3, Biochemistry 48 (2009) 6495–6501.
[9] B. Manta, M. Hugo, C. Ortiz, G. Ferrer-Sueta, M. Trujillo, A. Denicola, The peroxidase and peroxynitrite reductase activity of human erythrocyte peroxiredoxin 2, Arch. Biochem. Biophys. 484 (2009) 146–154.
[10] D. Parsonage, P.A. Karplus, L.B. Poole, Substrate specificity and redox potential of AhpC, a bacterial peroxiredoxin, Proc. Natl. Acad. Sci. U. S. A. 105 (2008) 8209–8214.
[11] A.V. Peskin, F.M. Low, L.N. Paton, G.J. Maghzal, M.B. Hampton, C.C. Winterbourn, The high reactivity of peroxiredoxin 2 with H(2)O(2) is not reflected in its reaction with other oxidants and thiol reagents, J. Biol. Chem. 282 (2007) 11885–11892.
[12] P. Nagy, K. Lemma, M.T. Ashby, Kinetics and mechanism of the comproportionation of hypothiocyanous acid and thiocyanate to give thiocyanogen in acidic aqueous solution, Inorg. Chem. 46 (2007) 285–292.
[13] P. Nagy, G.N. Jameson, C.C. Winterbourn, Kinetics and mechanisms of the reaction of hypothiocyanous acid with 5-thio-2-nitrobenzoic acid and reduced glutathione, Chem. Res. Toxicol. 22 (2009) 1833–1840.
[14] L.C. Adam, I. Fabian, K. Suzuki, G. Gordon, Hypochlorous acid decomposition in the pH 5-8 region, Inorg. Chem. 31 (1992) 3534–3541.
[15] C.M. Gerritsen, M. Gazda, D.W. Margerum, Non-metal redox kinetics: Hypobromite and hypoiodite reactions with cyanide and the hydrolysis of cyanogen halides, Inorg. Chem. 32 (1993) 5739–5748.
[16] W.A. Prutz, R. Kissner, T. Nauser, W.H. Koppenol, On the oxidation of cytochrome c by hypohalous acids, Arch. Biochem. Biophys. 389 (2001) 110–122.
[17] K.D. Fogelman, D.M. Walker, D.W. Margerum, Non-metal redox kinetics—hypochlorite and hypochlorous acid reactions with sulfite, Inorg. Chem. 28 (1989) 986–993.
[18] C.M. Gerritsen, M. Gazda, D.W. Margerum, Nonmetal redox kinetics—hypobromite and hypoiodite reactions with cyanide and the hydrolysis of cyanogen halides, Inorg. Chem. 32 (1993) 5739–5748.
[19] P. Nagy, M.T. Ashby, Reactive sulfur species: Kinetics and mechanisms of the oxidation of cysteine by hypohalous acid to give cysteine sulfenic acid, J. Am. Chem. Soc. 129 (2007) 14082–14091.
[20] P. Nagy, J.L. Beal, M.T. Ashby, Thiocyanate is an efficient endogenous scavenger of the phagocytic killing agent hypobromous acid, Chem. Res. Toxicol. 19 (2006) 587–593.
[21] D.I. Pattison, M.J. Davies, Reactions of myeloperoxidase-derived oxidants with biological substrates: Gaining chemical insight into human inflammatory diseases, Curr. Med. Chem. 13 (2006) 3271–3290.
[22] A.V. Peskin, C.C. Winterbourn, Kinetics of the reactions of hypochlorous acid and amino acid chloramines with thiols, methionine, and ascorbate, Free Radic. Biol. Med. 30 (2001) 572–579.

[23] O. Skaff, D.I. Pattison, M.J. Davies, Hypothiocyanous acid reactivity with low-molecular-mass and protein thiols: Absolute rate constants and assessment of biological relevance, Biochem. J. 422 (2009) 111–117.
[24] C.C. Winterbourn, Comparative reactivities of various biological compounds with myeloperoxidase-hydrogen peroxide-chloride, and similarity of the oxidant to hypochlorite, Biochim. Biophys. Acta 840 (1985) 204–210.
[25] X.L. Armesto, M. Canle, M.I. Fernandez, M.V. Garcia, J.A. Santabella, First steps in the oxidation of sulfur-containing amino acids by hypohalogenation: Very fast generation of intermediate sulfenyl halides and halosulfonium cations, Tetrahedron 56 (2000) 1103–1109.
[26] W.A. Prutz, R. Kissner, W.H. Koppenol, H. Ruegger, On the irreversible destruction of reduced nicotinamide nucleotides by hypohalous acids, Arch. Biochem. Biophys. 380 (2000) 181–191.
[27] M.T. Ashby, H. Aneetha, Reactive sulfur species: Aqueous chemistry of sulfenyl thiocyanates, J. Am. Chem. Soc. 126 (2004) 10216–10217.
[28] C.L. Hawkins, D.I. Pattison, N.R. Stanley, M.J. Davies, Tryptophan residues are targets in hypothiocyanous acid-mediated protein oxidation, Biochem. J. 416 (2008) 441–452.
[29] K. Lemma, M.T. Ashby, Reactive sulfur species: Kinetics and mechanism of the equilibrium between cysteine sulfenyl thiocyanate and cysteine thiosulfinate ester in acidic aqueous solution, J. Org. Chem. 73 (2008) 3017–3023.
[30] E.L. Thomas, T.M. Aune, Lactoperoxidase, peroxide, thiocyanate anti-microbial system—correlation of sulfhydryl oxidation with anti-microbial action, Infect. Immun. 20 (1978) 456–463.
[31] M.T. Ashby, A.C. Carlson, M.J. Scott, Redox buffering of hypochlorous acid by thiocyanate in physiologic fluids, J. Am. Chem. Soc. 126 (2004) 15976–15977.
[32] D.I. Pattison, M.J. Davies, Kinetic analysis of the reactions of hypobromous acid with protein components: Implications for cellular damage and use of 3-bromotyrosine as a marker of oxidative stress, Biochemistry 43 (2004) 4799–4809.
[33] P. Nagy, X. Wang, K. Lemma, M.T. Ashby, Reactive sulfur species: Hydrolysis of hypothiocyanite to give thiocarbamate-S-oxide, J. Am. Chem. Soc. 129 (2007) 15756–15757.
[34] X.G. Wang, M.T. Ashby, Reactive sulfur species: Kinetics and mechanism of the reaction of thiocarbamate-S-oxide with cysteine, Chem. Res. Toxicol. 21 (2008) 2120–2126.
[35] P. Nagy, M.T. Ashby, Reactive sulfur species: Kinetics and mechanism of the oxidation of cystine by hypochlorous acid to give N,N′-dichlorocystine, Chem. Res. Toxicol. 18 (2005) 919–923.
[36] P. Nagy, M.T. Ashby, Kinetics and mechanism of the oxidation of the glutathione dimer by hypochlorous Acid and catalytic reduction of the chloroamine product by glutathione reductase, Chem. Res. Toxicol. 20 (2007) 79–87.
[37] M.S.A. Coker, W. Hu, S.T. Senthilmohan, A.J. Kettle, Pathways for the decay of organic dichloramines and liberation of antimicrobial chloramine gases, Chem. Res. Toxicol. 21 (2008) 2334–2343.
[38] E.L. Thomas, Myeloperoxidase, hydrogen-peroxide, chloride anti-microbial system—nitrogen-chlorine derivatives of bacterial components in bactericidal action against Escherichia-Coli, Infect. Immun. 23 (1979) 522–531.
[39] M.B. Grisham, M.M. Jefferson, D.F. Melton, E.L. Thomas, Chlorination of endogenous amines by isolated neutrophils. Ammonia-dependent bactericidal, cytotoxic, and cytolytic activities of the chloramines, J. Biol.Chem. 259 (1984) 10404–10413.
[40] R.G. Midwinter, F.C. Cheah, J. Moskovitz, M.C. Vissers, C.C. Winterbourn, IkappaB is a sensitive target for oxidation by cell-permeable chloramines: Inhibition of NF-kappaB activity by glycine chloramine through methionine oxidation, Biochem. J. 396 (2006) 71–78.

[41] R.G. Midwinter, A.V. Peskin, M.C.M. Vissers, C.C. Winterbourn, Extracellular oxidation by taurine chloramine activates ERK via the epidermal growth factor receptor, J. Biol. Chem. 279 (2004) 32205–32211.
[42] A.V. Peskin, R.G. Midwinter, D.T. Harwood, C.C. Winterbourn, Chlorine transfer between glycine, taurine and histamine: Reaction rates and impact on cellular reactivity, Free Radic. Biol. Med. 15 (2004) 1622–1630.
[43] E.L. Thomas, M.B. Grisham, M.M. Jefferson, Cytotoxicity of chloramines, Methods Enzymol. 132 (1986) 585–593.
[44] T. Nauser, W.H. Koppenol, The rate constant of the reaction of superoxide with nitrogen monoxide: Approaching the diffusion limit, J. Phys. Chem. A 106 (2002) 4084–4086.
[45] J.W. Coddington, J.K. Hurst, S.V. Lymar, Hydroxyl radical formation during peroxynitrous acid decomposition, J. Am. Chem. Soc. 121 (1999) 2438–2443.
[46] M. Kirsch, H.G. Korth, A. Wensing, R. Sustmann, H. de Groot, Product formation and kinetic simulations in the pH range 1-14 account for a free-radical mechanism of peroxynitrite decomposition, Arch. Biochem. Biophys. 418 (2003) 133–150.
[47] R. Kissner, W.H. Koppenol, Product distribution of peroxynitrite decay as a function of pH, temperature, and concentration, J. Am. Chem. Soc. 124 (2002) 234–239.
[48] S.V. Lymar, R.F. Khairutdinov, J.K. Hurst, Hydroxyl radical formation by O-O bond homolysis in peroxynitrous acid, Inorg. Chem. 42 (2003) 5259–5266.
[49] S. Pfeiffer, A.C.F. Gorren, K. Schmidt, E.R. Werner, B. Hansert, D.S. Bohle, B. Mayer, Metabolic fate of peroxynitrite in aqueous solution—reaction with nitric oxide and pH-dependent decomposition to nitrite and oxygen in a 2:1 stoichiometry, J. Biol. Chem. 272 (1997) 3465–3470.
[50] D. Gupta, B. Harish, R. Kissner, W.H. Koppenol, Peroxynitrate is formed rapidly during decomposition of peroxynitrite at neutral pH, Dalton Trans. (2009) 5730–5736.
[51] R. Kissner, T. Nauser, P. Bugnon, P.G. Lye, W.H. Koppenol, Formation and properties of peroxynitrite as studied by laser flash photolysis, high-pressure stopped-flow technique, and pulse radiolysis, Chem. Res. Toxicol. 10 (1997) 1285–1292.
[52] C. Quijano, B. Alvarez, R.M. Gatti, O. Augusto, R. Radi, Pathways of peroxynitrite oxidation of thiol groups, Biochem. J. 322 (1997) 167–173.
[53] B. Alvarez, G. Ferrer-Sueta, B.A. Freeman, R. Radi, Kinetics of peroxynitrite reaction with amino acids and human serum albumin, J. Biol. Chem. 274 (1999) 842–848.
[54] R. Radi, J.S. Beckman, K.M. Bush, B.A. Freeman, Peroxynitrite oxidation of sulfhydryls. The cytotoxic potential of superoxide and nitric oxide, J. Biol.Chem. 266 (1991) 4244–4250.
[55] M. Trujillo, R. Radi, Peroxynitrite reaction with the reduced and the oxidized forms of lipoic acid: New insights into the reaction of peroxynitrite with thiols, Arch. Biochem. Biophys. 397 (2002) 91–98.
[56] R. Bryk, P. Griffin, C. Nathan, Peroxynitrite reductase activity of bacterial peroxiredoxins, Nature 407 (2000) 211–215.
[57] R. Ogusucu, D. Rettori, D.C. Munhoz, L.E. Netto, O. Augusto, Reactions of yeast thioredoxin peroxidases I and II with hydrogen peroxide and peroxynitrite: Rate constants by competitive kinetics, Free Radic. Biol. Med. 42 (2007) 326–334.
[58] M. Trujillo, A. Clippe, B. Manta, G. Ferrer-Sueta, A. Smeets, J.P. Declercq, B. Knoops, R. Radi, Pre-steady state kinetic characterization of human peroxiredoxin 5: Taking advantage of Trp84 fluorescence increase upon oxidation, Arch. Biochem. Biophys. 467 (2007) 95–106.
[59] M. Trujillo, G. Ferrer-Sueta, L. Thomson, L. Flohe, R. Radi, Kinetics of peroxiredoxins and their role in the decomposition of peroxynitrite, Subcell. Biochem. 44 (2007) 83–113.

[60] R.P. Szajewski, G.M. Whitesides, Rate constants and equilibrium-constants for thiol-disulfide interchange reactions involving oxidized glutathione, J. Am. Chem. Soc. 102 (1980) 2011–2026.
[61] J.M. Wilson, R.J. Bayer, D.J. Hupe, Structure-reactivity correlations for thiol-disulfide interchange reaction, J. Am. Chem. Soc. 99 (1977) 7922–7926.
[62] M.N. Hughes, M.N. Centelles, K.P. Moore, Making and working with hydrogen sulfide: The chemistry and generation of hydrogen sulfide in vitro and its measurement in vivo: A review, Free Radic. Biol. Med. 47 (2009) 1346–1353.
[63] Z. Szakacs, M. Kraszni, B. Noszal, Determination of microscopic acid-base parameters from NMR-pH titrations, Anal. Bioanal. Chem. 378 (2004) 1428–1448.
[64] H. Borsook, E.L. Ellis H.M. Huffman, Sulfhydryl oxidation—reduction potentials derived from thermal data, J. Biol. Chem. 117 (1937) 281–308.
[65] E.J. Cohn, J.T. Edsall, Proteins, Amino Acids and Peptides as Ions and Dipolar Ions, Reinhold Publ. Corp., New York, 1943.
[66] M. Calvin, Mercaptans and Disulfides, Academic Press, Inc., New York, NY, 1954, pp 8–11.
[67] D.D. Perrin, Dissociation Constants of Organic Bases in Aqueous Solution, Butterworths, London, 1965.
[68] H.A. Sober, CRC Handbook of Biochemistry: Selected Data for Molecular Biology, (2nd edn), Chemical Rubber Co, Cleveland, 1970.
[69] G.M. Bodner, Assigning the pKa's of polyprotic acids, J. Chem. Educ. 63 (1986) 246–247.
[70] M.A. Grafius, J.B. Neilands, Apparent dissociation constants of cysteine derivatives, J. Am. Chem. Soc. 77 (1955) 3389–3390.
[71] J.T. Edsall, R.B. Martin, B.R. Hollingworth, Ionization of individual groups in dibasic acids, with application to the amino and hydroxyl groups of tyrosine, Proc. Natl. Acad. Sci. U. S. A. 44 (1958) 505–518.
[72] R.E. Benesch, R. Benesch, The acid strength of the -SH group in cysteine and related compounds, J. Am. Chem. Soc. 77 (1955) 5877–5881.
[73] R.H. De Deken, J. Broekhuysen, J. Bechet, A. Mortier, Spectrophotometric study of the dissociation of the sulfhydryl group and molecular structure of cysteine, Biochim. Biophys. Acta 19 (1956) 45–52.
[74] E.L. Elson, J.T. Edsall, Raman spectra and sulfhydryl ionization constants of thioglycolic acid and cysteine, Biochemistry 1 (1962) 1–7.
[75] D. Garfinkel, J.T. Edsall, Raman spectra of amino acids and related compounds. 11. The ionization of cysteine, J. Am. Chem. Soc. 80 (1958) 3823–3826.
[76] J.T. Edsall, The ionization of cysteine and the possible role of hydrogen bonding by the thiol group, Biochemistry 4 (1965) 28–31.
[77] D.M.E. Reuben, T.C. Bruice, Reaction of thiol anions with benzene oxide and malachite green, J. Am. Chem. Soc. 98 (1976) 114–121.
[78] P.H. Connett, K.E. Wetterhahn, Reaction of chromium(Vi) with thiols—pH-Dependence of chromium(Vi) thio ester formation, J. Am. Chem. Soc. 108 (1986) 1842–1847.
[79] H. Lindley, Study of the kinetics of the reaction between thiol compounds and chloroacetamide, Biochem. J. 74 (1960) 577–584.
[80] E. Grunwald, K.C. Chang, P.L. Skipper, V.K. Anderson, Kinetics of bifunctional proton-transfer. 2. Lysine and cysteine in aqueous-solutions, J. Phys. Chem. 80 (1976) 1425–1431.
[81] W. Stricks, I.M. Kolthoff, Equilibrium constants of the reactions of sulfite with cystine and with dithiodiglycolic acid, J. Am. Chem. Soc. 73 (1951) 4569–4574.
[82] P. Nagy, M.T. Ashby, Reactive sulfur species: Kinetics and mechanism of the hydrolysis of cysteine thiosulfinate ester, Chem. Res. Toxicol. 20 (2007) 1364–1372.

[83] P. Nagy, K. Lemma, M.T. Ashby, Reactive sulfur species: Kinetics and mechanisms of the reaction of cysteine thiosulfinate ester with cysteine to give cysteine sulfenic acid, J. Org. Chem. 72 (2007) 8838–8846.
[84] D.L. Rabenstein, Nuclear magnetic-resonance studies of acid-base chemistry of amino-acids and peptides. 1. Microscopic ionization-constants of glutathione and methylmercury-complexed glutathione, J. Am. Chem. Soc. 95 (1973) 2797–2803.
[85] D.L. Rabenstein, D.A. Keire, Nuclear magnetic resonance spectroscopy of glutathione, Coenzymes Cofactors 3 (1989) 67–101.
[86] H.M.S. Patel, D.L.H. Williams, Nitrosation by alkyl nitrites. 6. Thiolate nitrosation, J. Chem. Soc. Perkin Trans. 2 (1990) 37–42.
[87] P.T. Chivers, K.E. Prehoda, B.F. Volkman, B.M. Kim, J.L. Markley, R.T. Raines, Microscopic pK(a) values of Escherichia coli thioredoxin, Biochemistry 36 (1997) 14985–14991.
[88] I. Krimm, S. Lemaire, E. Ruelland, M. Miginiac-Maslow, J.P. Jaquot, M. Hirasawa, D.B. Knaff, J.M. Lancelin, The single mutation Trp35 → Ala in the 35-40 redox site of Chlamydomonas reinhardtii thioredoxin h affects its biochemical activity and the pH dependence of C36-C39 H-1-C-13 NMR, Eur. J. Biochem. 255 (1998) 185–195.
[89] E. Mossner, H. Iwai, R. Glockshuber, Influence of the pK(a) value of the buried, active-site cysteine on the redox properties of thioredoxin-like oxidoreductases, FEBS Lett. 477 (2000) 21–26.
[90] R. Benesch, R.E. Benesch, Thiolation of proteins, Proc. Natl. Acad. Sci. U. S. A. 44 (1958) 848–853.
[91] K.J. Nelson, A.E. Day, B.B. Zeng, S.B. King, L.B. Poole, Isotope-coded, iodoacetamide-based reagent to determine individual cysteine pK(a) values by matrix-assisted laser desorption/ionization time-of-flight mass spectrometry, Anal. Biochem. 375 (2008) 187–195.
[92] K.J. Nelson, D. Parsonage, A. Hall, P.A. Karplus, L.B. Poole, Cysteine pK(a) values for the bacterial peroxiredoxin AhpC, Biochemistry 47 (2008) 12860–12868.
[93] H. Li, A.D. Robertson, J.H. Jensen, Very fast empirical prediction and rationalization of protein pK(a) values, Proteins: Struct. Funct. Bioinf. 61 (2005) 704–721.
[94] W.S. Allison, Formation and reactions of sulfenic acids in proteins, Acc. Chem. Res. 9 (1976) 293–299.
[95] S. Carballal, R. Radi, M.C. Kirk, S. Barnes, B.A. Freeman, B. Alvarez, Sulfenic acid formation in human serum albumin by hydrogen peroxide and peroxynitrite, Biochemistry 42 (2003) 9906–9914.
[96] L.B. Poole, H.R. Ellis, Identification of cysteine sulfenic acid in AhpC of alkyl hydroperoxide reductase, Methods Enzymol. 348 (2002) 122–136.
[97] L.B. Poole, P.A. Karplus, A. Claiborne, Protein sulfenic acids in redox signaling, Annu. Rev. Pharmacol. Toxicol. 44 (2004) 325–347.
[98] J.S. Stamler, D.I. Simon, J.A. Osborne, M.E. Mullins, O. Jaraki, T. Michel, D.J. Singel, J. Loscalzo, S-Nitrosylation of proteins with nitric-oxide—synthesis and characterization of biologically-active compounds, Proc. Natl. Acad. Sci. U. S. A. 89 (1992) 444–448.
[99] A. van der Vliet, P.A.C. Hoen, P.S.Y. Wong, A. Bast, C.E. Cross, Formation of S-nitrosothiols via direct nucleophilic nitrosation of thiols by peroxynitrite with elimination of hydrogen peroxide, J. Biol. Chem. 273 (1998) 30255–30262.
[100] D.A. Wink, R.W. Nims, J.F. Darbyshire, D. Christodoulou, I. Hanbauer, G.W. Cox, F. Laval, J. Laval, J.A. Cook, M.C. Krishna, W.G. Degraff, J.B. Mitchell, Reaction-kinetics for nitrosation of cysteine and glutathione in aerobic nitric-oxide solutions at neutral pH—insights into the fate and physiological-effects of intermediates generated in the NO/O_2 reaction, Chem. Res. Toxicol. 7 (1994) 519–525.

[101] G.I. Giles, C. Jacob, Reactive sulfur species: An emerging concept in oxidative stress, Biol. Chem. 383 (2002) 375–388.
[102] J.L. Kice, T.E. Rogers, Kinetic study of the reaction of mercaptans with phenyl benzenethiolsulfinate and benzenethiolsulfonate in aqueous dioxane, J. Am. Chem. Soc. 96 (1974) 8015–8019.
[103] S. Patai (Ed.), The Chemistry of Sulfenic Acids and Their Derivatives, John Wiley, New York 1990.
[104] L. Turell, H. Botti, S. Carballal, G. Ferrer-Sueta, J.A. Souza, R. Duran, B.A. Freeman, R. Radi, B. Alvarez, Reactivity of sulfenic acid in human serum albumin, Biochemistry 47 (2008) 358–367.
[105] S. Carballal, B. Alvarez, L. Turell, H. Botti, B.A. Freeman, R. Radi, Sulfenic acid in human serum albumin, Amino Acids 32 (2007) 543–551.
[106] P. Di Simplicio, S. Frosali, R. Priora, D. Summa, F.C. Di Simplicio, D. Di Giuseppe, A. Di Stefano, Biochemical and biological aspects of protein thiolation in cells and plasma, Antioxid. Redox Signal. 7 (2005) 951–963.
[107] E. Block, The organosulfur chemistry of the genus allium—implications for the organic-chemistry of sulfur, Angew. Chem. Int. Ed. Engl. 31 (1992) 1135–1178.
[108] Z.A. Wood, L.B. Poole, P.A. Karplus, Peroxiredoxin evolution and the regulation of hydrogen peroxide signaling, Science 300 (2003) 650–653.
[109] X. Fu, D.M. Mueller, J.W. Heinecke, Generation of intramolecular and intermolecular sulfenamides, sulfinamides, and sulfonamides by hypochlorous acid: A potential pathway for oxidative cross-linking of low-density lipoprotein by myeloperoxidase, Biochemistry 41 (2002) 1293–1301.
[110] M.J. Raftery, Z. Yang, S.M. Valenzuela, C.L. Geczy, Novel intra- and inter-molecular sulfinamide bonds in s100a8 produced by hypochlorite oxidation, J. Biol.Chem. 276 (2001) 33393–33401.
[111] A. Salmeen, J.N. Andersen, M.P. Myers, T.-C. Meng, J.A. Hinks, N.K. Tonks, D. Barford, Redox regulation of protein tyrosine phosphatase 1B involves a sulphenyl-amide intermediate, Nature 423 (2003) 769–773.
[112] R.L. van Montfort, M. Congreve, D. Tisi, R. Carr, H. Jhoti, Oxidation state of the active-site cysteine in protein tyrosine phosphatase 1B, Nature 423 (2003) 773–777.
[113] A. Claiborne, T.C. Mallett, J.I. Yeh, J. Luba, D. Parsonage, Structural, redox, and mechanistic parameters for cysteine-sulfenic acid function in catalysis and regulation, Adv. Protein Chem. 58 (2001) 215–276.
[114] A. Claiborne, J.I. Yeh, T.C. Mallett, J. Luba, E.J. Crane, V. Charrier, D. Parsonage, Protein-sulfenic acids: Diverse roles for an unlikely player in enzyme catalysis and redox regulation, Biochemistry 38 (1999) 15407–15416.
[115] H.J. Choi, S.W. Kang, C.H. Yang, S.G. Rhee, S.E. Ryu, Crystal structure of a novel human peroxidase enzyme at 2.0 angstrom resolution, Nat. Struct. Biol. 5 (1998) 400–406.
[116] S.W. Kang, I.C. Baines, S.G. Rhee, Characterization of a mammalian peroxiredoxin that contains one conserved cysteine, J. Biol. Chem. 273 (1998) 6303–6311.
[117] S. Boschi-Muller, S. Azza, S. Sanglier-Cianferani, F. Talfournier, A. Van Dorsselear, G. Branlant, A sulfenic acid enzyme intermediate is involved in the catalytic mechanism of peptide methionine sulfoxide reductase from Escherichia coli, J. Biol. Chem. 275 (2000) 35908–35913.
[118] K. Goto, M. Holler, R. Okazaki, Synthesis, structure, and reactions of a sulfenic acid bearing a novel bowl-type substituent: The first synthesis of a stable sulfenic acid by direct oxidation of a thiol, J. Am. Chem. Soc. 119 (1997) 1460–1461.
[119] K. Goto, K. Shimada, S. Furukawa, S. Miyasaka, Y. Takahashi, T. Kawashima, Formation of a stable sulfenic acid by hydrolysis of a thionitrate and a sulfenyl bromide, Chem. Lett. 35 (2006) 862–863.

[120] A. Ishii, K. Komiya, J. Nakayama, Synthesis of a stable sulfenic acid by oxidation of a sterically hindered thiol (Thiophenetriptycene-8-thiol) and its characterization, J. Am. Chem. Soc. 118 (1996) 12836–12837.
[121] N. Nakamura, A stable sulfenic acid, 9-triptycenesulfenic acid: Its isolation and characterization, J. Am. Chem. Soc. 105 (1983) 7172–7173.
[122] R. Tripolt, F. Belaj, E. Nachbaur, Unexpectedly stable sulfenic acid: 4,6-Dimethoxy-1,3,5-triazine-2-sulfenic acid; synthesis, properties, molecular and crystal structure, Z. Naturforsch. B Chem.Sci. 48 (1993) 1212–1222.
[123] T. Yoshimura, E. Tsukurimichi, S. Yamazaki, S. Soga, C. Shimasaki, K. Hasegawa, Synthesis of a stable sulfenic acid, trans-decalin-9-sulfenic acid, Chem. Commun. (Camb.). issue 18 (1992) 1337–1338.
[124] T. Nakamura, T. Yamamoto, M. Abe, H. Matsumura, Y. Hagihara, T. Goto, T. Yamaguchi, T. Inoue, Oxidation of archaeal peroxiredoxin involves a hypervalent sulfur intermediate, Proc. Natl. Acad. Sci. U.S.A. 105 (2008) 6238–6242.
[125] W. Panmanee, P. Vattanaviboon, L.B. Poole, S. Mongkolsuk, Novel organic hydroperoxide-sensing and responding mechanisms for OhrR, a major bacterial sensor and regulator of organic hydroperoxide stress, J. Bacteriol. 188 (2006) 1389–1395.
[126] H.A. Headlam, M. Gracanin, K.J. Rodgers, M.J. Davies, Inhibition of cathepsins and related proteases by amino acid, peptide, and protein hydroperoxides, Free Radic. Biol. Med. 40 (2006) 1539–1548.
[127] Z. Xu, L.S.M. Lam, L.H. Lam, S.F. Chau, T.B. Ng, S.W.N. Au, Molecular basis of the redox regulation of SUMO proteases: A protective mechanism of intermolecular disulfide linkage against irreversible sulfhydryl oxidation, FASEB J. 22 (2008) 127–137.
[128] J.M. Denu, K.G. Tanner, Specific and reversible inactivation of protein tyrosine phosphatases by hydrogen peroxide: Evidence for a sulfenic acid intermediate and implications for redox regulation, Biochemistry 37 (1998) 5633–5642.
[129] S.E. Leonard, K.G. Reddie, K.S. Carroll, Mining the thiol proteome for sulfenic acid modifications reveals new targets for oxidation in cells, ACS Chem. Biol. 4 (2009) 783–799.
[130] Y.H. Seo, K.S. Carroll, Profiling protein thiol oxidation in tumor cells using sulfenic acid-specific antibodies, Proc. Natl. Acad. Sci. U. S. A. 106 (2009) 16163–16168.
[131] M. Depuydt, S.E. Leonard, D. Vertommen, K. Denoncin, P. Morsomme, K. Wahni, J. Messens, K.S. Carroll, J.F. Collet, A periplasmic reducing system protects single cysteine residues from oxidation, Science 326 (2009) 1109–1111.
[132] J. Riemer, N. Bulleid, J.M. Herrmann, Disulfide formation in the ER and mitochondria: Two solutions to a common process, Science 324 (2009) 1284–1287.
[133] P.J. Hogg, Disulfide bonds as switches for protein function, Trends. Biochem. Sci. 28 (2003) 210–214.
[134] C.H. Lillig, C. Berndt, A. Holmgren, Glutaredoxin systems, Biochim. Biophys. Acta 1780 (2008) 1304–1317.
[135] C.H. Lillig, A. Holmgren, Thioredoxin and related molecules—from biology to health and disease, Antioxi. Redox Signal. 9 (2007) 25–47.
[136] E.S.J. Arner, A. Holmgren, Physiological functions of thioredoxin and thioredoxin reductase, Eur. J. Biochem. 267 (2000) 6102–6109.
[137] I. Carlberg, B. Mannervik, Glutathione-reductase, Methods Enzymol. 113 (1985) 484–490.
[138] D.A. Keire, E. Strauss, W. Guo, B. Noszal, D.L. Rabenstein, Kinetics and equilibria of thiol disulfide interchange reactions of selected biological thiols and related molecules with oxidized glutathione, J. Org. Chem. 57 (1992) 123–127.
[139] H.F. Gilbert, Thiol/disulfide exchange equilibria and disulfide bond stability, Methods Enzymol. 251 (1995) 8–28.

[140] M.M. Gallogly, J.J. Mieyal, Mechanisms of reversible protein glutathionylation in redox signaling and oxidative stress, Curr. Opin. Pharmacol. 7 (2007) 381–391.
[141] D.P. Jones, Radical-free biology of oxidative stress, Am. J. Physiol. Cell. Physiol. 295 (2008) C849–C868.
[142] M. Kemp, Y.M. Go, D.P. Jones, Nonequilibrium thermodynamics of thiol/disulfide redox systems: A perspective on redox systems biology, Free Radic. Biol. Med. 44 (2008) 921–937.
[143] P.L. Folkins, D.N. Harpp, Alpha-disulfoxides and other intermediates in the oxidation of disulfides, J. Am. Chem. Soc. 115 (1993) 3066–3070.
[144] C. Jacob, G.I. Giles, N.M. Giles, H. Sies, Sulfur and selenium: the role of oxidation state in protein structure and function, Angew. Chem. Int. Ed. 42 (2003) 4742–4758.
[145] C. Jacob, I. Knight, P.G. Winyard, Aspects of the biological redox chemistry of cysteine: From simple redox responses to sophisticated signalling pathways, Biol. Chem. 387 (2006) 1385–1397.
[146] T.J. Jonsson, A.W. Tsang, W.T. Lowther, C.M. Furdui, Identification of intact protein thiosulfinate intermediate in the reduction of cysteine sulfinic acid in peroxiredoxin by human sulfiredoxin, J. Biol. Chem. 283 (2008) 22890–22894.
[147] X. Roussel, G. Bechade, A. Kriznik, A. Van Dorsselaer, S. Sanglier-Cianferani, G. Branlant, S. Rahuel-Clermont, Evidence for the formation of a covalent thiosulfinate intermediate with peroxiredoxin in the catalytic mechanism of sulfiredoxin, J. Biol. Chem. 283 (2008) 22371–22382.
[148] X. Roussel, A. Kriznik, C. Richard, S. Rahuel-Clermont, G. Branlant, The catalytic mechanism of Sulfiredoxin from Saccharomyces cerevisiae passes through an oxidized disulfide Sulfiredoxin intermediate that is reduced by thioredoxin, J. Biol. Chem. 284 (2009) 33048–33055.
[149] G.I. Giles, K.M. Tasker, C. Collins, N.M. Giles, E. O'Rourke, C. Jacob, Reactive sulphur species: An *in vitro* investigation of the oxidation properties of disulphide S-oxides, Biochem. J. 364 (2002) 579–585.
[150] K.-P. Huang, F.L. Huang, P.K. Shetty, A.L. Yergey, Modification of protein by disulfide S-monoxide and disulfide S-dioxide: Distinctive effects on PKC, Biochemistry 46 (2007) 1961–1971.
[151] D.R. Hogg, J. Stewart, Nucleophilic substitution at bivalent sulfur. III. Kinetics and mechanism of the base-catalyzed hydrolysis of ethyl 2-nitro-4-(trifluoromethyl)benzenesulfenate, the corresponding sulfenyl chloride, and the disulfide, J. Chem. Soc. Perkin Trans. issue 1 (1974) 43–47.
[152] D.R. Hogg, P.W. Vipond, Nucleophilic substitution of bivalent sulfur. I. Kinetics and mechanism of the base-catalyzed hydrolysis of 2-nitrobenzenesulfenate esters, J. Chem. Soc. B. (1970) 1242–1247.
[153] S. Oae, T. Takata, Y.H. Kim, Alkaline hydrolyses of unsymmetrical thiosulfinates: evidence for selective attacking of hydroxide ion on sulfinyl atom, Tetrahedron Lett. issue 48 (1977) 4219–4222.
[154] C.C. Winterbourn, S.O. Brennan, Characterisation of the oxidation products of the reaction between reduced glutathione and hypochlorous acid, Biochem. J. 326 (1997) 87–92.
[155] A. Arora, C. Tripathi, Y. Shukla, Garlic and its organosulfides as potential chemopreventive agents: a review, Curr. Cancer Therapy Rev. 1 (2005) 199–205.
[156] E. Block, S. Ahmad, J.L. Catalfamo, M.K. Jain, R. Apitz-Castro, The chemistry of alkyl thiosulfinate esters. 9. antithrombotic organosulfur compounds from garlic: Structural, mechanistic, and synthetic studies, J. Am. Chem. Soc. 108 (1986) 7045–7055.
[157] Y. Cai, R. Wang, F. Pei, B.-B Liang, Antibacterial activity of allicin alone and in combination with b-lactams against Staphylococcus spp. Pseudomonas aeruginosa, J. Antibiot. (Tokyo) 60 (2007) 335–338.

[158] R. Gebhardt, H. Beck, K.G. Wagner, Inhibition of cholesterol biosynthesis by allicin and ajoene in rat hepatocytes and HepG2 cells, Biochim. Biophys. Acta 1213 (1994) 57–62.
[159] Y. Yamada, K. Azuma, Evaluation of the in vitro antifungal activity of allicin, Antimicrob. Agents Chemother. 11 (1977) 743–749.
[160] J.W. Finley, E.L. Wheeler, S.C. Witt, Oxidation of glutathione by hydrogen-peroxide and other oxidizing-agents, J. Agric. Food Chem. 29 (1981) 404–407.
[161] T.P.A. Devasagayam, A.R. Sundquist, P. Di Mascio, S. Kaiser, H. Sies, Activity of thiols as singlet molecular-oxygen quenchers, J. Photochem. Photobiol. 9 (1991) 105–116.
[162] E.L. Clennan, D.Y. Wang, C. Clifton, M.F. Chen, Geometry-dependent quenching of singlet oxygen by dialkyl disulfides, J. Am. Chem. Soc. 119 (1997) 9081–9082.
[163] E.L. Clennan, D.Y. Wang, H.W. Zhang, C.H. Clifton, Photooxidations of sulfenic acid-derivatives. 2. A remarkable solvent effect on the reactions of singlet oxygen with disulfides, Tetrahedron Lett. 35 (1994) 4723–4726.
[164] K.P. Huang, F.L. Huang, Glutathionylation of proteins by glutathione disulfide S-oxide, Biochem. Pharmacol. 64 (2002) 1049–1056.
[165] D. Fukushima, Y.H. Kim, T. Iyanagi, S. Oae, Enzymatic oxidation of disulfides and thiolsulfinates by both rabbit liver-microsomes and a reconstituted system with purified cytochrome-P-450, J. Biochem. (Tokyo) 83 (1978) 1019–1027.
[166] C. Teyssier, L. Guenot, M. Suschetet, M.H. Siess, Metabolism of diallyl disulfide by human liver microsomal cytochromes P-450 and flavin-containing monooxygenases, Drug Metab. Dispos. 27 (1999) 835–841.
[167] C. Teyssier, M.H. Siess, Metabolism of dipropyl disulfide by rat liver phase I and phase II enzymes and by isolated perfused rat liver, Drug Metab. Dispos. 28 (2000) 648–654.
[168] C.A. Joseph, M.J. Maroney, Cysteine dioxygenase: Structure and mechanism, Chem. Commun. (Camb.) (2007) 3338–3349.
[169] M. Hamann, T.Q. Zhang, S. Hendrich, J.A. Thomas, Quantitation of protein sulfinic and sulfonic acid, irreversibly oxidized protein cysteine sites in cellular proteins, Protein sensors and reactive oxygen species, Pt B, Thiol Enzymes Proteins 348 (2002) 146–156.
[170] A. Hall, P.A. Karplus, L.B. Poole, Typical 2-Cys peroxiredoxins—structures, mechanisms and functions, FEBS J. 276 (2009) 2469–2477.
[171] T.J. Jonsson, L.C. Johnson, W.T. Lowther, Structure of the sulphiredoxin-peroxiredoxin complex reveals an essential repair embrace, Nature 451 (2008) 98–U16.
[172] J.C. Moon, Y.S. Hah, W.Y. Kim, B.G. Jung, H.H. Jang, J.R. Lee, S.Y. Kim, Y.M. Lee, M.G. Jeon, C.W. Kim, M.J. Cho, S.Y. Lee, Oxidative stress-dependent structural and functional switching of a human 2-Cys peroxiredoxin Isotype II that enhances HeLa cell resistance to H2O2-induced cell death, J. Biol. Chem. 280 (2005) 28775–28784.
[173] K.S. Yang, S.W. Kang, H.A. Woo, S.C. Hwang, H.Z. Chae, K. Kim, S.G. Rhee, Inactivation of human peroxiredoxin I during catalysis as the result of the oxidation of the catalytic site cysteine to cysteine-sulfinic acid, J. Biol. Chem. 277 (2002) 38029–38036.
[174] B. Biteau, J. Labarre, M.B. Toledano, ATP-dependent reduction of cysteine-sulphinic acid by *S. cerevisiae* sulphiredoxin, Nature 425 (2003) 980–984.
[175] T.S. Chang, W. Jeong, H.A. Woo, S.M. Lee, S. Park, S.G. Rhee, Characterization of mammalian sulfiredoxin and its reactivation of hyperoxidized peroxiredoxin through reduction of cysteine sulfinic acid in the active site to cysteine, J. Biol. Chem. 279 (2004) 50994–51001.
[176] J.C. Lim, H.I. Choi, Y.S. Park, H.W. Nam, H.A. Woo, K.S. Kwon, Y.S. Kim, S.G. Rhee, K. Kim, H.Z. Chae, Irreversible oxidation of the active-site cysteine of

peroxiredoxin to cysteine sulfonic acid for enhanced molecular chaperone activity, J. Biol. Chem. 283 (2008) 28873–28880.
[177] J.H. Seo, J.C. Lim, D.Y. Lee, K.S. Kim, G. Piszczek, H.W. Nam, Y.S. Kim, T. Ahn, C.H. Yun, K. Kim, P.B. Chock, H.Z. Chae, Novel protective mechanism against irreversible hyperoxidation of peroxiredoxin N-alpha-terminal acetylation of human peroxiredoxin II, J. Biol. Chem. 284 (2009) 13455–13465.
[178] R.G. Hu, J. Sheng, X. Qi, Z.M. Xu, T.T. Takahashi, A. Varshavsky, The N-end rule pathway as a nitric oxide sensor controlling the levels of multiple regulators, Nature 437 (2005) 981–986.
[179] E. Graciet, R.G. Hu, K. Piatkov, J.H. Rhee, E.M. Schwarz, A. Varshavsky, Aminoacyl-transferases and the N-end rule pathway of prokaryotic/eukaryotic specificity in a human pathogen, Proc. Natl. Acad. Sci. U. S. A. 103 (2006) 3078–3083.
[180] T. Tasaki, Y.T. Kwon, The mammalian N-end rule pathway: New insights into its components and physiological roles, Trends Biochem. Sci. 32 (2007) 520–528.
[181] B.K. Sarma, G. Mugesh, Redox regulation of protein tyrosine phosphatase 1B (PTP1B): A biomimetic study on the unexpected formation of a sulfenyl amide intermediate, J. Am. Chem. Soc. 129 (2007) 8872–8881.
[182] D.T. Harwood, A.J. Kettle, C.C. Winterbourn, Production of glutathione sulfonamide and dehydroglutathione from GSH by myeloperoxidase-derived oxidants and detection using a novel LC-MS/MS method, Biochem. J. 399 (2006) 161–168.
[183] D.T. Harwood, S.L. Nimmo, A.J. Kettle, C.C. Winterbourn, M.T. Ashby, Molecular structure and dynamic properties of a sulfonamide derivative of glutathione that is produced under conditions of oxidative stress by hypochlorous acid, Chem. Res. Toxicol. 21 (2008) 1011–1016.
[184] J.M. Pullar, M.C.M. Vissers, C.C. Winterbourn, Glutathione oxidation by hypochlorous acid in endothelial cells produces glutathione sulfonamide as a major product but not glutathione disulfide, J. Biol. Chem. 276 (2001) 22120–22125.
[185] D.T. Harwood, A.J. Kettle, S. Brennan, C.C. Winterbourn, Simultaneous determination of reduced glutathione, glutathione disulphide and glutathione sulphonamide in cells and physiological fluids by isotope dilution liquid chromatography-tandem mass spectrometry, J. Chromatogr. B 877 (2009) 3393–3399.
[186] P. Wardman, C. von Sonntag, Kinetic factors that control the fate of thiyl radicals in cells, Biothiols, Pt A 251 (1995) 31–45.
[187] M.W. Foster, D.T. Hess, J.S. Stamler, Protein S-nitrosylation in health and disease: A current perspective, Trends Mol. Med. 15 (2009) 391–404.
[188] A. Keszler, Y. Zhang, N. Hogg, Reaction between nitric oxide, glutathione, and oxygen in the presence and absence of protein: How are S-nitrosothiols formed?, Free Radic. Biol. Med. 48 (2010) 55–64.
[189] G.H. Xu, M.R. Chance, Hydroxyl radical-mediated modification of proteins as probes for structural proteomics, Chem. Rev. 107 (2007) 3514–3543.
[190] M.Z. Hoffman, E. Hayon, Pulse-radiolysis study of sulfhydryl compounds in aqueous-solution, J. Phys. Chem. 77 (1973) 990–996.
[191] F.A. Davis, R.L. Billmers, Chemistry of sulfenic acids. 4. The 1st direct evidence for the involvement of sulfenic acids in the oxidation of thiols, J. Am. Chem. Soc. 103 (1981) 7016–7018.
[192] M.G. Bonini, O. Augusto, Carbon dioxide stimulates the production of thiyl, sulfinyl, and disulfide radical anion from thiol oxidation by peroxynitrite, J. Biol. Chem. 276 (2001) 9749–9754.
[193] M.D. Sevilla, D. Becker, M. Yan, The formation and structure of the sulfoxyl radicals $RSO^{\bullet}$, $RSOO^{\bullet}$, $RSO_2^{\bullet}$, and $RSO_2OO^{\bullet}$ from the reaction of cysteine, glutathione and penicillamine thiyl radicals with molecular oxygen, Int. J. Radiat. Biol. 57 (1990) 65–81.

[194] X.J. Zhang, N. Zhang, H.P. Schuchmann, C. Vonsonntag, Pulse-radiolysis of 2-mercaptoethanol in oxygenated aqueous-solution—generation and reactions of the thiylperoxyl radical, J. Phys. Chem. 98 (1994) 6541–6547.
[195] P. Wardman, Reactions of Thiyl Radicals in: L. Packer, E. Cadenas (Eds.), Biothiols in Health and Disease, Marcel Dekker Inc., New York, 1995, pp. 1–20.
[196] C.C. Winterbourn, Superoxide as an intracellular radical sink, Free Radic. Biol. Med. 14 (1993) 85–90.
[197] C.C. Winterbourn, D. Metodiewa, The reaction of superoxide with reduced glutathione, Arch. Biochem. Biophys. 314 (1994) 284–290.
[198] C.C. Winterbourn, D. Metodiewa, The reaction of superoxide with glutathione and other thiols, Methods Enzymol. 251 (1995) 81–86.
[199] H. Pichorner, D. Metodiewa, C.C. Winterbourn, Generation of superoxide and tyrosine peroxide as a result of tyrosyl radical scavenging by glutathione, Arch. Biochem. Biophys. 323 (1995) 429–437.
[200] C.C. Winterbourn, D. Metodiewa, Reactivity of biologically relevant thiol compounds with superoxide and hydrogen peroxide, Free Radic. Biol. Med. 27 (1999) 322–328.
[201] W.H. Koppenol, A thermodynamic appraisal of the radical sink hypothesis, Free Radic. Biol. Med. 14 (1993) 91–94.
[202] B.E. Sturgeon, H.J. Sipe, D.P. Barr, Jr, J.T. Corbett, J.G. Martinez, R.P. Mason, The fate of the oxidizing tyrosyl radical in the presence of glutathione and ascorbate. Implications for the radical sink hypothesis, J. Biol. Chem. 273 (1998) 30116–30121.
[203] N. Zhang, H.-P. Schuchmann, C. von Sonntag, The reaction of superoxide radical anion with dithiothreitol: A chain process, J. Phys. Chem. 95 (1991) 4718–4722.
[204] M. Benrahmoune, P. Therond, Z. Abedinzadeh, The reaction of superoxide radical with N-acetylcysteine, Free Radic. Biol. Med. 29 (2000) 775–782.
[205] G. Feroci, A. Fini, Voltammetric investigation of the interactions between superoxide ion and some sulfur amino acids, Inorg. Chim. Acta 360 (2007) 1023–1031.
[206] R.O. Beauchamp, J.S. Bus, J.A. Popp, C.J. Boreiko, D.A. Andjelkovich, A critical-review of the literature on hydrogen-sulfide toxicity, CRC Crit. Rev. Toxicol. 13 (1984) 25–97.
[207] T. Chiku, D. Padovani, W.D. Zhu, S. Singh, V. Vitvitsky, R. Banerjee, H_2S biogenesis by human cystathionine gamma-lyase leads to the novel sulfur metabolites lanthionine and homolanthionine and is responsive to the grade of hyperhomocysteinemia, J. Biol. Chem. 284 (2009) 11601–11612.
[208] R. Wang, Two's company, three's a crowd: Can H_2S be the third endogenous gaseous transmitter?, FESAB J. 16 (2002) 1792–1798.
[209] D.J. Lefer, A new gaseous signaling molecule emerges: Cardioprotective role of hydrogen sulfide, Proc. Natl. Acad. Sci. U. S. A. 104 (2007) 17907–17908.
[210] W.M. Zhao, J. Zhang, Y.J. Lu, R. Wang, The vasorelaxant effect of H_2S as a novel endogenous gaseous K-ATP channel opener, EMBO J. 20 (2001) 6008–6016.
[211] G.D. Yang, L.Y. Wu, B. Jiang, W. Yang, J.S. Qi, K. Cao, Q.H. Meng, A.K. Mustafa, W.T. Mu, S.M. Zhang, S.H. Snyder, R. Wang, H_2S as a physiologic vasorelaxant: Hypertension in mice with deletion of cystathionine gamma-lyase, Science 322 (2008) 587–590.
[212] E. Blackstone, M. Morrison, M.B. Roth, H_2S induces a suspended animation-like state in mice, Science 308 (2005) 518–518.
[213] D.L. Miller, M.B. Roth, Hydrogen sulfide increases thermotolerance and lifespan in Caenorhabditis elegans, Proc. Natl. Acad. Sci. U. S. A. 104 (2007) 20618–20622.
[214] C. Szabo, Hydrogen sulphide and its therapeutic potential, Nat. Rev. Drug Discov. 6 (2007) 917–935.

[215] G.A. Benavides, G.L. Squadrito, R.W. Mills, H.D. Patel, T.S. Isbell, R.P. Patel, V.M. Darley-Usmar, J.E. Doeller, D.W. Kraus, Hydrogen sulfide mediates the vasoactivity of garlic, Proc. Natl. Acad. Sci. U. S. A. 104 (2007) 17977–17982.
[216] J.W. Elrod, J.W. Calvert, J. Morrison, J.E. Doeller, D.W. Kraus, L. Tao, X.Y. Jiao, R. Scalia, L. Kiss, C. Szabo, H. Kimura, C.W. Chow, D.J. Lefer, Hydrogen sulfide attenuates myocardial ischemia-reperfusion injury by preservation of mitochondrial function, Proc. Natl. Acad. Sci. U. S. A. 104 (2007) 15560–15565.
[217] L. Li, A. Hsu, P.K. Moore, Actions and interactions of nitric oxide, carbon monoxide and hydrogen sulphide in the cardiovascular system and in inflammation—a tale of three gases!, Pharmacol. Ther. 123 (2009) 386–400.
[218] L. Li, M. Bhatia, P.K. Moore, Hydrogen sulphide—a novel mediator of inflammation?, Curr. Opin. Pharmacol. 6 (2006) 125–129.
[219] R.C.O. Zanardo, V. Brancaleone, E. Distrutti, S. Fiorucci, G. Cirino, J.L. Wallace, Hydrogen sulfide is an endogenous modulator of leukocyte-mediated inflammation, FASEB J. 20 (2006) 2118–2119.
[220] M.A. Mariggio, V. Minunno, S. Riccardi, R. Santacroce, P. De Rinaldis, R. Fumarulo, Sulfide enhancement of PMN apoptosis, Immunopharmacol. Immunotoxicol. 20 (1998) 399–408.
[221] L. Rinaldi, G. Gobbi, M. Pambianco, C. Micheloni, P. Mirandola, M. Vitale, Hydrogen sulfide prevents apoptosis of human PMN via inhibition of p38 and caspase 3, Lab. Invest. 86 (2006) 391–397.
[222] E.H. Berglin, J. Carlsson, Potentiation by sulfide of hydrogen peroxide-induced killing of Escherichia-Coli, Infect. Immun. 49 (1985) 538–543.
[223] Y. Kimura, H. Kimura, Hydrogen sulfide protects neurons from oxidative stress, FESAB J. 18 (2004) 1165–1166.
[224] K.D. Fogelman, D.M. Walker, D.W. Margerum, Nonmetal redox kinetics: Hypochlorite and hypochlorous acid reactions with sulfite, Inorg. Chem. 28 (1989) 986–993.
[225] R.C. Troy, D.W. Margerum, Non-metal redox kinetics: Hypobromite and hypobromous acid reactions with iodide and with sulfite and the hydrolysis of bromosulfate, Inorg. Chem. 30 (1991) 3538–3543.
[226] H. Laggner, M.K. Muellner, S. Schreier, B. Sturm, M. Hermann, M. Exner, B.M.K. Gmeiner, S. Kapiotis, Hydrogen sulphide: A novel physiological inhibitor of LDL atherogenic modification by HOCl, Free Radic. Res. 41 (2007) 741–747.
[227] M. Whiteman, J.S. Armstrong, S.H. Chu, S. Jia-Ling, B.S. Wong, N.S. Cheung, B. Halliwell, P.K. Moore, The novel neuromodulator hydrogen sulfide: An endogenous peroxynitrite 'scavenger'?, J. Neurochem. 90 (2004) 765–768.
[228] M.K. Muellner, S.M. Schreier, H. Laggner, M. Hermann, H. Esterbauer, M. Exner, B.M.K. Gmeiner, S. Kapiotis, Hydrogen sulfide destroys lipid hydroperoxides in oxidized LDL, Biochem. J. 420 (2009) 277–281.
[229] T. Siu, C.Q. Jia, Kinetic and mechanistic study of reaction between sulfide and sulfite in aqueous solution, Ind. Eng. Chem. Res. 38 (1999) 3812–3816.
[230] T. Siu, C.Q. Jia, Kinetics of reaction of sulfide with thiosulfate in aqueous solution, Ind. Eng. Chem. Res. 38 (1999) 1306–1309.
[231] G. Rabai, M. Orban, I.R. Epstein, Systematic design of chemical oscillators. 77. A model for the pH-regulated oscillatory reaction between hydrogen-peroxide and sulfide ion, J. Phys. Chem. 96 (1992) 5414–5419.
[232] M.R. Hoffmann, Kinetics and mechanism of oxidation of hydrogen-sulfide by hydrogen-peroxide in acidic solution, Environ. Sci. Technol. 11 (1977) 61–66.
[233] A.K. Mustafa, M.M. Gadalla, N. Sen, S. Kim, W. Mu, S.K. Gazi, R.K. Barrow, G. Yang, R. Wang, S.H. Snyder, H_2S signals through protein S-sulfhydration, Sci. Signal. 2 (2009) ra72.

CHAPTER 7

Toxicity of Silica Nanomaterials: Zeolites, Mesoporous Silica, and Amorphous Silica Nanoparticles

Anton Petushkov[1], Nicholas Ndiege[1], Aliasger K. Salem[2,*], *and* Sarah C. Larsen[1,**]

Contents

1. Introduction

Nanomaterials with unique properties are being incorporated into a diverse array of applications in areas such as electronics, catalysis, optics, and medicine. Carbon-based nanomaterials (carbon nanotubes, buckyballs), semiconductor quantum dots (CdSe), metal nanoparticles and nanorods

[1] Department of Chemistry, University of Iowa, Iowa City, IA, USA

[2] Division of Pharmaceutics and Translational Therapeutics, College of Pharmacy, University of Iowa, Iowa City, IA, USA

[*] Corresponding author. Tel.: +319 335-8810
Email address: aliasger-salem@uiowa.edu
[**] Corresponding author. Tel.: +319-335-1346
Email address: sarah-larsen@uiowa.edu

Advances in Molecular Toxicology, Volume 4
ISSN 1872-0854, DOI 10.1016/S1872-0854(10)04007-5

(gold, nickel, platinum), and nanosized metal oxides (TiO_2) are important nanomaterials that have been widely studied. For example, metal nanoparticles and nanorods (gold nickel and platinum) are being intensely investigated for applications in cancer detection [1,2], imaging [1], and gene delivery [3–5].

Silica-based materials including porous materials, such as mesoporous silica, microporous zeolites, nonporous amorphous silica, and crystalline silica, are important materials with a wide range of applications. Zeolites and mesoporous silica [6–10] have emerged as porous nanomaterials with new properties and many potential applications, in areas such as environmental catalysis [11], drug delivery [12,13], and imaging [14–18].

There is a growing use of silica-based nanomaterials in commercial products. In addition, natural crystalline silica materials, such as quartz and cristobalite, are major constituents of coal mine dust or coal fly ashes. It is therefore of critical importance to study their toxicity. The smaller size scale of nanoparticles may increase their toxicity or change the mechanism by which they induce toxicity. Toxicological data on "incidental" nanoparticles that are produced as a by-product cannot necessarily be extrapolated to engineered nanoparticles because they do not have the same size, composition, and surface properties [19]. Studies of the toxicity of nanomaterials are complex because nanomaterials have size- and shape-dependent properties that may affect toxicity. In addition, surface coatings are routinely used to control the surface chemistry and in many cases, this will affect the toxicity. Therefore, it is necessary to completely and thoroughly characterize the materials being studied.

Zeolites are crystalline aluminosilicate or silicate materials with very large surface areas due to their pores of less than ~2 nm. Mesoporous silica is a related porous material that is amorphous and has its pores of greater than ~2 nm. The structures of a common zeolite with the MFI structure, ZSM-5 (or silicalite-1 in the purely siliceous form), and mesoporous silica, MCM-41, are shown in Figure 1A and B, respectively. Zeolites and mesoporous

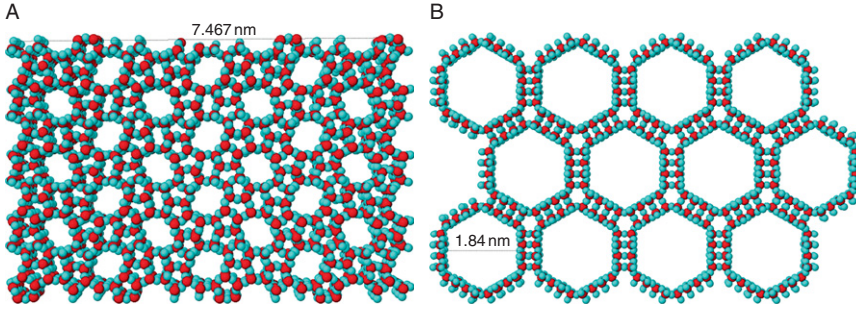

Figure 1 Representative structures of porous materials: (A) ZSM-5 zeolite and (B) MCM-41 mesoporous silica.

silica are important commercial materials widely used in traditional applications such as catalysis [20,21], separations [22], and water softening [22]. Recently, biomedical applications of zeolites and mesoporous silica in drug delivery, bloodclotting [23], and imaging [16,18,24–26] have been developed.

Zeolites and mesoporous silica can be synthesized with crystal sizes of 100 nm or less, giving these materials two dimensions on the nanoscale—the pore size and the crystal size. Nanoscale zeolites and mesoporous silica nanoparticles (MSNs) have large surface areas due to appreciable internal and external surface areas [27,28]. The external surface area of nanoscale zeolites is up to an order of magnitude larger than the external surface area of micron-sized zeolites and provides an additional surface for reaction or functionalization [29–31]. The external surface of nanoscale zeolites has been functionalized with organic functional groups for use in biomedical applications, such as imaging [32] and drug delivery [12], and in the development of low dielectric materials [33] for the semiconductor industry. Due to the larger pore sizes, MSNs can be functionalized on both the internal and external surfaces for applications in catalysis [34], imaging [17,35,36], and drug delivery [13,37].

Functionalizing silica-based nanoparticles can change the mechanisms and level of toxicity induced in cells. Cells can die by either of two major mechanisms: necrosis or apoptosis [38]. Necrosis, which can occur in a matter of seconds, is the death of the cells through external damage usually mediated via destruction of the plasma membrane or the biochemical supports of its integrity. The other major form of cell death, apoptosis, is much slower and is based on the concept of programmed cell death. Apoptosis requires from a few hours to several days, depending on the initiator. The manifestations of apoptosis, both biochemical and morphological, are unique and are completely different from those of necrosis [39]. The lactic dehydrogenase (LDH) release assay can be used to measure damage to the cell membrane, the caspase 3/7 activity assay can be used to measure key molecules involved in apoptosis, and the Annexin V–propidium iodide (PI) staining method provides visual confirmation of the types of cell death induced relative to the size and surface functionalization of the silicalite nanoparticles. The 3-(4,5-dimethylthiazol-2-yl)-2,5-diphenyltetrazolium bromide (MTT) assay is a colorimetric assay used to assess cytotoxicity. The activity of enzymes that reduce MTT to formazan which results in a purple color is measured spectrophotometrically. The LD_{50} value is the dose lethal to 50% of the cells.

Asefa and coworkers [40] and Martens and coworkers [41] have proposed that for materials in the solid phase, the conventional metric of cytotoxicity, LD_{50} measurement, is inappropriate since the particles are not soluble in aqueous media [40]. Asefa and coworkers prefer to

measure the number of particles needed to inhibit normal cell growth by 50%, which they call Q_{50}. The geometric area of the average particle is calculated from transmission electron microscopy (TEM) and X-ray diffraction (XRD) measurements. The number of particles per gram weight of the material is measured through the Brunauer, Emmett and Teller (BET) adsorption isotherm using nitrogen. Average viability of the cells is determined by light microscopy using a hemacytometer under standard trypan blue conditions. Martens and coworkers found that the cellular response was determined by the total mass/number/surface area of particles as well as concentration [41].

In proliferation assays, *in vitro* nanotoxicity assessment is commonly done whereby cellular reduction of tetrazolium salts produces formazan dyes. Cologenic assays, where colonies of highly proliferating cells are counted by visual inspection after exposure to nanomaterials, can be used where there is a need to avoid interactions between nanomaterials and probe molecules. Necrosis assays typically assess membrane integrity by monitoring:

(1) the uptake of a supravital dye, such as Trypan Blue, Neutral Red, or PI or
(2) the leakage of active enzymes into the cell media using the LDH assay.

DNA damage assays reveal DNA damage resulting from nanoparticle exposure leading to apoptosis[42].

As underscored in the previous paragraph, the importance of adequate methods to study the toxicity/cellular viability attributes of porous silicon (PSi) particles is paramount to evaluating their cytotoxic effects. The molecular cation MTT^+ is an important redox indicator that has been used in assays to study cytotoxicity, cell viability, and proliferation of living cells. This colorimetric assay method is based on the metabolic activity of viable cells. As a result, MTT is reduced to formazan (1-[4,5-dimethylthiazol-2-yl]-3,5-diphenylformazan).

$$\mathrm{MTT} + \mathrm{e}^- \Leftrightarrow \mathrm{MTT}^*$$

$$\mathrm{MTT}^* + \mathrm{e}^- \Leftrightarrow \mathrm{formazan}^-$$

However, the intermediate species reacts in a pH-dependent fashion:

$$\mathrm{MTT}^* + \mathrm{H}^+ \Leftrightarrow \mathrm{MTTH}^{*+}$$

$$\mathrm{MTTH}^{*+} + \mathrm{e}^- \Leftrightarrow \mathrm{formazanH}$$

$$\mathrm{formazanH} + \mathrm{H}^+ \Leftrightarrow \mathrm{formazanH_2}^+$$

Despite mitochondrial activity, the MTT reduction has also been attributed to nonmitochondrial enzymes as well as to endosomes and lysosomes rendering the exact reduction mechanism not well understood. Hirvonen and coworkers demonstrated that the use of the MTT assay as an agent for the determination of the cell viability in the presence of PSi microparticles can give erroneous information on the real cell viability [43]. PSi particles were able to reduce MTT directly, giving the same signal as is given by the metabolic activity of living cells. As a result, when used alone, the MTT assay was found to possibly underestimate the cytotoxicity of drug-loaded PSi microparticles. The redox activity of silicon particles was found to possibly cause unwanted reactions to occur in other systems containing redox-sensitive substances. This was not an issue for related materials, such as mesoporous silica.

Chen and coworkers found that determining whether nanomaterials are toxic depended greatly on diverse parameters, such as the structural properties of particles, their dosage forms, and their intended uses [44]. The location of particles relative to the cells was found to influence their cytotoxicity. Particles that were internalized into cells caused different cytotoxicity than particles mantling the cell membrane as discussed in more detail in Section 4 [44]. Commonly studied cells include human neuroblastoma (SK–N–SH) cells, human lung epithelial cells, skin and pulmonary fibroblast cells, HeLa cells, human bone marrow mesenchymal stem cells, 3T3-L1 cells, and Jurkat cells.

Toxicity studies of industrially important zeolites [45] and related crystalline silicas [46–52], such as quartz, have been reported in the literature. Studies of the natural zeolite, clinoptilolite, indicate that it is nontoxic and safe for human and veterinary use [8,53], but other studies have shown that crystalline silica materials exhibit toxicity through silicosis which is caused by inhalation of crystalline silica particles of respirable size. For example, in a study by Fubini and coworkers, the cytotoxicity of artificial crystalline silicas or porosils (differing size, morphology, surface area) to macrophages was investigated [45]. Macrophages were chosen because alveolar macrophages play a key role in silica-related diseases by clearing particles out of the lung or by causing chronic inflammation [44]. Similar toxicity was observed for calcined versus uncalcined crystalline silicas, suggesting that the internal surface does not play a significant role in silica toxicity for these materials. Recently, in a study on the cytotoxicity of nanocrystalline silicalite, we have shown that the toxicity was complex and depended on the size, surface functionalization, and cell line used in the cytotoxicity studies. The toxicity studies on zeolites will be reviewed in Sections 2 and 3 and are summarized in Table 1.

Mesoporous silicas, such as MCM-41, which in comparison with zeolites are amorphous, are being intensively investigated for biomedical applications [17,54,55]. There have been several studies recently focused

Table 1 Summary of toxicity studies of zeolites

Material	Cell line/ animal model	Concentration, exposure	Test (MTT, etc.)	Toxicity	Reference
Erinoite, mordenite	Mice	10–30 mg/mouse	Gross anatomical observation, light microscopy, histochemistry, electron microscopy	Toxic, mordenite less toxic than erionite	[62]
Asbestos, erionite, mordenite, zeolite 4A	Mice	0.5–20 mg/mouse	Gross anatomical, histological observation, tissue staining, histochemistry, electron microscopy	Toxic, mordenite less toxic than erionite, zeolite 4A has the smallest toxicity	[61]
Erionite, mordenite, asbestos	HTE, rat AM	2.5–25 $\mu g\,cm^{-2}$	Assay for generation of peroxide radicals, ^{51}Cr release assay, Collagen/ noncollagen	Erionite more toxic than mordenite, less toxic than crocidolite absestos	[59]

			protein synthesis detection assay.		
TON, MTT CRIS-rd, FAU, MFI-2, MFI-1,	Macrophage cell line (J774)	5–50 $\mu g\,mL^{-1}$	Cytotoxic effect to J774 cells of the six different porosils was determined on cells at confluence and on exponentially growing cultures	Shape-dependent toxicity	[45]
Erionite, mordenite	AS52 cell line	2–16 $\mu g\,cm^{-2}$ zeolite,2–20 μM $FeCl_2$	Cell viability study, mutagenesis study	Cytotoxic effect depends on the concentration of the zeolite and the amount of added iron (II)	[60]
Silicalite-1	HEK-293, RAW264.7	0.25–1 $mg\,mL^{-1}$	LDH release, caspase 3/7 activity assay, Annexin V-PI staining.	Cytotoxicity depends on the type of cell, zeolite functionalization, and concentration	[63]

on the interaction of mesoporous silica materials with cells [40,56–58]. The effect of surface functionalization of MCM-41 on cellular uptake [58] was investigated and showed that the cellular uptake varied with surface functionality in that the LD_{50} increased with decreasing ζ-potential. The toxicity study of MCM-41 and functionalized MCM-41 showed that unfunctionalized MCM-41 was more toxic on a per particle basis toward human neuroblastoma (SK-N-SH) than aminopropyl- and mercaptopropyl-functionalized MCM-41 and that the most toxic mesoporous silica materials studied were those with the largest BET surface areas [40]. Positively charged MCM-41 was shown to enhance cellular uptake and increased surface charge did not increase cytotoxicity [56]. Another recent study suggested that mesoporous silica inhibited cellular respiration [57]. Representative toxicity studies of mesoporous silica will be discussed in Section 4 and are summarized in Table 2.

Crystalline silica materials such as quartz are potential human carcinogens. In contrast, amorphous silica nanomaterials are generally thought to be safe and nontoxic. Extensive studies of crystalline silica materials such as quartz dusts have shown that physicochemical properties such as particle size, shape, surface area, and surface chemistry all impact toxicity [45–51]. The cytotoxicity of amorphous silica nanoparticles and crystalline silica will be discussed in Sections 5 and 6, respectively, and are summarized in Tables 3 and 4, respectively. Studies were chosen to highlight examples in which the properties of the materials such as size or surface functionalization could be correlated with cytotoxicity.

In this chapter, we provide a survey of the cytotoxicity of silica nanomaterials including porous silica materials such as zeolites and mesoporous silica, and amorphous silica nanoparticles and crystalline silica. Zeolites and mesoporous silica are unique relative to other classes of nanomaterials due to their porosity, which leads to very large internal and external surface areas and potentially increased surface reactivity. A comparison of the cytotoxicity of zeolites and mesoporous silica with related materials such as amorphous silica nanoparticles and quartz will be provided.

2. Toxicity Studies of Micron-Sized Synthetic and Natural Zeolites

Zeolites are important materials in many industrial processes. Since one of the most common pathways of zeolite exposure is inhalation, studies of zeolite interactions with lung tissue and epithelial lung cells are of particular interest. Several studies were conducted using epithelial [59], macrophage [45], and other cell lines [60], and live animals followed by extraction of their lung tissue and cells [59,61]. Several different types of

Table 2 Summary of cytotoxicity studies of mesoporous silica nanoparticles

Material	Cell line	Concentration ($\mu g\,mL^{-1}$)	Test (MTT, etc.)	Toxicity	Reference
MCM-41, MP-T (mercapto grafted), AP-T (aminopropyl grafted), SiO_2	SK-N-SH (human neuroblastoma)	40–800	Cell viability	LD_{50} increases in the following order: MCM-41 < MP-T < AP-T ~ SiO_2.	[40]
MCM-41, SBA-15, solid silica microsphere (SMS) and ammonium-functionalized analogues	Jurkat cells (lymphoid), SK-N-SH (human neuroblastoma)	50, 100, 200	Cell viability, TEM	Observed toxicity explained by changes in endocytosis; positively charged quaternary ammonium amines prevented toxicity; these positively charged particles were not endocytosed; for Jurkat cells, SMS exhibited instant and constant toxicity whether aminated or not.	[78]

(*continued*)

Table 2 (*continued*)

Material	Cell line	Concentration ($\mu g\,mL^{-1}$)	Test (MTT, etc.)	Toxicity	Reference
Mesoporous silica nanoparticles (MSNs) of type MCM-41	Human mesenchymal stem cells (hMSCs), 3T3-L1	100	Cell viability MTT	Uptake of MSNs is cell type and surface charge dependent.	[56]
MCM-41, SBA-15	HL-60 (myeloid), Jurkat (lymphoid)	25–500	Cell respiration studies	SBA-15 inhibited cellular respiration: MCM-41 had no effect on cellular respiration.	[57]
MCM-41	HeLa (human cervical cancer cells)	40	Guava ViaCount assay	ED_{50} increased as ζ-potential decreased with different surface functionalization.	[58]
MCM-41	Rabbit red blood cells				
Fluorescein isothiocyanate-conjugated MSNs (FITC-MSNs)	hMSCs, 3T3-L1	0–80	CCK-8 assay	Clathrin-dependent endocytosis; nontoxic to stem cells.	[79]

ED_{50}, effective dose for 50% of the cells; LD_{50}, lethal dose for 50% of the cells.

Table 3 Summary of cytotoxicity studies of silica nanoparticles

Material	Cell line	Concentration	Test (MTT, etc.)	Toxicity	Reference
Silica nanoparticles (varied from 14 to 335 nm diameter)	Human endothelial cells (EAHY926)	0–2500 $\mu g\,mL^{-1}$	MTT and LDH assays, Annexin V	Smaller silica nanoparticles are more toxic. For smaller particles, necrosis is observed within a few hours. Surface area is an important parameter.	[81]
Silica nanoparticles (2–335 nm)	Mouse macrophage (J774), human endothelial cells (EAHY926)	~1 $mg\,mL^{-1}$	MTT, WST1, EPR to evaluate hydroxyl radical formation	Cytotoxicity increases with decreasing particle size; radical formation observed that also increases with decreasing size.	[82]

(*continued*)

Table 3 (*continued*)

Material	Cell line	Concentration	Test (MTT, etc.)	Toxicity	Reference
Silica nanoparticles (15, 46 nm), crystalline silica (Min-U-Sil 5)	Human bronchoaleolar carcinoma-derived cells (A549)	10–100 $\mu g\,mL^{-1}$	Sulforhodamine (SRB) method, ROS	Both nanoparticles were more cytotoxic than crystalline silica; dose and exposure time dependent; ROS increased upon exposure to nanoparticles.	[83]
Silica (21, 80 nm), silica–chitosan composite (150–170 nm)	Fibroblast (WS1, CCD-966sk, MRC-5, MKN-28, HT-29)	4 $mg\,mL^{-1}$	MTT, LDH	Slightly toxic at high concentrations, high dosages were more toxic to normal human fibroblast cells than to cancer cells; toxicity was reduced for chitosan–silica composites.	[84]

Table 4 Summary of cytotoxicity studies of quartz particles

Material	Cell line	Concentration, exposure	Test (MTT, etc.)	Toxicity	Reference
Quartz	Rat alveolar macrophage cells	1 mg mL^{-1}	LDH release, peroxidation of unsaturated lipids, hemolysis assay	Freshly ground quartz sample has higher toxicity that diminishes as the sample is aged for 1–5 days.	[87]
Madagascar quartz	Murine alveolar macrophages	Up to 80 μg cm^{-2}	LDH activity, TBARS assay, Annexin V/propidium iodide cell staining, PPP activity assay, G6PD, 6PGD, GAPDH ctivity assays, G6PD expression, measurement of GSH	The sample was found to be toxic, likely to inhibit the G6PD activity. The proposed mechanism involves decreasing the ability of cells to counteract oxidative stress.	[88]

(*continued*)

Table 4 (*continued*)

Material	Cell line	Concentration, exposure	Test (MTT, etc.)	Toxicity	Reference
Bentonite, acid, alkaline, or organic activated, up to 6% quartz content	Human lung fibroblasts (IMR90)	Up to $50\,\mu g\,cm^{-2}$	Flow cytometry, Annexin V/propidium iodide cell staining, hemolytic potential, DNA fragmentation	Toxicity of bentonite depends on the quartz content as well as on the type of activation. Acid-activated particles with higher quartz content exhibited the highest cytotoxicity.	[89]

DQ-12 quartz, native, coated with aluminum lactate, polyvinylpyridine-*N*-oxide (PVNO)	Wistar rats, RLE cell line	2 mg per rat 40 $\mu g\,cm^{-2}$	Total cells, percentage of PMNs, total protein, LDH, alkaline phosphatase	Exposure to quartz leads to a persistent inflammation, as shown by *in vivo* and *ex vivo* approaches. The inflammatory response is associated with activation of NF-$\kappa\beta$ factor. Surface coating significantly reduces quartz cytotoxicity.	[90]

zeolitic materials were studied including naturally occurring erionite [45,59–62], crocidolite [59], mordenite [45,59–62], TON [45], and MTT [45] zeolites as well as synthetic zeolite 4A [61], faujasite [45], and MFI zeolites [45,63]. Studies of the zeolites mainly focused on the effect of zeolite type and morphology [45,59–62], specific surface area [45], the presence of iron cations on the surface of zeolite [60], and the effect of surface coating and functionalization [45,63] on cytotoxicity of the samples. A summary of these toxicity studies is provided in Table 1 and a more detailed discussion follows.

2.1. Carcinogenicity of naturally occurring fibrous zeolites

One of the first studies of zeolite biological activity and cytotoxicity was done by Baris *et al.*, who studied the cases of malignant mesothelioma and chronic fibrous pleuritis among residents of Karain, Turkey [64,65]. Similar diagnosis is usually linked to asbestos exposure. However, no natural or industrial sources of asbestos were found in the area. The small amount of asbestos fibers in drinking water was highly unlikely to cause the symptoms, as it was previously shown that the penetration of the ingested asbestos fibers through the walls of the gastrointestinal tract does not occur [66]. The authors proposed that the symptoms could be attributed to naturally occurring erionite zeolite found in the surrounding area and lung tissues of patients diagnosed with chronic fibrous pleuritis [64,65].

This work was followed by Suzuki, who used two naturally occurring zeolites, erionite and mordenite, to test their carcinogenic and fibrogenic effects on mice [62]. In the preliminary study, varying amounts of erionite and mordenite zeolites were intraperitoneally injected in mice and the effects were compared with positive (asbestos) and negative control specimins. It was shown that both erionite and mordenite can cause fibrosis and mesothelioma in mice lungs, the effect being more pronounced in the case of erionite zeolite consisting of thin fibers than mordenite, consisting of granular and fibrous particles.

In a later study, a larger group of animals was subjected to intraperitonial and intra-abdominal injection of different types of asbestos, natural erionite and mordenite zeolites, and synthetic zeolite 4A [61]. The animals were kept for up to 23 months after a single injection of particles and were either found dead or sacrificed. Gross anatomical and histological observations as well as electron microscopy were done for all animals. It was found that erionite zeolite samples were highly toxic, causing peritoneal fibrosis and leading to many cases of premature death. Fibrogenic effects of synthetic zeolite 4A (a nonfibrous zeolite) were the mildest of all samples. Mordenite-treated mice also developed peritoneal fibrosis, but the severity of fibrosis was decreased relative to the highly fibrous erionite sample. The authors concluded that there is a strong correlation between

fibrogenicity of zeolites and their carcinogenicity that leads to formation of tumors and fibrosis.

2.2. Effect of crystal morphology and surface area of zeolites

The effect of crystal morphology has been one of the most commonly investigated parameters for zeolite toxicity studies. Zeolite crystal morphology is dictated by the crystal structure and varies from one zeolite to another. In some cases, the zeolite crystal morphology can be controlled by varying the synthetic conditions.

The cytotoxic effect of fibrous versus spheroid-shaped zeolite particles was studied in a series of papers [45,59]. In a study by Mossman and coworkers, rat alveolar macrophage (AM) cells and a hamster tracheal epithelium (HTE) cell line were used to study the effect of fibrous and nonfibrous mineral particles on the generation of superoxide species, release of ^{51}Cr as well as the rates of collagen and noncollagen protein synthesis [59]. The zeolite, erionite, was chosen among other minerals as an example of a highly fibrous material and the zeolite, mordenite, was chosen for its nonfibrous morphology. The results demonstrated that chemically similar fibrous and nonfibrous dusts have different cytotoxicities. The fibrous zeolite, erionite, was characterized by a significantly higher rate of superoxide species generation in comparison with nonfibrous mordenite. The presence of $5\,\mu m\,cm^{-2}$ erionite increased the amount of generated superoxide up to 750% compared to the control run. In order to attain a similar rate of superoxide generation, $25\,\mu m\,cm^{-2}$ mordenite was required.

The ^{51}Cr assay was used to measure the release of the radioactive chromium isotope from the cells as a result of their death. The chromium-51 assay study has shown increased release of ^{51}Cr from the cells in presence of fibrous particles in comparison with nonfibrous ones, although the authors have not shown the results for the zeolitic particles, that is, erionite and mordenite. Similarly, the presence of fibrous minerals in the cells resulted in increased synthesis of collagen proteins, while nonfibrous particles did not show enhanced synthesis of collagen. Excessive synthesis of collagen in the cells is an indication of fibrosis.

Fubini *et al.* provided a more detailed study on the effect of particle morphology on cytotoxicity [45]. Several types of purely siliceous zeolites were chosen for the study including Theta-1 (TON), ZSM-23 (MTT), CRIS, ZSM-5 (MFI), and faujasite (FAU). The shape of particles was evaluated quantitatively by calculating their aspect ratios (*ar*) using the following equation:

$$ar = \frac{a}{\sqrt{b \cdot c}}$$

where *a, b*, and *c* are the three dimensions of the crystals, *a* being the largest one.

The following types of zeolites (*aspect ratio* shown in parentheses) were used in this study: fibrous TON (14.8), MTT (8.1), and CRIS-rd (7.1) zeolites; rod-shaped MFI-2 (8.2); spherical MFI-1 (1.2); and FAU (1.0) (Figure 2). The cytotoxic effect of different zeolite samples was studied using a monocyte–macrophage cell line (J774). The cells were exposed to zeolite powder, with concentrations ranging from 5 to 50 $\mu g\,mL^{-1}$. The ratio of surviving cells to the control samples after 24 h was used to evaluate cytotoxicity. It was shown that zeolites with small aspect ratios, that is, spheroid form, exhibited low levels of cytotoxicity even at high concentrations in the cell medium, while fibrous zeolites, such as MTT and TON, were toxic even at small concentrations. Increasing the fibrous zeolite concentration in the cell medium further increased the cytotoxic effect of these zeolites.

Another important parameter of zeolites as porous materials which was considered to have an influence on cytotoxicity of particles is the available surface area. The external surface area of particles varied from 1.7 to 31.3 $m^2\,g^{-1}$, while the internal surface area varied from 10.5 to 776 $m^2\,g^{-1}$. When uncalcined zeolite samples in which the pores were still blocked by the respective template molecules were used, no change in toxicity was observed, indicating that the internal surface area does not have any significant effect on toxicity. Both uncalcined and calcined TON zeolite samples exhibit large cytotoxicity despite the fact that the uncalcined TON does not have any accessible internal surface area.

Based on these results, the authors concluded that the particle shape is the key factor in the cytotoxic potential. Fibrous particles of sufficient size cannot be fully engulfed by macrophage cells and uptake of such particles may result in rupture of the cell membrane, release of lysosomal content, and ultimately cell death. Two of the most toxic zeolites used in the study have a fibrous structure. At the same time, a zeolite with relatively high aspect ratio, MFI-2, did not show any significant toxicity. This is explained by the fact that while MFI has a relatively high aspect ratio, the length of the crystals is on the order of 10 μm, which makes them too large to be phagocytized by macrophage cells.

2.3. Surface reactivity and reactive oxygen species

One of the factors associated with the biological activity of aluminosilicate dusts is the generation of reactive oxygen species (ROS) by their surface. One of the most common and important oxygen free radicals is the superoxide anion (O_2^-), which can be dismutated to form H_2O_2 and the highly reactive hydroxyl radical (·OH) [67]. Generation of ROS can be facilitated either by the surface of aluminosilicates or in the presence of certain metal ions, particularly iron (Fenton chemistry). Studies have shown that silicon oxygen radicals can be generated by a freshly fractured surface of silica.

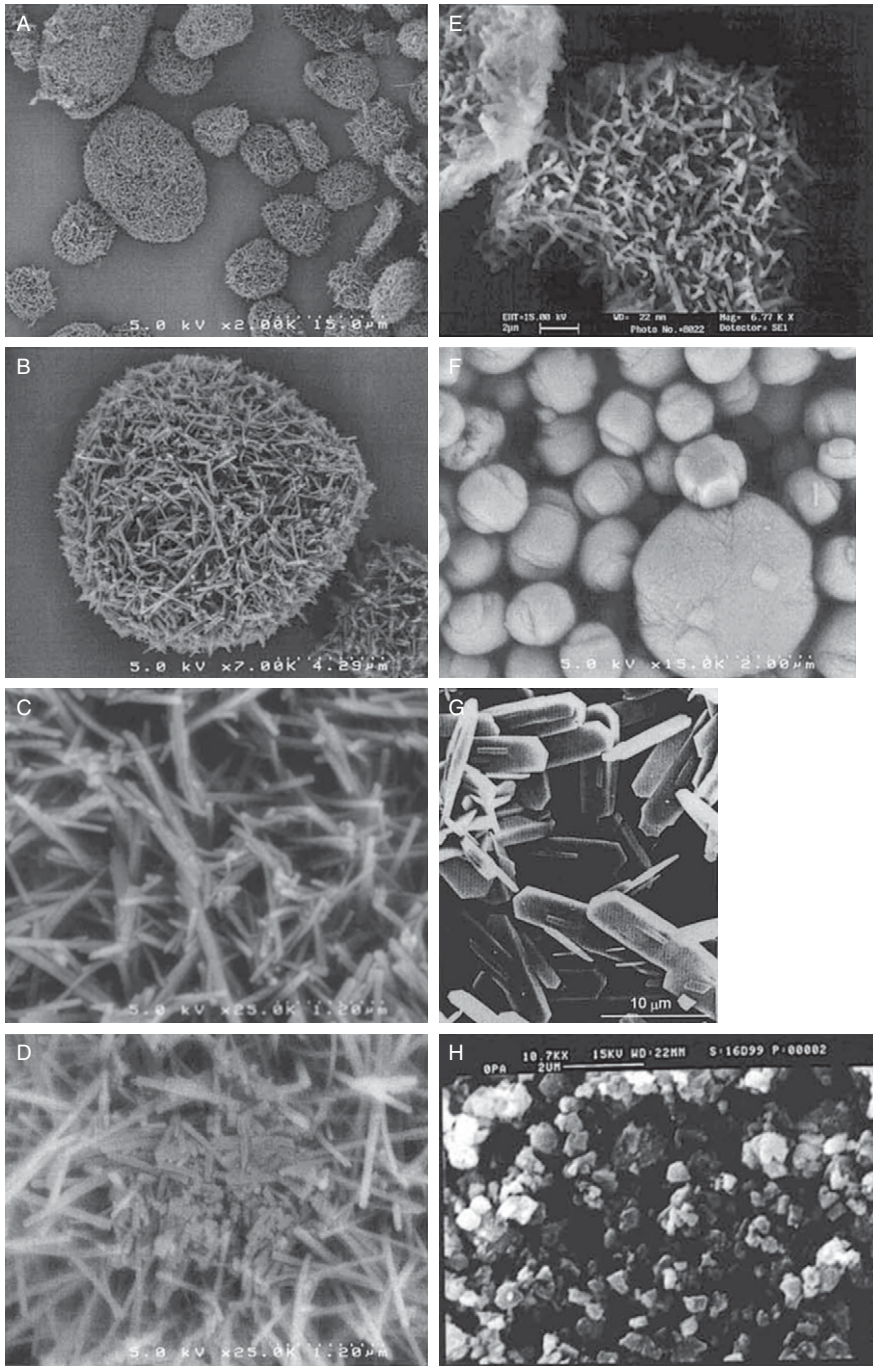

Figure 2 Scanning electron microscopy (SEM) images: (A–C) TON at increasing magnification, (D) MTT, (E) CRIS-rd, (F) MFI-1, (G) MFI-2, and (H) FAU. Reprinted with permission from Fenoglio *et al.* [45]. Copyright 2000 American Chemical Society.

When in contact with aqueous medium, the free radicals on the silica surface can give rise to ·OH radicals [67]. Generated ROS can react with biomolecules inside the cell causing cell damage and inflammation.

Another source of ROS comes from the presence of Fe^{2+} ions on the silica surface. A schematic representation of Fenton chemistry is shown below:

$$\mathrm{O_2 + \text{cellular reductants} \rightarrow O_2^{\bullet -} + H_2O_2}$$
$$\mathrm{Fe(III) + O_2^{\bullet -} \rightarrow Fe(II) + O_2}$$
$$\mathrm{2O_2^{\bullet -} + 2H^+ \rightarrow O_2 + H_2O_2}$$
$$\mathrm{Fe(II) + H_2O_2 \rightarrow Fe(III) + {}^{\bullet}OH + OH^-}$$

$$\mathrm{O_2^{\bullet -} + H_2O_2 \xrightarrow{Fe(III)/Fe(II)} O_2 + {}^{\bullet}OH + OH^-}$$

Since iron ions act as a catalyst in this reaction, even a small amount of iron present in the cell can cause the generation of large amount of radicals.

In a study by Fach *et al.*, two zeolites, mordenite and erionite, were investigated with respect to their cytotoxic potential toward the Chinese hamster ovary AS52 cell line as well as the effect of iron in the zeolite on the cytotoxicity [60]. The rationale for studying the toxicity of the zeolites in the presence of iron is because of their ion-exchange capabilities and the fact that naturally occurring zeolites can accumulate iron on their surface. A mutagenesis study was performed by exposing the cells to various concentrations of zeolites and iron. The cells were treated with 6-thioguanine (TG), were incubated for 10–14 days, and were examined for the development of TG-resistant (TGr) clones. Cytotoxicity was determined by measuring the relative cloning efficiency (RCE) and comparing it with untreated control samples.

Similar to the results of other studies, erionite, a fibrous zeolite, exhibited a larger cytotoxicity than mordenite. The percent viability in the case of erionite was as low as 20%, while for mordenite, cell viability increased to 40% under similar conditions. The cytotoxic effect also depends on the concentration of the zeolite and the amount of added iron (II).

The cytotoxicity of the zeolites was enhanced by ferrous ions, albeit only at high concentrations of both zeolite and iron (II). Mordenite was not mutagenic and ferrous ion did not alter mordenite's mutagenic potential. On the other hand, the mutagenic potential of erionite zeolite was significantly higher and the presence of ferrous cations further increased it. The difference in cytotoxic and mutagenic potentials of mordenite and erionite is explained by higher rate of ROS generation by the latter as well as higher iron (II) uptake from the environment. Another explanation of different effect of iron (II) on the two zeolites is that they have different crystal structures and, therefore,

different ion exchange sites. This difference can affect the Fenton chemistry by limiting the access of iron cations to hydrogen peroxide or changing the iron redox potential.

Fubini *et al.* investigated surface reactivity of the zeolite samples to provide more insight into the effect of OH radical generation on the cytotoxicity of the samples [45]. The samples were classified in the following order of ROS generation activity: FAU, MFI-2 < MTT < CRIS-rd and TON < MFI-1. The rate of radical generation varied from one zeolite to another and did not show any significant correlation with the toxicity of the zeolites. For example, MFI-1 zeolite that shows the lowest cytotoxicity has the highest rate of OH radical generation, while TON zeolite that has the highest cytotoxicity in the series showed a medium rate of radical generation.

The reactivity of the zeolite surface can be suppressed by coating the surface. Fubini *et al.* used aluminum lactate coating on TON, the most toxic zeolite used in their study. Treatment of TON with 3% w/v aluminum lactate solution decreased the toxicity of both calcined and noncalcined samples [45]. The decrease of cytotoxicity after surface coating was less pronounced in case of calcined samples, as adsorbates are more likely to concentrate inside the pores, while the external surface coverage becomes smaller.

3. Crystal Size and Surface Functionalization of Nanoscale Silicalite

New biomedical applications are currently being developed for zeolites and mesoporous silica materials (discussed in Section 4) including drug delivery and imaging. For these applications to be realized, the cytotoxicity of these materials in solution under biological conditions should be investigated. The cytotoxicity of silicalite-1 with varying crystal size (~30, 150, and 500 nm) and surface functionalization (amine, thiol, carboxylic acid) was investigated in phosphate buffer solution [63]. Silicalite-1, which has the MFI structure (Figure 1A) is the purely siliceous form of the zeolite ZSM-5 [27,28]. The silicalite external surface was functionalized by grafting of aminopropyl, mercaptopropyl, and carboxy functional groups onto the external zeolite surface as shown schematically in Figure 3. These functional groups were chosen so that the effect of surface charge on cytotoxicity could be systematically investigated [63]. The cytotoxicity of the silicalite samples with different crystal sizes and different surface functional groups was investigated using human embryonic kidney 293 (HEK-293) cells and the RAW264.7 macrophage cell lines.

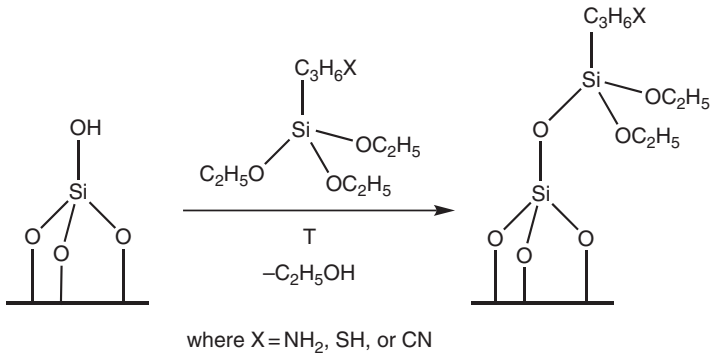

Figure 3 Reaction scheme depicting the reaction of the surface silanol groups with the organosilanes (APTES, MPTS, and CPTS) to form amino-, thiol-, and cyano-functionalized silicalite-1. The cyano-functionalized silicalite-1 was treated with sulfuric acid to form carboxy-functionalized silicalite-1. Reprinted with permission from Petushkov *et al.* [63]. Copyright 2009 American Chemical Society.

3.1. Physicochemical properties of nanoscale silicalite

Silicalite was synthesized in three different crystal sizes (~30, 150, and 500 nm) and the samples were subsequently calcined and then functionalized with 3-aminopropyltriethoxysilane (APTES), 3-mercaptopropyltriethoxysilane (MPTS), and (3-ethoxysilyl)propionitrile (CPTS) functional groups as shown schematically in Figure 3. The smallest CPTS-functionalized zeolite sample was 50 nm in diameter. The silicalite crystal structure was confirmed by powder XRD. The crystal morphology from the SEM images is approximately cubic and did not noticeably change when the sample was functionalized. Functionalization of silicalite nanoparticles results in a decrease in the total specific surface area by up to 20% in case of APTES and up to 40% in case of CPTS. The ζ-potential represents the surface charge of the particles in solution and varies with pH and ionic strength. Functionalization of silicalite with APTES leads to a marked positive shift of ζ-potential in comparison with the calcined silicalite sample. The ζ-potential for APTES-silicalite-1 is more positive than the ζ-potential for the calcined silicalite. The ζ-potential for CPTS-silicalite-1 is governed by dissociation of the surface carboxy groups, which shifts the ζ-potential to more negative values.

3.2. Effect of size and surface functionalization on toxicity of nanoscale silicalite

The cytotoxicity of the silicalite samples with different crystal sizes and different surface functional groups was investigated using HEK-293 cells and the RAW264.7 macrophage cell lines [63]. The rationale behind this

selection of cell models is that the RAW264.7 cell line is a model macrophage cell line commonly used to represent the physiological scavengers of foreign nanoparticles. HEK-293 cells were selected for evaluation in cytotoxicity studies because of their relevance and wide utility in the development of drug and gene delivery vehicles.

The cytotoxic potential of the silicalite-1 nanocrystals was evaluated using the LDH release assay, the caspase 3/7 activity assay, and Annexin V–PI staining. The leakage of LDH from cells provides a direct measure of the damage/integrity to the cell membrane. Caspases participate in a proteolytic cascade that leads to the programmed death of cells. Initiator caspases such as caspases 8 and 10 have an early role in the cascade, while effector caspases such as caspases 3, 6, and 7 are involved at later stages. As a result, measuring caspase 3/7 activity allows for a strong correlation of the degree of apoptosis occurring in a cell population. The Annexin V–PI staining method was then used to provide visual confirmation of the type of cell death induced by the different functionalized silicalite nanoparticles. Annexin-V FITC is a 35.8 kDa protein that has a strong natural affinity for phosphatidylserine, a membrane phospholipid that, soon after apoptosis initiates, translocates from the inner to the outer surface of the cell plasma membrane. Cells with preserved membranes are impermeable to PI. However, PI enters those cells with a damaged membrane, staining the DNA red.

The degree of LDH release of cells treated with silicalite nanoparticles is dependent on dose, particle size, and cell type (Figure 4). In HEK-293 cells, an increase from 0.5 to 1 mg mL^{-1} for 30 and 150 nm silicalite nanoparticles significantly increased LDH release, while an increase of 0.5 to 1 mg mL^{-1} for 500 nm nanoparticles did not significantly increase LDH levels in HEK-293 cells. In contrast to the HEK-293 cells, increasing the dose of 30 nm silicalite nanoparticles from 0.5 to 1 mg did not cause a significant increase in toxicity when incubated in RAW264.7 cells. However, increasing the dose of 150 and 500 nm silicalite nanoparticles from 0.5 to 1 mg did cause a significant increase in toxicity when incubated in RAW264.7 cells. Increasing the dose of larger silicalite nanoparticles increased toxicity in RAW264.7 cells, while increasing the dose of smaller silicalite nanoparticles increased toxicity in HEK-293 cells.

The biological characteristics of each of these cell lines can be used to rationalize these results. HEK-293 cells, which are a hypotriploid human cell line derived from the kidney and commonly used for drug and gene delivery efficacy testing, preferentially internalize particles <300 nm by clathrin-mediated endocytosis [68]. Particles above the 250–300 nm threshold for endocytosis such as the 500 nm silicalite nanoparticles would probably have greater difficulty entering the cell by this route and the toxicity of these particles even with increasing dose would be reduced. In contrast, the RAW264.7 cells are a macrophage-like cell line that has a greater capacity

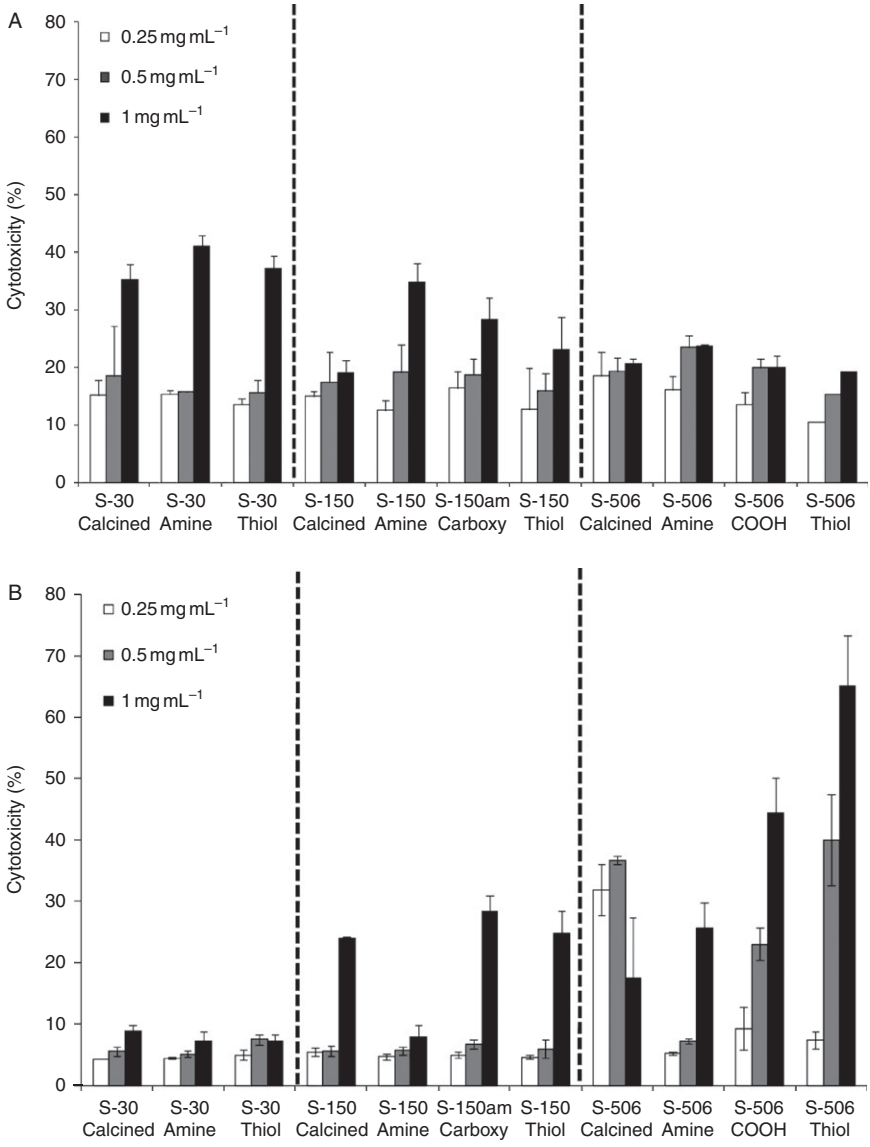

Figure 4 Cytotoxicity of calcined, amine-functionalized, thiol-functionalized, and carboxy-functionalized silicalite nanoparticles after 4 h of incubation in (A) HEK-293 cells and (B) RAW264.7 macrophages as measured by the extent of LDH release. The extent of enzyme leakage is expressed as a percentage of the total activity (mean ± SD of three separate experiments). Reprinted with permission from Petushkov *et al.* [63]. Copyright 2009 American Chemical Society.

to phagocytose micron-size range particles. Therefore, 500 nm particles would be expected to be internalized more easily in RAW264.7 cells when compared to HEK-293 cells accounting for the dose-dependent toxicity at higher particle sizes. A recent study by Thrall et al has shown that changing the size of silica nanoparticles from 10 to 500 nm did not significantly change any of the 1009 gene sets they tested, which were present in RAW264.7 cells [69]. This study by Thrall *et al.* implies that it is not genotoxicity that is being affected by the size of the silicalite nanoparticles [69]. The surface area does not correlate with cytotoxicity as indicated by the fact that 30 nm silicalite particles have the largest external surface area, yet show markedly lower toxicity relative to the largest 500 nm silicalite particles.

The dominant parameters affecting increased LDH release in HEK-293 cells were dose and particle size independent of surface functionalization. However, LDH release activity in RAW264.7 cells was connected to dose, particle size, and surface functionalization. The degree of toxicity did not change with surface functionalization in RAW264.7 cells incubated with 30 nm silicalite nanoparticles but did change toxicity induced by the 150 and 500 nm silicalite nanoparticles. The larger 500 nm silicalite nanoparticles showed dose-dependent increases in toxicity that increased with surface functionalization in the order of amine < carboxylic acid < thiol. The amine-functionalized silicalite which has the largest positive surface charge had the lowest toxicity for both the 150 and 500 nm silicalite particles, suggesting a correlation with surface charge. Nitric oxide (NO) production which is also linked to *S*-nitrosoglutathione (GSNO) production is inhibited by thiol groups [70–72]. One possible reason that thiol-functionalized 500 nm silicalite nanoparticles trigger strong LDH release but not apoptosis may be related to interference with levels of GSNO and NO production. Toxicity in macrophages that is predominantly caused by necrosis results when GSNO is depleted [70]. This could account for the large LDH release but low caspase 3/7 activity observed in RAW264.7 cells when treated with thiol-functionalized 500 nm silicalite nanoparticles.

Significantly higher levels of caspase 3/7 activity were generated by carboxylic acid-functionalized 500 nm silicalite nanoparticles when compared to all other groups. Previous studies comparing quantum dots coated functionalized with either amine groups or carboxylic acid groups have shown that the quantum dots coated with COOH groups are significantly more toxic. These particles stimulated significantly higher proinflammatory cytokines such as interleukin (IL)-6, IL-8, and IL-10 that have been reported to be correlated with immunotoxicity and apoptosis [73]. Other studies have shown that COOH coated nanoparticles are efficiently taken up by cells such as macrophages [74]. COOH-coated silicalite nanoparticles generate the strongest ROS production, which has been reported to be correlated with high levels of caspase 3/7 activity and apoptosis [75]. Studies on quartz dusts have shown that surface modification can

dramatically influence the toxicity [51,76]. For example, quartz modified with aluminum lactate or polyvinylpyridine-*N*-oxide (PVNO) was significantly less toxic and this was correlated with lower production of hydroxyl radicals when the modified quartz was exposed to hydrogen peroxide [76]. We investigated the radical generating ability of our silicalite samples in the presence of hydrogen peroxide and did not observe a clear correlation with toxicity.

4. Cytotoxicity of Mesoporous Silica

Mesoporous silica consists of silica channels/pores (>2 nm in diameter) capable of adsorbing small molecules (Figure 1B). The surface of mesoporous silica can be functionalized with different organic groups through grafting or cocondensation methods for applications in catalysis, imaging (markers and contrast agents), drug delivery, gene delivery, and sensing applications. The biological field has shown a keen interest in mesoporous silica for these applications due to its high surface area ($>1000\,m^2\,g^{-1}$), large pore volume, and well-defined and tunable pore size (1.5–10 nm). Reduction of particle size to the nanosize regime allows for optimal cell uptake. Mesoporous silica also shows high compatibility with biological media at concentrations adequate for pharmacological applications. However, concerns of cytotoxicity have resulted in various studies of their toxicity in an effort to determine the extent of any toxicity of the MSNs. An overview of the cytotoxicity studies discussed in this section is provided in Table 2.

4.1. Effect of surface functionalization on toxicity and cellular uptake

Surface-functionalized mesoporous silica materials offer numerous unique features, such as stable mesoporous structures, large surface areas, tunable pore sizes and volumes, and well-defined surface properties for site-specific delivery and for hosting molecules with various sizes, shapes, and functionalities. This is ideal for a controlled release mechanism where any premature release of guest molecules poses a challenging problem, for example, the delivery of many toxic antitumor drugs requires "zero release" before reaching the targeted cells or tissues. The possible cytotoxicities of MSNs could result from cellular injuries through a variety of mechanisms, such as membrane peroxidation, glutathione depletion, mitochondrial dysfunction, and DNA damage, eventually leading to cell death. Further reports on cytotoxicity of MSNs suggested that low concentrations of MSNs were more biocompatible than high doses. MSNs were nontoxic or less toxic to

local tissues but induced serious systemic toxicity. These toxicities could be lessened by decorating surfaces of the particles with certain functional groups. The mesoporous silicas impacted mitochondrial functions in a manner dependent on their physical properties. Several groups have investigated the effect of organic functionalization of MSNs on cytotoxicity.

Slowing, Trewyn, and Lin reported the synthesis of a series of organic functionalized MSNs (similar to scheme in Figure 3) and investigated the cytotoxicity and the mechanism of endocytosis of these materials with different charge profiles on human cervical cancer cells (HeLa) [58]. Three functional groups were grafted onto the surface of fluorescein-functionalized MCM-41-type MSN (FITC-MSN): 3-aminopropyl (AP), *N*-(2-aminoethyl)-3-aminopropyl (AEAP), and *N*-folate-3-aminopropyl (FAP). The ED_{50} (effective dose for 50% of the cells) for FITC-MSN, AP-MSN, and FAP-MSN decreased in the order $12.35 > 10.95 > 2.7\,\mu g\,mL^{-1}$ suggesting dose-responsive endocytosis [58]. The increase in ED_{50} correlated with a decrease in ζ-potential.

Cellular uptake of these materials (shown schematically in Figure 5) in the presence of specific inhibitors was tested to investigate the possible mechanism of endocytosis. It was found that the FITC- and FAP-MSNs are endocytosed via a clathrin-pit-mediated uptake mechanism. Additionally, uptake of FAP-MSN was partially inhibited by folic acid, whereas endocytosis of FITC-MSN was not perturbed. These findings suggested that the mechanism of endocytosis for this material is mediated by folic acid receptors on the HeLa cell surface. In contrast, endocytosis of AP- and GP-MSNs was affected by a caveolar inhibitor, genistein, suggesting that these materials are endocytosed via a caveolae-mediated mechanism. In further analysis of surface functionality on endosomal escape, it was found that the more negatively charged FITC- and AP-MSNs appeared to be able to escape from endosomes within 6 h, while those with more positive ζ-potentials (GP-MSNs, FAP-MSNs) remained trapped within the endosomes.

Huang and coworkers evaluated the effect of surface charge on the cell uptake of MSNs and elucidated the uptake mechanism [56]. MSNs were found to have a high cellular labeling efficiency and subsequently the positive surface charge had negligible effect on the uptake efficiency of MSNs. It was inferred that the uptake of MCM-41-type MSNs by human mesenchymal stem cells (hMSCs) can be regulated by a threshold of positive surface charge but also implied that the modulation of surface charge on MSNs uptake is specific to cell type [56]. At low surface charge, the normal clathrin- and actin-dependent mechanisms operate, which by themselves are already quite efficient for hMSC and 3T3-L1 cells. Above this threshold, a new but unknown mechanism takes effect for hMSC. Surface charge functionalization with different amounts of positively charged quaternary ammonium group did not affect the biocompatibility of MSNs.

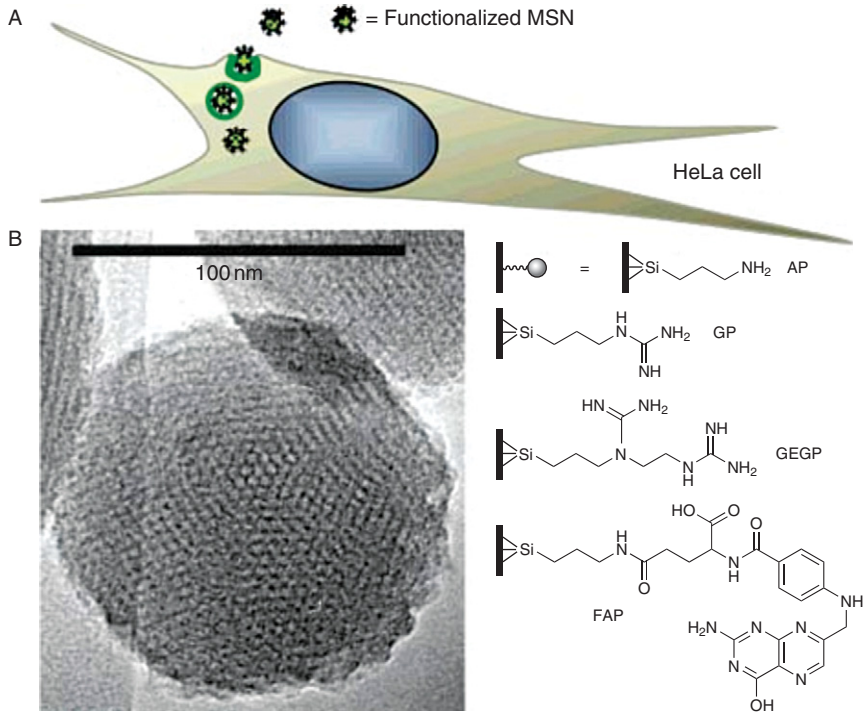

Figure 5 Schematic representation of (A) the endocytosis of organically functionalized mesoporous silica nanoparticles (MSNs) by a human cervical cancer cell (HeLa). (B) TEM image of a fluorescein-functionalized MSN (FITC-MSN). Reprinted with permission from Slowing *et al.* [58]. Copyright 2006 American Chemical Society.

Amorphous silica materials are known to cause hemolysis of mammalian red blood cells, raising serious biosafety concerns over the use of amorphous silica for intravenous drug delivery. It is widely accepted that the hemolytic activity of silica is related to surface silanol groups. Lin and coworkers investigated the hemolytic properties of MSNs with mammalian (rabbit) red blood cells [77]. The researchers showed that hemolytic amorphous silica actually contained less silanol groups than nonhemolytic MSNs, implying that the hemolytic properties of these silica materials were not proportional to the total amount of silanol groups. They further showed that there was significant difference between the surface charge properties of amorphous silica and MSNs in aqueous media via electrophoretic light scattering. This suggested that the external surface of amorphous silica is more abundant in negatively charged species than that of the MSNs; thus, even if MSNs had more silanol groups than amorphous silica, not all of these groups contribute to the electrophoretic mobility of the particles. Thus, despite MSNs having

more silanol groups than amorphous silica, most of these groups are inaccessible for any direct interaction with the cell membrane. Amorphous silica possesses many nanoscale domains with abundant silicates on its external surface which are responsible for strong and continuous electrostatic interactions with trimethylammonium head groups of the membrane lipids as shown in Figure 6. MSNs on the other hand have a low surface density of silanol groups for MSNs caused by the unique honeycomb-like structure with arrays of 3 nm mesopores resulting in low hemolytic behavior.

Several groups have studied the cellular uptake of MSNs. Asefa and coworkers investigated the mesoporosity dependence and functional group dependence of cytotoxicity and endocytosis of MSNs [78]. In their study, the uptake of MCM-41, SBA-15, and solid silica microsphere (SMS, ~300 nm) and the ammonium-functionalized analogues (MCM-41-N, SBA-15-N, and SMS-N) of each of these were investigated on Jurkat cells (lymphoid) and SK-N-SH (human neuroblastoma) cells [78]. MCM-41 has a larger surface area but a smaller pore size compared to SBA-15. SMS has very low surface area and low porosity. The cytotoxicity of SBA-15 on Jurkat cells

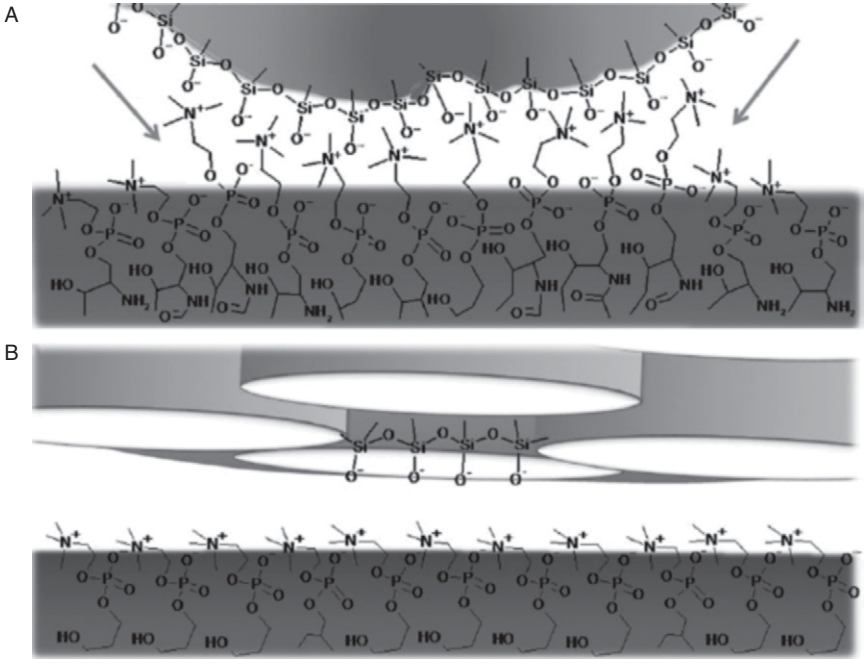

Figure 6 Representation of the interaction of (A) amorphous silica nanoparticles and (B) MSNs with the RBC membrane (bottom rectangular surfaces). Arrows show the disruption of the membrane due to the cumulative interaction between silanol groups and phospholipids. Reprinted with permission from Slowing *et al.* [77]. Copyright 2009 Wiley–VCH.

was both dose dependent and time dependent. In contrast, MCM-41 did not cause significant cytotoxicity unless there was a long exposure time (greater than ~1 day). No significant cytotoxicity was observed when SBA-15 and MCM-41 were functionalized with positively charged ammonium. In general, SK-N-SH cells were more resistant to the MSNs whether aminated or not. SMS was toxic to Jurkat cells in both forms.

The observed toxicity was explained by changes in endocytosis. Positively charged ammonium-functionalized MSNs prevented toxicity; these positively charged particles were not endocytosed. The endocytosis was studied using transmission electron microscopy (TEM) and the results are shown in Figure 7. In Figure 7A and B, the endocytosis of SBA-15 and

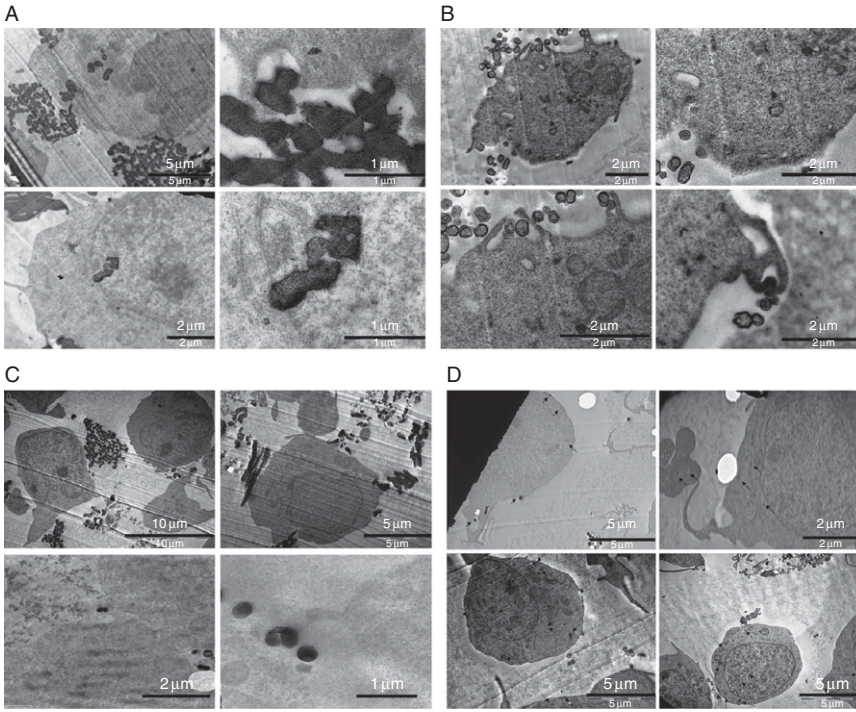

Figure 7 TEM images that visualized the uptake of silica nanoparticles by Jurkat cells. (A) Endocytosis of SBA-15. The cytoplasm membranes inclined to fold with an intension to absorb the material from outside. In addition, an internalized SBA-15 nanoparticle was observed penetrating the nuclear membrane. (B) Endocytosis of MCM-41. Particles are ingested by cells as cell membranes hug around MCM-41 nanoparticles, forming a pseudopodium. (C) Endocytosis of SBA-N (upper panel) or MCM-N (lower panel). No efficient endocytosis can be observed, as particles stay outside of cells in the medium. (D) Endocytosis of SMS (upper panel) or SMS-N (lower panel). Internalized solid nanoparticles are indicated by arrows. Reprinted with permission from Tao *et al.* [78]. Copyright 2009 American Chemical Society.

MCM-41, respectively, by Jurkat cells, was observed in the TEM images. In Figure 7C, no endocytosis of MCM-41-N and SBA-15-N by Jurkat cells was observed. Finally, in Figure 7D, SMS and SMS-N were both endocytosed. Based on these results, Asefa and coworkers concluded that the cytotoxicity is both particle dependent as well as cell-type dependent [78].

In a related study by Chen and coworkers, the efficient cellular internalization of fluorescein isothiocyanate-conjugated mesoporous silica nanoparticles (FITC-MSNs) with highly ordered hexagonal pores and well-defined hexagonal edges was demonstrated [79]. The mechanisms of cellular uptake of FITC-MSNs in 3T3-L1 cells and hMSCs was further investigated. Microscopy experiments demonstrated that the intracellular internalization detected by flow cytometry was not a result of adherence to the cell surface. hMSCs internalized FITC-MSNs more efficiently than the 3T3-L1 cells. hMSCs reserved the intracellular FITC-MSNs longer, implying that FITC-MSNs could be a viable candidate for stem cell tracking. FITC-MSN internalization did not affect cell viability, cell proliferation, and the immunophenotypic profiles of surface markers in hMSCs. Further evidence of FITC-MSN biocompatibility was the exertion of equal (to untreated cells) adipogenic differentiation ability by the labeled 3T3-L1 cells after cellular internalization of the FITC-MSNs. FITC-MSNs could be found in the late endosomes or lysosomes after internalization and its uptake was significantly reduced after inhibition of clathrin but not caveolae, indicating the involvement of clathrin-dependent endocytosis in the uptake pathway [79].

FITC-MSNs retained their architectonic integrity after internalization and appeared to escape from endolysosomal vesicles. Due to the absence of cytotoxicity, it was inferred that FITC-MSNs escaped from endolysosomal vesicles via the localized destabilization of endolysosomal membrane but not via the rupture of endolysosomal vesicles with surface cationization. The results support a claim for potential application of these nanoparticles in stem cell tracking.

However, according to a study by Peters and coworkers, human endothelial cells possess a large capacity for the internalization of particulate matter in the nanometer scale [80]. This capacity allows for nanoparticulate incorporation mostly into vacuoles. Particle containing vacuoles possess an autophagic function since these vacuoles also contain varying amounts of amorphous cellular material and membranes.

4.2. Effect of MSNs on cellular respiration

In a study by Asefa and coworkers, MSNs (SBA-15 and MCM-41) were found to induce mitochondrial oxidative stress and deplete cellular glutathione [57]. Their results confirmed a concentration-dependent

interference by SBA-15 in glucose-supported respiration. MCM-41 was observed to affect glucose processing but not respiration. They also confirmed that ATP hydrolysis (consumption) is not significantly altered in the nanoparticle-treated cells. It was thus unlikely that significant ROS was generated in the nanoparticle-treated cells. Both SBA-15 and MCM-41 were equally toxic to the mitochondria and SMP. It appeared that the physical properties of nanoparticles determined their effects on cellular bioenergetics. MCM-41 had only a small effect on cellular respiration. The minimal effect of MCM-41 was likely due to limited access to cellular mitochondria. The cellular uptake of MCM-41 was likely hindered by its high surface area per unit mass.

5. Silica Nanoparticle Toxicity

Silica (SiO_2) can be produced inexpensively, is generally regarded as relatively safe, and is used in a multitude of different applications. Of particular interest is the use of silica in biomedical applications. The cytotoxicity of amorphous, nonporous silica nanoparticles has been investigated and a brief summary of representative results is presented here for comparison with the porous silica nanomaterials, zeolites, and mesoporous silica.

Hoet and coworkers investigated the cytotoxicity of amorphous silica nanoparticles (sizes varied from 14 to 335 nm in diameter) in endothelial cells (EAHY926) [81]. Their amorphous silica samples were stable monodisperse dispersions that were stable against aggregation. The particle size distributions were measured by dynamic light scattering (DLS). They determined that smaller silica nanoparticles are more toxic when the particle morphologies are similar and the doses are expressed in mass concentration. The 14 and 16 nm silica nanoparticles have $ED_{50} = 33$ and $47\,\mu g\,cm^{-2}$, respectively, compared to the 104 and 335 nm silica particles that have $ED_{50} = 1095$ and $1087\,\mu g\,cm^{-2}$, respectively. The surface area was also an important factor in toxicity and when the toxicity was compared in terms of surface area ($cm^2\,cm^{-2}$), the toxicity was similar for different sized silica particles. The mechanism for cell death was also investigated and it was found that, for smaller particles, necrosis is observed within a few hours.

In a subsequent study, Martens and coworkers investigated cytotoxicity of amorphous silica nanoparticles (sizes varied from 2 to 335 nm diameter) in endothelial cells (EAHY926) and mouse macrophages (J774) [82]. The cytotoxicity was observed to increase with decreasing particle size as shown by the correlation between ED_{50} and particle size in Figure 8. The ability of the silica to generate hydroxyl radicals from hydrogen peroxide was also investigated using the spin trap, 5,5-dimethyl-1-pyrroline-*N*-oxide (DMPO), and electron paramagnetic resonance (EPR) spectroscopy to

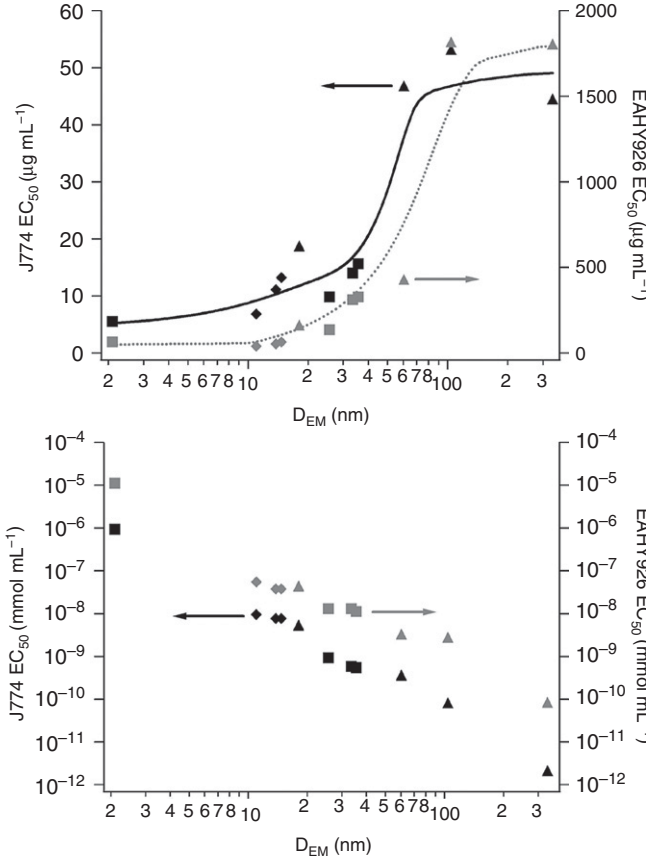

Figure 8 Cytotoxicity expressed as half-maximum effective dose (ED_{50} value) in g mL^{-1} (upper panel) and in mmol mL^{-1} (lower panel) of SNP in human endothelial (EAHY926, gray) and mouse monocyte macrophage (J774, black) cell lines in function of silica nanoparticle diameter. Different symbols are applied to distinguish SNP synthesis procedure: Lys-Sil, squares; Stober, triangles; Ludox, diamonds. Reprinted with permission from Thomassen *et al.* [82]. Copyright 2009 American Chemical Society.

detect the hydroxyl adduct, 2,2-dimethyl-5-hydroxy-1-pyrrolidinyloxyl (DMPO-OH). On a per mass basis, the radical-generating activity decreased with increasing particle size, suggesting that the radical formation which is a surface property correlates with cytotoxicity. This was the first report of radical formation on amorphous silica nanoparticles in aqueous solution [82].

Ma and coworkers evaluated the cytotoxicity of SiO_2 nanoparticles (15 nm, 46 nm) in human bronchoalveolar carcinoma-derived cells, using crystalline silica as a positive control [83]. Prior to their work, studies had

shown that SiO_2 nanoparticles caused aberrant clusters of topoisomerase I (topo I) in the nucleoplasm in cells, proinflammatory stimulation of endothelial cells, and fibrogenesis in Wistar rats. On the other hand, an *in vivo* mouse study showed that silica nanoparticles are not toxic in an apparent contradiction. Ma *et al.* observed that the cytotoxicity of the 46 nm SiO_2 nanoparticles was not significantly different from that of the 15 nm SiO_2 nanoparticles in the 10–100 $\mu g\,mL^{-1}$ dosage range possibly due to aggregation or a similar hydrodynamic radius [83]. Both sizes of SiO_2 nanoparticles produced greater cytotoxicity than the crystalline silica in the 50–100 $\mu g\,mL^{-1}$ range. A strong correlation between decreased cell viability and increased ROS level after 48 h exposure was observed. The reverse correlation between the decreased cell viability and the increased LDH activity suggested that cell death was the primary cause of the reduction in cell number. The authors concluded that the ROS generated by exposure to the nanoparticles produces oxidative stress in these cells as reflected by the reduced glutathione levels and the elevated production of malondialdehyde and LDH, indicative of lipid peroxidation and membrane damage.

In a related study by Kong and coworkers, the cytotoxicity was shown to correlate with the metabolic activity of the cell line [84]. They determined that silica nanoparticles are nontoxic at low concentrations but cause cell membrane damage at higher concentrations as indicated by increased LDH. The high doses were found to be more toxic to human fibroblast cells which have long doubling times relative to tumor cells which have shorter doubling times.

6. Cytotoxicity of Quartz

Exposure to crystalline silicates, such as quartz, occurs during quarrying, mining, or processing. A number of silicate materials are known for their cytotoxic potential that leads to pulmonary inflammation and pulmonary fibrosis when the particles are inhaled [85]. Hochstrasser and Antonini have show that Si and Si–O radicals are present on the surfaces of freshly cleaved silica and quartz [86]. These surface radicals can react with other molecules, such as CO_2, and produce new radicals. In a series of works, Shi and coworkers showed that freshly cleaved crystalline silica has a higher potential to generate hydroxyl radicals than the sample that was aged for several days in air [67,87]. The relative intensity of ESR signal of DMPO–OH adduct decreased 2.5-fold in comparison with a freshly ground sample [67]. This work was followed by a more detailed study of the fresh versus aged quartz hydroxyl radical generation and cytotoxic potential toward alveolar macrophage cells [87]. It was shown that the treatment of alveolar macrophages with freshly ground silica resulted in higher secretion of hydrogen peroxide and higher rate of LDH release in

comparison with aged quartz. Freshly ground quartz particles also exhibited a much higher hemolytic potential to red blood cells than the aged samples.

An in-depth study on the mechanism of quartz toxicity was done by Polimeni *et al.* [88], who used murine alveolar macrophage cell line (MH-S) to evaluate oxidative stress imposed by quartz crystals. Pure quartz powder with particle size ranging from 1 to 10 μm was obtained by grinding Madagascar quartz crystals. Several methods were used to determine the oxidative effect of quartz in the cells. Release of LDH in the extracellular environment was used to monitor cytotoxic effect of quartz. The thiobarbituric acid reactive substances (TBARS) assay was used as a screening method for lipid peroxidation. Cell apoptosis was detected using Annexin V and PI assays. The pentose phosphate pathway (PPP) activity was measured as it is one of the metabolic pathways most sensitive to a cell oxidative stress. PPP is activated in the cells in response to an oxidative stress. During the oxidative phase of the pathway, the reduced form of nicotinamide adenine dinucleotide phosphate (NADPH) is synthesized. NADPH acts as a redox cofactor for many antioxidant enzymes. However, PPP activation was not observed when the cells were incubated with quartz particles. Moreover, the presence of quartz particles inhibited the PPP activity, while the glutathione/oxidized glutathione ratio (GSH/GSSG ratio) that serves as an indicator of oxidative stress in the cells was decreasing.

The PPP pathway in the cells is regulated by a glucose-6-phosphate dehydrogenase (G6PD) enzyme that catalyzes the rate-limiting step in the pathway. The measurement of G6PD activity in the studied system showed significant decrease of its activity in presence of quartz. The authors hypothesized that the decrease of G6DP enzyme activity by quartz particles goes via an oxidative mechanism. It was concluded that the presence of quartz particles in the cells decreases their ability to counteract oxidative stress by inhibiting activity of certain enzymes.

The effect of quartz content in bentonite mineral, a mineral containing up to 6% of α-quartz, as well as activation of the particles with alkaline, acidic, and organic solutions was studied by Geh *et al.* [89]. The particles were also treated with alkaline, acidic, and organic solutions, and the cytotoxic effect of particle activation was studied. The IMR-90 human lung fibroblast cell line was chosen for evaluation of bentonite cytotoxicity. The cellular uptake of bentonite particles was studied with TEM. The degree of uptake depended on the type of activation. Alkaline-activated particles exhibited the largest uptake in comparison with untreated particles, ~3.5-fold higher than the untreated particles.

Cytotoxicity was analyzed using flow cytometry and by measuring of the cell respiratory activity. Cell staining (Annexin/FITC, PI) was used to distinguish between early apoptotic cells (Annexin V-positive, PI-negative), late apoptotic/necrotic cells (Annexin V-positive, PI-positive), and necrotic cells (Annexin V-negative, PI-positive).

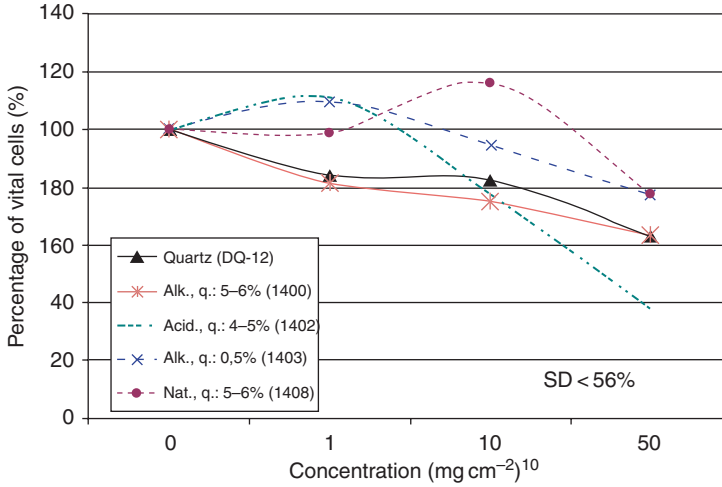

Figure 9 Cytotoxicity of different bentonite particles in IMR-90 cells in relation to quartz, measured by Coulter Counter, exposure time 24 h. Reprinted with permission from Geh *et al.* [89]. Copyright 2006 Springer.

Flow cytometry has shown that cytotoxicity of bentonite is both quartz concentration and activation dependent. Increase of the quartz concentration in the bentonite samples led to higher toxicity (Figure 9). Particle activation played a significant role. For example, acid-treated samples containing 5–6% quartz showed higher cytotoxicity than DQ-12 quartz used as a positive control. These effects appeared at higher concentration of bentonite, while at lower concentration the presence of bentonite in cell cultures resulted in their proliferation. Relatively low positive control (pure quartz) toxicity was attributed to the fact that the quartz powder was not freshly prepared, while freshly ground quartz powders are known to have higher cytotoxicity than aged ones [87]. The authors also claimed that the cytotoxicity of bentonite samples may originate not only from the presence of quartz but also from iron, a transition metal known to cause generation of ROS. Based on the experimental data, the authors have concluded that the cytotoxic effect of bentonite particles was slightly more necrotic than apoptotic, caused by rupture of the cell membrane.

Albrech *et al.* focused on the effect of quartz surface coating on cytotoxicity of particles [90]. DQ12 (Dörentruper quartz) was used for evaluation of cytotoxicity in rat alveolar macrophages over time. Rat bronchoalveolar lavage was analyzed for cell toxicity parameters using several techniques. Rat lung macrophage cell line NR8383 was used as a model to study the quartz effect on the epithelial cells. The bronchoalveolar lavage fluid (BALF) was analyzed for the number or macrophage and

neutrophil cells, total protein, amount of released LDH, and concentration of alkaline phosphatase.

The exposure of rats to untreated quartz particles resulted in significant steady increase of the number of cells in BALF over time. Neutrophils constituted up to 65% of the total number of cells in the lavage, a characteristic of inflammatory process occurring in rat lungs. Also, the amount of LDH released (as a result of cell membrane rupture) increased especially after 90-day period. At the same time, coating the quartz particles with aluminum lactate or PVNO resulted in significant decrease of parameters linked to cytotoxic and inflammatory processes. PVNO appeared to be a more effective coating than aluminum lactate as shown by the above mentioned methods.

Measurement of β-glucuronidase and macrophage inflammatory protein MIP-2 was performed to characterize the activity of inflammatory cells in the rat lung after animal treatment. It was shown that the presence of native DQ-12 quartz results in higher concentrations of β-glucuronidase and MIP-2 indicates an enhanced amount of inflammatory cells in BALF in comparison with coated quartz particles and negative control samples.

In order to investigate the role of epithelial lung cells in the inflammatory response to the presence of quartz particles, nuclear translocation factor nuclear factor-kappaB (NF-κβ) was studied. NF-κβ is an important transcription factor involved in inflammatory cellular responses. Activity of NF-κβ was measured by means of immunohistochemistry as well as by measuring the concentration of IκBα inhibitor protein in lung homogenates. The studies have shown that the concentration of the inhibitor protein is significantly lower in animals treated with native quartz particles in comparison with control samples. Treatment with PVNO-coated quartz did not change the concentration of IκBα in the rat lungs significantly at any time point. Immunostaining of lung sections showed that an enhanced amount of NF-κβ was detected in lungs treated with native quartz. The NF-κβ signal appears to be acute and subchronic after 3 and 90 days from quartz instillation, respectively. In comparison with native quartz particles, lungs treated with coated quartz show lower amounts of NF-κβ.

7. Summary

In this chapter, an overview of the toxicity of silica-based nanomaterials was presented. Porous materials, such as crystalline, microporous zeolites, and mesoporous silica materials, have two nanoscale aspects: nanoscale pores which provide large internal surface areas and nanoscale crystal or particle sizes which may lead to unique external surface reactivity. The nonporous silica materials are crystalline silica (most commonly quartz or

cristobalite) and amorphous silica, with the focus here being on amorphous silica nanoparticles. Particular attention was given to studies in which the physicochemical properties of silica-based materials were correlated with toxicity. For most of the toxicity studies discussed here, the reported toxicity was complex and often depended on cell type, dosage, length of exposure, and chemical properties of the material.

Toxicity studies of zeolites suggest that the internal surface does not appear to influence the toxicity of the zeolites most likely because the internal surface does not interact with the biological system of interest [44]. This does not rule out a secondary toxicity that could be associated with toxic species located in the internal pore surface that could then be released; however, a study of this proposed secondary effect has not been reported. The impact of particle aspect ratio is critical for zeolites and crystalline silicas which exhibited increased toxicity at high aspect ratios [44,60–61]. These particles cannot be completely endocytosed by macrophage cells, for example, and may rupture the cell membrane leading to cell death.

The effect of particle size and surface functionalization was also investigated by comparing the toxicity and endocytosis of mesoporous and nonporous silica nanoparticles [75,76]. It was found that the toxicity of the materials could be correlated with the endocytotic efficiency of the MSNs which depends on particle size and surface functionalization. Aminated MSNs exhibited less toxicity and this was due to the less effective endocytosis of the aminated MSNs relative to the untreated MSNs [76]. It was also further demonstrated that the endocytosis could be controlled by varying the surface functionalization [75]. For zeolites, coating the surface with aluminum lactates decreased the toxicity substantially [44]. However, the variation in toxicity with surface functionalization for silicalite nanoparticles was complex [62]. For nonporous silica nanoparticles, the smaller particles were found to be more toxic when endothelial or mouse macrophage cell lines were used [80].

The formation of ROS was investigated for several different materials in order to explain toxicity results. For quartz, it was shown that a freshly cleaved quartz surface generates more radicals than an aged quartz surface which correlated with a higher rate of LDH release. For nonporous amorphous silica nanoparticles and endothelial and mouse macrophage cells, the ROS-generating ability increased with increasing cytotoxicity and decreasing particle size. [80]. In contrast, for zeolites and MSNs, the ROS-generating ability did not correlate with cytotoxicity [44,56].

The results from the literature presented here underscore the importance of careful materials characterization since the toxicity depends on the particle size, porosity, shape, surface area, surface functionalization, and surface treatment. In addition, the toxicity may vary based on the cell line, concentration, and exposure time in a complex way. The formation of

ROS and the endocytosis can often be correlated with observed cytotoxicity. As new silica-based nanomaterials are synthesized with careful control of size and surface properties, it remains critically important to evaluate the toxicity of the materials prior to the development of widespread applications.

Acknowledgments

A.K. Salem and S.C. Larsen acknowledge grant support from NSF NER (CMMI-0608977) and the Center for Health Effects and Environmental Contamination (CHEEC) at the University of Iowa. ND acknowledges support from Grant Number UL1RR024979 from the National Center for Research Resources (NCRR), a part of the National Institutes of Health (NIH). The contents of this chapter are solely the responsibility of the authors and do not necessarily represent the official views of the Clinical and Translational Science Awards (CTSA) or NIH.

REFERENCES

[1] H.F. Wang, T.B. Huff, D.A. Zweifel, W. He, P.S. Low, A. Wei, J.X. Cheng, In vitro and in vivo two-photon luminescence imaging of single gold nanorods, Proc. Natl. Acad. Sci. U. S. A. 102 (2005) 15752–15756.
[2] I.H. El-Sayed, X.H. Huang, M.A. El-Sayed, Surface plasmon resonance scattering and absorption of anti-EGFR antibody conjugated gold nanoparticles in cancer diagnostics: Applications in oral cancer, Nano Lett. 5 (2005) 829–834.
[3] A.K. Salem, C.F. Hung, T.W. Kim, T.C. Wu, P.C. Searson, K.W. Leong, Multicomponent nanorods for vaccination applications, Nanotechnol. 16 (2005) 484–487.
[4] A.K. Salem, M. Chen, J. Hayden, K.W. Leong, P.C. Searson, Directed assembly of multisegment Au/Pt/Au nanowires, Nano Lett. 4 (2004) 1163–1165.
[5] A.K. Salem, P.C. Searson, K.W. Leong, Multifunctional nanorods for gene delivery, Nat. Mater. 2 (2003) 668–671.
[6] M. Kralj, Biomedical and environmental potential of nanoporous materials, Period. Biol. 105 (2003) 99–107.
[7] M. Kralj, K. Pavelic, Medicine on a small scale, EMBO Rep. 4 (2003) 1008–1012.
[8] K. Pavelic, M. Hadsija, L. Bedrica, J. Pavelic, I. Dikic, M. Katic, M. Kralj, M. Bosnar, S. Kapitanovic, M. Poljak-Blazi, S. Krizanac, R. Stojkovic, M. Jurin, B. Subotic, M. Colic, Natural Zeolite clinoptilotite: New adjuvant in anticancer therapy, J. Mol. Med. 78 (2001) 708–720.
[9] L. Tosheva, V.P. Valtchev, Nanozeolites: Synthesis, crystallization mechanism, and applications, Chem. Mater. 17 (2005) 2494–2513.
[10] S.C. Larsen, Nanocrystalline zeolites and zeolite structures: Synthesis, characterization, and applications, J. Phys. Chem. C 111 (2007) 18464–18474.
[11] G.H. Li, C.A. Jones, V.H. Grassian, S.C. Larsen, Selective catalytic reduction of NO2 with urea in nanocrystalline NaY zeolite (234, 401, 2005), J. Catal. 235 (2005) 431–431.

[12] M.E. Pearce, H.Q. Mai, N. Lee, S.C. Larsen, A.K. Salem, Silicalite nanoparticles that promote transgene expression, Nanotechnology 19 (2008) 175103–175109.
[13] B.G. Trewyn, S. Giri, I.I. Slowing, V.S.Y. Lin, Mesoporous silica nanoparticle based controlled release, drug delivery, and biosensor systems, Chem. Commun. (2007) 3236–3245.
[14] C.P. Tsai, Y. Hung, Y.H. Chou, D.M. Huang, J.K. Hsiao, C. Chang, Y.C. Chen, C.Y. Mou, High-contrast paramagnetic fluorescent mesoporous silica nanorods as a multifunctional cell-imaging probe, Small 4 (2008) 186–191.
[15] R. Matheoud, C. Secco, S. Ridone, E. Inglese, M. Brambilla, The use of molecular sieves to simulate hot lesions in F-18-fluorodeoxyglucose—Positron emission tomography imaging, Phys. Med. Biol. *53* (2008) N137–N148.
[16] W.S. Li, Z.F. Li, F.Y. Jing, X.G. Yang, X.J. Li, F.K. Pei, X.X. Wang, H. Lei, Zeolites Mn2+-NaY as oral gastrointestinal tract contrast agents in magnetic resonance imaging, Acta Chim. Sin. 65 (2007) 2029–2033.
[17] Y.S. Lin, Y. Hung, J.K. Su, R. Lee, C. Chang, M.L. Lin, C.Y. Mou, Gadolinium (III)-incorporated nanosized mesoporous silica as potential magnetic resonance imaging contrast agents, J. Phys. Chem. B 108 (2004) 15608–15611.
[18] K.J. Balkus, J.M. Shi, A study of suspending agents for gadolinium(III)-exchanged hectorite. An oral magnetic resonance imaging contrast agent, Langmuir 12 (1996) 6277–6281.
[19] V.L. Colvin, The potential environmental impact of engineered nanomaterials, Nat. Biotechnol. 21 (2003) 1166–1170.
[20] G.H. Li, C.A. Jones, V.H. Grassian, S.C. Larsen, Selective catalytic reduction of NO2 with urea in nanocrystalline NaY zeolite, J. Catal. 234 (2005) 401–413.
[21] G.H. Li, S.C. Larsen, V.H. Grassian, Catalytic reduction of NO2 in nanocrystalline NaY zeolite, J. Mol. Catal. Chem. 227 (2005) 25–35.
[22] D.W. Breck, Zeolite Molecular Sieves: Structure, Chemistry, and Use, Wiley-Interscience, New York, 1974.
[23] J. Galownia, J. Martin, M.E. Davis, Aluminophosphate-based, microporous materials for blood clotting, Microporous Mesoporous Mater. 92 (2006) 61–63.
[24] I. Bresinska, K.J. Balkus, Studies of Gd(III)-exchanged Y-type zeolites relevant to magnetic-resonance-imaging, J. Phys. Chem. 98 (1994) 12989–12994.
[25] S.W. Young, F. Qing, D. Rubin, K.J. Balkus, J.S. Engel, J. Lang, W.C. Dow, J.D. Mutch, R.A. Miller, Gadolinium zeolite as an oral contrast agent for magnetic-resonance-imaging, J. Magn. Reson. Imaging 5 (1995) 499–508.
[26] C. Platas-Iglesias, L. Elst, W. Zhou, R.N. Muller, C. Geraldes, T. Maschmeyer, J.A. Peters, Zeolite GdNaY nanoparticles with very high relaxivity for application as contrast reagents in magnetic resonance imaging, Chem. Europ. J. 8 (2002) 5121–5131.
[27] W. Song, V.H. Grassian, S.C. Larsen, High yield method for nanocrystalline zeolite synthesis, Chem. Commun. (2005) 2951–2953.
[28] W. Song, R.E. Justice, C.A. Jones, V.H. Grassian, S.C. Larsen, Size-dependent properties of nanocrystalline silicalite synthesized with systematically varied crystal sizes, Langmuir 20 (2004) 4696–4702.
[29] W. Song, J.F. Woodworth, V.H. Grassian, S.C. Larsen, Microscopic and macroscopic characterization of organosilane-functionalized nanocrystalline NaZSM-5, Langmuir 21 (2005) 7009–7014.
[30] K. Barquist, S.C. Larsen, Chromate adsorption on amine-functionalized nanocrystalline silicalite-1, Microporous Mesoporous Mater. 116 (2008) 365–369.
[31] B.-Z. Zhan, M.A. White, M. Lumsden, Bonding of organic amino, vinyl, and acryl groups to nanometer-sized NaX zeolite crystal surfaces, Langmuir 19 (2003) 4205–4210.

[32] F. Lerouge, O. Melnyk, J.O. Durand, L. Raehm, P. Berthault, G. Huber, H. Desvaux, A. Constantinesco, P. Choquet, J. Detour, M. Smaihi, Towards thrombosis-targeted zeolite nanoparticles for laser-polarized Xe-129 MRI, J. Mater. Chem. 19 (2009) 379–386.
[33] C.M. Lew, Z.J. Li, S. Li, S.J. Hwang, Y. Liu, D.I. Medina, M.W. Sun, J.L. Wang, M.E. Davis, Y.S. Yan, Pure-silica-zeolite MFI and MEL low-dielectric-constant films with fluoro-organic Functionalization, Adv. Funct. Mater. 18 (2008) 3454–3460.
[34] S. Huh, J.W. Wiench, B.G. Trewyn, S. Song, M. Pruski, V.S.Y. Lin, Tuning of particle morphology and pore properties in mesoporous silicas with multiple organic functional groups, Chem. Commun. (2003) 2364–2365.
[35] M. Liong, J. Lu, M. Kovochich, T. Xia, S.G. Ruehm, A.E. Nel, F. Tamanoi, J.I. Zink, Multifunctional inorganic nanoparticles for imaging, targeting, and drug delivery, ACS Nano 2 (2008) 889–896.
[36] W.J. Rieter, J.S. Kim, K.M.L. Taylor, H.Y. An, W.L. Lin, T. Tarrant, W.B. Lin, Hybrid silica nanoparticles for multimodal imaging, Angew. Chem. Int. Ed. 46 (2007) 3680–3682.
[37] I.I. Slowing, B.G. Trewyn, S. Giri, V.S.Y. Lin, Mesoporous silica nanoparticles for drug delivery and biosensing applications, Adv. Funct. Mater. 17 (2007) 1225–1236.
[38] D. Kanduc, A. Mittelman, R. Serpico, E. Sinigaglia, A.A. Sinha, C. Natale, R. Santacroce, M.G. Di Corcia, A. Lucchese, L. Dini, P. Pani, S. Santacroce, S. Simone, R. Bucci, E. Farber, Cell death: Apoptosis versus necrosis (review), Int. J. Oncol. 21 (2002) 165–170.
[39] S.Y. Proskuryakov, V.L. Gabai, A.G. Konoplyannikov, I.A. Zamulaeva, A.I. Kolesnikova, Immunology of apoptosis and necrosis, Biochemistry (Mosc.) 70 (2005) 1310–1320.
[40] A.J. Di Pasqua, K.K. Sharma, Y.L. Shi, B.B. Toms, W. Ouellette, J.C. Dabrowiak, T. Asefa, Cytotoxicity of mesoporous silica nanomaterials, J. Inorg. Biochem. 102 (2008) 1416–1423.
[41] D. Lison, L.C.J. Thomassen, V. Rabolli, L. Gonzalez, D. Napierska, J.W. Seo, M. Kirsch-Volders, P. Hoet, C.E.A. Kirschhock, J.A. Martens, Nominal and effective dosimetry of silica nanoparticles in cytotoxicity assays, Toxicol. Sci. 104 (2008) 155–162.
[42] B. Marquis, S. Love, K. Braun, C. Haynes, Analytical methods to assess nanoparticle toxicity, Analyst. 139 (2009) 425–439.
[43] T. Laaksonen, H. Santos, H. Vihola, J. Salonen, J. Riikonen, T. Heikkila, L. Peltonen, N. Kurnar, D.Y. Murzin, V.P. Lehto, J. Hirvonent, Failure of MTT as a toxicity testing agent for mesoporous silicon microparticles, Chem. Res. Toxicol. 20 (2007) 1913–1918.
[44] K.E. Driscoll, The toxicology of crystalline silica studied in vitro, J. Occup. Environ. Hyg. 10 (1995) 1118–1125.
[45] I. Fenoglio, A. Croce, F. Di Renzo, R. Tiozzo, B. Fubini, Pure-silica zeolites (porosils) as model solids for the evaluation of the physicochemical features determining silica toxicity to macrophages, Chem. Res. Toxicol. 13 (2000) 489–500.
[46] B. Fubini, G. Zanetti, S. Altilia, R. Tiozzo, D. Lison, U. Saffiotti, Relationship between surface properties and cellular responses to crystalline silica: Studies with heat-treated cristobalite, Chem. Res. Toxicol. 12 (1999) 737–745.
[47] B. Fubini, Surface reactivity in the pathogenic response to particulates, Environ. Health Perspect. 105 (1997) 1013–1020.
[48] B. Fubini, Surface chemistry and quartz hazard, Ann. Occup. Hyg. 42 (1998) 521–530.
[49] B. Fubini, C.O. Arean, Chemical aspects of the toxicity of inhaled mineral dusts, Chem. Soc. Rev. 28 (1999) 373–381.

[50] Z. Elias, O. Poirot, M.C. Daniere, F. Terzetti, A.M. Marande, S. Dzwigaj, H. Pezerat, I. Fenoglio, B. Fubini, Cytotoxic and transforming effects of silica particles with different surface properties in Syrian hamster embryo (SHE) cells, Toxicol. In Vitro 14 (2000) 409–422.
[51] M. Giovine, M. Pozzolini, I. Fenoglio, S. Scarfi, M. Ghiazza, U. Benatti, B. Fubini, Crystalline silica incubated in ascorbic acid acquires a higher cytotoxic potential, Toxicol. Ind. Health 18 (2002) 249–255.
[52] K. Donaldson, P.J.A. Borm, The Quartz hazard: A variable entity, Ann. Occup. Hygiene 42 (1998) 287–294.
[53] M. Grce, K. Pavelic, Antiviral properties of clinoptilolite, Microporous Mesoporous Mater. 79 (2005) 165–169.
[54] S. Giri, B.G. Trewyn, M.P. Stellmaker, V.S.-Y. Lin, Stimuli-responsive controlled-release delivery system based on mesoporous silica nanorods capped with magnetic nanoparticles, Angew. Chem. Int. Ed. 44 (2005) 5038–5044.
[55] D.R. Radu, C.-Y. Lai, K. Jeftinija, E.W. Rowe, S. Jeftinija, V.S.-Y Lin, A polyamidoamine dendrimer-capped mesoporous silica nanosphere-based gene transfection reagent, J. Am. Chem. Soc. 126 (2004) 13216–13217.
[56] T.H. Chung, S.H. Wu, M. Yao, C.W. Lu, Y.S. Lin, Y. Hung, C.Y. Mou, Y.C. Chen, D.M. Huang, The effect of surface charge on the uptake and biological function of mesoporous silica nanoparticles 3T3-L1 cells and human mesenchymal stem cells, Biomaterials 28 (2007) 2959–2966.
[57] Z.M. Tao, M.P. Morrow, T. Asefa, K.K. Sharma, C. Duncan, A. Anan, H.S. Penefsky, J. Goodisman, A.K. Souid, Mesoporous silica nanoparticles inhibit cellular respiration, Nano Lett. 8 (2008) 1517–1526.
[58] I. Slowing, B.G. Trewyn, V.S.Y. Lin, Effect of surface functionalization of MCM-41-type mesoporous silica nanoparticleson the endocytosis by human cancer cells, J. Am. Chem. Soc. 128 (2006) 14792–14793.
[59] T. Brooke, A.M.S. Mossman, In vitro assays to predict the pathogenicity of mineral fibers, Toxicology 60 (1990) 53–61.
[60] E. Fach, R. Kristovich, F.J. Long, W.J. Waldman, K. Prabir Dutta, V. Marshall Williams, The effect of iron on the biological activities of erionite and mordenite, Environ. Int. 29 (2003) 451–458.
[61] Y. Suzuki, N. Kohyama, Malignant mesothelioma induced by asbestos and zeolite in the mouse peritoneal cavity, Environ. Res. 35 (1984) 277–292.
[62] Y. Suzuki, Carcinogenic and fibrogenic effects of zeolites: Preliminary observations, Environ. Res. 27 (1982) 433–445.
[63] A. Petushkov, J. Intra, J.B. Graham, S.C. Larsen, A.K. Salem, Effect of crystal size and surface functionalization on the cytotoxicity of silicalite-1 nanoparticles, Chem. Res. Toxicol. 22 (2009) 1359–1368.
[64] Y.I. Baris, A.A.S.M. Ozesmi, I. Kerse, E. Ozen, B. Kolacan, M. Altinors, A. Goktepeli, An outbreak of pleural mesothelioma and chronic fibrosing pleurisy in the village of Karain/Urgup in Anatolia, Thorax 33 (1978) 181–192.
[65] Y. lzzettin, M.A. Baris, A. Altay Sahin, Environmental mesothelioma in Turkey, Ann. N. Y. Acad. Sci. 330 (1979) 423–432.
[66] P. Gross, R.A.H.L.M. Swinburne, J.M. Davis, W.B. Greene, Ingested mineral fibers. Do they penetrate tissue or cause cancer? Arch. Environ. Health 29 (1974) 341–347.
[67] X.D. Shi, N.S. Vallyathan, ESR evidence for the hydroxyl radical formation in aqueous suspension of quartz particles and its possible significance to lipid peroxidation in silicosis, J. Toxicol. Environ. Health 25 (1988) 237–245.
[68] M. Marsh, H.T. McMahon, Cell biology—The structural era of endocytosis, Science 285 (1999) 215–220.

[69] K.M. Waters, L.M. Masiello, R.C. Zangar, B.J. Tarasevich, N.J. Karin, R.D. Quesenberry, S. Bandyopadhyay, J.G. Teeguarden, J.G. Pounds, B.D. Thrall, Macrophage responses to silica nanoparticles are highly conserved across particle sizes, Toxicol. Sci. 107 (2009) 553–569.
[70] V. Borutaite, G.C. Brown, Nitric oxide induces apoptosis via hydrogen peroxide, but necrosis via energy and thiol depletion, Free Radic. Biol. Med. 35 (2003) 1457–1468.
[71] K.S. Kumar, V.K. Singh, W. Jackson, T.M. Seed, Inhibition of LPS-induced nitric oxide production in RAW cells by radioprotective thiols, Exp. Mol. Pathol 74 (2003) 68–73.
[72] R. Zamora, K.E. Matthys, A.G. Herman, The protective role of thiols against nitric oxide-mediated cytotoxicity in murine macrophage J774 cells, Euro. J. Pharmacol. 321 (1997) 87–96.
[73] J.P. Ryman-Rasmussen, J.E. Riviere, N.A. Monteiro-Riviere, Surface coatings determine cytotoxicity and irritation potential of quantum dot nanoparticles in epidermal keratinocytes, J. Invest. Dermatol. 127 (2007) 143–153.
[74] M.J.D. Clift, B. Rothen-Rutishauser, D.M. Brown, R. Duffin, K. Donaldson, L. Proudfoot, K. Guy, V. Stone, The impact of different nanoparticle surface chemistry and size on uptake and toxicity in a murine macrophage cell line, Toxicol. Appl. Pharmacol. 232 (2008) 418–427.
[75] E.J. Park, K. Park, Oxidative stress and pro-inflammatory responses induced by silica nanoparticles in vivo and in vitro, Toxicol. Lett. 184 (2009) 18–25.
[76] R.P.F. Schins, R. Duffin, D. Hohr, A.M. Knaapen, T.M. Shi, C. Weishaupt, V. Stone, K. Donaldson, P.J.A. Borm, Surface modification of quartz inhibits toxicity, particle uptake, and oxidative DNA damage in human lung epithelial cells, Chem. Res. Toxicol. 15 (2002) 1166–1173.
[77] I.I. Slowing, C.W. Wu, J.L. Vivero-Escoto, V.S.Y. Lin, Mesoporous silica nanoparticles for reducing hemolytic activity towards mammalian red blood cells, Small 5 (2009) 57–62.
[78] Z.M. Tao, B.B. Toms, J. Goodisman, T. Asefa, Mesoporosity and functional group dependent endocytosis and cytotoxicity of silica nanomaterials, Chem. Res. Toxicol. 22 (2009) 1869–1880.
[79] D.M. Huang, Y. Hung, B.S. Ko, S.C. Hsu, W.H. Chen, C.L. Chien, C.P. Tsai, C.T. Kuo, J.C. Kang, C.S. Yang, C.Y. Mou, Y.C. Chen, Highly efficient cellular labeling of mesoporous nanoparticles in human mesenchymal stem cells: Implication for stem cell tracking.FASEB J19 (2005) 2014–2016.
[80] K. Peters, R.E. Unger, C.J. Kirkpatrick, A.M. Gatti, E. Monari, Effects of nano-scaled particles on endothelial cell function in vitro: Studies on viability, proliferation and inflammation, J. Mater. Sci. Mater. Med. 15 (2004) 321–325.
[81] D. Napierska, L.C.J. Thomassen, V. Rabolli, D. Lison, L. Gonzalez, M. Kirsch-Volders, J.A. Martens, P.H. Hoet, Size-dependent cytotoxicity of monodisperse silica nanoparticles in human endothelial cells, Small 5 (2009) 846–853.
[82] L.C.J. Thomassen, A. Aerts, V. Rabolli, D. Lison, L. Gonzalez, M. Kirsch-Volders, D. Napierska, P.H. Hoet, C.E.A. Kirschhock, J.A. Martens, Synthesis and characterization of stable monodisperse silica nanoparticle sols for in vitro cytotoxicity testing, Langmuir 26 (2009) 328–335.
[83] W.S. Lin, Y.W. Huang, X.D. Zhou, Y.F. Ma, In vitro toxicity of silica nanoparticles in human lung cancer cells, Toxicol. Appl. Pharmacol. 217 (2006) 252–259.
[84] J.S. Chang, K.L.B. Chang, D.F. Hwang, Z.L. Kong, In vitro cytotoxicitiy of silica nanoparticles at high concentrations strongly depends on the metabolic activity type of the cell line, Environ. Sci. Technol. 41 (2007) 2064–2068.
[85] Diseases associated with exposure to silica and nonfibrous silicate minerals, Arch. Pathol. Lab. Med. 112 (1988) 673–720.

[86] G. Hochstrasser, J.F. Antonini, Surface states of pristine silica surfaces, Surface Sci. 32 (1972) 644–664.
[87] V. Vallyathan, X. Shi, N.S. Dalal, W. Irr, V. Castranova, Generation of free radicals from freshly fractured silica dust. Potential role in acute silica-induced lung injury, Am. J. Respir. Dis. 138 (1988) 1213–1219.
[88] M. Polimeni, E.G.M. Ghiazza, I. Fenoglio, A. Bosia, B. Fubini, D. Ghigo, Quartz inhibits glucose 6-phosphate dehydrogenase in murine alveolar macrophages, Chem. Res. Toxicol. 21 (2008) 888–894.
[89] S. Geh, R.Y.R. Duffin, C. Albrecht, P.J.A. Borm, L. Armbruster, M. Raulf-Heimsoth, T. Bruning, E. Hoffmann, A.W. Rettenmeier, E. Dopp, Cellular uptake and cytotoxic potential of respirable bentonite particles with different quartz contents and chemical modifications in human lung fibroblasts, Arch. Toxicol. 80 (2006) 98–106.
[90] C. Albrecht, R.P.F.S.D. Höhr, A. Becker, T. Shi, A.M. Knaapen, P.J.A. Borm, Inflammatory time course after Quartz instillation role of tumor necrosis factor and particle surface, Am. J. Respir. Cell Mol. Biol. 31 (2004) 292–301.

INDEX

Note: The letters 't' and 'f' following locators refer to tables and figures respectively.

B

C

D

E

F

I

J

K

L

M

R

S